Roles of Wnt Signalling during Neural Differentiation of Embryonic Stem (ES) Cells

Norshariza Nordin

Submitted for the Degree of Doctor of Philosophy
University of Edinburgh

June 2006

This thesis is dedicated to....

My late father : 1947-1997
My late grandfather : 1918-1997
My late grandmother : 1923-1997

My in-laws and my mother

&

Foremost

My lovely daughters
Qistina and Jannah

Declaration

I (Norshariza Nordin) declare that the work presented in this thesis is my own, except where otherwise clearly stated. All experiments were designed by me, or in collaboration with my supervisors Dr. John Mason and Dr. Meng Li. No part of this work has been, or being, submitted for any other degree or qualification.

Signed:

Date: 28/7/06

Acknowledgements

First of all I would like to thank the Malaysian Government for the financial support and also to Associate Professor Dr Rozita Rosli of UPM for her encouragement in me pursuing this PhD.

Special thanks go to my supervisors, Dr John Mason and Dr Meng Li for their patience, advice, support and encouragement during the whole period until the completion of this thesis. Especially to John, thank you for being such an understanding and supportive supervisor, and in making me realized that taking breaks can make you even more productive.

Thanks go out to members of the Mason, Price, Kind and Spears laboratories for making DBUG such a brilliant place to work. Full credit goes to Dr Tom Pratt and Katy Gillies for being so helpful in every way. Technical support from Linda Wilson in taking the confocal images and Shonna Johnston for helping me with the flowcytometry techniques is much appreciated. I would also like to thank Rowena Smith for patiently coping with me in ESTC room and especially in preparing me the 1% gelatine.

Special appreciation goes to Dr Ian Simpson for his time in teaching me about ES cells, Mark Barnett who taught me about SyBr Green light cycler and also Ben Martynoga for his good tips on flowcytometry. Thanks also to Mark Hillen for the primers. Catherine Naughton also did a good job in teaching me about Western blot and Ben Fernby for his help with cloning strategies. Dr Vassiliki Fotaki also deserves special thanks for all the help regarding molecular techniques. I must also thank Tammy Yu for always there in doing me favours during my crucial times.

Special thanks to Catherine Carr who has done an excellent job babysitting my children whenever my experiments didn't go as planned. I would also like to thank everyone in the lab for accepting me the way I am. I really enjoyed myself for the last 3 years and 7 months.

To all my Malaysian friends wherever you are, thank you for all the support and friendship, particularly to Zahidah, Rowiyah and Aida for babysitting my kids, Roziyah Yusup for being such a great listener, Azila Kassim for the laughs and everyone who knows me.....

To my family, thank you for believing in me. Last but not least, my grateful thanks go to my husband for the advice, patience and importantly in making me realized that I am not a "superwoman". Thank you for the popcorn too.

Table of contents

Common Abbreviations

4′-OHT	4′-Hydroxytamoxifen
ATRA	*All trans* retinoic acid
ß-gal	ß-galactosidase
bHLH	Basic helix loop helix
BMP	Bone morphogenetic protein
bp	Base pairs
BSA	Bovine serum albumin
cDNA	Complementary DNA
CNS	Central nervous system
DMSO	Dimethylsulphoxide
DNA	Deoxyribonucleic acid
dNTPS	Deoxyribonucleotides triphosphates
E	Embryonic day
EBs	Embryoid bodies
EGF	Epidermal growth factor
En	Engrailed
eGFP	Enhanced green fluorescent protein
ER	Estrogen receptor
ES	Embryonic stem
FACS	Fluorescence activated cell sorting
FBS	Foetal bovine srum
FCS	Foetal calf serum
FGF	Fibroblast growth factor
HA	Haemeagglutinin
HEK	Human embryonic kidney
ICM	Inner cell mass
Id	Inhibitor of differentiation
Kb	Kilobase
LiCl	Lithium chloride
LIF	Leukaemia inhibitory factor
MHB	Midbrain-hinbrain boundary
NPCs	Neural precursor cells
NSC	Neural stem cells
Pac	Puromycin resistant gene
PCR	Polymerase chain reaction
PNS	Peripheral nervous system
POU	Pit-Oct-Unc

qRT-PCR	Quantitative RT-PCR
RA	Retinoic acid
RNA	Ribonucleic acid
rpm	Revolutions per minute
RT	Room temperature
RT-PCR	Reverse transcription polymerase chain reaction
SAP	Shrimp alkaline phosphatase
SDS-PAGE	SDS polyacrylamide gel electrophoresis
SHH	Sonic hedgehog
SOX	SRY-like HMG box
Tp	Puromycin resistant clone after treatment with tamoxifen
UTR	untranslated region

List of Tables

List of Figures

Abstract

Embryonic stem (ES) cells are unique cells with the capacity to self-renew and differentiate into every cell type in the body even after prolonged culture. They provide an ideal system in which to study genetic mechanisms that regulate differentiation along specific lineages. Further, once such differentiation can be precisely controlled *in vitro*, ES cells hold great promise for a variety of therapeutic applications. This study concerns the mechanisms that regulate neural differentiation of ES cells, and specifically in the possible role of Wnt signalling in this process. Wnt proteins are a large family (19 members in mammals) of signalling molecules that have well-established roles in regulating embryonic patterning, cell proliferation and cell determination.

Activation of Wnt signalling has previously been shown to inhibit the differentiation of ES cells to neural precursors. Further, there is preliminary evidence that Wnt signalling may promote the differentiation of these neural precursors into neurons. In order to investigate how Wnt signalling affects the differentiation of ES cells into neurons *in vitro*, RNA expression of all 19 Wnt genes together with two Wnt antagonists, *Dkk1* and *sFRP2*, during the process was first determined by RT-PCR. Of 19 Wnt genes, the expression of 12 with particularly interesting patterns was subsequently analysed by quantitative RT-PCR (qRT-PCR). Neural differentiation of ES cells was induced through the formation of embryoid bodies (EBs) and the addition of retinoic acid (RA). The gene expression was determined in five different stages of the process including undifferentiated ES cells, early EBs prior to the addition of RA, EBs in the presence of RA, attached EBs after withdrawal

of RA and finally neuron-like cells grown on an adhesive substratum. Many *Wnt* genes showed dynamic alterations in expression levels during neural differentiation.

In order to test the effect of expressing Wnts at different stages, we developed an inducible expression system. The system is based on a cre-*loxP* strategy and allows for stimulation or inhibition of Wnt signalling at specific steps of the differentiation process. Overexpression of *Wnt1*-HA and *Wnt3a* at early and late stages of the process in addition to constitutive expression of these genes was carried out. Additionally, inhibition of Wnt signalling by overexpressing *Dkk1* at early and late stages as well as its constitutive expression during the differentiation process was also conducted. The effects of altered Wnt signalling on the formation of neural precursor cells (NPCs) and neuronal cells was analysed using specific protein markers by immunocytochemistry and fluorescent-activated cell sorting (FACS) analysis.

It was found that overexpression of *Wnt1* and *Wnt3a* at the early stages of the differentiation process significantly reduced the formation of NPCs while inhibition of Wnt signalling at this stage by induction of *Dkk1* significantly increased the number of NPCs. A Significant increase in the percentage of neuron formation was observed when *Dkk1* and *Wnt1* were overexpressed at early stages of the process. In contrast, overexpression of *Wnt3a* at this stage significantly reduced the number of neurons.

Formation of neurons was stimulated by overexpression of *Wnt3a* at late stages of neural differentiation process, whereas induction of *Wnt1* at this

stage enhanced the percentage of neurons in cultures. Overexpression of *Dkk1* at this stage however significantly decreased the formation of neurons.

Additionally, cconstitutive stimulation or inhibition of Wnt signalling during the process was observed to reduce the ability of ES to differentiate into NPCs and neurons. These observations therefore highlight the complexity of probable function of stage-dependent response to Wnt signalling during neural differentiation.

Chapter 1: Introduction

1.1 Embryonic Stem cells

1.1.1 Mouse Embryonic Stem (ES) Cells

At the time of implantation, the early mouse embryo is composed of three distinct cell types termed the trophectoderm, the primitive endoderm and the inner cell mass (ICM). Among these, the ICM will be organized into the epiblast, which then during gastrulation develops into the three primary germ layers (ectoderm, mesoderm and definitive endoderm), and the extraembryonic mesoderm of the yolk sac and amnion. The primary germ layers consist of progenitor cells which are capable to differentiate into all types of fetal and adult tissues (Loebel *et al.*, 2003; Eiges and Benvenisty, 2002; Wobus, 2001). At around embryonic day 3.5 (E3.5)[1], the cells of the ICM are relatively undifferentiated, pluripotent[2] cells prior to differentiating into the specific tissues. Within a few days, the embryo from the ICM/blastocyst stage (~E5.0) develops to gastrulation (~E7.0) stage by which point most of these pluripotent cells have differentiated (Figure 1.1, Loebel *et al.*, 2003; Hadjantonakis and Papaioannou, 2001; Wobus, 2001). Understanding the basic properties of these cells, especially their capacity to self-renew as well as to differentiate would offer a great deal of advantages in understanding mammalian development. Therefore, it would be advantageous to have a system that can recapitulate the proliferation and differentiation processes of these cells *in vitro*. Besides having the chance to

[1] E0.5 is taken as midday on the day that vaginal plug is detected.
[2] The cells are able to differentiate into virtually any cell type present in the body. At this point the cells are expressing *Oct4*, a marker for pluripotent cells and also *Rex1*, which is specifically expressed in the ICM (Scholer *et al.*, 1990)

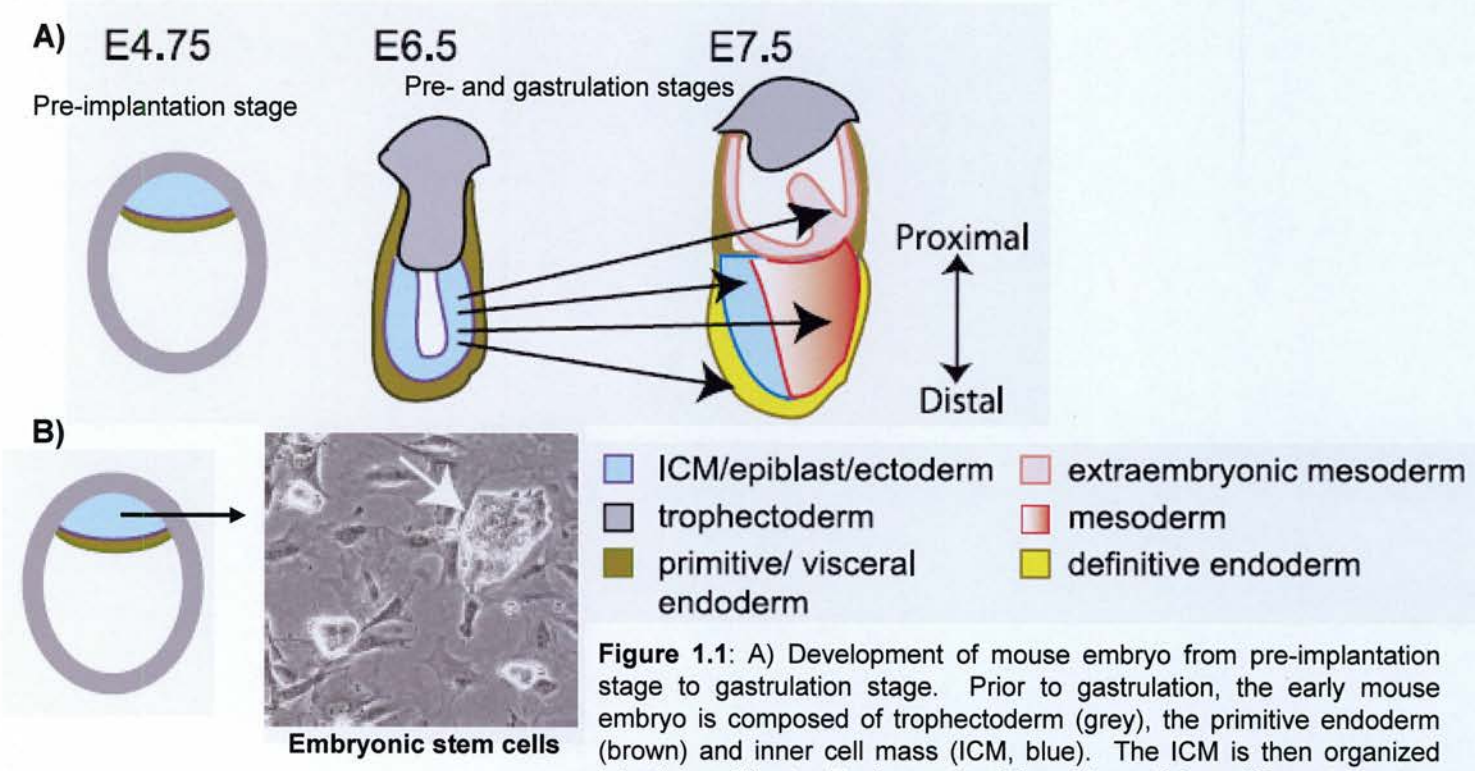

Figure 1.1: A) Development of mouse embryo from pre-implantation stage to gastrulation stage. Prior to gastrulation, the early mouse embryo is composed of trophectoderm (grey), the primitive endoderm (brown) and inner cell mass (ICM, blue). The ICM is then organized into the epiblast. During gastrulation, the epiblast differentiates into ectoderm (blue), mesoderm (red) and definitive endoderm (yellow). B) Establishment of embryonic stem (ES, white arrow) cells *in vitro* derived from the ICM of mouse embryo during pre-implantation stage. Diagram is adapted from Loebel *et al.,* 2003.

study the mechanisms in a more simplified environment, the system will also serve as an invaluable tool/model for genetic manipulation as well as potentially providing a renewable cell source of cell-replacement therapies. These are the cells that most people refer to as embryonic stem (ES) cells when growing *in vitro*.

1.1.2 Origin and Properties of Embryonic Stem (ES) cell lines

The establishment of mouse ES cell lines by several independent groups in the 1980s (Evans and Kaufman, 1981; Martin, 1981; Axelrod, 1984; Wobus *et al.*, 1984) has given us invaluable tools for the analysis of genetics and development as well as a great model system to understand lineage differentiation and as a source of cells for transplantation (O'Shea, 2001). Mouse ES cells have normally been derived from either dissociated morulae (Eistetter, 1988), intact blastocysts (Evans and Kaufman, 1981), or entire ICM (Martin, 1981). In addition, Brook and Gardner (1997) also found a source of ES progenitor cells in the primitive ectoderm or epiblast. In most cases, the cells were derived from E3.5 ICM (Figure 1.1) of mouse blastocyst (O'Shea, 2001) into tissue culture and propagating them as undifferentiated cell lines in the presence of leukemia inhibitory factor (LIF) [Smith *et al.*, 1988] or mouse embryonic fibroblasts (MEFs), which provide a source of LIF (Hadjantonakis and Papaioannou, 2001). Apparently, the cells are able to replicate unlimitedly in tissue culture without losing their pluripotency. A characteristic that is well suited for cell genetic manipulations. Upon withdrawal of LIF, the cells spontaneously differentiate (Li *et al.*, 1998a; Smith, 2001; Murray and Edgar, 2001).

Similar to the ICM and the early epiblast, ES cells are capable to differentiate into multiple cell types in culture (Rossant and McKerlie, 2001), in teratomas (ref Hadjantonakis and Papaioannou, 2001), or in chimeric embryos and can even form the entire fetus when transferred back into blastocysts of an early embryo (Nagy *et al.*, 1990, 1993). However, ES cells have not been demonstrated to contribute to either the trophectoderm or visceral endodermal lineages (Loebel *et al.*, 2003). The cells also retain a normal, euploid karyotype when propagated *in vitro*. The majority of established ES cell lines are male (XY), since the XX karyotype seems to be unstable, and often the X chromosome is lost (Smith, 2001). Other characteristics of undifferentiated ES cells are high alkaline phosphatase activity, expression of embryonic antigens SSEA-1 (Solter and Knowles, 1978; Resnick *et al.*, 1992), a high nucleo-cytoplasmic ratio and high telomerase activity (Thomson *et al.*, 1998; Burdon *et al.*, 1999; Prelle *et al.*, 1999).

1.1.3 Maintenance of ES cells

Two major invaluable properties of ES cells are their ability to self-renew indefinitely *in vitro* and their capacity to differentiate into virtually any cell type present in the body (pluripotent cells), even after prolonged culture (Suda *et al.*, 1987). Therefore, understanding the factors controlling these mechanisms is essential in order to conclusively provide a continuous genuine resource of embryonic stem cells *in vitro* with these properties preserved. Presently, there are at least five signalling pathways that are thought to be co-operatively involved in maintaining self renewal and pluripotency of mouse ES cells (Nakashima *et al.*, 2004; Temple, 2003).

One of the key regulators of ES cell pluripotency and differentiation is Oct4 (also known as Oct3), which belongs to the POU (Pit-Oct-Unc) transcription factor superfamily (Pesce and Scholer, 2001; Scholer *et al.*, 1991). Oct4 appears to be exclusively expressed in ES cells and, is downregulated upon commitment to differentiation (Fuhrmann *et al.*, 2001). In the mouse embryo, its expression is restricted to the ICM and downregulated in the trophectoderm and the primitive endoderm. Mice with targeted disruption of *Oct4* produced embryos devoid of the pluripotent ICM (Nichols *et al.*, 1998), suggesting the importance of the gene in maintaining pluripotency. However, Niwa and colleagues (2000) demonstrated that increased expression of Oct4 causes ES cells to differentiate. Quantitative analysis of Oct4 expression also demonstrated that a high and a low level of Oct4 expression directed ES cells towards the extra-embryonic mesoderm or endoderm lineages, and trophectoderm, respectively. Nevertheless, ES cells with normal level of Oct4 remain pluripotent (Pan *et al.*, 2002; Niwa *et al.*, 2000; Niwa, 2001). In addition, these cells still require LIF for self-renewal (Niwa *et al.*, 2000) indicating that there is more than one regulatory element or pathway involved in maintaining these properties of ES cells.

A major signalling pathway that sustains long term self-renewal of mouse ES cells with maintained undifferentiated cell characteristics, pluripotency and embryo colonization capability (Smith, 2001; Ying *et al.*, 2003a) involves leukaemia inhibitory factor (LIF). LIF acts by binding a heterodimeric receptor complex comprising the LIF receptor (LIFR) and glycoprotein 130 (gp130) (Yoshida *et al.*, 1994; Smith 1998; Smith and Treutlien, 1998; Ernst *et al.*, 1999; Burdon *et al.*, 2002). This receptor complex results in activation of gp130 signaling through the Janus Kinase (Jak)/signal transducer and

activator of transcription-3 (Stat-3) pathway. Activation of the latent transcription factor STAT3 by LIF is sufficient to maintain mouse ES cells self-renewal in serum containing cultures (Matsuda *et al.*, 1999; Niwa *et al.*, 1998). Several cytokines related to LIF bind to the LIFR/gp130 heterodimer and can also substitute LIF *in vitro*, such as ciliary neurotrophic factor, cardiotropin 1 and oncostatin M (Hadjantonakis and Papaioannou, 2001). Inhibition of STAT3 was also found to induce differentiation of ES cells (Niwa *et al.*, 1998; Ernst *et al.*, 1999). However, in the absence of serum, LIF alone cannot maintain the cells self-renewal; instead, they differentiate into neural-like cells (Temple, 2003). Therefore, another factor(s), which may be present in the serum, together with LIF must be needed in order to preserve this invaluable property of ES cells.

This observation, thus, has led to the study of neurogenesis inhibitor element as a target in another pathway that may be involved in maintaining self-renewal in mouse ES cells. In the study conducted by Ying *et al.* (2003a), an early embryo anti-neurogenesis factor (Wilson and Edlund, 2001; Wilson and Hemmati-Brivanlou, 1995), bone morphogenetic protein (BMP), in combination with LIF was found to inhibit neural differentiation, thus, enhancing self-renewal of mouse ES cells in serum-free cultures. Interestingly, they discovered that BMP alone neither activated STAT3 nor modulated gp130 signal transduction in ES cells, indicating that a BMP signalling pathway directly contributes to the self-renewal of ES cells. Ying and colleagues (2003a) proposed the Smad pathway as a transducer of the self-renewal signal through activation of expression of inhibitor of differentiation (Id) genes. Id proteins are negative regulators for basic helix-loop-helix (bHLH) transcription factors that specify various cell lineages

(Ying *et al.*, 2003a; Nakashima *et al.*, 2001). Together with LIF, overexpression of Id has been observed to maintain undifferentiated ES cells in serum-free medium. On the other hand, BMP alone has been discovered to promote differentiation of ES cells to non-neural cells (ref. Ying *et al.*, 2003a; Ying *et al.*, 2003b), besides being demonstrated to antagonize neural differentiation of ES cells in serum-free cultures (Tropepe *et al.*, 2001, Ying *et al.*, 2003b). Therefore, the effect on self-renewal of ES cells may be dependent totally on co-stimulation and balancing with LIF pathway, since both pathways have stimulatory and inhibitory effects on self-renewal of ES cells (Temple, 2003).

Even though LIF seems to be the central player in maintaining these properties of ES cells, previous studies have shown that mutant embryos deficient in the LIF/gp130/Stat3 pathway formed normal ICM and LIF-deficient mice developed normally (Stewart 1994) arguing against the fundamental role of LIF/gp130/Stat3 for pluripotency. As a result, the existence of a novel pathway(s) that maintains pluripotency in both ICM and ES cells has been proposed (Mitsui *et al.*, 2003). Mitsui *et al.* (2003) and Chambers *et al.* (2003) demonstrated the involvement of a divergent homeobox transcription factor, Nanog, in maintaining self-renewal of ES cells independently of the LIF/STAT3 pathway. Similar to Oct4, Nanog is expressed in the ICM as well as in ES cells, and downregulated upon differentiation of ES cells (Cavaleri and Scholer, 2003; Chambers *et al.*, 2003). Mitsui and colleagues discovered that *nanog*-deficient ES cells lost pluripotency and differentiated into extraembryonic endoderm lineage, and *nanog*-deficient ICM failed to generate epiblast and only produced parietal endoderm-like cells. In addition, Chambers *et al.* (2003) demonstrated that overexpression of nanog cannot revert the differentiation of ES cell induced

by downregulation of Oct4. They also discovered that Nanog was still expressed in Oct4-deficient embryos, suggesting that Nanog and Oct4 may be working side by side in supporting ES cells potency and self-renewal. Stat3-activated self-renewal of ES cells was also not affected by overexpression of Nanog. Therefore, Nanog, Oct4 and Stat3 seem to be operating three different transcriptional pathways in maintaining self-renewal and pluripotency of ES cells.

The other pathway, which has recently been proposed to be sufficient in maintaining self-renewal as well as the pluripotency of ES cells, is the canonical Wnt pathway. Wnt proteins are signalling proteins, which are believed to participate in the control of gene expression, proliferation, differentiation and cell polarity (Nakashima *et al.*, 2004). In this pathway, also referred to as the Wnt/ß-catenin pathway, the binding of Wnt to its receptor, frizzled, results in inactivation of glycogen synthase kinase-3 (GSK-3 ß), which then stabilizes ß-catenin and activates the transcription of target genes (Miller, 2002). In a study conducted by Sato and colleagues (2004), the pathway was activated by a new GSK-3-specific pharmacological inhibitor, BIO. BIO-treated mouse ES cells were found to be morphologically and pluripotency maintained in the absence of LIF. Therefore, activation of Wnt pathway seems to be sufficient to sustain the self-renewal of ES cells. Expression of known genes involved in mouse ES cells maintenance such as zinc-finger protein Rex-1, POU family transcription factor Oct-4 and the newly identified homeodomain protein Nanog were detected in these cells, indicating their pluripotency property is maintained. The cells were also able to differentiate into the expected lineages upon the withdrawal of BIO. Earlier studies have also indicated the involvement of the canonical Wnt

pathway in maintaining the proliferation of various multipotent stem cells such as haematopoetic stem cells (Reya *et al.*, 2003), neural stem cells (Chenn and Walsh, 2002), skin stem cells (Alonso and Fuchs, 2003) as well as mouse embryonic stem cells (Kielman *et al.*, 2002). The observations made by Sato and colleagues may indicate the possibility that LIF induces self-renewal of ES cells partly through activation of the Wnt pathway. Additionally, a recent study also has suggested the convergence of Wnt/ß-catenin and LIF pathways on activation of STAT3 in preventing differentiation of ES cells (Hao *et al.*, 2006). The study found that activation of STAT3 protein by Wnt/ß-catenin is not enough to maintain ES cells without the presence of LIF in the culture.

1.1.4 Differentiation of ES cells

Studies with mouse ES cells have led to the successful development of many *in vitro* differentiation systems. Most of them involve culturing the ES cells as small aggregates, called embryoid bodies (EBs), in the absence of the cytokine leukemia inhibitory factor (LIF) on a non-adhesive substratum (reviewed in Gottlieb and Huettner, 1999). The differentiation of ES cells to specific lineages is often directed using growth factors and/or retinoic acid (Rohwedel *et al.*, 1999; Lee *et al.*, 2000a; Liu *et al.*, 2000a; Buttery *et al.*, 2001; Lumelsky *et al.*, 2001) or by blocking certain inhibitory pathways (Tropepe *et al.*, 2001; Gratsch and O'shea,2002). In addition, differentiation can also be achieved by growing the cells in co-culture with various differentiated cell types (Rathjen *et al.*, 1999; Kawasaki *et al.*, 2000; Wichterle *et al.*, 2002; Mummery *et al.*, 2002) or by forced expression of transcription factors known to be essential for specific differentiation lineages, such as GATA factors toward differentiation into visceral endoderm (Fujikura *et al.*, 2002).

One of the *in vitro* differentiation systems established is the differentiation of ES cells into early primitive ectoderm-like (EPL) cells (Rathjen *et al.*, 1999). The primitive ectoderm of the mouse embryo arises from the ICM between E4.75 and E5.25 just prior to formation of the three primary germ layers (Rathjen *et al.*, 1999). Gene expression profiles of ES and EPL cells recapitulate the expression of ICM and epiblast, respectively (Loebel *et al.*, 2003). Thus, EPL cells are believed to resemble the epiblast in the embryo. However, unlike ES cells, these EPL cells cannot contribute to tissues in chimeric embryos (Rathjen *et al.*, 1999; Pelton *et al.*, 2002). Interestingly, EPL cell-derived EBs are predisposed to mesodermal differentiation even though these EPL cells are a step closer to ectodermal commitment (Loebel *et al.*, 2003). Nevertheless, continuous exposure to conditioned medium could also direct the EPL cells to a neural fate (Rathjen *et al.*, 2002). Interestingly, these cells can revert to an ES cell-like state upon withdrawal of conditioned medium, with the ability for *in vitro* differentiation and contribution to tissues in chimeric mice (Rathjen *et al.*, 1999; Lake *et al.*, 2000).

The foremost important contribution of ES cells is their ability to differentiate into all primary germ layer tissues *in vitro*. Depending on the culture supplements and conditions, differentiation of ES cells can be directed to ectodermal, mesodermal and endodermal derivatives (Table 1). The endothelial and haematopoietic cells are the earliest mesodermal derivatives to be differentiated from ES cells in cultures. Other mesodermal derivatives that have been differentiated *in vitro* are the smooth muscle cells, heart tissues, skeletal muscles, mast cells, adipocytes, chondrocytes, osteoblasts and osteoclasts. As for endodermal derivatives, ES cells have been demonstrated to differentiate into pancreatic islet cells, insulin- producing

Table 1.1: Different differentiated cell types derived from ES cells *in vitro*

Embryonic Germ Layer	Cell Type	References
Ectoderm (external layer)	Neural progenitor cells	Li *et al.*, 1998
	Neurons	Bain *et al.*, 1995; Strubing *et al.*, 1995; Okabe *et al.*, 1996
	Cortical neurons	Bibel *et al.*, 2004
	Dopaminergic neurons	Lee *et al.*, 2000a; Bjorklund *et al.*, 2002; Kim *et al.*, 2003
	Motor neurons	Wichterle *et al.*, 2002
	Interneurons	Renoncourt *et al.*, 1998
	Oligodendrocytes	Brustle *et al.*, 1999; McDonald *et al.*, 1999; Liu *et al.*, 2000a
	Astrocytes	Billon *et al.*, 2002; Fraichard *et al.*, 1995
	Dendritic cells	Fairchild *et al.*, 2000
Mesoderm (middle layer)	Adipocytes	Dani 1999
	Cardiomycetes	Wobus *et al.*, 1991; Maltsev *et al.*, 1993; Wobus *et al.*, 1997; Wobus and Guan, 1998; Boheler *et al.*, 2002
	Chondrocytes	Kramer *et al.*, 2000
	Haematopoietic cells	Wiles, 1993; Robb and Begley, 1996; Kennedy *et al.*, 1997; Kyba *et al.*, 2002
	Lymphoic precursors	Gutierrez-Ramos and Palacios, 1992
	Endothelial cells	Bagutti *et al.*, 1996, 2001; Gualandris *et al.*, 2000; Yamashita *et al.*, 2000; Feraud *et al.*, 2001, 2003.
	Osteoblasts	Buttery *et al.*, 2001; Phillips *et al.*, 2001
	osteoclasts	Hemmi *et al.*, 2001
	Skeletal muscle cells	Rohwedel *et al.*, 1994; Ridgeway *et al.*, 2000
	Smooth muscle cells	Yamashita *et al.*, 2000
	Mast cells	Tsai *et al.*, 2000; Lindmark *et al.*, 2004
Endoderm (internal layer)	Pancreatic-like islets	Lumelsky *et al.*, 2001; Hori *et al.*, 2002
	Insulin-producing cells	Soria *et al.*, 2000; Blyszczuk *et al.*, 2004
	Hepatic progenitors	Yin *et al.*, 2002
	Hepatocytes	Hamazaki *et al.*, 2001; Jones *et al.*, 2002

cells, hepatic progenitors and liver. For ectodermal commitment, ES cells have been successfully differentiated into neural precursors, dendritic cells,

various types of neurons, and glial cells both the astrocytes and oligodendrocytes.

1.1.5 Neural differentiation of ES cells *in vitro*

Numerous methods have been established in order to achieve populations enriched in neural lineage cells from ES cells in culture. Among the methods established are treatment with retinoic acid (RA) in the presence of serum (Bain *et al.*, 1995), coculture with a particular stromal cell line, PA6 (Kawasaki *et al.*, 2000), adherent monoculture in serum-free medium with N2 and B27 supplements (Ying *et al.*, 2003b), the use of selective medium (Okabe *et al.*, 1996; Tropepe *et al.*, 2001) and the use of genetically modified ES cells and antibiotic selection for cells expressing early neural precursor cells (Li *et al.*, 1998). Additionally, the use of the growth factors EGF (epidermal growth factor) and FGF-2 together with insulin contained in N2 have been recently shown to sufficiently sustain the specific expansion of neural stem (NS) cells derived from ES cells (Conti *et al.*, 2005). The study has successfully generated NS cell lines, that only express neural genes but not of mesoderm- and endoderm-specific genes or even of pluripotent cell-specific transcription factors Oct4 and Nanog, derived from at least ten ES cell lines in this condition.

The most common method used for neural differentiation of mouse ES cells is the spontaneous formation of three-dimensional multicellular aggregates termed embryoid bodies (EBs). Upon withdrawal of LIF, dissociated ES cells spontaneously form EBs when grown in a non-adhesive substratum dish (Figure 1.2). Based on gene expression analysis, the structure of EBs recapitulates certain aspects of early embryogenesis in which lineage specific

region similar to that found in the embryo appears (Gottlieb and Huettner, 1999; Rodda *et al.*, 2002). Upon further culturing, differentiation in EBs resembles the formation of egg cylinder-stage embryos which contains a double-layered structure with an inner ectodermal layer and outer layer of endoderm enclosing a cavity, followed by the appearance of mesodermal cell types (Figure 1.2). However, only a small percentage of neural lineage cells are produced by spontaneous differentiation of EBs (Strubing *et al.*, 1995).

In order to enhance neural differentiation, a method, which was optimized based on neuronal differentiation from teratocarcinoma cells (Jones-Villeneuve *et al.*, 1982), referred to as the 4-/4+ protocol (Bain *et al.*, 1995) was developed. In the 4-/4+ protocol, EBs are cultured for 4 days in the absence of retinoic acid (RA), or specifically *all-trans* retinoic acid (ATRA), followed by 4 days in the presence of RA. RA has been demonstrated to induce differentiation in human teratocarcinoma (NT2) (Pleasure and Lee, 1993; Pleasure *et al.*, 1992), P19 embryonal carcinoma (EC) cells (Boudjelal *et al.*, 1997; Bouillet *et al.*, 1996) and D3 ES cell line (Bain *et al.*, 1995). RA is believed to have important regulatory functions during embryonic development (Morriss-Kay and Sokolova, 1996), although this is controversial. *In vitro*, RA induces differentiation of ES cells into specific cell types in a time- and concentration-dependent manner (Drab *et al.*, 1997).

In the 4-/4+ protocol, the events occurring during the first 4 days in culture are parallel to the ones occurring between embryonic days 4-6 (E4-6). One of the major events occurring at this stage is the expression of a transcription factor for pluripotent embryonic cells encoded by the *Oct-4* gene. *Oct-4* is

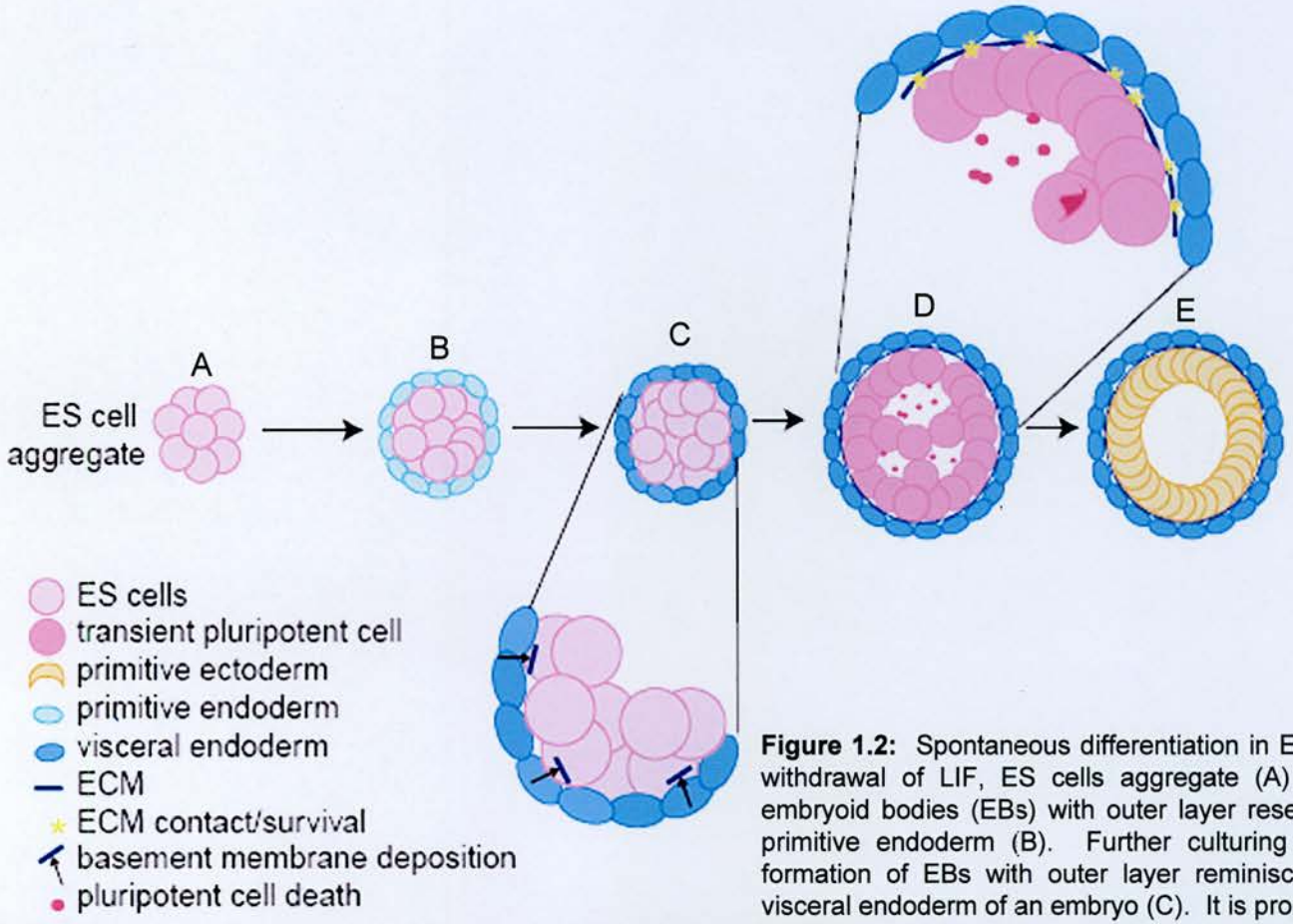

Figure 1.2: Spontaneous differentiation in EBs. Upon withdrawal of LIF, ES cells aggregate (A) and form embryoid bodies (EBs) with outer layer resembles the primitive endoderm (B). Further culturing results in formation of EBs with outer layer reminiscent of the visceral endoderm of an embryo (C). It is proposed that basement membrane induces an alteration in the pluripotent cell state so that the cells that are in contact with the membrane survive and reorganise into an inner ectodermal layer (primitive ectoderm) (E) while those centrally located undergo cell death (D) forming a cavity (E). Diagram is adapted from Lake *et al.*, 2002.

expressed in undifferentiated ES cells and downregulated as the EBs mature (Niwa *et al.*, 2000). Its expression is also extinguished between E5 and E8 embryo as committed lineages emerge (reviewed in Gottlieb and Huettner, 1999). Based on marker expression, the outer layer of EBs also consists of cells resembling visceral endoderm cells as found in E5 embryo (Duncan *et al.*, 1997) in addition to the formation of epiblast-like cells inside the EBs (Doetschman *et al.*, 1985). Besides these events, the cells undergoing neural differentiation *in vitro* also express many regulatory genes expressed in very early brain development, such as *Wnt1, MASH-1, Sox 1, Sox 2, Pax6, Pax3, and delta 1.* These events, therefore, demonstrate that the *in vitro* pathway of neural development of neurons through a series of cellular progenitors may resemble that *in vivo* (Gottlieb and Huettner, 1999).

Treatment with RA at early stage of EBs (on day 2 or day 4) with high concentration of ATRA (100-1000 nM) results in almost 100% of cells in each EBs differentiating into neural cells compared to low frequency of neural differentiation from spontaneous differentiation (Strubing *et al.*, 1995; Fraichard *et al.*, 1995). A recent study by Plactha *et al.*, 2004 has demonstrated that RA appears to restrict the differentiation of ES cell-derived progenitors to a CNS fate. The finding was based on transplantation of RA-treated EBs into a chick neural tube which resulted in the formation of the CNS restricted neuronal cells compared to development of the CNS and PNS restricted neuronal cells on the untreated neural tube. RA-treated EBs also generate various type of neural cells including excitatory and inhibitory neurons and glial cells (Bain *et al.*, 1995, 1996; Fraichard *et al.*, 1995; Strubing *et al.*, 1995; Finley *et al.*, 1996).

A posteriorising effect of RA during neural development *in vivo* and *in vitro* has been suggested (Blumberg *et al.*, 1997; Maden, 2002; Barberi *et al.*, 2003; Du and Zhang, 2004-references therein) even though there is little evidence to prove that RA is actually inducing neural specification from ES cells. RA indeed has been shown to be required for differentiation of EBs into spinal motorneurons (Wichterle *et al.*, 2002) and neuronal cell types characteristic of ventral CNS; somatic motorneurons, cranial motorneurons and interneurons (Renoncourt *et al.*, 1998). On the other hand, Bibel and colleagues (2004) have managed to differentiate RA-treated EBs into Pax6 positive radial glial cells which leads to generation of a defined neural lineage characteristic of cortical pyramidal neurons. These findings therefore imply that treatment with RA could generate various types of neurons within the CNS.

1.2 Wnt Signalling Pathways

1.2.1 Wnt Genes

In 1982, a signalling molecule, the proto-oncogene *Int-1*, correlated with development of mammary tumours in mice was discovered by Nusse and Varmus (Nusse and Varmus, 1982). Not long after the discovery its homolog was then identified in Drosophila *Wingless* (*Wg*) which plays an important role in segment polarity (Cabrera *et al.*, 1987). Interestingly, the Int-1 protein was later discovered to be required for midbrain and cerebellar development (McMahon and Bradley, 1990; McMahon *et al.*, 1992). Consequently, the amalgamation of *Wg* and *Int* led to the name Wnt. Wnt proteins are now recognized as one of the important signalling molecules, together with other families such as the fibroblast growth factors (FGFs), the transforming growth factors (TGFs), the bone morphogenetic proteins (BMPs) and hedgehog (HH) proteins that have been implicated in a wide variety of

biological processes. With its pleiotropic signals, Wnt has been seen to be involved in regulating embryonic patterning, cell proliferation and cell differentiation (Brown and Moon, 1998; Wodarz and Nusse, 1998; Logan and Nusse, 2004). Wnt genes encode a large family of secreted glycoproteins varying between 350-440 amino acids in length with all proteins have highly conserved spacing of 23-24 cysteine residues (Figure 1.3), suggesting that the protein folding may depend on the formation of multiple intramolecular disulfide bonds (Miller, 2001).

Once secreted, Wnt proteins associate with glycosaminoglycans in the extracellular matrix (ECM) and bind tightly to the cell surface (Bradley and Brown, 1990; Reichsman *et al.*, 1996). It is also possible to collect active Wnt protein from the medium of cultured cells [Wnt3a conditioned medium (CM): Shibamoto *et al.*, 1998; Wg CM: VanLeeuwen *et al.*, 1994] even though they are found in tight association with the plasma membrane. Unfortunately, they are notoriously insoluble to be purified in active form, hence hampering attempts on protein characterization. Studies by Willert and colleagues (2003), however have finally managed to unravel the mystery of the insolubility of Wnt proteins. They found Wnt proteins to be unexpectedly hydrophobic and post-translationally modified by palmitoylation, which was found to be on a conserved cysteine residue. Palmitate was found to be critical for signalling. They also discovered that different results were obtained when haematopoietic stem cells (HSCs) were treated with purified Wnt3a protein compared to treatment with Wnt3a CM suggesting that the presence of other factor in the medium might have underscored the function of Wnt protein in the medium. The availability of purified Wnt proteins will therefore be useful in determining the role of each

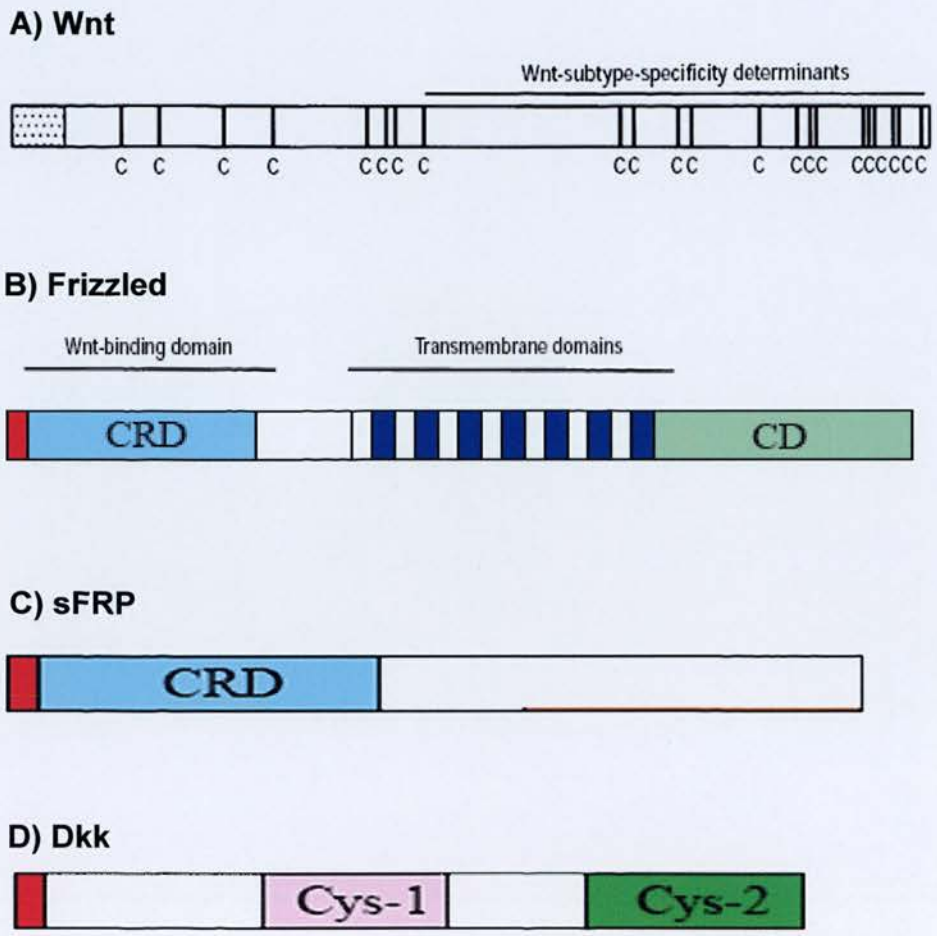

Figure 1.3: A) Structure of Wnt showing 23-24 cysteine residues with their spacing conserved. B) Structure of Frizzled (Fzd) showing cysteine rich domain (CRD) for Wnt binding and the seven transmembrane domains with cytoplasmic carboxyl domain (CD). C) Structure of secreted frizzled related proteins (sFRP) showing CRD that is 30-50% sequence homology with CRD with Fzd. D) Dkk structure showing the two cysteine-rich domains (Cys-1 and Cys-2). Diagrams are adapted from Miller, 2002, and Kawano and Kypta, 2003.

Wnt genes as well as other Wnt signalling components during development. The transduction of Wnt signals involves post-translational modification and secretion of Wnts, binding to transmembrane receptors, activation of cytoplasmic effectors, and transcriptional regulation of target genes. Most information on Wnt signalling is based on genetic studies in *Drosophila* and *Caenorhabditis elegans*, ectopic gene expression in *Xenopus*, and gene knockouts in the mouse (Wodarz and Nusse, 1998). Presently, in vertebrates: 16 members have been found in Xenopus, 11 in chick, 12 in zebrafish, 19 in mouse and humans, while in invertebrates: 7 members have been found in Drosophila, 5 in *Caenorhabiditis elegans* and 1 in hydra. More specific information and updates on Wnt genes including Wnt mutant phenotypes can be obtained from Roel Nusse's webpage: http://www.stanford.edu./~rnusse/wntwindow.html.

1.2.2 Components of Wnt Pathway

1.2.2.1 Wnt Receptors

There are at least three different receptors that are involved in the reception of Wnt signals. The first well known Wnt receptors which were first identified in Drosophila studies are the members of the Frizzled (Fzd) gene family (Bhanot *et al.*, 1996). The gene encodes an amino-terminal cysteine-rich domain (CRD), seven-transmembrane spanning domain (Figure 1.3) and cytoplasmic carboxy-terminus consisting of a S/T-X-V motif which bind to PDZ domain (Songyang *et al.*, 1997). The CRD is believed to be important for Wnt binding. There are 10 known members in human and mice, four in Drosophila and three in *C. elegans* (Miller, 2002). The interaction between

receptors and ligand is promiscuous, in that different Wnt proteins can bind to multiple Fzd's and vice versa (Bhanot *et al.*, 1999).

It is also hypothesized that Fzd receptors may use heterotrimeric G proteins to transduce Wnt signals; based on the structure of these receptors that resembles the seven-transmembrane G-protein-coupled receptors. Several studies have demonstrated that G-protein signalling has able to mediate calcium release and activate protein kinase C (PKC) in ß-catenin-independent Wnt signalling pathway (Sheldahl *et al.*, 1999; Liu *et al.*, 1999a; Kuhl *et al.*, 2000a,b; Slusarski *et al.*, 1997).

Fzd also forms a ternary complex with Wnt and either one or both of two members of low-density lipoprotein receptor-related protein (LRP) family, LRP-5 and LRP-6 (Tamai *et al.*, 2000). These are single transmembrane receptors that act as co-receptor and upon forming the ternary complex activates Dishveled (Dsh), which then leads to inhibition of ß-catenin degradation (see section 1.2.3.1). Similar developmental defects as observed from mutations in certain individual Wnt genes were detected in mice with mutations in LRP-6 (Pinson *et al.*, 2000). Overexpression of LRP-6 also resulted in axis duplication and activation of Wnt-responsive gene in Xenopus, while overexpression of a truncated form of LRP-6 was found to block Wnt activity in the same assay (Tamai *et al.*, 2000). In Drosophila, *arrow*, the orthologue of LRP-5 and LRP-6, is needed for optimal Wg signalling (Wehrli *et al.*, 2000). These studies therefore demonstrate the importance of these receptors in transduction of Wnt signals in vertebrate as well as in invertebrate.

Recently, another Wnt receptor that has a Wnt-interacting WIF domain at its extracellular region (Hsieh *et al.*, 1999), the tyrosine kinase receptor Derailed

which belongs to the RYK (in mammals) subfamily has been described. Derailed is believed to be Dwnt5 receptor and through its unclear signal transduction appears to regulate axon guidance in the *Drosophila* CNS (Yoshikawa *et al.*, 2003). Similar phenotype that displays misrouting of neuronal projections across the midline was observed both in Dwnt5 mutant embryos as well as those lacking Derailed. Wnt4 and Wnt5 have been implicated in axon guidance in vertebrate (Hall *et al.*, 2000; Lyuksyutova *et al.*, 2003) and therefore it will be interesting to see whether the interaction between Wnts to Fzd/LRP and RYK receptors occur and function in the same tissues and cellular processes simultaneously or in parallel pathways (Logan and Nusse, 2004).

In addition to the Fzd and LRP receptors, cell-surface proteoglycans also have been suggested to play a role in transduction of Wnt signals. Studies in Drosophila have shown that Heparan sulphate proteoglycans (HSPGs) are required as co-receptors during Wg signalling (Lin *et al.*, 1999). Mutations in genes encoding enzymes necessary for the formation of heparan sulphate defect Wg signalling (Cumberledge and Reichsman,, 1997; Lin *et al.*, 1999). In vertebrates, HSPGs are also required for Wnt signalling. QSulf1, an avian protein related to heparan-specific N-acetyl glucosamine sulfatases has been shown to regulate heparan-dependent Wnt signalling in cultured cells (C2C12), implying that it can regulate Wnt signals by desulphation of cell-surface proteoglycans (Dhoot *et al.*, 2001). However, to date, it is unclear how proteoglycans modulate Wnt signalling (Miller, 2002) although emerging evidence implies its role in the transport or stabilization of Wnt (Logan and Nusse, 2004).

1.2.2.2 Wnt Antagonists

Many extracellular molecules have been found to regulate Wnt activity. Proteins that act as Wnt antagonists can be categorized into two classes, the secreted Frizzled related protein (sFRP) class and the Dickkopf (Dkk) class. Members of sFRP class, which includes Wnt inhibitory factor-1 (Wif-1) and Cerberus in addition to members of sFRP members, bind directly to Wnts hence resulting in alteration of their binding specificity to the Wnt receptor complex. Members of the Dkk class, which consist of certain Dkk family protein and Wise, inhibit Wnt signalling by binding to the LRP-5/LRP-6 component of Wnt receptor complex. Therefore it is suggested that the members of the sFRP class could inhibit both canonical and non-canonical pathways whereas those of the Dkk class could only inhibit the canonical pathway (reviewed in Kawano and Kypta, 2003; Logan and Nusse, 2004).

1.2.2.2.1 sFRPs

Presently there are eight known members of the sFRP family. Each member protein contains a cysteine-rich domain (Figure 1.3, CRD) that is 30-50% homologous to Fzd protein and has 10 conserved cysteine residues at the amino terminus (Melkonyan *et al.*, 1997). However it is unclear whether sFRP inhibits Wnt signalling by binding to Wnt ligands through the CRD (Lin *et al.*, 1997) or the carboxyl-terminus that lies outside the CRD (Uren *et al.*, 2000). Interestingly, the CRD of sFRP1 appears to interact with Wnt ligand and the Fzd receptor suggesting that sFRPs may block Wnt signalling by forming non-functional interactions with either Wnts or Frizzled receptors (Bafico *et al.*, 1999). Nevertheless, in addition to acting as Wnt antagonists,

sFRPs may also promote Wnt signalling depending upon their expression levels or cellular context (Uren *et al.*, 2000).

Many of the sFRPs have been found to be expressed in the developing nervous system (Mayr *et al.*, 1997; Hoang *et al.*, 1998; Leimeister *et al.*, 1998; Lescher *et al.*, 1998). In a functional analysis of sFRP2, it was discovered that the protein may enhance survival and expansion of neural precursor cells during neural differentiation of ES cells, thus highlighting the importance of Wnt signalling and Wnt antagonism during the process (Aubert *et al.*, 2002). The finding may indirectly prove the antagonizing effect on Wnt signalling by sFRPs *in vivo* as many of the genes have been discovered to be expressed in the developing nervous system normally in close proximity to Wnt responsive tissues (reviewed in Kawano and Kypta, 2003). However more precise studies need to be carried out in order to understand how sFRPs could control Wnt activity in healthy tissue. It is interesting to know which Wnts each sFRP can bind and whether they could be acting as agonists in addition to as antagonists at a particular time point and in particular tissues during development.

1.2.2.2.2 Dkks

Dkk proteins are the best characterized secreted Wnt signalling inhibitors that have not been found in invertebrates (Logan and Nusse, 2004). Four Dkk genes have been found in vertebrate (*Dkk1, -2, -3* and *-4*) and each gene contains two cysteine rich domain (Cys1 and Cys2, Figure 1.3) separated by a linker at different length (Glinka *et al.*, 1998; Krupnik *et al.*, 1999). Dkk1 and Dkk4 are inhibitors while, depending on cellular context, Dkk2 can either be

an inhibitor or activator of Wnt signalling (Brott and Sokol, 2002; Mao and Niehrs, 2003). Little is known about the function of Dkk3.

Among the Dkk family, the most studied member is Dkk1. Dkk1 does not bind to either Wnts or Fzd at all, instead it binds to LRP5/6 with high affinity (Bafico *et al.*, 2001; Mao *et al.*, 2001; Semenov *et al.*, 2001) and to another class of transmembrane molecules, the Kremens (Mao and Niehrs, 2003; Mao *et al.*, 2002). Upon forming a complex with LRP5/6 and Kremen (Krm), Dkk1 (and also Dkk2, Mao *et al.*, 2002) promotes the internalization of LRP preventing LRP5/6 from binding to Wnt, and might also inhibit recruitment of Axin[3] to the plasma membrane resulting in negative regulation of Wnt signalling (Mao *et al.*, 2001). Dickkopf which means "fat head" has been known for its head inducing activity through experiments with Dkk1 in *Xenopus*, zebrafish and mouse embryos. Based on overexpression of Wnts during gastrulation, which leads to microcephaly in *Xenopus* (McGrew *et al.*, 1997) and possibly in mouse (Popperl *et al.*, 1997), it has been suggested that Wnt signalling is capable of inhibiting the Spemann organizer. Dkk1, which is expressed in the anterior endomesoderm of the organizer where head inducing activity exists, is therefore believed to antagonize Wnt activity that inhibits the organizer during head induction. Overexpression of *Dkk1* in *Xenopus* and zebrafish also results in embryos with enlarged heads (Glinka *et al.*, 1998; Hashimoto *et al.*, 2000; Shinya *et al.*, 2000). Additionally, coexpression of *Dkk1* with a dominant-negative mutant of the BMP2/4 receptor is able to induce complete duplication of head structures in *Xenopus* embryos (Glinka *et al.*, 1998). Observation of early mouse embryos with a *Dkk1* null mutation reveals a requirement for the inhibition of Wnt signalling during mouse axis formation

[3] Wnt-activated LRP5 recruits Axin (intercellular antagonist) to the plasma membrane and promotes its degradation, leading to stabilization of ß-catenin (Mao *et al.*, 2001), hence activates canonical Wnt signalling pathway (section 1.2.3.1).

in addition to limb morphogenesis (Mukhopadhyay *et al.*, 2001). Specifically, severe truncation of forebrain and cephalic neural crest-derived head tissues were observed in these mice. Besides these studies, Krm proteins also have been shown to inhibit Wnt activity during early anteroposterior patterning of the Xenopus CNS (Davidson *et al.*, 2002). Taken together, all these findings suggest that Dkk1 acts as a Wnt antagonist and is essential for brain formation. In general the inhibition of Wnt signalling is necessary for proper development in vertebrate. In addition, it is interesting to see whether inhibition of Wnt/β-catenin signalling pathway by Dkk1 is required for induction of apoptosis. Dkk1 is known as a transcriptional target of p53 and is induced by various agents such as ultraviolet (UV) and chemotherapeutic agents lead to DNA damage (Shou *et al.*, 2002).

1.2.3 Different Wnt signalling pathways

Wnt signalling diversifies into three main pathways (Figure 1.4); the classical, canonical Wnt/β-catenin pathway, the Wnt/Calcium (Ca^{2+}) pathway and the planar cell polarity (PCP) pathway (Lustig and Behrens, 2003). Based upon their ability to transform C57MG mammary epithelial cells and to induce secondary axis formation in early Xenopus embryos, Wnts have been classified into two functional groups (*Wnt1* and *Wnt5a*) [reviewed in Yamaguchi, 2001]. Unlike members of the Wnt1 group which when overexpressed are able to transform C57MG and to induce the secondary axis formation, overexpression of each of Wnt5a group members does not transform C57MG cells or induce a secondary axis (Wong *et al.*, 1994; Du *et al.*, 1995). At present, it is still uncertain which Wnt acts through which pathway. Depending on the receptor, it is possible that Wnt can act through

more than one pathway. Nevertheless, members of *Wnt1* class (*Wnt1, -2, -2b, -3, -3a, -6, -7b, -8a and-8b*) are thought to primarily signal through the canonical Wnt/β-catenin pathway (Kemp *et al.,* 2005). Members of *Wnt5a* (*Wnt4, -5a* and *-11*) group may signal through the Wnt/Ca^{2+} pathway that involves protein kinase C (PKC). Interestingly, Wnt7a has been shown to activate both the canonical (Lucas and Salinas, 1997; Caricasole *et al.,* 2003; Hirabayashi *et al.,* 2004) and PCP (Kengaku *et al.,* 1998; Dabdoub *et al.,* 2003; Winn *et al.,* 2005) pathways. Other Wnt genes (*Wnt5b, -7b, -9a, -9b, -10a, -10b* and *-16*) are still unclassified. The major function of the canonical Wnt/β-catenin pathway is to regulate cell fate determination during development (Miller, 2002), whereas the β-catenin-independent pathway primarily involves in modulation of cell movements and cytoskeletal organization (reviewed in Kohn and Moon, 2005).

1.2.3.1 Canonical Wnt/β-Catenin Pathway

The Wnt signalling pathway originally identified as β-catenin-dependent pathway and which now is known as the canonical Wnt/β-catenin pathway has been the most studied. The elevation of cytoplasmic β-catenin protein levels is the hallmark of canonical Wnt signalling activation. In the absence of Wnt, β-catenin is initially phosphorylated by casein kinase Iα (CKIα) (Amit *et al.,* 2002) followed by the serine/threonine kinase glycogen synthase kinase-3β (GSK-3β) (Yost *et al.,* 1996). GSK-3β also phosphorylates Axin and APC[4] (Hart *et al.,* 1998; Kishida *et al.,* 1998) which then act as the scaffolding proteins facilitating the interaction between these kinases and β-catenin. These proteins form a β-catenin destruction complex which allows

[4] Adenomatous Polyposis coli (APC)

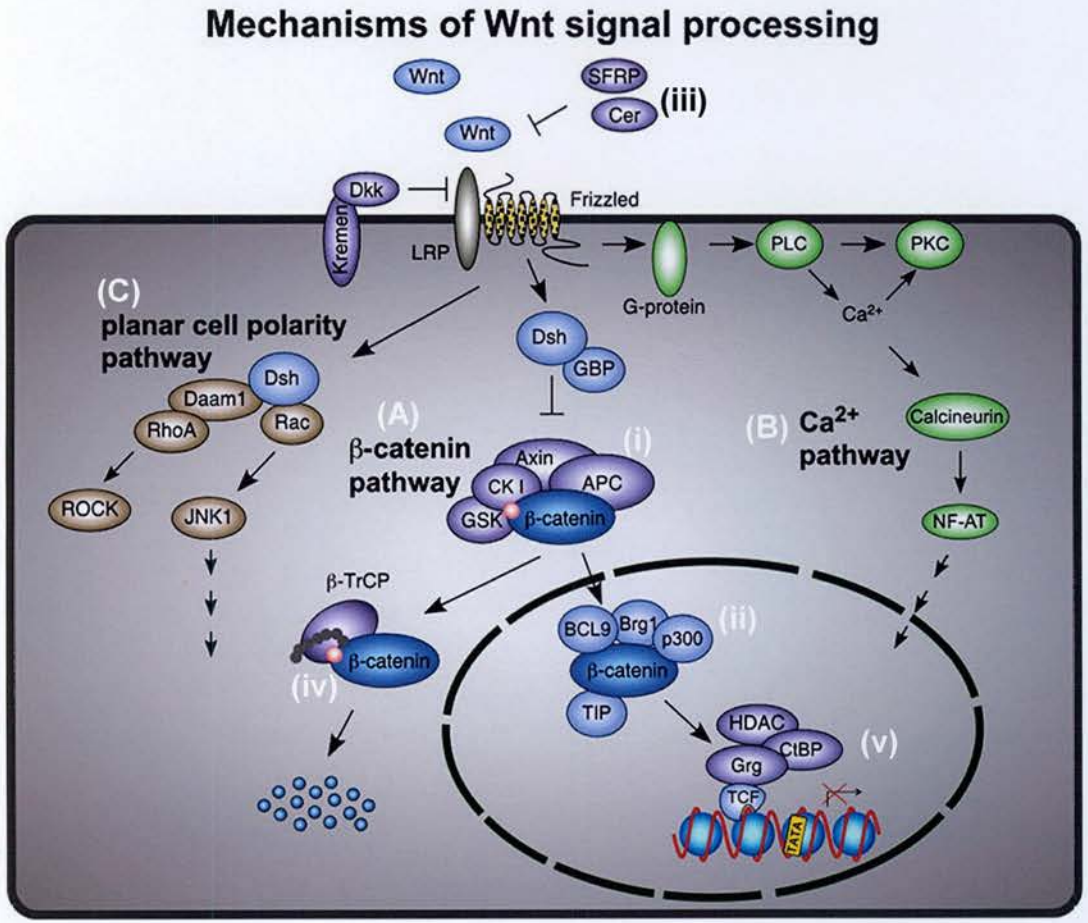

Figure 1.4: Three main Wnt siganlling pathways. A) Canonical Wnt/ß-catenin pathway involves stabilisation of ß-catenin by dissociation of ß-catenin-destruction complex (i) and accumulation of ß-catenin into the nucleus. In the nucleus, it then forms transcriptional activation complex with TCF and CBP/p300 as co-activator (ii) to activate Wnt target genes. Inhibition of Wnt signalling by its antagonists (iii) such as Dkk, sFRP, or Cer leads to phosphorylation of ß-catenin which then recognised by ß-TrCP and degraded by proteosome (iv). In the nucleus, TCF forms repressor complex thus represses activation of Wnt target genes (v). B) Calcium pathway and finally (C) planar cell polarity. Diagram is adapted from http://www.fdm.uni-freiburg.de/SysBio/Bilder/Wnt-signaling-Hecht-800.jpg

phosphorylated β-catenin, especially at positions 33, 37 and 41 by GSK-3β, to be recognized by the E3 ligase β-TrCP (Latres *et al.*, 1999), targeted by ubiquitination (Winston *et al.*, 1999) and degraded by the proteasome (Aberle *et al.*, 1997; Kitagawa *et al.*, 1999).

In the presence of Wnt, degradation of β-catenin is inhibited leading to its nuclear accumulation (Moon and Miller, 1997; Cox *et al.*, 1999; Tolwinski and Wieschaus, 2004; Logan and Nusse, 2004) and activation of target genes through binding to transcription factors T-cell factor (TCF)/lymphoid-enhancing factor (LEF) and co-activators p300 and CBP (cyclic AMP resonse element-binding protein) [Behrens *et al.*, 1996; Molenaar *et al.*, 1996; van de Wetering *et al.*, 1997; Seidensticker and Behrens, 2000]. One of the mechanisms is the phosphorylation of Dshevelled (Dsh), a cytoplasmic scaffold protein, upon formation of ternary complex between Wnt, Fzd and LRPs. Dsh through its interaction with Axin then recruits GSK-3β binding protein, Frat-1/GBP[5], to inhibit GSK-3β activity which could thereby block phosphorylation of β-catenin as well as Axin and APC (Li *et al.*, 1999; Farr *et al.*, 2000; Salic *et al.*, 2000). Alternatively, upon reception of Wnt signal, the ternary complex could trigger the recruitment of Axin, removing it from the destruction complex and promotes stabilization of β-catenin (Cliffe *et al.*, 2003; Tamai *et al.*, 2004). A mutant form of β-catenin that lacks the phosphorylation sites for its degradation is unresponsive to Wnt and can constitutively activate Wnt target genes (Munemitsu *et al.*, 1996; Yost *et al.*, 1996).

[5] Frat-1 (frequently rearranged in T-cell lymphomas) in the mouse and its homolog GBP (GSK3 binding protein) in *Xenopus* (Salic *et al.*, 2000).

In the absence of a Wnt signal, TCF forms a repressor complex with Groucho (Cavallo *et al.*, 1998), which is mediated by interactions with histone deacetylases (HDAC) [Chen *et al.*, 1999]. Once in the nucleus, β-catenin is believed to convert the repressor complex into transcriptional activator complex together with CBP which acts as coactivator (Hecht *et al.*, 2000; Takemaru and Moon, 2000). Similar to its interaction with TCF/LEF, β-catenin also has been shown to interact with other binding partners in the nucleus. One example is its binding to Pitx2 which then leads to conversion of Pitx2 from a transcriptional repressor into an activator (Kioussi *et al.*, 2002). The complexity of the regulation of gene expression by nuclear β-catenin is added by activity of a number of proteins which are controlling Wnt signalling events in the nucleus. These include Chibby, a nuclear antagonist that binds to carboxyl-terminus of β-catenin (Takemaru *et al.*, 2003), and ICAT, a β-catenin-binding protein which blocks the binding of β-catenin to TCF (Tago *et al.*, 2000) and destroys the complexes between β-catenin, LEF and CP/p300 (Daniels and Weis, 2002; Graham *et al.*, 2001).

The important function of TCF/LEF- β-catenin binding complex in activating Wnt signalling target genes is seen in TCF-1/LEF-1 double knock-out mice which result in an early embryonic phenotype that resembles that of the Wnt3a knock-out (Galceran *et al.*, 1999). β-catenin-mediated activation of a Wnt responsive repoter gene which is driven under the control of a promoter that contains multiple TCF/LEF consensus binding motifs upstream from a cFos minimal promoter (TOP, TCF optimal promoter) has been developed. The first TOP to be used which drives activity of luciferase was built by inserting the TOP sequence upstream of a luciferase coding region (TOP-FLASH) in a promoterless vector (Korinek *et al.*, 1997). Wnt1-expressing

C57MG cells transiently-transfected with TOPFLASH have been shown to increase luciferase activity indicating the activation of TCF reporter construct in response to Wnt signal as opposed to the cells transiently transfected with a mutated version of TOP, FOPLASH, which did not increase the activity of luciferase (Korinek *et al.*, 1998). However, TOPFLASH only measures the activity of luciferase from the whole population of cells, but not the specific cells, that respond to Wnt signals. Consequently, many other TOP derivatives such as TOP-Galactosidase (TOP-GAL, Das-Gupta and Fuchs, 1999), ß-catenin activated transcription-galactosidase (BAT-GAL, Maretto *et al.*, 2003), TOP-RED (Megason and McMahon, 2002) and TOP-destabilized green fluorescent protein (TOP-dGFP, Dorsky and Moon, 2002) which allow direct visualization of the cells that are responding to Wnt signals were established. These reporter gene constructs therefore would be useful in detecting the cells that are responding to Wnt signals in a specific population of cells at specific time during development.

1.2.3.2 Wnt/Ca^{2+} Pathway

Calcium was first discovered as a second messenger in Wnt signalling pathway when injection of *Wnt5a* (Slusarski *et al.*, 1997) or *Wnt11* (Westfall *et al.*, 2003) mRNA into 1-cell zebrafish embryo increased the frequency of calcium transients in the enveloping layer of the blastodisc. Based on studies with overexpression of *Wnt5a* and *-11* in *Xenopus* (Shedahl *et al.*, 1999; Kuhl *et al.*, 2000), elevation of intracellular calcium activates calcium-sensitive proteins, calcium/calmodulin-dependent kinase II (CamKII) and protein kinase C (PKC), most probably via frizzled receptor, and Knypek and Ror2 (reviewed in Kohn and Moon, 2005). The pathway, however, is not well-elaborated, and it is not clear whether this pathway is conserved in

mammals, even though the pathway can counteract the canonical pathway (Yamaguchi, 2001; Lustig and Behrens, 2003).

1.2.3.3 Planar Cell polarity Pathway

The last pathway, the planar cell polarity pathway does not directly lead transcription of target genes but instead involves small GTPases such as RhoA and Cdc42 and Jun Kinase (JNK) and controls cytoskeletal rearrangements by regulating cell motility, shape and polarity (Veeman *et al.*, 2003; reviewed in Kohn and Moon, 2005). Its main role is the temporal and spatial control of embryonic development, as exemplified in the polar arrangement of cuticular hairs in Drosophila or the convergent-extension movements in Xenopus where intercalation of mesenchymal and neuroectodermal cells along anterior-posterior (A-P) axis results in elongation and narrowing of embryo and neural plate during gastrulation (Heisenberg *et al.*, 2000; Wallingford *et al.*, 2000; Lustig and Behrens, 2003). It is uncertain whether there is a relationship between this pathway and the Wnt/Ca^{2+} pathway (Yamaguchi, 2001).

1.3 Brief overview of vertebrate Central Nervous System (CNS) development

The central nervous system (CNS) develops through a series of rather complicated steps. The first step is the specification of neuroepithelium from ectoderm cells through a process known as neural induction, which also requires an inductive interaction with nascent mesoderm and endoderm. Ectodermal cells appear during gastrulation stage together with mesodermal and endodermal cells, forming the three primary germ layers (Figure 1.1). In the mouse, gastrulation begins at E6.5 with the formation of the primitive

streak (PS) at the posterior end of the embryo which lengthens towards the anterior end as the gastrulation proceeds. Before this, around E6.0, distal visceral endoderm cells migrate anteriorly and form the anterior visceral endoderm (AVE). Signals secreted by the AVE and newly formed anterior PS induce anterior structures in the presumptive neural ectoderm (review in Sasai and De Robertis, 1997; Yamaguchi *et al.*, 2001; Stern, 2005).

Neural ectoderm is a derivative of ectoderm which is formed as a result of neural induction process and neurulation. Neuralution is a process where neural plate, which is induced by the underlying notochord, folds along the craniocaudal axis forming a hollow neural tube (Figure 1.5). Formation of the neural tube results in ectodermal derivatives; skin ectoderm which gives rise to epidermis and epidermal derivatives such as hair, glands and nails, neural crest ectoderm that lead to formation of the peripheral nervous system (PNS) including various types of nerves, ganglia and receptors, and finally the neural ectoderm which gives rise to the central nervous system containing neurons, oligodendrocytes and astrocytes (Figure 1.5). Induction of neural tissue as opposed to epidermal tissues is believed to be responsibility of an organiser; the Spemann organiser (dorsal lip of the amphibian, blastopore in zebrafish) or Hensen's node as in birds and mammals (Spemann and Mangold, 1924; reviewed in Stern *et al.*, 2001) also known as the default model. According to this model, secreted factors of the bone morphogenetic protein (BMP) family functions as neural inhibitors and epidermal inducers. The organiser thus secrets BMP antagonists to antagonise BMP activity and signals nearby cells to become nervous system, while cells further away that do not receive these signals develop into skin (Hawley *et al.*, 1995; Wilson and Hemmati-Brivanlou, 1995). However,

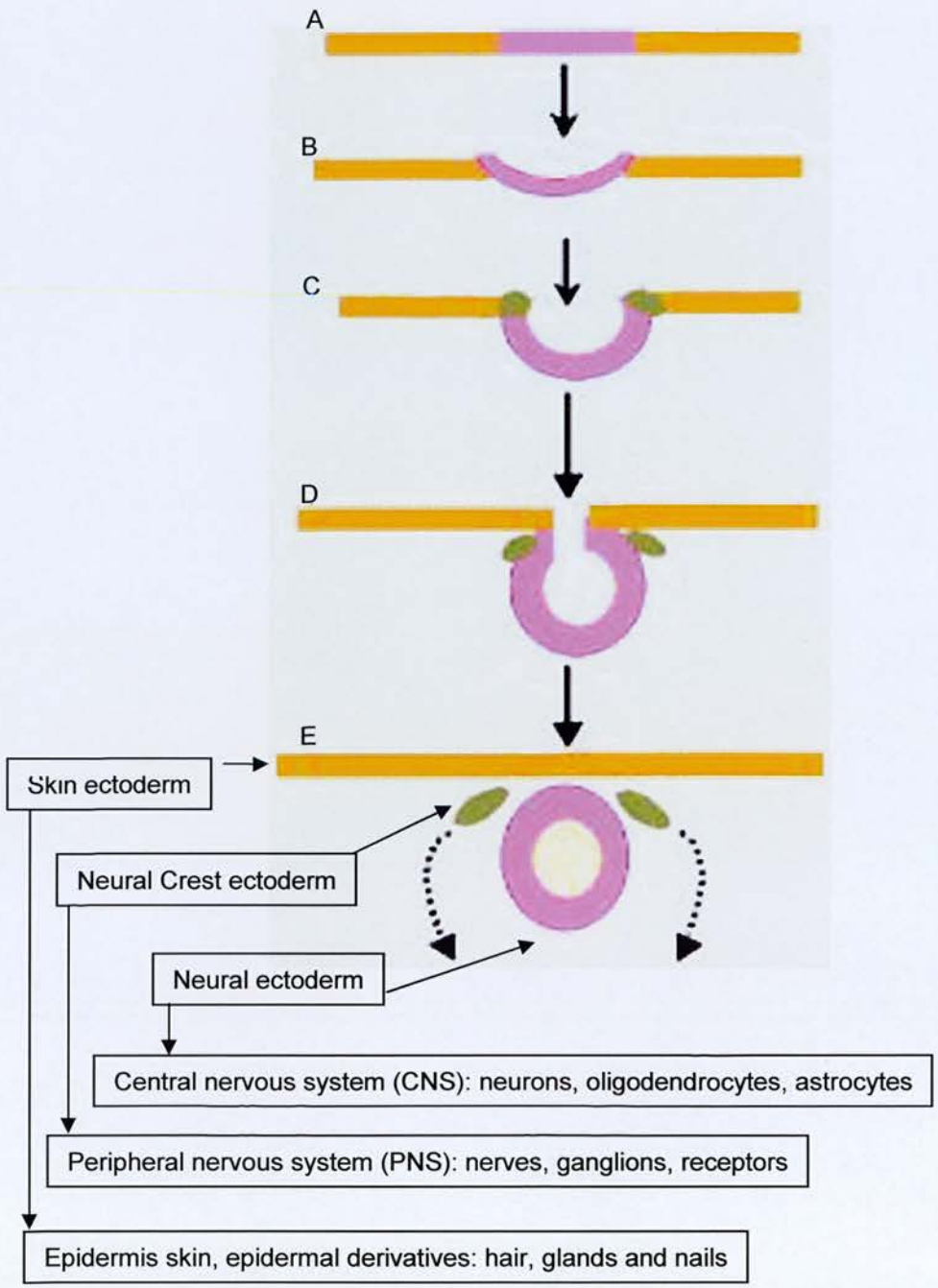

Figure 1.5: Formation of neural tube begins with induction of neural plate by underlying notocord (A). Then the neural plate begins to fold converting it to a neural groove (B), which deepens and forms a neural tube (C). Subsequently two masses of ectoderm at the edges of the neural plate form neural crest (C,D) which later separate neural ectoderm and skin ectoderm (E). Skin ectoderm, Neural crest ectoderm and neural ectoderm then gives rise to epidermis and epidermal derivatives, the PNS and the CNS, respectively. Diagram and legends are adapted and modified from Professor A. Cuschieri at http://staff.um.edu.mt/acusl/fourthweek.htm.

studies with chick embryos and some amphibians suggest that induction by this organiser only presents the earliest inductive events and that neural induction may involve rather more complex steps (Stern, 2001).

The second step in development of the CNS involves patterning of neural tube along the anterior-posterior (A-P) axis. At least three interesting models have been proposed for neural induction and regulation of neural tube patterning process. Mangold (1933) proposed the existence of several distinct organisers for the head, trunk and tail. However these organisers cannot induce neural fate by itself as demonstrated in experiments with chicks (Tam and Steiner, 1999; Foley *et al.*, 2000). Additionally, in the activation-transformation model, Nieuwkoop *et al.* (1952) proposed double-gradient stages for the regulation of neural tube patterning. Initial induction (activation) stage underlined by BMP antagonists produced nervous system with rostral (anterior) character followed by activity of posteriorizing molecules (transforming) that gradually generated more caudal (posterior) region (reviewed by Ciani and Salinas, 2005). However, various experiments conducted within the last five decades never really agreed with either of these two models. Recently, studies by Stern (2001, 2004) proposed a model that reconciles the classical models on how the neuraxis is patterned. They believe that an initial event similar to the activation step of Nieuwkoop's is required for induction of unstable expression of early neural markers such as Sox3 and Otx2, but required additional signal(s) for stabilisation of anterior neural development followed by a set of third signals, equivalent to Nieuwkoop's transformation step for formation of posterior axis.

As mentioned above, the AVE participates in the formation of the A-P axis even before gastrulation and later during gastrulation specifies anterior neural ectoderm. In addition, several families of secreted signalling molecules have been implicated in the process, in particular members of Wnt and TGF-ß/BMP families. While inhibition of BMP signalling leads to the formation of neural tissues, inhibition of both Wnt and BMP signals (Figure 1.6) are required for anterior neural patterning (Niehrs, 1999). Interestingly, posterior neural patterning depends on three posteriorizing molecules; Wnts (McGrew *et al.*, 1997; Houart *et al.*, 2002; Wilson and Houart, 2004), FGFs (Cox and Hemmati-Brivanlou, 1995; Pownall *et al.*, 1998) and RA (Durston *et al.*, 1989; Blumberg *et al.*, 1997; Kudoh *et al.*, 2002; Martynoga et al., 2005) in addition to inhibition of BMP (Figure 1.6).

The entire neural tube is divided into four longitudinal divisions; the floor, basal, alar and roof-plates, which enclose a neural canal (Figure 1.6, Rossant and Tam, 2002). Patterning of dorsal-ventral (D-V) axis of neural tube occurs by signalling molecules initially produced by the adjacent ectoderm and axial mesoderm (formed from cells at the anterior primitive streak, Beddington, 1994) and later in the roof and floor plates of the neural tube (reviewed in Campbell, 2003). The patterning of neural tube leads to the formation of three primary brain vesicles, the prosencephalon, mesencephalon and rhombencephalon, and the spinal cord in the neural canal along the entire neural tube (Figure 1.6). The prosencephalon (forebrain) then divides into the telencephalon which gives rise to cerebrum, hippocampus and olfactory lobes, and diencephalon that forms thalamic and hypothalamic regions. Additionally, the mesencephalon (midbrain) gives rise to tectum which

UNIV. EDINBURGH

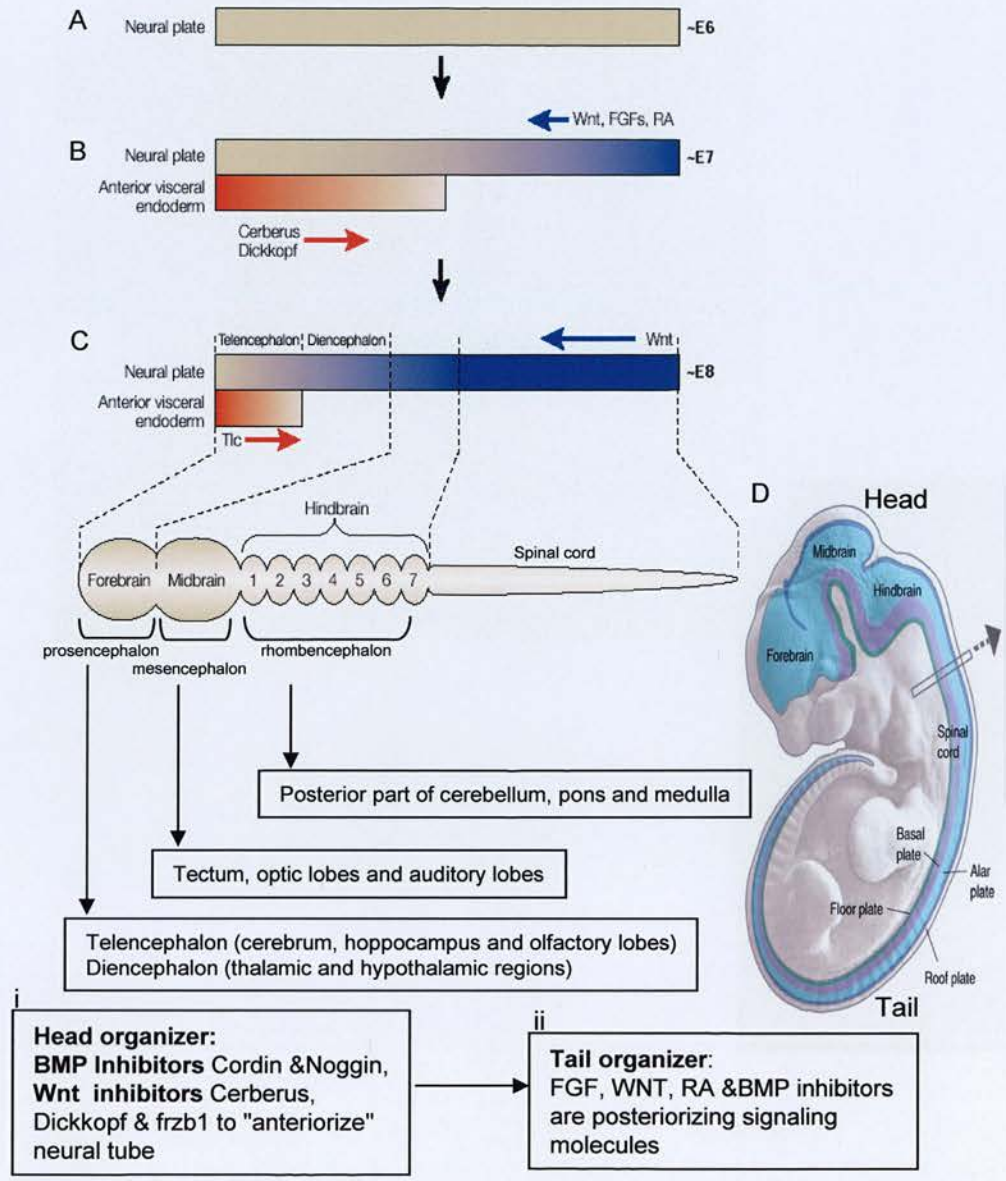

Figure 1.6: Development of the CNS begins with the formation of neural plate when gastrulation starts around E6 (A). At this time, anterior-posterior (head-tail) axis appears with the formation of anterior visceral endoderm (AVE) and anterior primitive streak secreting signals to induce anterior neural development. Anterior CNS formation is induced by anti BMPs and Wnt inhibitors (i), while posterior CNS depends on FGF, Wnt and RA in addition to BMP inhibitors (ii). Around E7, neural plate undergoes a process celled neurulation forming a hollow neural tube (B). Along its entire length the neural tube is subdivided into four longitudinal domains: the floor plate, basal plate, alar plate, and roof plate. Motor neurons are derived from the basal plate (D). Neuralation (around E8) subsequently divides the neural tube into prosencephalon, mesencephalon and rhombencephalon and the spinal cord with each giving rise to regions as described in C. The diagram is adapted from http://www.cvm.tamu.edu/labbott/13.

includes the optic lobes and the auditory lobes, while the rhombencephalon (hindbrain) develops into posterior part of cerebellum, pons and medulla (reviewed by Ciani and Salinas, 2005).

Highly proliferative cells in the ventricular and subventricular zones of the neural tube serve as progenitor cells (neural precursor cells, NPCs) for most different types of neurons such as interneurons and motor neurons (Muroyama *et al.*, 2002, 2004) and cortical neurons (Levers *et al.*, 2001). In the developing mouse brain, NPCs give rise to neurons mostly between E10 and E17 (Qian *et al.*, 2000). A variety of signalling molecules are believed to regulate maintenance and proliferation/differentiation of NPCs (Edlund and Jessell, 1999). Among these, BMPs have been shown to promote neuronal differentiation of cortical ventricular zone precursors (Li *et al.*, 1998b). Notch signalling, FGF2 and epidermal growth factor (EGF) can also maintain neural stem cells in an undifferentiated state (Reynolds and Weiss, 1992; Ohtsuka *et al.*, 2001; Hitoshi *et al.*, 2002). Besides that Wnt signalling also has been shown to promote differentiation of the posterior forebrain and also involved in the formation of dorsal spinal neurons (Lee and Pfaff, 2001; Dickinson *et al.*, 1994). The signalling molecule Sonic Hedgehog (Shh) secreted from the notochord and floor plates has been shown to function as a gradient signal for generation of motor neuron and ventral spinal neurons (Roelink *et al.*, 1995; Tanabe *et al.*, 1995; Ericson *et al.*, 1996; Tanabe and Jessell, 1996; Jessell, 2000). The roof plate, in addition, has been indicated as a major source of inductive signals controlling the generation of dorsal interneurons (Lee and Jessell, 1999). Moreover, expression of secretory proteins of the BMP, FGF and Wnt families has also been detected from cells at the dorsal end of the

neural tube at around the time when the dorsal interneurons are generated (Lee and Jessell, 1999).

The regulation of these signalling molecules is regulated through the expression of various transcription factors which control a number of unique genes to perform different functions during development. These include, Emx2 and Pax6, which help to regulate early regionalisation of neocortex (Muzio *et al.*, 2002), Gli3 expression, which is essential for telencephalon maintenance (Rallu *et al.*, 2002), Foxg1, which is required for the correct projection of thalamocortical tract (Pratt *et al.*, 2002) and a major regulator for telecephalic neurogenesis (Martynoga *et al.*, 2005), and the proneural basic-helix-loop-helix (bHLH) neurogenin (Ngn1 and 2) proteins are needed for neurogenesis of neocortex (Schuurmans et al., 2004). It is therefore important to note that the development of the CNS requires activities and interaction between different sets of player genes ranging from different types of signalling molecule families to different functions of transcription factors. Understanding the mechanisms of each individual player during the development process is essential in order to understand the process itself. The information gained hence would be useful, among many others, in recapitulating the process in ES cells especially for future use of ES cells as a potential source for transplantation replacement therapies. One of the players worth examining is Wnt signalling.

1.4 Wnts and neurogenesis

1.4.1 Developmental Patterning of Wnt Expression in the CNS

A number of RNA expression studies by *in situ* hybridization, quantitative reverse transcription polymerase chain reaction (qRT-PCR) and microarrays have revealed the expression of Wnt genes since the very early stages of

embryogenesis which later demonstrates the central nervous system as the primary region for expression of mouse Wnt genes (Gavin *et al.*, 1990; McMahon *et al.*, 1992a; Parr *et al.*, 1993; Lloyd *et al.*, 2003; Hamatani *et al.*, 2004; Mohamed *et al.*, 2004; Wang *et al.*, 2004; Kemp *et al.*, 2005). Specifically, these studies demonstrate the expression of *Wnt1, -2b, -3, -3a, -4, -5a, -5b, -6, -7a, -7b, 10b* and *-11* at preimplantation stages with highest expression of *Wnt3a, -6, -7a, -9a* and *-10b* in the blastocyst (Kemp *et al.*, 2005). In accordance with this, Wang and co-workers (2004) discovered nuclear localization of ß-catenin in the ICM at this stage, which indicates the probable function of the canonical Wnt/ ß-catenin signalling pathway in the region; most of the Wnt genes expressed in the blastocyst/ICM have been shown to activate the canonical pathway (reviewed in Wodarz and Nusse, 1998). Just before gastrulation, around E6.25, Wnt3 is expressed in the prospective anterior and posterior proximal embryonic ectoderm, after the establishment of AVE (Liu *et al.*, 1999b). Mouse embryos lacking Wnt3 lack primitive streak and display gastrulation defects with no appearance of A-P axis formation and inhibition of neural differentiation (Liu *et al.*, 1999; Yamaguchi *et al.*, 1999). These two studies clearly demonstrate the requirement of a specific Wnt in particular developmental event (Logan and Nusse, 2004). Additionally, TOP-GAL activity was also observed at E6.5-7.0 along the forming primitive streak (Merrill *et al.*, 2004) indicating the presence of canonical Wnt signals. A number of Wnt antagonists such as sFRPs, Dkks and Cerebrus also have been shown to be expressed prior to and during early gastrulation (Belo et al., 1997; Kemp *et al.*, 2005) consistent with the suggestion that subsequent induction of forebrain requires inhibition of Wnt signalling (Huelsken *et al.*, 2000; Mukhopadhyay *et al.*, 2001; Yamaguchi, 2001; Ishikawa *et al.*, 2003). In agreement to this, Ishikawa and colleagues (2003) show that Apc mutant

mouse embryos formed truncated forebrain. Besides that, Wnt signalling also has been shown to inhibit the formation of neuroectoderm and anterior PS as it is observed that *LRP5*$^{+/-}$*LRP6*$^{-/-}$ mouse embryos generate more neuroectoderm and display an expanded anterior PS during gastrulation (Kelly *et al.*, 2004).

During late gastrulation stage, around the time of neural tube closure (E8-8.5), *Wnt7b* and *-3a* RNA are detected in the presumptive diencephalon, anterior to the midbrain-forebrain junction. By E9.5, various expression patterns of Wnt genes are found to encircle the entire neural tube (Parr *et al.*, 1993). At this time, Wnt1 and Wnt3a are detected in dorsal midbrain, Wnt4 and Wnt7b at dorsal forebrain and *Wnt5* and *Wnt7a* at ventral forebrain. Studies by Grove *et al.* (1998) and Lee *et al.* (2000b) also have identified a potential source of patterning signals regulated by multiple Wnt genes (*Wnt2b, -3a, -5a, -7a, -7b and -8b*) expressed in the embryonic medial telencephalon (cortical hem). Their expression in the cortical hem may imply that at least one of the proteins is involved in hippocampal development. Indeed, a loss of the hippocampal region was observed in *Wnt3a* and *LEF1* mutant mice (Lee *et al.*, 2000b; Galceran *et al.*, 1999). Mouse with deletion of ß-catenin in the dorsal telecephalon also formed hippocampal region similar to those observed in *Wnt3a*$^{-/-}$ and *LEF*$^{-/-}$ mutants. In an earlier study, *Wnt5a* transcripts were also demonstrated to be present in the developing CNS, specifically in the ventral portion of the entire midbrain (Gavin *et al.*, 1990).

In addition, Wnt expression is also detected at midbrain-hindbrain boundary (MHB, Parr *et al.*, 1993; Panhuysen *et al.*, 2004)). *Wnt1*, the first Wnt identified, is expressed in the dorsal midline of diencephalon to spinal cord

including the MHB (McMahon *et al.*, 1992b). Loss of Wnt1 activity has been shown to result in deletion of midbrain and dorsal metencephalic structures (McMahon and Bradley, 1990; Thomas and Capecchi, 1990; McMahon *et al.*, 1992). However, no phenotypic abnormalities were observed in the diencephalon, caudal hindbrain and spinal cord of the *Wnt1* mutant mice even though its normal expression has been detected in these regions. Together with *Wnt1*, *Wnt3a* and *-7b* are also expressed in the MHB (Parr *et al.*, 1993; Panhuysen *et al.*, 2004). Interestingly, a wider region of the CNS is affected in *Wnt1/Wnt3a* double knockout compared to when only *Wnt1* or *Wnt3a* is deleted (Ikeya *et al.*, 1997). This case represents several cases where full mutant phenotypes are revealed only when multiple Wnt genes are eliminated (Logan and Nusse, 2004). A similar scenario was observed when downstream Wnt pathway components were deleted. Defects similar to Wnt3a mutants were observed in *LEF1* and *TCF1* mutants but only when both *LEF1* and *TCF1* were eliminated (Galceran *et al.*, 1999). Besides *Wnt1* and *Wnt3a, Wnt5a, -7a* and *-7b* are also expressed in hindbrain region with each expression restricted to its specific subregions (Parr *et al.*, 1993).

Expression of Wnt genes in the spinal cord is a continuation of the expression profiles in the hindbrain which results in emergence of three expression patterns. First, expression of *Wnt1, -3* and *-3a* which are detected in dorsal roof plate region, except for expression of Wnt3 which does not extend into the most posterior region of the spinal cord (Parr *et al.*, 1993). A second pattern of expression was demonstrated by *Wnt5a, -7a* and *-7b* which are expressed in more ventral portions of the spinal cord (Gavin *et al.*, 1990). However, none of these are expressed in the floor plate while expression of *Wnt5a* is restricted to the most anterior part of the spinal cord (Parr *et al.*,

1993). Finally, *Wnt4* is expressed at dorsal domain and the only Wnt gene that is expressed in the floor plate of the spinal cord at this stage, E9.5. The expression patterns of these Wnt genes are observed at the same time that the first spinal cord neurons are born (around E9.5, Nornes and Carry, 1978) which may imply the function of these genes in the specification of neuron types or formation of neuronal connections. Indeed, Muroyama and co-workers (2002) discovered that *Wnt1* and *Wnt3a* proteins are required for proper generation of interneuron subclasses in the spinal cord. Additionally, *Wnt3* expressed in motorneurons regulates terminal arborisation of muscle sensory afferents in the spinal cord demonstrating the role of Wnt protein in the formation of the sensory-motor connections in the mouse spinal cord (Krylova *et al.*, 2002). *Wnt7a* has also been shown to regulate axonal remodelling and presynaptic differentiation of pontine mossy fibers (Hall *et al.*, 2000). Moreover, *Wnt7a* mutant mice also show morphology of delayed maturation of synapses in the cerebellum (Hall *et al.*, 2000). *Wnt4* that is specifically expressed in a rostrocaudal gradient in the floorplate is believed to be involved in axon guidance in commissural axons (Lyuksyutova *et al.*, 2003).

Expression profiles of Wnt genes during the development of CNS clearly suggest the important role of Wnt activity in the process as well as the complexity of Wnt signal transduction mechanisms. Its knockout phenotypes which closely correlate with the expression patterns, very importantly, indicate the requirement of that particular Wnt gene in the specific event during the development (Logan and Nusse, 2004). In addition, the complexity of Wnt signalling is also added by the redundant function of Wnt signalling components (*LEF1*$^{-/-}$ and *TCF1*$^{-/-}$ double mutants, Galceran *et*

al., 1999) as well as by the activity of different Wnt genes (*Wnt1*$^{-/-}$ and *Wnt3a*$^{-/-}$ double mutants, Ikeya *et al.*, 1997; McMahon *et al.*, 1992b). Promiscuous Wnt/Fzd interactions as well as activation of at least three different pathways also add up to the complexity of Wnt signalling. Wnt also forms gradients which through direct or indirect interaction with other secreted signalling molecules and transcription factors regulate the expression of target genes in a concentration-dependent manner (Wodarz and Nusse, 1998). Nevertheless, Wnt signalling has been seen to be involved in controlling the initial formation of neural plate and many subsequent patterning decisions in the embryonic nervous system, dorsal-ventral (Megason and McMahon, 2002; Saint-Jeannet *et al.*, 1997) and anterior-posterior (McMahon and Bradley, 1990) patterning of the CNS as well as axon guidance and synapse formation (reviewed in Ille and Sommer, 2005). Specifically, it is reasonable to believe that one of the main functions of Wnt signalling in the development of CNS is to regulate cell fate decision; between promoting cell proliferation or differentiation.

1.4.2 Multiple roles of Wnt signalling during CNS Development

A balance between proliferation and differentiation rate of progenitors/neural stem cells is essential for proper development of the CNS. Unfortunately, due to overlapping and redundant functions of individual Wnt genes besides being difficult to be isolated in active form proteins, understanding the roles of Wnt signalling in mouse neural development *in vivo* mostly comes from transgenic mice overexpressing downstream Wnt signalling pathway components, specifically ß-catenin or APC (Chenn and Walsh, 2002; Kielman *et al.*, 2002; Zechner *et al.*, 2003; Israsena *et al.*, 2004; Backman *et al.*, 2005). As it is believed that the components of the Wnt

pathway may be involved in promoting proliferation of primitive cells in the human skin (Zhu and Watt, 1999) and the mouse gut (Korinek *et al.*, 1998), the components also have been indicated through regulation of Wnt signalling to be involved in proliferation of progenitors/neural stem cells in the mouse brain (Chenn and Walsh, 2002).

In vitro and *in vivo* studies of neural stem cells, specifically, have implicated the role of Wnt signalling in regulating proliferation or differentiation of these cells (reviewed by Patapoutian and Reichardt, 2000; Kleber and Sommer, 2004). Transgenic mice overexpressing a stabilized form of ß-catenin in neural progenitors (under the control of nestin enhancer) increased the number of progenitor cells and decreased neuronal differentiation, which resulted in massive enlargement of the cerebral cortex (Chenn and Walsh, 2002, 2003; Zechner *et al.*, 2003). On the contrary, retroviruses overexpressing ß-catenin in NPCs isolated from mouse E14 cortex produced increased number of neurons upon withdrawal of FGF2 even though in the presence of this mitogenic stimulus the NPCs produced high number of neurospheres (Israsena *et al.*, 2004). Even though there was a concern raised against the use of FGF2 that led to the different roles of ß-catenin between these two studies; in promoting proliferation and also differentiation of cortical cells. However, it is believed that the difference is most likely due to the timing at which the stabilized form of ß-catenin is expressed (Hirabayashi *et al.*, 2004). Similar to the study by Israsena and colleagues, a study by Hirabayashi *et al.* (2004) also revealed that a stabilized form of ß-catenin promoted neuronal differentiation of cortical NPCs harvested from E11.5 neocortex. The difference between these studies compared to that of Chenn and Walsh (2002) is that the ectopic expression of the stabilized form of ß-catenin in the

earliest study was activated at around E8.5 as activation of nestin enhancer is known to be at around E8.5. Therefore these studies strongly suggest that the response of NPCs to Wnt signalling, in particular the canonical Wnt/ ß-catenin pathway is stage dependent; exposure of NPCs to Wnt signalling at early stage increases proliferation of NPCs but also promotes the formation of neurons upon exposure to Wnt activity at the late stage during development.

Many other studies also exhibit the same phenomena. In an *ex vivo* study, Viti and co-workers (2003) also show that cell proliferation of neural progenitors from E10.5-13.5 mouse forebrain (dorsolateral cortex) transfected with a retrovirus expressing HA-tagged *Wnt3a, -7a* or *-7b* increased while delaying the differentiation of these cells into neurons. When the viruses expressing Wnt7a-HA were injected into the lateral ventricles of E10.5 mice, more progenitors were diverted to subventricular zone (SVZ) instead of differentiating into neurons as normal. Interestingly, they also discovered that Wnt7a did not enhance proliferation when the progenitors were infected at later stage, E16. Their studies clearly demonstrate that Wnt is able to promote proliferation of early cortical progenitor cells *in vivo* and *in vitro.* Additionally, Hirabayashi and colleagues (2004) also demonstrated that inhibition of Wnt signalling results in reducing number of neurons when NPCs were infected with a retrovirus expressing Axin and that retrovirus-mediated expression of Wnt7a in dorsal cerebral cortex at late stage promotes the formation of neurons. In another study, treatment of Wnt3a conditioned medium (CM) onto neural stem cells isolated from E11.5 mouse embryos inhibits the formation of neurospheres but promoted and enhanced neuronal differentiation of these forebrain neurospheres when treated with Wnt3a CM

at late stages (Muroyama *et al.*, 2002, 2004) and also increased self-renewal activity of neurospheres from ganglionic eminence (Israsena *et al.*, 2004). The absence of hippocampus region in Wnt3a mutant mice also implies the involvement of Wnt3a-mediated proliferation in the specification of hippocampal cell fate (Lee *et al.*, 2002). In further analysing the Wnt3a mutant mouse, the authors discovered that Wnt3a regulates the proliferative expansion of caudomedial cortical progenitor cells at E10.5. These studies therefore obviously imply the importance role of Wnt signalling in maintenance, proliferation and differentiation of forebrain progenitor cells *in vivo* and *in vitro*.

The effect of Wnt signalling on the proliferation and differentiation of progenitors is also observed in the midbrain. Studies by Castelo-Branco *et al.* (2003), demonstrate that treatment of Wnt1-HA or Wnt3a-HA CM increases the proliferation of dopaminergic precursor cells obtained from ventral midbrain (VM) precursors, while treatment with Wnt5a-HA CM increases differentiation of these precursors into dopaminergic neurons (DA). The authors also discovered that treatment with Wnt1-HA CM on the VM cells increased the number of both DA and non-DA VM neurons. Similar result was also obtained in a recent study when rat VM E14.5 precursor cultures were treated with purified Wnt5a-HA (Schulte *et al.*, 2005); Wnt5a promotes differentiation of dopaminergic precursors into DA neurons at midbrain region. Wnt signalling also has been shown to strictly regulate cell proliferation of progenitor cells in the mid/hindbrain boundary (MHB) region in a spatiotemporal manner which is essential in maintaining the MHB region (McMahon and Bradley, 1990; Thomas and Capecchi, 1990; Panhuysen *et al.*, 2004). Overexpression of *Wnt1* in mouse embryos under

control of the engrailed (En1) promoter from E8.5 of embryonic development strongly increases the proliferation of neural progenitors in the dorsal region but not in the ventral region of MHB (Panhuysen *et al.*, 2004). Ectopic expression of Wnt1 under a control of the Hoxb-4 region A enhancer also increased the proliferation of spinal cord precursor cells when analysed at E10.5 and E12.5 (Dickinson *et al.*, 1994).

These studies undeniably suggest the important roles of Wnt signalling in cell fate specification for forebrain, midbrain, hindbrain and spinal cord regions for proper development of the CNS. The different roles played by this complex signalling pathway highly depend on the cellular contexts and very stage specific. Based on these studies, it is reasonable to suggest that early exposure to Wnt signals promotes the proliferation rate of neural precursor cells while the formation of neurons seems to be enhanced upon exposure to Wnt signals at late stages during development. Nevertheless, it is worth noting that constitutive overexpression of genes leading to continuous activation of Wnt signalling pathway seem to inhibit the formation of neural lineages.

1.5 Wnts and neural Differentiation of ES cells *in vitro*

To date, not many studies have been carried out to unravel the roles of Wnt signalling during neural differentiation of mouse ES cells in culture. In an effort to identify genes that could play a role in the commitment or specification of neural lineage in ES cells, Aubert and colleagues (2002), by using microarray technique, identified the Wnt antagonist sFRP2 as a major unregulated gene during neural differentiation. When functionally evaluated, using an episomal expression technology, they discovered that

overexpression of sFRP2 enhances neural development of ES cells in culture, implying the inhibitory effect of Wnt activity to neural differentiation process. To further examine the effect of Wnt signalling during the process, they used *Wnt1*-overexpressing ES cells and also lithium chloride treatment, which partially mimics Wnt signalling by inhibiting the activity of GSK-3ß. Results from both experiments showed that Wnt activity suppressed neural differentiation.

A study by Kielman *et al.* (2002) also showed that ES cells lacking APC were unable to differentiate into neural lineages. In addition, inhibition of neural differentiation was also observed from APC-deficient and stably transfected dominant active ß-catenin ES cells (Heagele *et al.*, 2003). In the study, both of these ES cell lines activated Wnt signalling target genes suggesting modulation of Wnt signals in the differentiation of ES cells. Interestingly, a recent study by Watanabe *et al.* (2005) demonstrated that treatment with Wnt3*a* at late culture stages in neural differentiation process increased the number of neural cells, while exposure to Wnt3*a* at the early culture stages strongly suppressed neural conversion. Another study by Schmidt and colleagues (2001) also suggested a specific influence of lithium chloride on neuronal differentiation. The study discovered that upon treatment with LiCl, mRNA expression of Mash and En1 were decreased while mRNA levels of neuron-specific genes such as synaptophysin and neurofilament, NFM, were increased, implying that Wnt signalling inhibits the formation of NPCs but also promotes differentiation into neurons. These studies are also supported by a recent study by Otero *et al.* (2004) which demonstrates that an increase in ß-catenin signalling by treatment with Wnt3a CM or overexpression of ß-catenin induces neuronal lineage commitment.

Therefore, these studies indicate that Wnt signalling also affect neuronal differentiation of ES cells *in vitro*.

Taken together, these studies seem to suggest that Wnt signalling inhibits the formation of neural precursor cells, and also stimulates the differentiation of these cells into neurons. Thus, Wnt activity appears to be stage-dependent, which depends on the cell-intrinsic properties at a particular point during neural differentiation process. Therefore, it would be interesting to monitor the effect of stimulating or inhibiting the activity of Wnt signal at different stages during neural differentiation of mouse ES cells *in vitro*.

1.6 Conditional Gene Expression System

One major drawback toward understanding the mechanisms underlying the control of self-renewal and differentiation of ES cells is the lack of an inducible expression system that would allow overexpression of certain gene of interest to be turned on in undifferentiated as well as their differentiated derivatives both *in vivo* and *in vitro* (Vallier *et al.*, 2000). The system not only provides an invaluable tool that overcomes the lethality problem with constitutive expression of knockouts but also gives us the ability to tightly control gene expression in a temporal-, spatial- and tissue-specific manner. In other words, it would be useful to have a system that could control the timing of transgene expression, avoid the problem with transgene extinction, for example, during differentiation and also any toxicity problem upon constitutive overexpression of a transgene. This type of control can be accomplished using binary transgenic systems, which fall into two categories. One of the categories uses an effector that transactivates transcription of the transgene and is normally used to activate transgene in

gain-of-function experiments. The second uses an effector which is a site-specific DNA recombinase that rearranges the transgene and is normally used to activate or silent target gene (reviewed in Lewandoski, 2001; Van der Weyden *et al.*, 2002). For the purpose of this study, only the site-specific DNA recombination category will be described.

1.6.1 Site-specific DNA Recombination

The conditional gene expression by site-specific recombination system is composed of a recombinase enzyme and its target sequence, which, depending on the orientation and location of the target sequence, allows for the deletion, insertion, inversion or translocation of specific regions of DNA. Presently, two members of the λ-integrase family, Cre, (cause recombination) from bacteriophage P1 (Sauer and Henderson, 1989) and Flp, from *Saccharomyces cerevisiae* (O'Gorman *et al.*, 1991), have been used in this system. Cre and Flp recombinases catalyse a DNA recombination event between two 34-bp recognition sites known as *loxP* and *FRT*, respectively. Cre appears to be more effective in recombining a transgene array *in vitro* and *in vivo* than Flp (Ringrose *et al.*, 1998), and Cre/*loxP* has been the most widely used site-specific DNA recombinase system in both ES cells and mice (Van der Weyden *et al.*, 2002). The system is known for its simplicity, no loss of gain of nucleotides after recombination, small 34-bp target site (*loxP*) which does not affect adjacent genes in the chromosome, long distance function and function in a wide range of cell types. However, Cre recombinase can also cause chromosomal rearrangements or aberrations (Loonstra *et al.*, 2001).

Chemically inducible forms of Cre have been used in order to create spatiotemporally controlled transgene expression. Tamoxifen-dependent Cre-mediated recombination which uses the ligand-binding domain of mutated human estrogen receptor, ER^T and ER^{T2}, fused to Cre (Cre-ER^T and Cre-ER^{T2}) is often used. Cre is activated upon exposure to tamoxifen or synthetic estrogen, 4-hydroxytamoxifen (4-OHT, Feil *et al.*, 1996, 1997; Indra *et al.*, 1999). Cre-ER^{T2} recombinase is more sensitive to 4'-OHT than the original Cre-ER^T (Feil *et al.*, 1996; Indra *et al.*, 1999).

1.6.2 Inducible expression of Wnts

Dramatic phenotypes ranging from embryonic lethality and CNS abnormalities to kidney and limb defects were observed in vertebrates with loss of a single Wnt gene (review in Logan and Nusse, 2004). An inducible expression system, therefore, would be useful in order to circumvent the problem with lethality from constitutive deactivation or even constitutive overexpression of a particular Wnt gene. However, few studies, looking for the function of Wnts in neural development have used the system. As far as this study is concerned, to date, very few studies have ever described the use of conditional transgenic mice embryos overexpressing Wnt gene to study a specific Wnt function at a particular time during development of the CNS. Only tissue-specific and no temporally controlled of transgenic expression has been described. A recent study by a group of researchers in Germany has managed to generate transgenic mouse embryos ectopically expressing *Wnt1* under the control of En1 promoter using a conditional knock-in approach ($En1^{+/Wnt1}$, Panhuysen *et al.*, 2004). Dickinson and co-workers (1994) used transgenic mouse embryos overexpressing Wnt1 under the control of

the Hoxb-4[6] Region A enhancer. Conditional expression of a stabilized form of ß-catenin under a control of nestin promoter also has been described by Backman *et al.*, 2005.

Similarly, when looking for the roles of Wnt signalling during neural differentiation of ES cells, most of the studies have either used constitutive overexpression or deactivation of a specific gene of interest (Aubert et al., 2002; Kielman et al., 2002; Haegele et al., 2003; Otero et al., 2004). A system that gives us the ability to tighly control transgene expression in temporally-controlled manner during neural differentiation of ES cells in culture condition, therefore, would be useful in avoiding the problem with Wnt toxicity besides circumventing the effect of conditioned medium underscoring the function of Wnt protein if Wnt conditioned medium were to be used. Unfortunately, few of the existing inducible systems designed test for inducible expression restricted to both undifferentiated and differentiated derivative of ES cells *in vitro*. An interferon-based conditional expression of the chloramphenicol aceyltransferase (CAT) gene has been successfully regulated in undifferentiated ES cells. However, the interferon-mediated CAT expression in the differentiated-derivatives of ES cells *in vitro* was not tested (Whyatt *et al.*, 1993). In another study, tamoxifen-dependent Cre-mediated recombination has also been shown to activate a stably integrated lacZ reporter gene in ES cells. Again, only undifferentiated ES cells were tested for tamoxifen-mediated expression of lacZ (Zhang *et al.*, 1996). In addition, high dose of tamoxifen, which far exceeded the threshold above which tamoxifen becomes detrimental to cell growth (Danielian *et al.*, 1998), was required to induce the expression in the study in addition to

[6] The gene is expressed in proliferating NPCs (ventricular zone) of the hindbrain and spinal cord (Dickinson *et al.*, 1994)

strong background expression. One study reported tightly controlled expression of the Oct3/4 transgene driven under a tetracycline-regulated transactivator, tTA, which in responding to low dosed of tetracycline induced the expression of the transgene in undifferentiated ES cells (Niwa *et al.*, 2000). The study also, since only interested in analysing the effect of Oct3/4 in pluripotent cells, reported no induction of the transgene in differentiated ES cells.

A study by Vallier *et al.* (2001) has successfully managed to develop a conditional gene expression system that allows an expression of human-alkaline phosphatase (hAP) to be tighly controlled both in undifferentiated as well as differentiated ES cells *in vitro* and also *in vivo*. Transgene expression in the study was tightly controlled in response to a nondetrimental dose of tamoxifen. The study thus provides an invaluable approach in inducing ectopic expression of gene during differentiation of ES cells directed to various lineages. Hence allowing for a variety of gene functional analyses to be carried out in efforts to understand the mechanisms behind differentiation process of ES cells.

1.7 AIMS

Previous *in vivo* and *in vitro* studies have strongly suggested the important roles of Wnt signalling during neural development. A few studies using ES cells also seem to imply that Wnt inhibits the differentiation of ES cells into NPCs, and, at later stage, promotes the differentiation of these precursors into neurons. Using an invaluable system that allows the analysis of gene

function to be carried out in a more simplified environment, ES cells, this study therefore was conducted in order to unravel the roles of Wnt signalling during neural development *in vitro* with a focus to the hypothesis that Wnt signalling may inhibit differentiation of ES cells into NPCs, and may also stimulate the differentiation of NPCs into neurons. The general aims of this thesis are as follows:

1) **To examine the expression profiles of all 19 mouse Wnt genes and two Wnt antagonists during neural differentiation of ES cells.**

2) **To generate and characterise inducible and reporter gene expression systems in ES cells**

3) **To analyse the effect of overexpressing Wnt and Wnt antagonist at particular time points during neural differentiation of ES cells**

Chapter 2: Materials and Methods

2.1 Materials

2.1.1 Suppliers and equipment

All chemicals used were of analytical, molecular biology or tissue culture grade, where appropriate, and were supplied by Sigma, Merck or Fisher Scientific unless otherwise stated. Electrophoresis grade agarose was from Flowgen (Seakem LE agarose). Restriction and modifying enzymes were from Roche Molecular Biochemicals or New England Biolabs. All primers were synthesized by MWG Biotech AG.

All centrifugations using 1.5 ml and 0.2 ml tubes were carried out using bench-top centrifuge Biofuge Pico (Heraeus) at room temperature (RT) or Biofuge Fresco at 4°C. Centrifugations using 20 ml universal bottle for tissue culture were carried out using Biofuge Primo at 1000 rpm at RT for 5 minutes.

2.1.2 Solutions

Solutions used:

Name	Contents
1X PBS	2.67 mM KCl, 1.47 mM KH_2PO_4, 137.93 mM NaCl, 8.06 mM Na_2HPO_4-$7H_2O$
1X TBE	0.1 M Tris Borate, 0.02 M EDTA
1X TBS	100 mM Tris base, pH 7.5, 150 mM NaCl
1X TBS-T	1X TBS, 0.1% Tween-20

2X YT broth	1.6% Tryptone, 1% yeast extract, 0.5% NaCl; autoclaved at 121°C for 20 minutes
4% PFA	50 mM NaOH, 4% paraformaldehyde in 1X PBS. Heat to dissolve at 55°C, stored aliquots at -20°C.
Ampicillin	100 mg/ml in double distilled water, sterile filter (0.22 μm, Nalgene)
EBM	ESM without LIF
ESM	1X GMEM (BHK-21, Gibco), 10% (v/v) Foetal calf serum (Gibco), 1% MEM non-essential amino acids (Gibco), 1 mM sodium pyruvate (Gibco), 0.1 mM 2-mercaptoethanol (Gibco), 2 mM L-glutamine (Gibco), LIF 100U/ml Human recombinant Leukaemia inhibitory factor (LIF) was made in house by Mrs Rowena Smith by transfection of COS-7 cells with an expression plasmid harbouring the human LIF construct.
HEK-M	RPMI 1640 medium (Gibco), 10% (v/v) foetal calf serum (FCS, Gibco), 20 mM L-Glutamine (Gibco), 20 U/ml Penicillin (Gibco), 20 mg/ml streptomycin (Gibco)
Immuno-blocking solution	0.3% BSA, 1% appropriate serum, 0.1% Tween-20 in 1X PBS, sterile filter (0.22 μm, Nalgene)
LB/2x YT agar	1.5% agar (w/v) in appropriate broth; autoclaved at 121°C for 20 minutes
Luria-Bertani (LB) broth	1% (w/v)Tryptone, 0.5% (w/v)yeast extract, 0.5% (w/v) NaCl; autoclaved at 121°C for 20 minutes

Mowiol	2.4g Mowiol (Calbiochem Cat no 475904), 4.76 ml Glycerol (Fisher Scientific) and 12 ml ddH$_2$O-mixed overnight at RT. 12ml of 0.2M Tris (ph8.5) was added and heated at 50°C for 1-2 hours. The solution was spun at 2000 rpm for 15 minutes. Finally, 2.5 % of antifade [1,4-diazobicyclooctane (DABCO) Sigma] was added. Store in aliquots at -20°C.
Protein-lysis buffer	TENT buffer with 1.0 μg/ml Aprotinin, 1.0 μM Leupeptin, 2.0 μM Pepstatin, 1 μg/ml Pefabloc (Calbiochem)
Orange loading dye	50% glycerol, 2 mM EDTA, few grains of orange G dye in double distilled water
PBSG	5% goat serum in 1X PBS
Permeabilisation solution	1% Triton-X100 in 1X PBS
TE	10 Mm Tris-HCl, 1 mM EDTA, pH 7.4
TENT buffer	20 mM Tris pH 8, 2 mM EDTA, 150 mM NaCl, 1% Triton-X100
Western-transfer buffer	20% methanol, 0.1 M glycine, 0.01M Tris-base in double distilled water or 20% methanol in 1X transfer buffer (NP0006, Invitrogen)
Western blot-blocking buffer	10% (w/v) skimmed milk (Marvel) in 1X TBS-T

2.2 Cell culture techniques

2.2.1 ES Cell lines

All ES cell lines used were obtained from Institute for Stem Cell Research, University of Edinburgh. Background information on the cell lines is described in later chapters of this thesis. Among the cell lines used were 46C

ES cell line, a *Sox1*-GFP knock-in reporter ES cell line (Aubert *et al.*, 2003), and R26CT2S cell line, a Cre-expressing cell line (Grotewold, unpublished). 46C was used in screening for the Wnt expression profiles during neural differentiation process, and was also used for transfection with TOP-Red2 construct for determination of specific cells that were responding to the Wnt signalling during the process (more details are described in Chapter 3 and 4 of this thesis).

2.2.2 Other mammalian cell line

The only other cell line used was human embryonic kidney (HEK 293) cells obtained from European Cell Culture Collection. This cell line was used to test the functionality of a plasmid construct that was built, TOP-Red2 prior to transfecting the construct into an appropriate ES cell line.

2.2.3 Routine work

Sterile conditions according to Class II procedures were applied during maintainance of all cell lines. Culture wastes and glassware were soaked and washed in 5% Virkon after use. The wastes were then autoclaved at 121°C for 20 minutes prior to disposal.

2.2.3.1 Pre-coating plate

2.2.3.1.1 Gelatin

Plates or flasks for growing embryonic stem (ES) cells were pre-coated with pre-warmed 0.1% gelatin (Sigma) in 1X PBS for at least 10 minutes at room temperature. The excess gelatin was pipetted out prior to plating the cells.

2.2.3.1.2 PDL/laminin

Plates and glass chamber slides used to grow dissociated embryoid bodies (EBs) for the formation of neural precursor and neuron-like cells were pre-coated with 10 μg/ml of poly-D-lysine (PDL, Sigma) or 2 μg/ml of laminin (Sigma), in 1X PBS. They were coated with PDL for at least 20 minutes at room temperature, washed with 1X PBS twice prior to coating with laminin for at least 20 minutes at room temperature. The excess laminin was pipetted out before plating the cells.

Alternatively, PDL-coated plate could be left dry at 4°C up to several weeks. The plates could also be kept at 4°C overnight in laminin.

2.2.3.2 Thawing cells

Frozen cells from liquid nitrogen tank were quickly thawed in 37°C water-bath (Grant) for about 1 minute with shaking after being transported into ES tissue culture room in dry ice. The thawed cells were then gently transferred into 9 ml of pre-warmed complete ES medium (ESM, refer to section 2.1.2) and spun down for 5 minutes at 1000 rpm. Depending on the size of the pellet, which approximately indicates the amount of cells present, an appropriate volume of ESM was used to resuspend the pellet. Normally, 7 ml, 5 or 1 ml of pre-warmed ESM was used to resuspend the pellet before plating the cells into gelatin-coated (refer to section 2.1.3) T25 flask, 6- or 24-well plate (Nulge-Nunc or Greiner), respectively. The cells were then grown in 37°C incubator in an atmosphere of 5% CO_2 (Sanyo).

2.2.3.3 Splitting cells

The cells were ready to be split once they were 90-100% confluent for HEK 293 or 70-90% confluent for ES cells. The cells were rinsed with 1X PBS twice after the medium had been aspirated off, followed by an incubation in an appropriate volume (Table 2.1) of 1X trypsin-EDTA (Gibco-Invitrogen) in 37°C incubator for 1-3 minutes until the cells detached from the flask. The trypsin was then deactivated in an appropriate volume of ESM or HEK-M (Table 2.1) before the cell suspension was triturated 6-12 times to dislodge the cells. Subsequently, the cells were collected by spinning the suspension at 1000 rpm at RT for 5 minutes, and resuspended in an appropriate volume before being counted using haemocytometer. The cells were then seeded into a desired flask (pre-coated with 0.1% gelatin for ES cells see section 2.1.3) at appropriate density (Table 2.1), and incubated in 37°C incubator in an atmosphere of 5% CO_2 (Sanyo) until confluent.

Table 2.1 : Splitting cells

	1X Trypsin (ml)	ESM or HEK-M for deactivation of trypsin (ml)	Cell density for plating cells
96-well plate	0.04	0.10	-
24-well plate	0.10	0.25	3-5 X 10^3
48-well plate	0.25	0.25	3-5 X 10^4
6-well plate	0.5	0.5	2-4 X 10^5
T25 flask	1.0	4.0	1-2 X 10^6
T75 flask	2.0	8.0	1.5-2.5 X 10^6
T180 flask	4.0	16.0	4-5.5 X 10^6
60 mm dish	0.5	1.0	2-4 X 10^5
100 mm dish	2.0	8.0	1.5-2.5 X 10^6

2.2.3.4 Freezing cells

In general, 70-80% confluent monolayer grown cells were trypsinised as described in section 2.4.3.2. Following the deactivation of trypsin in an

appropriate volume of ESM (Table 2.1), the cell suspension was spun after the addition of an equal volume of freezing medium (10% DMSO, 10% FCS in ESM) at 1000 rpm for 5 minutes at RT. The cell pellet was then resuspended in an appropriate volume of freezing medium (2.0 ml for T25 flask or 4.0 ml for T75 flask) prior to freezing at -80°C for a few days until permanently stored in liquid nitrogen, in 1.0 ml aliquot per cryovial (Nalgene).

2.3 Molecular Biology Techniques

2.3.1 RNA extraction

RNA was extracted with all standard precautions in handling RNA taken. Gloves and sterile filter tips and tubes were used throughout the whole procedure. The extracted RNA was kept at -20°C for a short storage, and at -70°C for longer storage.

2.3.1.1 Whole embryo

RNA was extracted from whole mouse embryo E10.5, 11.5 and 12.5, where E0.5 is taken as midday on the day hat plug was detected. The mouse was killed by cervical dislocation and the whole embryos were taken out and washed in sterile 1X PBS. The embryos were kept on ice in the PBS until processed.

RNA extraction was carried out using TRIZOL (GibcoBRL), a phenol-chloroform based protocol, following the manufacturer's protocol. The embryo was weighed on a cleaned weighing boat prior to chunking them using a sterile blade. The tissue was lysed in the appropriate amount of TRIZOL following the manufacturer's recommendation. The RNA pellet

was properly dried before being reconstituted in nuclease-free water (Qiagen).

2.3.1.2 Cell lines

RNA extraction from cell lines was carried out using RNAeasy mini kit (Qiagen), a spin column based protocol, following the protocol described by the manufacturer with slight modifications, where appropriate. In general, most extractions were carried out from cell lines trypsinized from 6-well plate. After trypsinization, the cells were washed twice with 1X PBS and the cells were collected by spinning the cells at 10,000 rpm in 1.5 ml centrifuge tube at room temperature. The cell pellet could then be stored at -70°C or immediately processed for RNA extraction.

The number of single cells harvested from a well of 6-well plate would normally be lysed in 400 µl of guanidine-isothiocyanate contained lysis buffer [1 ml RLT buffer (Qiagen) + 10 µl 2-mercaptoethanol (Sigma)]. The cell lysate was pipetted and vortexed to completely lyse and homogenize the lysate. It is very important to ensure that the cells are completely lysed in order to have a good yield and quality RNA. In order to promote a selective binding of total RNA to the silica-gel-membrane, an equal volume of 70% of ethanol in nuclease-free water was added into the lysate prior to applying the sample into a spin column. The spin column was spun at 13,000 rpm for 15 seconds and the flow-through was discarded. Following the manufacturer's suggestion, RNase-free DNAse (Qiagen) treatment was conducted to efficiently remove any DNA contamination. The column was washed several times as suggested by the manufacturer, prior to eluting the

RNA in appropriate volume (normally 25-30 μl) of RNase-free water into a spun-dried column membrane.

2.3.1.3 Embryoid bodies (EBs)

RNA extraction from EBs was also carried out using RNAeasy mini kit (Qiagen) following the protocol described by the manufacturer. The EBs were transferred into a 20 ml universal tube using a pastette. By letting the EBs settle down for 5 minutes, the medium was pipetted off using 20 ml disposable plastic pipette as it has a wider tip. Using the same method, the EBs were then washed with 1X PBS twice before being transferred into a 1.5 ml tube, where they were finally collected by spinning at 10,000 rpm at RT. The EBs pellet was either stored at -70°C or immediately processed for RNA extraction, as described in section 2.2.1.2, except that the EBs were passed through sterile 21 gauge needle for several times for complete cell lysis. Generally, EBs from 60 mm dish would be lysed in 600 μl lysis buffer (Qiagen) after passing them through the gauge needle fitted on an RNAse-free syringe.

2.3.2 DNA/plasmid extraction

Plasmid DNA was extracted from overnight grown bacterial culture using Qiagen mini-, midi-or maxi-preps kits depending on the volumes of the cultures as recommended by the manufacturer. Bacterial cultures were either grown at 37°C (Sanyo) or 30°C (SI-600R, Lab Companion) with shaking at 225 rpm. A 2 ml-starter culture for maxi- and midi-preps kits was incubated at the appropriate temperature with the indicated speed of shaking for 6 hours prior to growing the culture in a larger volume of

cultures in 1 in 500 dilutions overnight (16-18 hours) with an appropriate antibiotic.

2.3.3 DNA precipitation

Precipitation of DNA was conducted when certain concentration of DNA was required for specific molecular applications; DNA sequencing or introducing DNA construct into bacterial cells via electroporation.

The required volume of DNA was pre-determined before the DNA could be precipitated, or directly precipitated from ligation mixture. 0.4 volume (0.4Y μl) of 5M ammonium acetate (NH_4 OAc, pH 5.5) and 2.5 volumes (2.5Y μl) of absolute ethanol were added to the required volume of DNA (Y μl). The mixture was vortexed to mix and the DNA was precipitated by centrifugation at 13,000 rpm for 30 minutes at 4°C. The DNA pellet was then washed with 500 μl of 75% absolute ethanol twice by centrifugation, as above, for 15 minutes. The pellet was then dried at 37°C for 5-10 minutes before being sent for sequencing or reconstituted in the required volume of 2 μl prior to electroporation.

2.3.4 DNA sequencing

Plasmid DNA was sequenced using the MWG Biotech Sequencing Facility (http://www.mwg-biotech.com). In general, the DNA was precipitated (refer section 2.2.4) to the required amount by the company, and posted off for sequencing. Normally, 1 μg of plasmid DNA was required for one sequencing reaction. Sequencing primers were either supplied or synthesized upon given primer sequence on-site, by the company, or sent together (10 pmol/μl) with the plasmid.

2.3.5 Agarose electrophoresis

DNA and RNA were visualized on agarose gel. The gel was prepared by heat-dissolving the agarose powder in 1X TBE (0.1 M Tris Borate, 0.02 M EDTA) buffer using a microwave oven (Panasonic). Then the agarose solution was cooled to 50°C before the addition of 0.5 μg/ml ethidium bromide solution. The solution was poured onto a gel tray where a flat-tooth comb was used to make up wells. The solution took 15 to 20 minutes to solidify before the samples could be loaded into the wells. Depending on the concentration of the agarose gel, samples were run in 1X TBE buffer at appropriate constant voltage, or electrophoresed at 45 mA/cm for appropriate duration of time. The bands were then viewed under ultra-violet (UV) light.

2.3.6 RNA quantification

RNA was quantified using an UV spectrophotometer (Jenway) by measuring the absorbance at λ=260 nm. RNA was also run on a gel to confirm the integrity of the RNA.

2.3.7 DNA quantification

Plasmid DNA was quantified using agarose gel electrophoresis. The plasmid was linearised by restriction enzyme digestion prior to running it on the gel alongside with known quantity of DNA ladder (100 base pair and 1 kilobase pair ladders, New England Biolabs). The combination of ethidium bromide and UV transilluminator with the use of imaging software were used in this procedure, where the intensity of linearised band was compared to the intensity of a same size band on a known concentration DNA ladder.

Normally, the average concentration from different dilutions of linearised plasmid ran on the gel was used as the final concentration.

2.3.8 Protein extraction

Protein was extracted from either monolayer grown cell line or three dimensional cell aggregates, embryoid bodies (EBs).

2.3.8.1 Cell lines

Protein extraction was normally carried out from confluent monolayer cell lines grown in T25 or T75 flasks after being washed with 1X PBS twice. The cells were then scraped using a tissue culture grade cell scraper (Nalgene) in 1 ml 1X PBS. The detached cells were transferred into 1.5 ml tube and spun at 10,000 rpm at RT for 5 minutes. The cells were then lysed in 80 µl or 200 µl of ice-cold protein-lysis buffer (see section 2.1.2) depending on the flasks they originated from; T25 or T75, respectively, on ice for 20 minutes. The cell lysate was spun at 13,000 rpm for 20 minutes at 4°C to harvest the protein. Alternatively, the lysate was kept at -20°C before being spun as described above. The supernatant was transferred into a new 1.5 ml centrifuge tube and kept at -70°C.

2.3.8.2 Embryoid bodies

Protein was also extracted from EBs growing in 100 mm bacterial grade plates. The EBs were collected into a universal bottle and washed with ice-cold 1X PBS twice. After the last wash, 1 ml of EBs in PBS was transferred into a 1.5 ml tube and spun at 10,000 rpm for 5 minutes at 4°C. The EBs were lysed in 150 µl of ice-cold lysis buffer and processed as described above (section 2.3.1.1).

2.3.9 Protein quantification

Quantification of total protein was conducted using the BCA Protein Assay Reagent Kit (Pierce), following the manufacturer's instructions. It is a colourimetric based detection technique which detects the colour produced by the reaction between a unique reagent containing bicinchoninic acid (BCA) with cuprous ions present in the protein. Protein concentrations were determined with reference to series of dilutions of known concentrations of bovine serum albumin (BSA) as the standard protein. The protein samples were assayed alongside with the standards in duplicates where the absorbance was then measured at 562 nm in 96-well plate using a spectrophotometer plate reader (Dynex) or in disposable plastic cuvettes using a spectrophotometer (Jenway). The protein concentration was finally calculated from a linear regression of a standard curve of known range of BSA concentrations, where 10-20 μg of total protein was used for western blotting.

2.4 Immunodetection

2.4.1 Western blotting

Western blotting was conducted in order to detect expression of certain protein of interest using commercial antibodies (Appendix A for the list of antibodies used). Samples were run as denatured and reduced protein in TENT buffer alongside a pre-stained protein marker (SeeBlue Plus 2, Invitrogen) for western blotting. The marker was used for band sizing and confirmation of complete protein transfer.

2.4.1.1 SDS-PAGE

A total volume of 20 µl containing 10-20 µg of total protein, 1X sample buffer (NP0007, Invitrogen), and 1X reducing agent (NP0004, Invitrogen) in TENT buffer was loaded into 12% Tris/glycine polyacrylamide Novex pre-cast gel (EC60058, Invitrogen) setup in the Xcell SureLock Mini-Cell (Invitrogen) . The solution was vortexed to mix and boiled at 95°C for 5 minutes prior to loading into a lane of the gel filled with 1X NuPage MOPS SDS running buffer (NP0001, Invitrogen). The protein samples together with the protein marker were run for 1 hour and 30 minutes at constant voltage of 150 V. Upon completion, the gel was equilibrated in transfer buffer (NP0006, Invitrogen) for a few minutes before being setup for protein transfer.

2.4.1.2 Protein transfer

Mini Trans-Blot Electrophoretic Transfer Cell Unit (Bio-Rad Laboratories, USA) was used to electrophoretically transfer the protein bands from the gel onto a membrane. During the electrophoresis of the SDS-PAGE gel, a pre-cut PVDF membrane (Bio-Rad), Whatman 3 MM papers (Whatmann, USA) and fibre pads (provided in the transfer set) were pre-soaked in transfer buffer (NP0006, Invitrogen) for at least 10 minutes at RT. Following exactly the instructions in the manual provided by the manufacturer, the unit was assembled and operated accordingly. Transfer was conducted in transfer buffer at a constant current of 400mA (150 V) for an hour or 50mA for 16 hours in the cold room (4°C). Upon completion, the membrane was stained with Ponceau S (Sigma) for few seconds and rinsed with ddH_2O to visualise transferred proteins. The image was then scanned (GS-710 Calibrated Imaging Densitometer, BioRad) and recorded (Quantity One 4.0.3, BioRad), and the membrane was ready for immunodetection.

2.4.1.3 Protein detection

Immunoblotting began with blocking the membrane in Western-blocking buffer (section 2.1.2) overnight at 4°C or 2 hours at RT. Then, the membrane was incubated with shaking in appropriate dilution of primary antibody (Appendix A for the list of antibodies used) in blocking buffer for 2 hours at RT or at 4°C overnight. The antibody was drained off prior to washing the membrane with TBS-T (section 2.1.2) for 10 minutes at RT three times. The procedure proceeded with incubation with an appropriate dilution of peroxidase-conjugated secondary antibody in Western-blocking buffer for an hour at RT with slow shaking prior to washing the membrane as described above. Immunodetection was then carried out using ECL Plus Western Blotting Detection Reagents (Amersham Biosciences) following the protocol suggested by the manufacturer and exposed to X-ray film, which subsequently developed and processed in an automatic X-ray processor.

2.4.2 Immunocytochemistry

Immunocytochemistry was generally conducted in 4-well plate (Delta,Nunc) or 8-well glass slide chamber (Fisher Scientific). The attached cells were gently rinsed with 1X PBS prior to being fixed in 4% paraformaldehyde (PFA) (section 2.1.2) for 30 minutes at RT before being permeabilised in 1% Triton-X100 in 1X PBS (permeabilization solution, section 2.1.2) for 15 minutes at RT. Cells were then blocked for 30 minutes at RT in Immuno-blocking buffer (section 2.1.2) prior to incubating the cells in an appropriate dilution of primary antibody (Appendix A for the list of antibodies used) in the blocking buffer for 2 hours at RT or overnight at 4°C. After rinsing with 1X PBS twice, the cells were then incubated with diluted secondary antibody (Appendix A for the list of antibodies used) for 1-2 hours at RT in the dark.

The cells were then counterstained with TO-PRO3 (Molecular Probes) or propidium iodide (Sigma), where appropriate, for 10-15 minutes at RT after being rinsed with 1X PBS twice. The cells were either left in PBS or mounted in mowiol (section 2.1.2), and kept in the dark until viewing under fluorescent microscope (Axiovert 132, Ziess).

2.4.2.1 Cell counting

Cell counting was carried out from at least 3 different fields from at least 2 duplicate wells of 4-well plate (Delta Nunc). The percentage of positive cells stained for certain antibody was taken over the total cells stained with nuclei staining such as ToPRO3 or propidium iodide. Counting for cells stained with specific antibody was done manually using Image Tool while counting for cells stained with nuclei staining was performed using IMARIS software programme.

2.4.3 Flowcytometry

Analysis by fluorescent activated cells sorting (FACS) was carried out using FACS calibur (Becton Dickinson) on live and fixed cells.

2.4.3.1 Detection of GFP

Expression of enhanced green fluorescent protein (eGFP) from 46C EBs was detected and analysed by FACS using live cells. Day 4, 6, 8, 12 and 14 EBs from 46C ES cells were trypsinized in 4X trypsin (section 2.7). Instead of using EBM to deactivate the trypsin, FACS wash buffer (10% foetal calf serum in 1X PBS) was used and the single cells were immediately analysed by FACS. EBs from non-expressing eGFP cell line (R26CT2S) was used as the negative control and also for gate setting.

2.4.3.2 Antibody staining

FACS was also used to detect percentage of positive cells by antibody staining. Antibody staining was carried out on trysinised neural precursor and neuron-like cells grown on PDL/laminin coated 60 mm dish (Greiner). After neutralization of trypsin, the cells were washed in 1X PBS twice by spinning the cells at 6500 rpm in 1.5 ml tube for 3 minutes at RT prior to fixing them in 200 µl of 70% ethanol for 15 minutes at RT. Then, the ethanol was diluted in 1 ml of 1X PBS before being kept at -20°C.

On the day of the analysis by FACS was to be carried out, the samples were thawed at RT and 300 µl of PBSG (5% goat serum in 1X PBS) was added into the tube prior to spinning the tube at 6500 rpm for 3 minutes at RT. Subsequently, 150 µl of diluted primary antibody (Table 2.2) was gently mixed into the cells and incubated at RT for an hour. Once completed, 1 ml of PBSG was added into the tube, inverted to mix and incubated for 2 minutes to wash the cells before spinning the cells as described above. Incubation with 150 µl of secondary antibody [R-Phycoreithrin (PE) conjugated antibody (1:100 dilutions)] was carried out in the dark for 30 minutes at RT. The cells were then washed as described above prior to finally be resuspended the cell pellet in 350 µl of PBSG for the analysis by FACS.

For analysis purposes, fixed cells, fixed cells stained with primary antibody only and fixed cells stained with secondary antibody alone were run together with the samples for checking the sensitivity and specificity of the antibodies used, and for gate setting.

Table 2.2 : List of antibodies for FACS

Primary Antibody	Secondary antibody
Nestin (1:50) (Mouse IgG1, DSHB)	Goat anti mouse IgG1-PE (1:100) (P21129, Molecular Probes)
Pax6 (1:200) (Mouse IgG1, DSHB)	Goat anti mouse IgG1-PE (1:100) (P21129, Molecular Probes)
ß-tubulin (1:800) (Mouse IgG2b, Sigma)	Goat anti mouse IgG2b (1:100) (P21149, Molecular Probes)
NeuN (1:200) (Mouse IgG1, Abcam)	Goat anti mouse IgG1-PE (1:100) (P21129, Molecular Probes)
GFAP (1:800) (Rabbit IgG, DakoCytomation)	Goat Anti Rabbit IgG-PE (1:100) (P2771, Molecular Probes)

2.5 Construction of Transgenic ES cells

Chapter 4 will describe the details of the construction of transgenic ES cell lines. The construction began with building the plasmid construct in *E. coli* followed by introducing the plasmid into ES cells by GeneJuice (Novagen). The same procedure was applied when constructing transient or stable transfected HEK 293 cells.

2.5.1 Bacterial work

All bacterial work used *E. coli* strain JM109 (Promega) or its derivative, Stbl2 or Stbl4 (Invitrogen).

2.5.1.1 Cloning and subcloning

All cloning and subcloning strategies in constructing the appropriate DNA constructs are described in Appendix B.

2.5.1.1.1 Restriction endonucleases

In preparing the appropriate digested vector or digested DNA fragment for cloning or subcloning purposes, at least 4 μg of DNA was digested with 40 units of enzyme in a total volume where the volume of the enzyme did not exceed 10% of the total volume. The digestion was carried out using manufacturer's suggested buffer and BSA (Roche) at 37°C for 5 hours, prior to running the digested DNA on a 0.8% agarose gel to check for the complete digestion. Upon the completion of the digestion, the digested DNA was either directly purified or run on agarose gel for excision of the desired band using QIA-quick gel extraction kit (Qiagen).

Clones were screened using an enzyme that cut both the insert and the vector to verify the orientation of the insert inside the vector. For screening purposes, 0.5 μg of plasmid/DNA was digested in 5 units of enzyme in a total volume of 20 μl for 90 minutes at 37°C, together with 1X buffer with or without 1X BSA as recommended by the manufacturer (Roche). The reaction was scaled up for a digestion that resulted in 200 bp or lower digested band size.

2.5.1.1.2 Dephosphorylation and ligation

Dephosphorylation was performed whenever there were possibilities of self religation from digested vectors. The procedure was carried out using shrimp alkaline phosphatase (SAP, Roche) following the manufacturer's

recommendation as the phosphatase could be completely deactivated by heating the mixture at 65°C for 15 minutes. The DNA was then either purified (QIA-quick gel extraction kit, Qiagen) or directly quantitated (by running on agarose gel, section 2.2.7) prior to ligation.

The purified DNA fragment was directly ligated into appropriate purified digested-cloning vector. Generally, 50 or 100 ng of purified vector was used to ligate appropriate amount of the purified DNA fragment (the insert) based on the formula described in Table 2.3 as the guideline. The ligation was carried out using 1.5 Weiss units of T4 DNA ligase (Roche, UK) in 1X ligation buffer (Roche, UK) where a total volume of 12 µl was incubated at 16°C for 16 hours or for 5 hours at RT. A ligation mixture with the insert and the vector alone were also included as the negative controls, and for checking the ligation efficiency. Subsequently, 5.5 µl of the ligation mixture was used for transformation.

Table 2.3: Ligation formula

$$\text{ng of insert} = \frac{\text{ng of vector} \times \text{size of insert (kb)}}{\text{size of vector (kb)}} \times \text{molar ratio of } \frac{\text{insert}}{\text{vector}}$$

ng = nano gram, kb = kilobase

2.5.1.2 Transformation

In most cases, transformation was carried out using JM109 competent cells. However, for cloning involving unstable inserts such as direct repeats, MAX Efficiency Stbl2 or Stbl4 competent cells were used. Stbl2 was transformed by heat-shocking while Stbl4 via electroporation.

2.5.1.2.1 Antibiotics

Depending on the plasmid, 100 μg/ml of ampicillin or 50 μg/ml of kanamycin were used for selection.

2.5.1.2.2 Heat-shock

Transformation was carried out by incubating the mixture of the ligated vector or plasmid DNA with competent cells in ice-cold sterile 17 X 100 mm polypropylene tube (Falcon) on ice for at least 10 minutes. Depending on the type of vector involved, the competent cells used were either JM109 (Promega), for stable vector, or Stbl2 (Invitrogen) for unstable vector. Normally 50-200 μl of competent cells were mixed with 5-10 μl of ligation mixture or 1-50 ng of purified plasmid DNA by gently flicking the tube. After 10 minutes on ice, the mixture was heat-shocked for 60 seconds at 42°C in a water bath without shaking (Grant). The transformants were then propagated in one ml pre-warmed (37°C) Luria-Bertani (LB) broth for JM109 cells, or SOC medium (provided with Stbl2, Invitrogen) for Stbl2 cells for 90 minutes at 37°C or 30 °C, respectively, with shaking. Following this, the bacterial cell cultures were transferred into 1.5 ml tube and spun at 6000 rpm at RT for 30 seconds. The supernatant was poured off, leaving approximately 200 μl of the supernatant in the tube to fully resuspend the pellet. For each transformation reaction, 100 ul of the undiluted cells or 1:100 dilutions were plated on LB or 2xYT agar containing appropriate antibiotic at either 37°C or 30 °C overnight.

2.5.1.2.3 Electroporation

Transformation via electroporation was carried out for certain ligation mixtures involving unstable vector using Stbl4 competent cells (Invitrogen).

The ligation mixtures were purified by ethanol precipitation (see section 2.2.3), and reconstituted in 2 μl TE buffer (10mM Tris-HCl, 1 mM EDTA, pH 7.4) prior to adding into 20 μl of Stbl4 competent cells in 1.5 ml tube. The cell suspension was properly mixed by gently flicking the tube before being electroporated at 1.2 kV, 0.25 μF and 200 Ω in disposable electroporation cuvettes (BioRad) using GenePulser (BioRad). Immediately, using a long pipette tip the cell suspension was transferred into 1.0 ml SOC medium in 14 ml round bottom Falcon tube and incubated for 90 minutes at 30°C with shaking at 225 rpm. The cells were plated on LB agar plate with 50 μg/ml ampicillin as described above (section 2.5.1.2.1).

2.5.2 Introduction of construct plasmids into ES cells

2.5.2.1 GeneJuice

Among the transfection reagents tested, GeneJuice (Novagen) was found to give high transfection efficiency based on the number of colonies formed after about one week in selective medium. The procedure was conducted following the manufacturer's recommendation with slight modifications, as described in Table 2.4 below. The ES cells were seeded one day before transfection was to be carried out, so that the cells would be about 20-60% confluent on the day of transfection. The transfection began with mixing pre-warmed serum-free BHK21 medium (Gibco: 21710-025) with GeneJuice by tapping the tube prior to incubating the mixture for 5 minutes at RT. Following the incubation, the plasmid DNA was then added into the mixture, tapped to mix and incubated at RT for another 15-60 minutes to build DNA-GeneJuice complex. Once the incubation was completed, the DNA/GeneJuice complex was added to the cells that had been grown in

serum-free medium, and incubated for 2-8 hours in 37°C incubator (Sanyo). The medium with DNA/GeneJuice was discarded and the cells were grown in complete medium (ESM) in the incubator until the cells were confluent. The cells were then either analysed for transient transfection, or selected in selective medium for stable transfection.

Table 2.4: Transfection using GeneJuice (Novagen)

	100 mm dish	60mm dish/ 6 well-plate	4-well plate	8-well slide chambers
Number of ES cells	$1X10^6$	$2\text{-}4 X 10^5$	$1\text{-}2 X 10^4$	$0.5\text{-}1 X 10^4$
Serum-free BHK21 medium	150 µl	100 µl	30 µl	20 µl
GeneJuice	3 µl	3 µl	1 µl	0.75 µl
DNA/Plasmid	1-2 µg	0.5-1 µg	0.2-0.5 µg	0.2 µg
Serum-free into plate/ES cells	2 ml	1 ml	150 µl	100 µl
Growth medium (ESM)	10 ml	5 ml	1 ml	500 µl

2.5.2.2 Selection medium

All of the constructs built carried a neomycin resistance gene which confers resistance to geneticin (G418). Thus, screening for the positive clones was carried out using G418 selective medium. With exception of constructs carrying pCAG-floxed neomycin pA IRES puromycin cassette, the neomycin resistant clones were then subjected to screening for puromycin resistant clones upon excision of the neomycin floxed cassette with tamoxifen (more details are discussed in Chapter 4 of this thesis).

2.5.2.3.1 Geneticin (G418)

Neomycin resistant clones were selected by growing the cells in 400 μg/ml geneticin (G418) in ESM as soon as the cells reached confluency. The selective medium was changed every other day until the cells n the non-transfected control plate died off. The transfected plates were incubated until the clones appeared which normally took about 7-10 days after the initiation of selection. The clones were then picked using a yellow tip (Greiner) attached to P200 pipette (Gilson) and transferred into gelatin-coated 96-well plate after being washed in 1X PBS twice, and grown in the selective medium in 37°C incubator. Once confluent, the cells were trypsinized and grown in gelatin-coated 24-well plate in the selective medium. The procedure was repeated and the cells were split in 6-well plate. The selection was stopped once the cells were grown in a T25 flask. The positive clones were frozen and kept in liquid nitrogen.

2.5.2.3.2 Puromycin

Cells carrying a complete pCAG-floxed neomycin pA IRES puromycin cassette were further screened using 1 μg/ml puromycin. The positive clones for neomycin resistant genes were seeded into 24-well plate and grown in ESM containing 0.2, 0.5 and 1μM tamoxifen (4'-Hydrotamoxifen, 4-OHT, Sigma) for the excision of the neomycin-pA cassette which would then allow for the expression of puromycin resistant gene protein. The cells were selected in puromycin selective medium 2 days after being exposed to tamoxifen, at which time the cells were about 80-90% confluent. The clones that survived puromycin were selected as the positive clones for carrying the complete cassette, and were subjected to the manipulation of the

overexpression of the gene of interest during neural differentiation of ES cells (more details in Chapter 5 of this thesis).

2.6 Inducible ES cells system: Activation of Cre by tamoxifen

Chapter 4 will discuss in detail the inducible ES cell system. The expression of the gene of interest was induced by activation of Cre-recombinase upon exposure of the cells harbouring the complete pCAG-floxed-neomycin-pA-IRES-puromycin (Figure 4.1) to tamoxifen. Optimal conditions for the induction of Cre-recombinase were determined by exposing the undifferentiated and differentiated (EBs D0 of neural differentiation protocol, section 2.7) clone cells to 0.2, 0.5, 0.8 and 1.0 μM tamoxifen for 24 or 48 hours before being harvested for total RNA and protein. The undifferentiated ES cells were seeded into 6-well plate at a density of 2-4 X 10^5 cells per well (Table 2.1), while the EBs were formed in 60 mm dish (Greiner).

2.7 Neural differentiation of Mouse ES cells

The differentiation of ES cells into neurons was carried out through the formation of embryoid bodies (EBs) using *all-trans* retinoic acid (ATRA) following the 4-/+4 protocol (Bain *et al.*, 1995). Around 5x10^5/ml of lightly trypsinised 46C cells were allowed to aggregate in suspension culture (EBs day 0, D0) in the absence of LIF in non-tissue culture-treated petri dishes (Greiner) for four days before the addition of 10^{-6}M of ATRA for another 4 days. On D8, some of the embryoid bodies (aggregates) were trypsinised in high concentration of trypsin (4X Trypsin-EDTA, 4% chicken serum in 1X PBS) at 37°C water bath for 5 minutes. The trypsinized cells were then

stained with trypan blue (Sigma) and counted using heamacytometer prior to plating on PDL and laminin coated plate (Li *et al.*, 1998) at $2x10^6$ cells in 6-well plate ($1\text{-}2x10^5/cm^2$) for terminal differentation in DMEM/F12 suplemented with N2 (Gibco) and neurobasal medium supplemented with B27 (Gibco). Trypan blue was used to exclude apoptotic cells during cell counting. The rest of the EBs were transferred into smaller petri dishes as to get higher density of EBs population (details are described in Chapter 3 of this thesis).

Detail description on neural differentiation assay for manipulation of Wnt signalling during neural differentiation process of mouse ES cells is discussed in chapter 5 of this thesis.

2.8 Polymerase Chain Reaction (PCR)

PCR has been widely used throughout the whole project. Chapter 3 of this thesis specifically applied this important technique in determining the expression profile of all 19 Wnt genes, besides other genes, during neural differentiation of mouse ES cells.

2.8.1 Primer design

Primers were designed using Primer 3 programme at http://frodo.wi.mit.edu/cgi-bin/primer3/primer3www.cgi and Web Primer: DNA and Purpose Entry at http://seq.yeastgenome.org/cgi-bin/web-primer. The DNA sequences were taken from Nucleotide sequence (Genebank) at http://www.ncbi.nlm.nih.gov/entrez/query.fcgi?db=Nucleotide or Ensembl Mouse Genome website at

http://www.ensembl.org/Mus musculus/index.html. The designed primer sequences were synthesized by MWG Biotech AG (http://www.mwg-biotech.com). Primers for light cycler were designed based on guidelines provided in the Quantitect SYBR Green PCR handbook (Qiagen).

2.8.2 Optimization of PCR parameters

Positive samples were used in optimizing the conditions for PCR parameters. Thus, cDNA synthesized from total RNA extracted from mouse embryo day 8.5, 10.5 and 12.5 were used in optimizing the PCR conditions for each Wnt gene. All 19 Wnt genes are expressed during development of mouse embryo. Opimization conditions for each gene began with amplification of the gene transcript using 1.5 mM $MgCl_2$ with annealing temperature taken from the melting point of its corresponding forward and reverse primers, following [2 (A + T) + 4 (G + C)] formula as the guideline. Different concentration of $MgCl_2$ and annealing temperature were applied until the best conditions were discovered.

2.8.3 cDNA synthesis

The cDNA was synthesized by adding 1.0 μg of extracted RNA to 100 ng of random hexanucleotide primers (PROMEGA) in nuclease-free water in a total volume of 15 μl at 70°C for 10 minutes followed by a quick chill on ice (about 2 minutes). The synthesis was continued in a total volume of 25 μl containing the RNA/random primers mix, together with 1X RT-buffer (Promega), 1.0 mM of the four deoxyribonucleoside 5'-triphosphates (dNTPs, Promega), 1 unit of RNase inhibitor (Promega) and 200 units of MMLV reverse transcription enzyme (Promega) at 42°C for an hour. All components were properly mixed by vortexing prior to a quick spin before being loaded

into a PCR machine (MJ Research) for the incubation. The reverse transcriptase was deactivated and the RNA-cDNA hybrid was denatured by incubating the mixture at 95°C for five minutes. Finally, the samples were either kept on ice for immediate amplification of cDNA or stored at -20°C until used.

2.8.4 Reverse-transcription (RT)-PCR

RT-PCR was carried out in a total volume 20 μl consisting of 1 μl of synthesized cDNA, 1.5 mM $MgCl_2$, 0.2 mM of dNTPs, 7.0 pmol of both forward and reverse primers and 1 unit of Taq polymerase enzyme (Promega). PCR parameters for the amplification of each gene are specifically described below in Appendix C.

2.8.5 Quantitative RT-PCR (qRT-PCR)

Quantitaive RT-PCR was performed using Quantitect SYBR Green PCR master mix (Qiagen) in DNA Engine Opticon (MJ Research) following the suggestions described in Quantitect SYBR Green PCR handbook (Qiagen). A total reaction of 25 μl containing 1X SYBR Green PCR master mix, 10 pmols of each forward and reverse primers, and 1μl of synthesized cDNA in nuclease-free water was properly mixed in 8-well strip (BioRad) prior to loading into the machine. Normally, 5-8 dilution series of purified plasmid carrying the transcript sequence of interest or a sample known to express the gene of interest were used as the standards and were run together with the samples. Arbitrary units for amplification of each transcript were generated from these standards. The cycle began with the initial activation step at 95°C to activate DNA polymerase for 15 minutes, followed by 35 cycles of denaturation step at 94°C for 15 seconds, annealing step at 50-60°C (refer to

Appendix C) for 30 seconds and extension step at 72°C for 30 seconds. In order to verify the specificity and identity of the PCR product, melting curve analysis was performed for every reaction between 65°C and 95°C following the instructions provided by the manufacturer.

Amplification of the target transcript sequence was quantified using relative quantification where the ratio between the value of target and a suitable housekeeping gene transcript was determined. ß-Actin was used as the housekeeping gene as its expression during neural differentiation process was found to be the most stable as compared to other housekeeping gene tested. In addition the gene has been frequently used in previous studies involving the differentiation of mouse ES cells (Lako *et al.*, 2001; Conti *et al.*, 2005). The differential gene expression in different samples was compared as relative expression to ß-Actin or relative expression to non-treated sample following the formulae described in Table 2.5.

Table 2.5 : Quantitative differential gene expression by light cycler

Relative Expression to ß-Actin

$$= \frac{\text{unit expression of gene of interest}^{(\text{sample})}}{\text{unit expression of ß-Actin}^{(\text{sample})}}$$

Relative Expression to non-treated sample

$$= \frac{\text{unit expression of gene of interest}^{(\text{sample})}}{\text{unit expression of ß-Actin}^{(\text{sample})}} \Big/ \frac{\text{unit expression of gene of interest}^{(\text{non-treated sample})}}{\text{unit expression of ß-Actin}^{(\text{non-treated sample})}}$$

Chapter 3: Expression profiles of Wnt genes during neural differentiation of mouse ES Cells

3.1 Introduction

As discussed in chapter 1, Wnts have been implicated to play important roles in regulating development of the nervous system. Therefore, they are strong candidates for regulating aspects of the *in vitro* differentiation process of ES cells into neurons. However, knowledge of their function during this process is limited. Preliminary findings have suggested that they may influence neural development of ES cells in culture. It is believed that Wnts may inhibit the differentiation of ES cells into neural precursor cells (NPCs) but may also promote the differentiation of NPCs into neurons.

One study found that Wnt antagonist sFRP2 is upregulated during neural differentiation of ES cells *in vitro* (Aubert *et al.*, 2002). The gene function analysis from the study demonstrated an increase of neural precursor cell differentiation from sFRP2-overexpressing ES cells implying an inhibitory effect of Wnt activity on neural differentiation. Inhibition of neural differentiation was also observed from ES cells treated with lithium chloride, which partially mimics Wnt signalling, as well as from forced expression of *Wnt1*. This study has been supported, among other studies, by a recent study which demonstrated that treatment with Wnt3*a* at late culture stages in neural differentiation increased the number of neural cells, while exposure to Wnt3*a* at early culture stages strongly suppressed neural conversion (Watanabe *et al.*, 2005). Taken together, these studies suggest a role for Wnts in inhibiting the differentiation of ES cells to NPCs, but also promoting the

differentiation of NPCs to neurons. Therefore, looking at the expression profiles of all members of the family gene during the process would be a first step to determining whether or not Wnts may be involved in neural differentiation of ES cells *in vitro*.

In this chapter, the expression profiles of all 19 Wnt genes and two Wnt antagonists, *Dkk1* and *sFRP2*, during neural differentiation of mouse ES cells *in vitro* were examined. Neural differentiation was induced through the formation of embryoid bodies (EBs) in the absence of LIF followed by the addition of retinoic acid (RA) for four days [Bain *et al.*, 1995; Li *et al.*, 1998a]. The expression of all 19 Wnt genes was screened in five different stages during the process; undifferentiated ES cells (day 0, D0), early formed EBs (D2 and D4), RA-treated EBs (D6 and D8), attached EBs (D10, D12 and D14) and neuron-like cells (D14 or six days after re-plating). Figure 3.1 shows a schematic flowchart for the steps involved.

Neural differentiation was carried out using an ES-cell line engineered to monitor the formation of neural precursor cells (NPCs), 46C ES cell line. This line carries a *Sox1* reporter allele constructed by insertion of the coding sequence of enhanced green fluorescent protein (eGFP) into the *Sox1* open reading frame (ORF, Aubert *et al.*, 2003). As the endogenous *Sox1*, the expression of eGFP was silent in undifferentiated ES cells but activated upon neural induction. Sox1 is the earliest specific marker for neural precursor cells (NPCs) and is only expressed in proliferating progenitors in the lens and throughout the CNS in the mouse embryo (Wood and Episkopou, 1999; Aubert *et al.*, 2003). It is not expressed in undifferentiated ES cells but is specifically expressed in NPCs upon induction of neural differentiation of ES

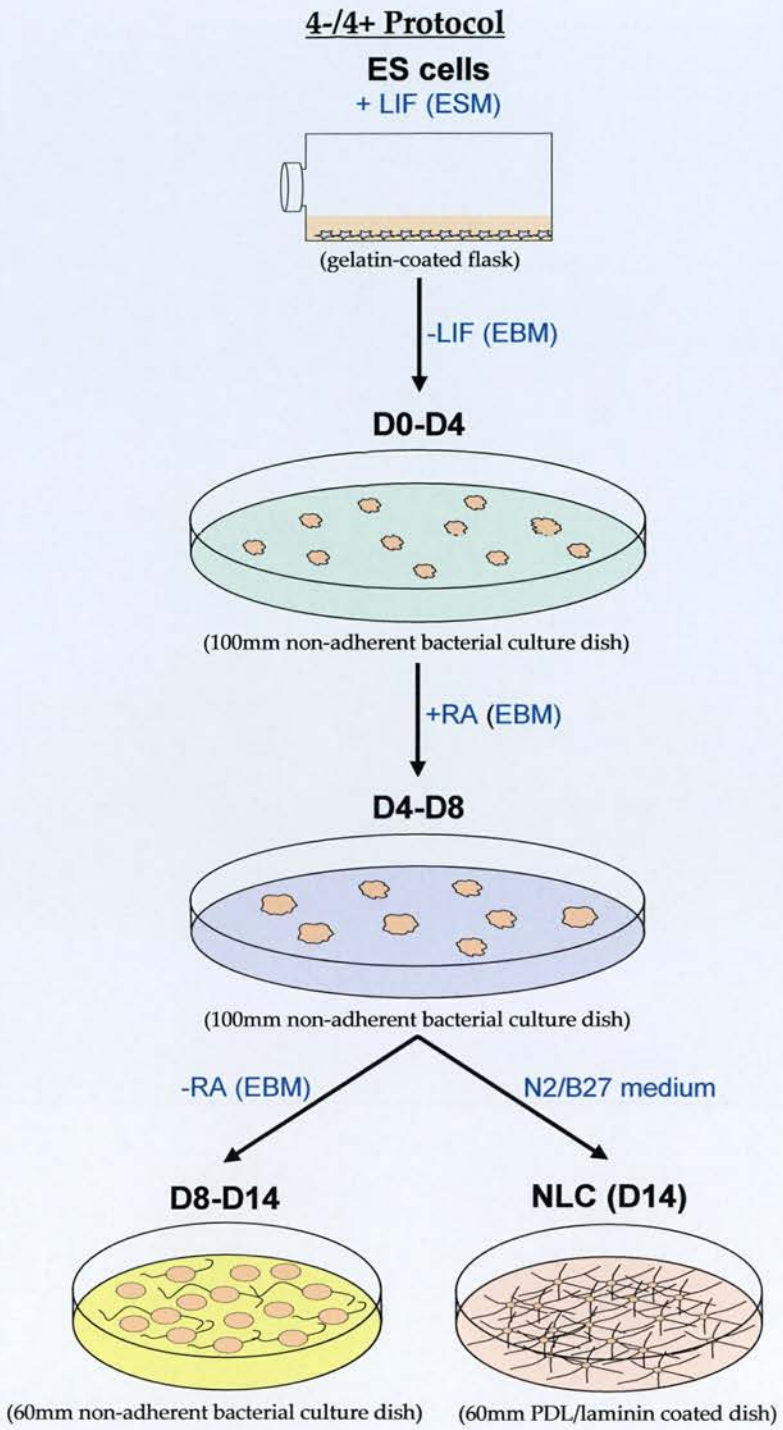

Figure 3.1: Schematic diagram of neural differentiation assay for 46C cells using the 4-/4+ protocol. RA was added for four days (D4-8) after the aggregates (EBs) were grown for four days (D0-4) without LIF. On D8, the EBs were either transfer into smaller dishes to promote attachment and neurite outgrowth or dissociated and plated on PDL/laminin-coated plates.

cells (Pevny *et al.*, 1998; Ying *et al.*, 2003b). 46C ES cells were used to facilitate the identification of NPCs, thus allowing us to monitor the success of the neural differentiation protocol. In addition, the presence of NPCs that are expressing GFP upon neural induction, after the addition of RA, therefore can be quantitated by FACS analysis.

In the next part of this study, the specific Wnts expressed during the neural differentiation process were identified by RT-PCR from total RNA harvested from each stage as described earlier (Figure 3.2 describes in detail the time points for RNA extraction for each stage). The expression of selected Wnt genes that showed particularly interesting expression profiles was further quantitated using light cycler (SYBR Green), quantitative RT-PCR (qRT-PCR). Hence, the expression of Wnts at the specific time points along the process was determined.

3.2 Results

3.2.1 Neural Differentiation of Mouse ES cells (46C) *In vitro*

In this study, we applied the most common approach, 4-/4+ protocol, for the induction of neuronal differentiation of ES cells (Bain *et al.*, 1995). As described in Figure 3.1 and 3.2, the EBs were treated with 1.0 μM *all-trans* retinoic acid (ATRA) for four days after being grown for four days in the absence of LIF. The formation of multicellular aggregates, EBs, was observed the next day (D1) after the withdrawal of LIF. As previously observed, the EBs appeared small with irregular boundaries after two days in culture without LIF. On D4, the EBs looked mature, in which they became larger and mostly were spherical with more prominent smooth boundaries (Figure 3.3; Bain *et al.*, 1995; Lake *et al.*, 2000). As expected, two days after the

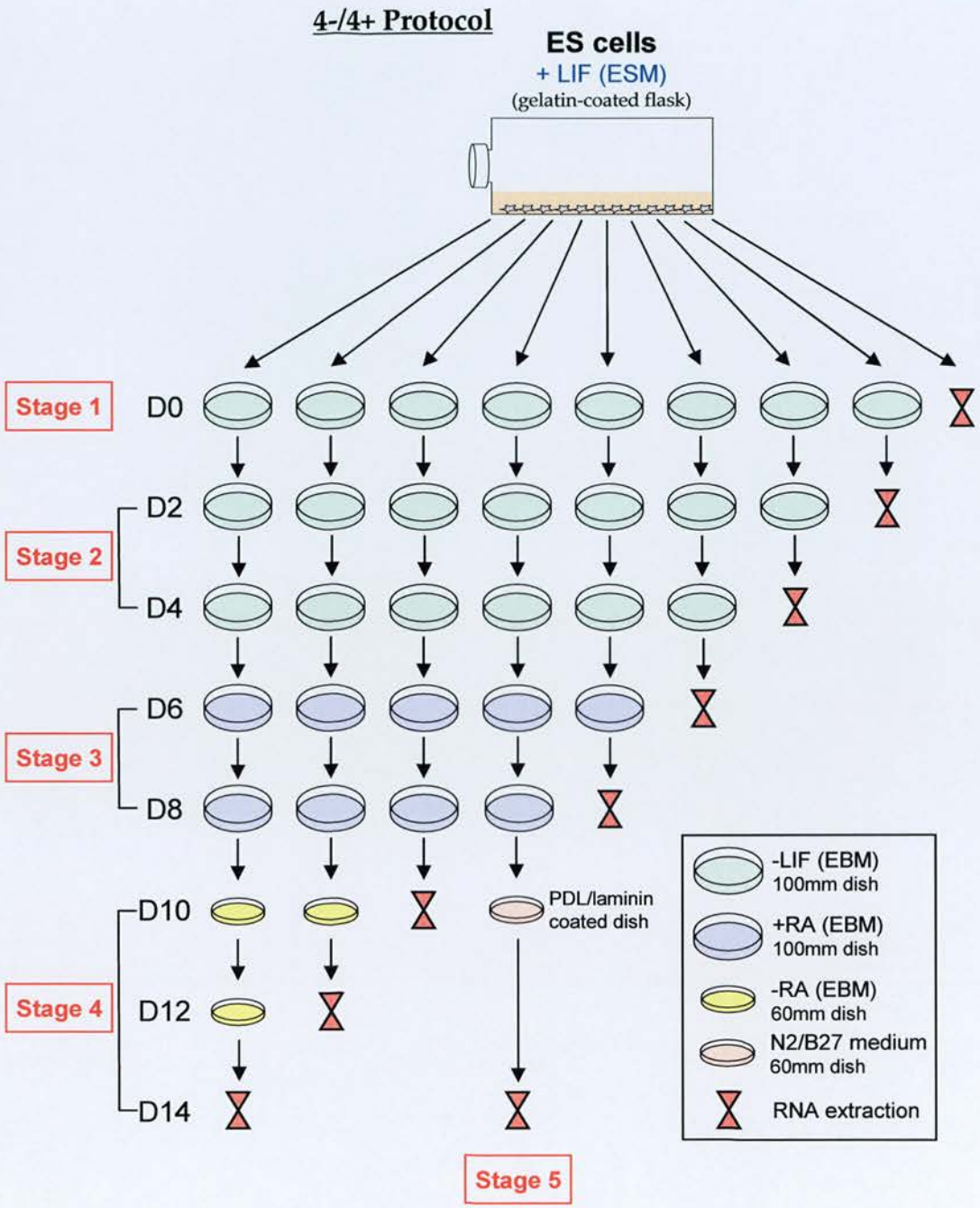

Figure 3.2: Detailed schematic diagram of neural differentiation assay for 46C cells *in vitro* showing the specific time point where the cells were harvested for RNA extraction. Stage 1 is the undifferentiated ES cells (D0). Stage 2 and 3 are the EBs before and after the addition of *all-trans* Retinoic acid (ATRA), respectively. Stage 4 contains mostly the attached EBs. Stage 5 is the neuron-like cells (NLC) grown on a PDL/laminin coated plate.

addition of ATRA (D6), cells expressing GFP were visible under fluorescence microscope (Figure 3.3E) indicating the presence of dividing neural precursor cells, as *Sox1* is the earliest specific marker of neural precursors in the mouse embryo (Wood and Episkopou, 1999). After 4 days in ATRA (on D8), the EBs were either transferred onto smaller petri dishes to encourage the attachment of EBs to the plate since low density of EBs resulted in slower attachment of EBs to the dish, or dissociated and plated on PDL/laminin-coated plates.

On D10, many EBs in the smaller dish were attached and started to form outgrowth of neurites (Figure 3.4A). The EBs were monitored until D14 to observe the growth of the neurites. On D14, almost all the attached EBs were hardly seen as a ball-shaped clumps as they seemed to have dispersed, forming more dense growth of neurites (Figure 3.4D). In addition, the expression of GFP was still observed indicating that neural precursor cells were still present (Figure 3.4E). Alternatively, the GFP expression might be due to its half-life (maximum half-life for GFP is 54 hours, Sacchetti *et al.*, 2001). The GFP expression was also analysed and confirmed by fluorescence-activated cell sorting (FACS) analysis (Figure 3.5). FACS analysis demonstrated that the highest number of cells expressing GFP (about 70%) was seen at D8.

Two days after plating the dissociated EBs on PDL/laminin-coated plates (D10) in the medium supplemented with N2/B27, the dissociated cells started to form clumps and gave rise to a network of neuron-like cells with apparent death of other cell types. Six days after the re-plating, more distinct neuron-like networking (Figures 3.4) and more positively stained cells for class III β-tubulin were observed, as previously described (Bain *et al.*, 1995; Li *et al.*,

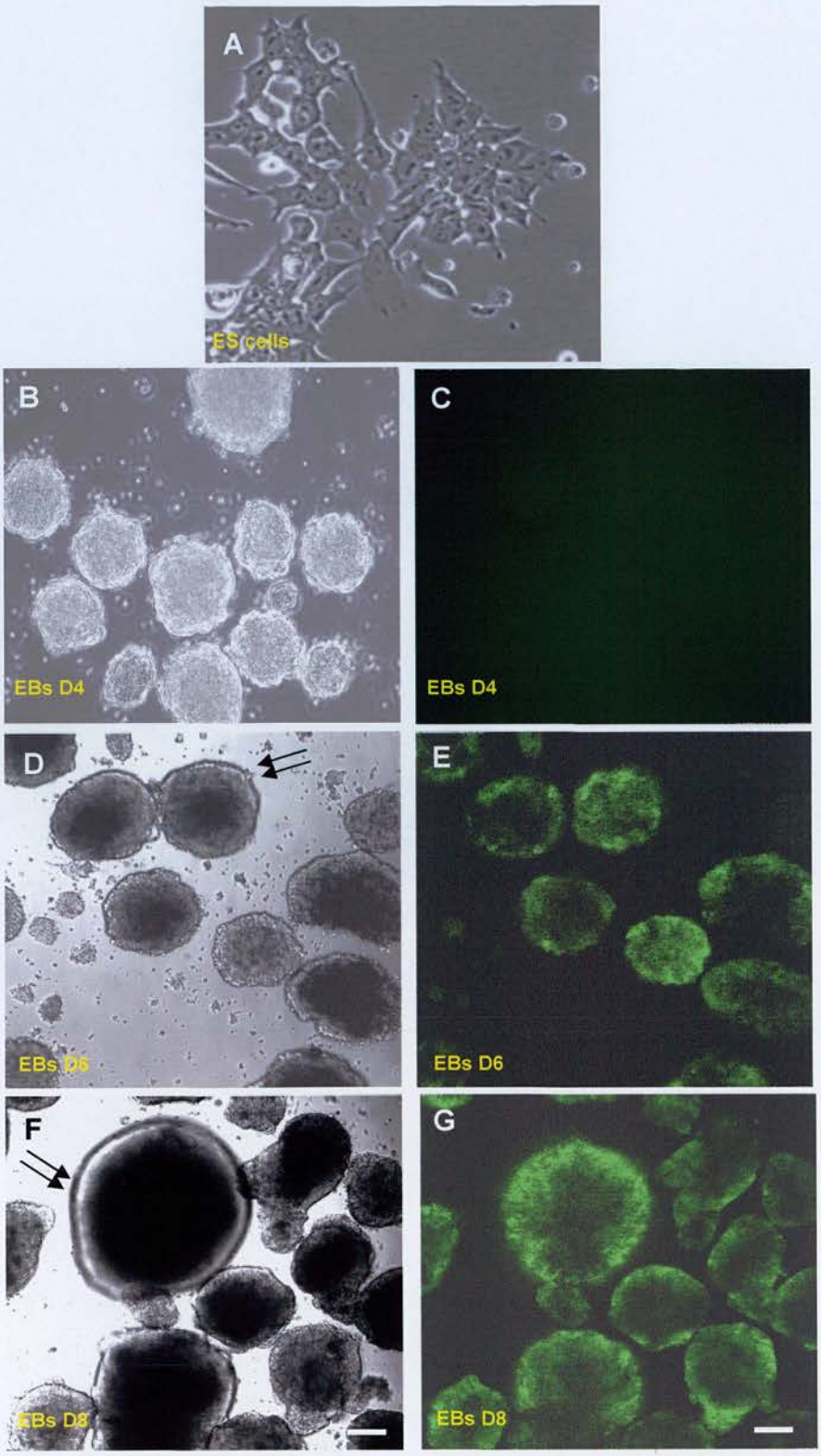

Figure 3.3: Expression of Sox1-GFP during neural differentiation of 46C ES cells *in vitro*. (A) Morphology of undifferentiated 46C ES cells. (B, D and F) phase contrast pictures of embryoid bodies (EBs) at D4, D6 and D8. (C, E and G) fluorescent images of the EBs shown in B, D and F demonstrating clear expression of Sox1-GFP at D6 and D8. Double arrows show the smooth boundaries of mature-looking EBs. Scale bar is 100 μm.

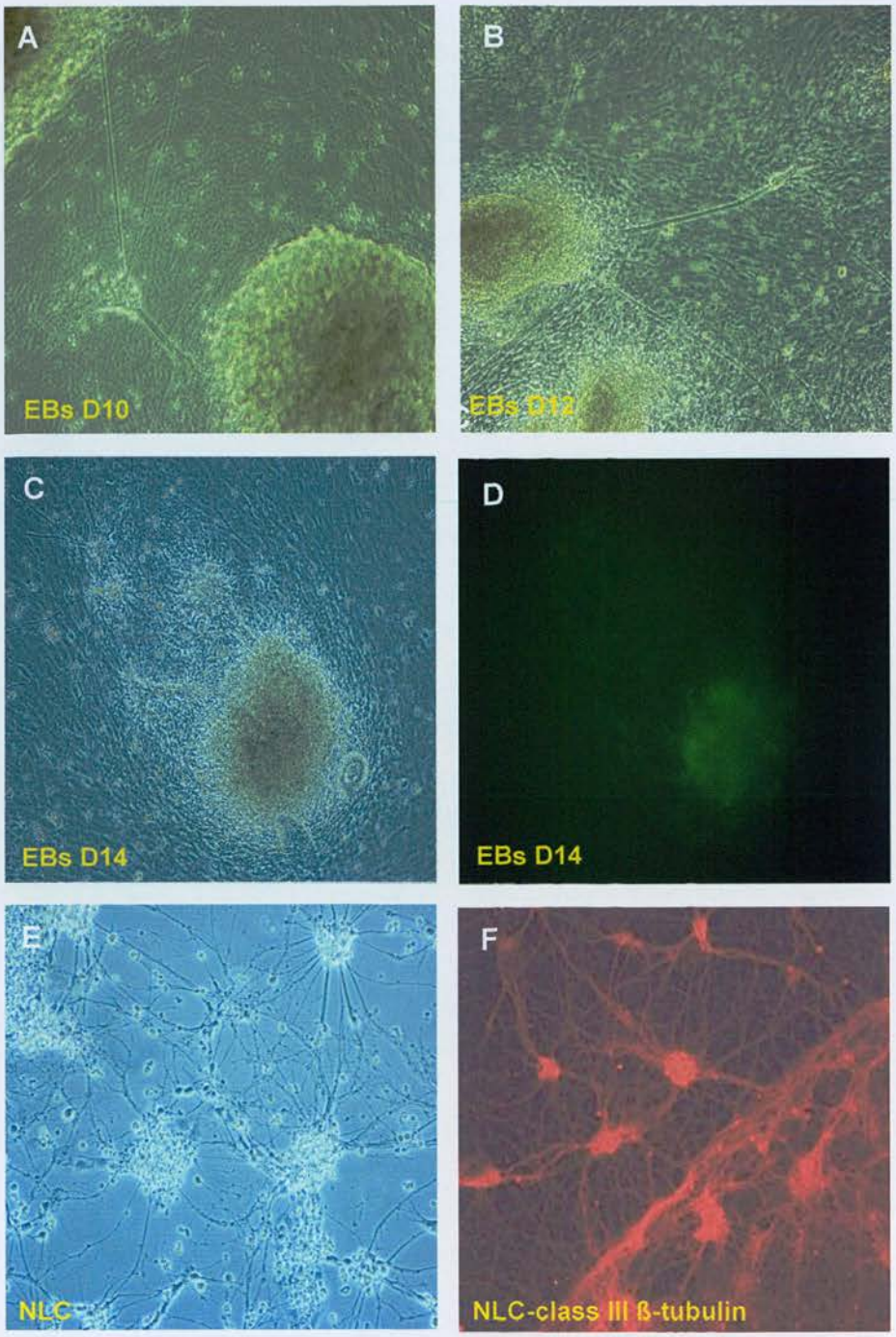

Figure 3.4: Formation of neurites and neuron-like cells (NLC) from neural differentiation of 46C cells. (A, B and C) phase contrast pictures of EBs at D10, D12 and D14 showing the formation of neurites outgrowth in cultures with higher density of EBs. (D) the fluorescent image of C showing a faint expression of GFP at D14 indicating reduced number of dividing npc. (E and F) phase contrast picture and expression of neuronal marker, class III ß-tubulin, respectively, of NLC 6 days after plating on PDL-laminin-coated plate indicating the formation of neurons.

1998a). The protocol also gives rise to a small percentage of GFAP, and RC2 positive cells for astrocytes, and radial glial cells, respectively (Figure 3.6). At this stage, no expression of GFP was observed demonstrating the absence of neural precursor cells. These results show that RA is able to induce extensive differentiation of neurons when plated on a permissive substrate, and that the protocol activates a pathway that leads to expression of neuron associated genes as previously described (Bain *et al.*, 1995).

3.2.2 Efficiency of Neural Differentiation of 46C cells *in vitro*

To further analyze the efficiency, reproducibility and success of the differentiation protocol of 46C ES cells into neurons, gene expression profiles for specific cell population markers was carried by RT-PCR for *Oct4*, *Sox1* and *Wnt1*. RT-PCR analysis was conducted on total RNA extracted from EBs D0-14 and NLC from three independent 46C ES cell neural assays; 46C ES cells passage 17, 19 and 23 for batch A, B and C, respectively (Figure 3.7). The expression pattern of *Oct-4*, a marker for undifferentiated ES cells *in vivo* as well as *in vitro* (Scholer *et al.*, 1989, 1990; Pesce *et al.*, 1999; Pesce and Scholer, 2000, 2001) demonstrates that the differentiation protocol was successful (Figure 3.7). *Oct-4* is expressed in undifferentiated ES cells and downregulated as differentiation occurs (Niwa *et al.*, 2000). As expected, expression of *Sox1*, a marker for neural precursor cells, was observed upon induction of neural cells, on D6, indicating the presence of NPCs in agreement with the FACS analysis (Figure 3.5). However, D6 EBs seem to have the highest RNA expression of *Sox1*, a disagreement with the protein expression level by FACS analysis, which demonstrates D8 EBs as to have the highest Sox1-GFP expression (Figure 3.5 and 3.7). This might be due to the time required for the green fluorescent protein to be correctly folded

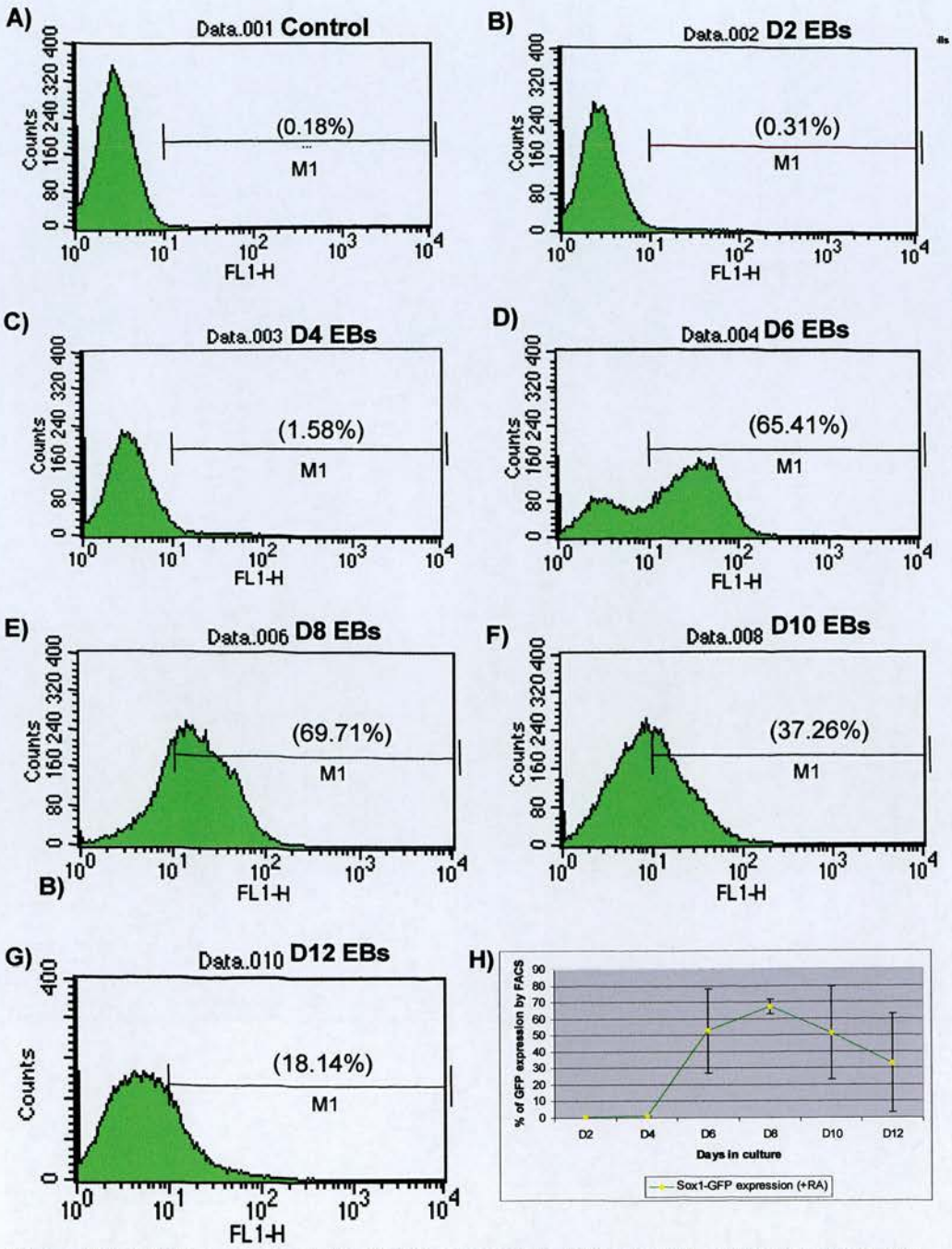

Figure 3.5: FACS analysis of *Sox1*-GFP expression during neural differentiation of 46C cells. (A) FACS profile of D6 EBs of control cells, non-GFP expressing cells (R26CT2S), which were used to set the M1 gate. (B and C) FACS profiles for D2 and D4 EBs of 46C cells, respectively, showing almost no expression of Sox1-GFP before the addition of ATRA. (D, E, F and G) FACS profiles for D6, D8, D10 and D12 EBs after the addition of ATRA, respectively, clearly showing high expression of Sox1-GFP at D6 and D8 of the process. The percentage of cells expressing GFP is shown in parentheses. (H) Graph showing the percentage of cells expressing Sox1-GFP from D2, D4, D6, D8, D10 and D12 EBs during the process. Error bars show the mean ± the range between the highest and the lowest values from two independent experiments.

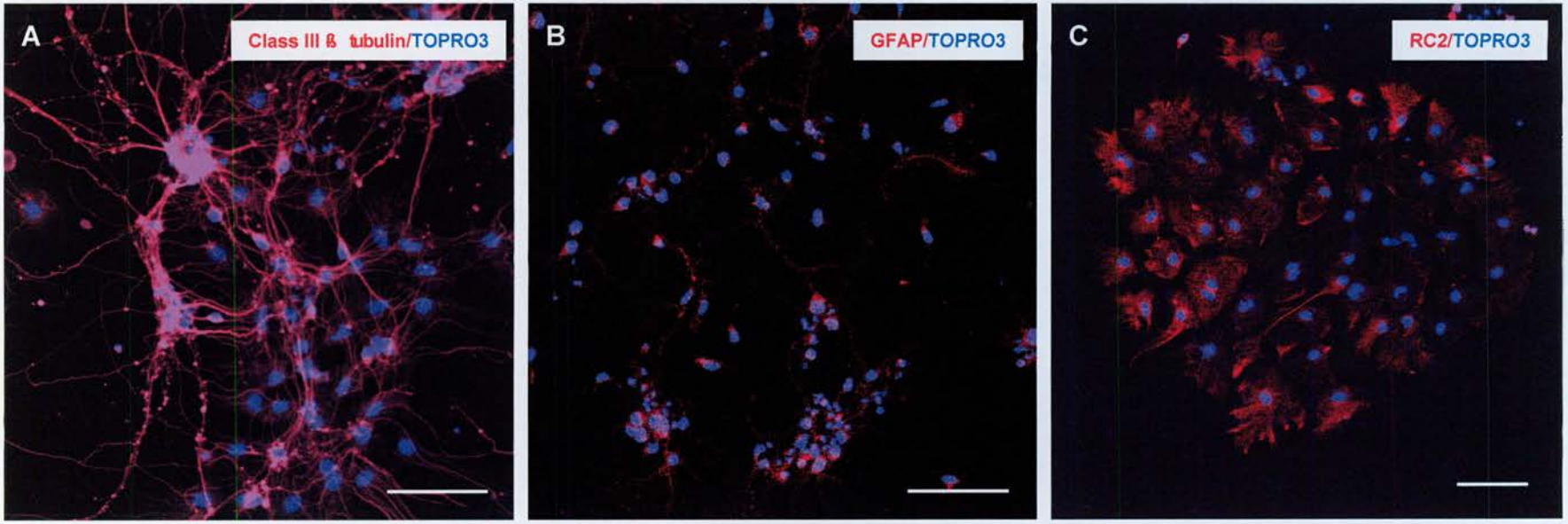

Figure 3.6: Expression of cell type specific markers after neural differentiation of 46C cells. Expression of (A) neuronal marker, ß-tubulin, (B) astrocytes (glial fiblliary protein, GFAP) and (C) radial glial marker, RC2. Cell nuclei were counterstained with TOPRO3 (blue). Scale bar is 100 µm

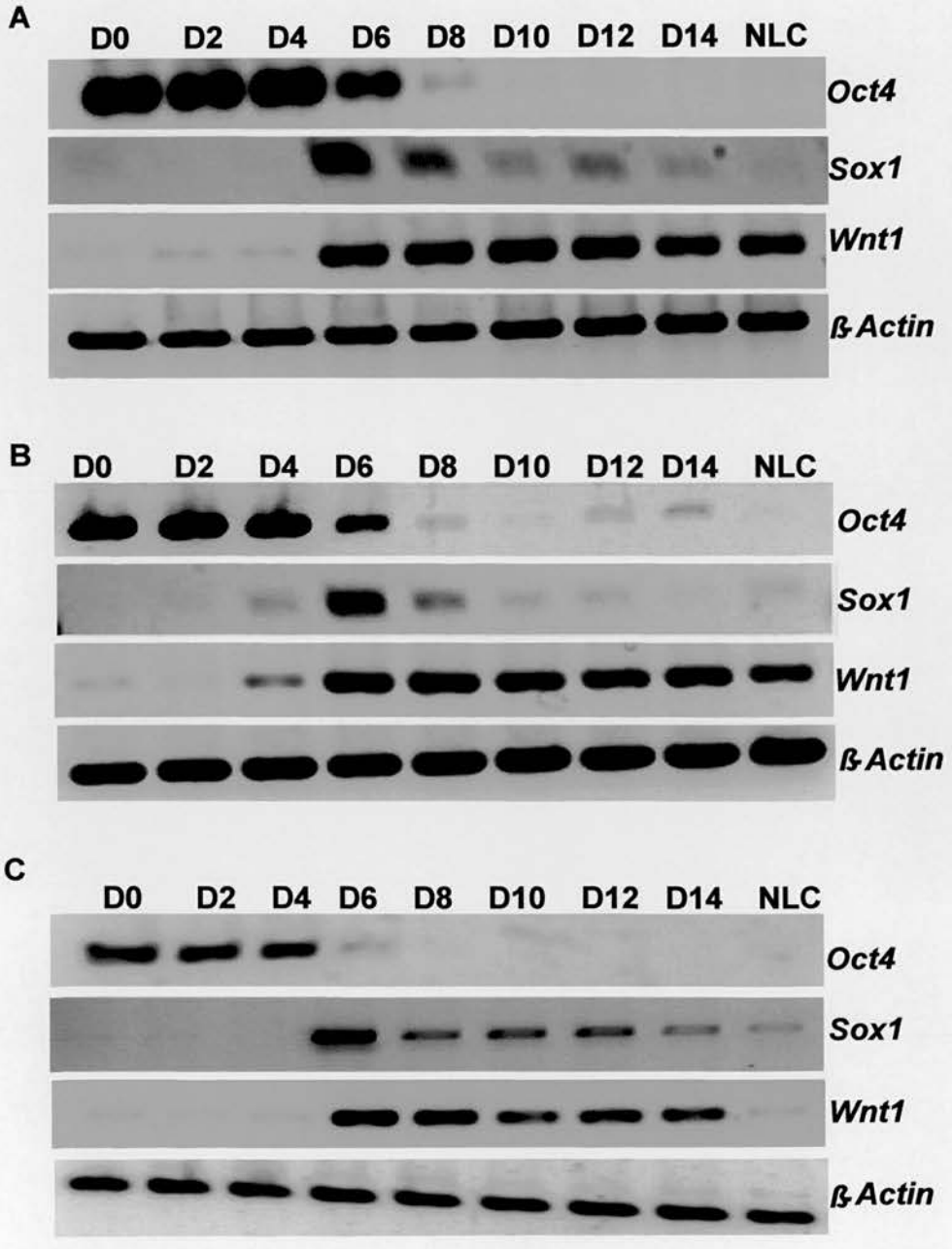

Figure 3.7: Efficiency of neural differentiation of mouse ES (46C) cells *in vitro.* RT-PCR from total RNA extracted from cells at 2 day intervals. The expression patterns of *Oct4* (marker for undifferentiated ES cells), *Sox1* (marker for dividing neural precursor cells), *Wnt1* (known to be RA-induced) and *ß-actin* from 3 different batches of neural assay demonstrates the reproducibility and efficiency of the protocol in directing differentiation towards neural lineage. (A, B and C) show the genes expression patterns from 46C cells passage 17, 19 and 23 respectively. The PCR was carried out for 30 cycles for *Oct4* and *Sox1, and* 35 cycles for *Wnt1 and ß-actin.*

before being able to be detected and analysed. The expression profile of these genes shows that the differentiation has successfully been directed towards the neural lineage.

In addition, the study also confirmed the success of the differentiation protocol by the expression pattern of *Wnt1*, which is known to be RA-induced (St-Arnaud *et al.*, 1989). As expected, expression of *Wnt1* was detected on D6 onwards (after the addition of RA) with low expression in the neuron-like cells, NLC, in one of the batches (Figure 3.7). Quantitative RT-PCR, however, has confirmed the reproducibility of *Wnt1* RNA expression profile from these three batches (Figure 3.12).

3.2.3 Expression Profiles of Wnt genes by RT-PCR during neural differentiation *in vitro*

The expression of Wnt genes was monitored from D0-D14 to ascertain which Wnt genes were differentially expressed during the differentiation process. At this time, the target was to identify the expression of Wnt gene(s) from the whole population of five different stages during the differentiation process; undifferentiated ES cells (stage 1, D0), early formed EBs (stage 2, D2 and D4), RA-treated EBs (stage 3, D6 and D8), attached EBs (stage 4, D10, D12 and D14) and neuron-like cells (stage 5, D14 or six days after re-plating) [Figures 3.1 and 3.2]. Suitable primer pairs for all 19 mouse Wnt genes primers were optimized using total RNA extracted from whole mouse embryos day 10.5, 11.5 and 12.5, as the embryos at these stages express all Wnt genes (Parr *et al.*, 1993; Parr and McMahon, 1994; Kemp *et al.*, 2005). Most of the primers were

designed to span an intronic region as a way to check for any contamination with genomic DNA. All gene primers were run at least twice.

The expression patterns of all 19 Wnt genes are shown in Figure 3.8. Out of 19 Wnt genes that were screened, two genes (*Wnt8b and Wnt10a*) were detected at a very low level of expression. *Wnt10a* was consistently detected at a very low level on D12 going up to a slightly higher expression level on D14 with no expression detected in neuron-like cells. No expression of this gene was ever detected at stage 1-3 and on D10. Expression of *Wnt8b* was detected inconsistently at a very low level between stages 2-3. The other gene with low expression level is *Wnt2a*, which is first expressed on D4. The expression was down-regulated on D8 onwards with no expression detected in neuron-like cells. Expression of *Wnt3, -9b(15)* and *-16* were detected in undifferentiated ES cells (D0 EBs) at different level of expression. High expression of *Wnt3* was also detected at later stages of the process (D10, D12 and D14) with very low expression detected on D6, D8 and NLC. For *Wnt9b*, high expression was detected on D4, D8 and D10 with no expression detected in NLC. Low level of *Wnt9b* expression was seen on D2, D6, D12 and D14. *Wnt5b* and *-7b* were detected at high level at all stages with low expression level in NLC.

At least six Wnts (*Wnt1, -2b, -3a, -4, -5a, -10b and -11*) have been shown to have dynamic expression patterns during the differentiation process. Among these, only *Wnt3a* is highly expressed in neuron-like cells, while *Wnt4* was not expressed in these cells at all. While *Wnt5a* was expressed at low level in neuron-like cells, a very low level expression of Wnt*10b* and *-11* were also detected in these cells. High expression of *Wnt2b* started on D10

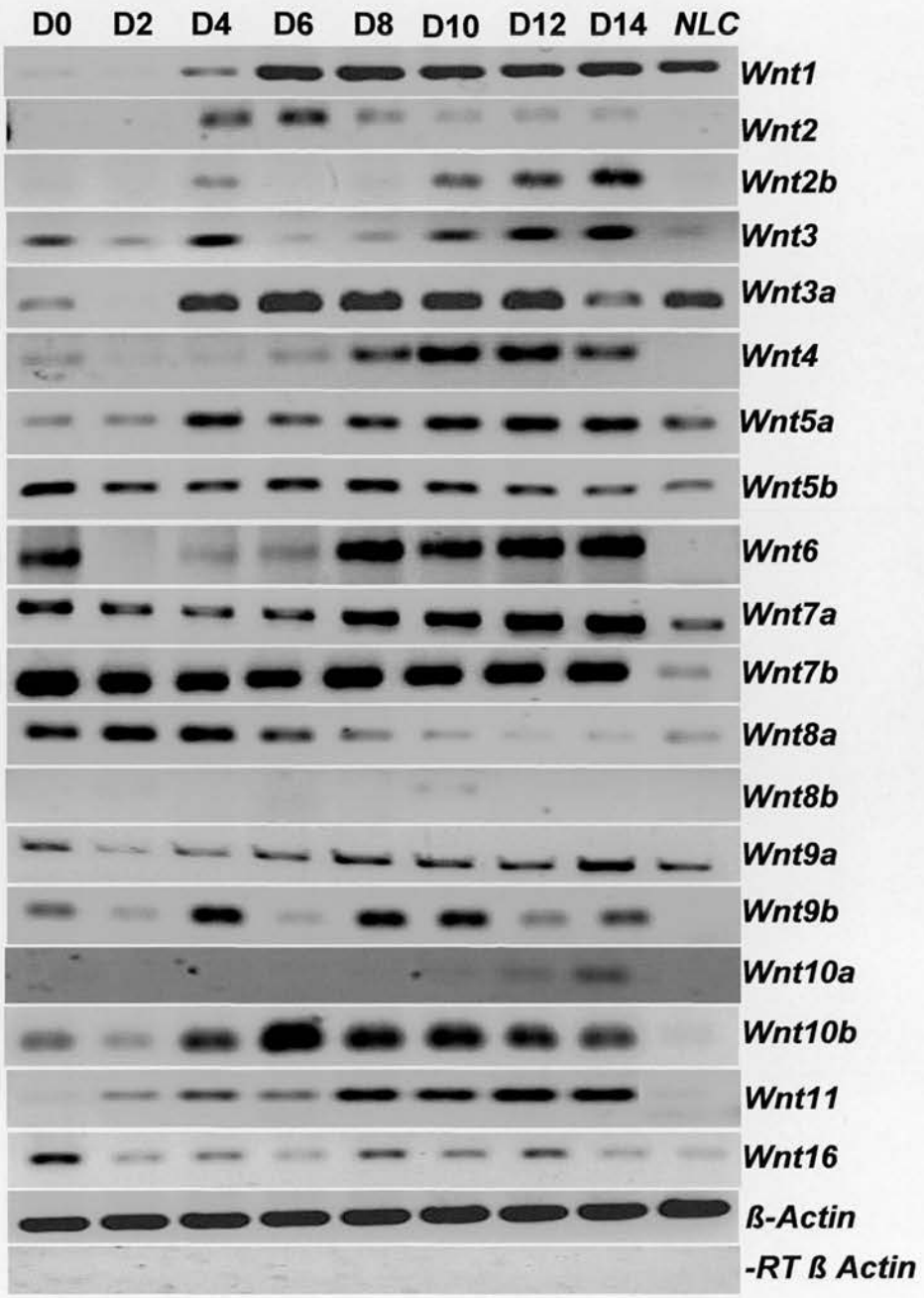

Figure 3.8: Expression profile of Wnt genes during neural differentiation of mouse ES cells (46C) *in vitro* by RT-PCR. RNA extracted on D0-14 EBs and neuron-like cells (NLC) was subjected to RT-PCR with all 19 mouse Wnt genes, as indicated. The EBs were exposed to ATRA for four days after being grown in the absence of LIF for four days. NLC were harvested 7 days after plating the dissociated D8 EBs on PDL/laminin plates. The results were from a single experiment from the same synthesized cDNA. The PCR cycles were 35 for all genes except for *Wnt3, Wnt8b, Wnt9b, Wnt10a* and *Wnt16* which were 30 cycles.

while for *Wnt4* and *-11*, their high expression began at D8. The expression for *Wnt3a* and *-10b* started on D4 with the highest expression detected on D6. *Wnt1* gave the expected expression pattern as being induced on D6, after the addition of RA and low expression level in neuron-like cells.

The other interesting expression patterns are the expression of *Wnt6, -7a* and *-9a.* High expression of *Wnt6* was detected on D0 and D8-14 with no expression on D2 and NLC, and low level of expression on D4-6. For *Wnt7a,* its expression seemed to be downregulated on D2-D6, but it is highly expressed in undifferentiated ES cells (D0). However, the expression went up again on D8 onwards except in neuron-like cells, which showed low expression level. The same scenario was observed with *Wnt9a.* The gene was also expressed in undifferentiated ES cells (D0) and downregulated on D2-6. The expression was then continued on D8 onwards including the neuron-like cells. On the contrary, high expression of *Wnt8a* has been observed to occur in undifferentiated ES cells (D0) as well as in non RA-treated treated EBs (D2-4), with low expression detected on D6-8 and in neuron-like cells. No expression of *Wnt8a* was detected on D10-14.

These RT-PCR results, therefore, show that many Wnt genes are expressed during neural differentiation of mouse ES cells *in vitro.* Among all, *Wnt5b, -6, -7a, -7b, -8a, -9a* and *-16* were expressed at high level in undifferentiated ES cells (stage 1). In early formed EBs (D2 and D4, stage 2), high level of *Wn3, -3a, -5a, -5b, -7b, -8a, -9b* and *-10b* were detected. In stage 3 EBs after the addition of ATRA (D6 and D8), *Wnt1, -3a, -5a, -5b, -6, -7a, -7b, -9a, -9b, -10b,* and *-11* were detected at high level of expression. In stage 4 which mainly contained attached EBs (D10, D12 and D14), *Wnt1, -2b, -3, -3a, -4, -5a, -5b, -6, -*

7a, -7b, -9a, -10b and *-11* were detected. A high level expression of only one gene (*Wnt3a*) was detected in neuron-like cells (stage 5), while Wnt*5a*, 5b, *7a* and *9a* were detected at low level in these cells. However, these results were based on RT-PCR results which are not quantitative and may be influenced by the number of PCR cycles. Thus, the Wnt genes with interesting expression patterns were subsequently subjected to quantitative RT-PCR.

3.2.4 Evaluation of qRT-PCR analysis

In this analysis, the expression level of each gene at specific time points during the differentiation process was normalized to the expression of *ß-Actin*, as the reference gene. The expression level for each gene was then expressed as relative to *ß-Actin* and relative to the expression of undifferentiated ES cells (fold increase to D0, refer to Chapter 2 for their specific formulae). ß-Actin was used as the reference gene since the gene was found to be expressed at constant level throughout the differentiation process (Appendix D). Besides that, it has also been widely used in previous studies (Aubert *et al.*, 2003; Otero *et al.*, 2004; Israsena *et al.*, 2004; Kemp *et al.*, 2005. Therefore, the amount of RNA present in the population cells was not absolutely quantified. Instead, the ratio between the amount of target (Wnt genes, *Dkk1* or *sFRP2*) and a reference transcript (*ß-Actin*) within the same sample was calculated. Thus, differential gene expression in different samples (D0-14 EBs and NLC) can then be compared using the normalized value.

In this study, the standards used were a series of diluted synthesized cDNAs from EBs that have the highest expression level of the gene of interest as shown by RT-PCR. The same cDNA was also used in setting up the

standards for *ß-Actin.* Subsequently, a set of the same arbitrary units for the standards were setup for the amplification of both transcripts. It does not matter what units were used as the results were given in ratio. A value of 1 would indicate the expression level of the gene of interest is the same as the reference gene, and the value of more or less than 1 would indicate a relative higher or lower expression of the gene of interest accordingly. The value of relative expression to ß-actin can therefore be used in comparing the differential gene expression between the expression levels of different genes in the same set of samples (since ß-actin is consistently expressed through out the process) in addition to the comparison of the differential gene expression in the same set of sample using the same gene. Relative expression of the normalized gene expression (to ß-actin) to the gene expression on D0 or undifferentiated ES cells (stage 1) was also determined. This gives the information on fold induction between the expression in undifferentiated and differentiated cells throughout the whole differentiation process.

The other important factor is the level of background fluorescence from primer dimers, since the amplification is detected by SYBR Green which fluoresces when bound to double-stranded DNA (dsDNA). Therefore the fluorescence from artifact dsDNA of primer dimer could impede proper quantification. Fortunately, melting curve analysis and gel electrorophoresis of the DNA amplified never indicated such problem in our work. This problem was avoided by designing appropriate primers, optimum concentrations for all components and optimized SYBR Green-PCR conditions (as described in Chapter 2).

Based on this study, we find that qRT-PCR is a good technique for analysis of differential gene expression, provided that all the factors influencing the analysis are carefully taken into account. Besides that the analysis between different samples should be done in parallel with proper choice of standards. Finally, the qRT-PCR analysis should be qualitatively confirmed by other method, such as *in situ* hybridization or northern blotting, or may be quantitatively extended using TaqMan real time PCR, which was not done in this study. This is because the main objectives for this part of study are to confirm the expression profiles as demonstrated by RT-PCR and quantified the expression level of each gene at different stages during the differentiation process by qRT-PCR.

3.2.5 Expression Profiles of Wnt antagonists by qRT-PCR: *Dkk1* and *sFRP2*

Expression profiles of two Wnt antagonists were examined during the differentiation process (Figure 3.9, Table 3.1 section 3.2.6). *Dkk1*, which antagonizes Wnt signalling by direct interaction with Wnt receptor, LRP5/6, and *sFRP2*, which antagonizes Wnt signalling by directly bind to Wnts (as described in Chapter 1), were included. In addition, *sFRP2* was also included since its expression has been shown to be upregulated during neural induction (4-/4+) of ES cells and downregulated in differentiated neurons and glial in mouse brain (Aubert *et al.*, 2002).

Interestingly, *Dkk1* was found to be highly expressed at stage 2 during the differentiation process, which mainly consists of *Sox1* negative EBs (Figure 3.9). The highest expression was detected on D4 with a 30 fold increase

Table 3.1: Grouping of Wnt genes based on relative expression to ß-actin by qRT-PCR

Group		Stage 1	Stage 2		Stage 3		Stage 4			Stage 5
		D0	D2	D4	D6	D8	D10	D12	D14	NLC
A	*Wnt8a*	++	+++	++++	+	+	+	+	+	+
B	*Wnt6,*	++	+	+	++	++	++	++	++	+
	Wnt7a	+++	+	+	+	++++	++++	++++	++++	++++
	Wnt7b	+++	+	+	++	++++	++++	+++	+++	+++
C	*Wnt1*	-	+	+	++++	++++	++++	+++	+++	++
	Wnt3a	+	-	++	++++	++++	++++	+++	+	+
	Wnt10b	+	-	+	++	++	+++	+	+	-
D	*Wnt2b*	+	-	++	+	++	++++	++++	++++	+
	Wnt4	+	+	+	+	+++	+++	++++	+++	+
	Wnt5a	+	-	+	+	+	++	+++	++++	++
	Wnt9a(14)	+	+	+	++	++++	+++	+++	++++	++
	Wnt11	+	+	++	+	++	++++	++++	++++	+
Dkk1		+	+++	++++	++	++	++	+++	+++	++
sFRP2		+	+++	+++	+++	++++	+++	++	+++	+++

(Based on relative to ß-actin value (x); - = x ≤ 0.01; + = 0.01 < x ≤0.25; ++ = 0.25 < x ≤ 0.5; +++ = 0.5 < x ≤ 1; ++++ = x > 1)

Canonical pathway, Non-canonical pathway, both pathways, unclassified.

☐ Upregulation of expression

compared to its expression on D0. The expression was, however, downregulated on D6 onwards, where the formation of NPCs was detected, consistent with downregulation of *Dkk1* expression upon neural induction.

sFRP2 was found to be expressed at all stages of the process with D8 having the highest expression level. The highest expression was increased five fold compared to expression on D0. Lower levels of sFRP2 expression were then observed at stages 4 and 5. In agreement with the published results by Aubert and colleagues (2002), we also observed high expression of sFRP2 in

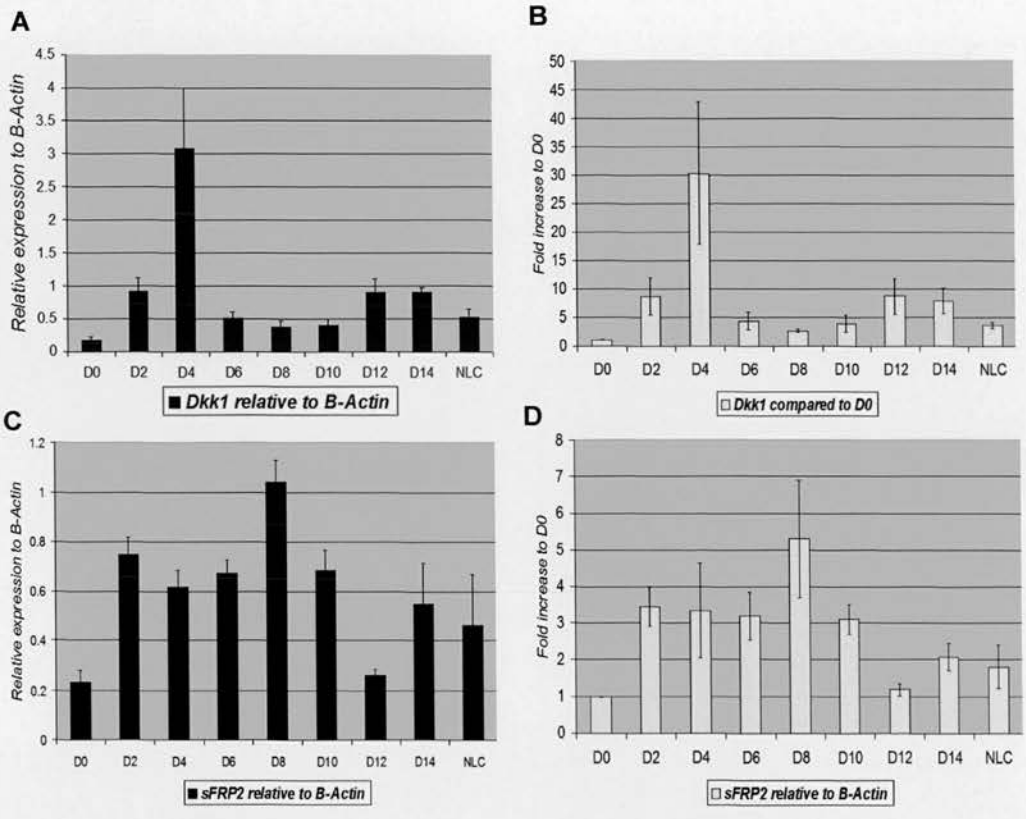

Figure 3.9 : Expression profile of Wnt Antagonists by qRT-PCR. Expression profiles of *Dkk1* and *sFRP-2* during neural differentiation of mouse ES cells *in vitro*. (A and C) Expression of *Dkk1* and *sFRP-2* normalized to *ß-Actin*, respectively. (B and D) are expression of the respective genes (normalized to *ß-actin*) relative to D0 or undifferentiated ES cells. Standard error bars show mean ± SEM from three independent experiments.

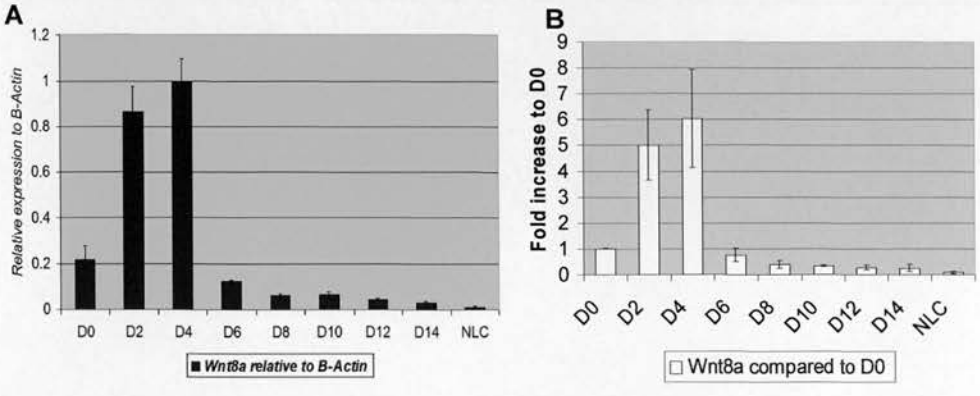

Figure 3.10 Group A - Wnt Expression profile by qRT-PCR. Group A consists of only *Wnt8a*, which is up-regulated during early stages of neural differentiation process (D2 and 4) and seems to be down-regulated upon induction of neural fate. (A) Expression of *Wnt8a* normalized to ß-Actin. (B) Its normalized expression relative to D0 or undifferentiated ES cells. Standard error bars show mean ± SEM from three independent experiments.

NPCs (stage 3) followed by lower expression level of the gene in differentiated neuronal cells (stage 4 and -5). The expression profile of sFRP2 in our assay therefore may imply an inhibitory effect on Wnt signalling by sFRP2 activity during the differentiation process, as demonstrated by the study. However, in overall expression, the expression of *Dkk1* was higher than that of *sFRP2* in this neural differentiation assay. The highest expression level of *Dkk1* was discovered to be 3-fold higher than that of *sFRP2* relative to ß-actin.

3.2.6 Expression profile of Wnt genes by quantitative PCR (qRT-PCR) during neural differentiation *in vitro*

12 of the Wnt genes with an interesting expression pattern demonstrated by RT-PCR results were quantitatively analysed using SYBR green real time PCR (qRT-PCR). Besides Wnt genes, two of the Wnt antagonists, *Dkk1* and *sFRP2*, were also analysed by qRT-PCR. Total RNA from three independent experiments were analysed for the expression of the 12 Wnt genes and the two Wnt antagonists.

Based on qRT-PCR results, the expression of Wnt genes during the differentiation process have been classified into four groups (Table 3.1); group A genes which are expressed at stage 1 and 2 (D2 and D4 EBs), group B genes which are highly expressed at stage 1 (D0/undifferentiated ES cells), 3 (D6 and D8 EBs) and 4 (D10, D12 and D14 EBs), group C genes which were up-regulated at stage 3 and finally group D genes which were highly expressed at stage 4.

3.2.6.1 *Expression of Group A gene: Wnt 8a*

Wnt8a was observed to have a dynamic expression pattern starting from high expression at stage 1 (D0) going to a higher expression level at stage 2 (D2 and D4, Figure 3.10, Table 3.1). Its highest expression level on D4 increased 8-fold compared to its expression on D0. It was found to be down-regulated upon the induction of neural cells. Interestingly the expression was down-regulated in the EBs of stages 3 and 4 after the addition of ATRA with almost no expression detected in NLC. The expression profile agrees with the expression described by RT-PCR (Figure 3.6).

3.2.6.2 *Expression of Group B genes: Wnt 6, -7a and-7b*

Interestingly, Wnt genes in this group showed biphasic expression (Figure 3.11, Table 3.1). Wnt6, -7a and -7b were expressed in undifferentiated ES cells but were down-regulated at stage 2 (D2 and D4), that mainly contains young EBs before the addition of ATRA. The genes seemed to be expressed at high levels of expression starting from D6-D14 for *Wnt6* (1-1.2 fold increase from its expression on D0) and D8-D14 for *Wnt7a* and *Wnt7b* (1.5-2 and 5-6 fold increase from their expression on D0, respectively). However, the expression of *Wnt6* was detected at low level in NLC while *Wnt7a* and *Wnt7b* were detected at high level in these cells indicating both genes were expressed in neuronal cells.

3.2.6.3 *Expression of group C genes: Wnt1, -3a and -10b*

The expression of Wnt genes in this group were upregulated at stage 3 (Figure 3.12, Table 3.1). *Wnt1, Wnt3a* and *Wnt10b* exhibit the highest expression level on D6-10, two days after the addition of ATRA. Very low

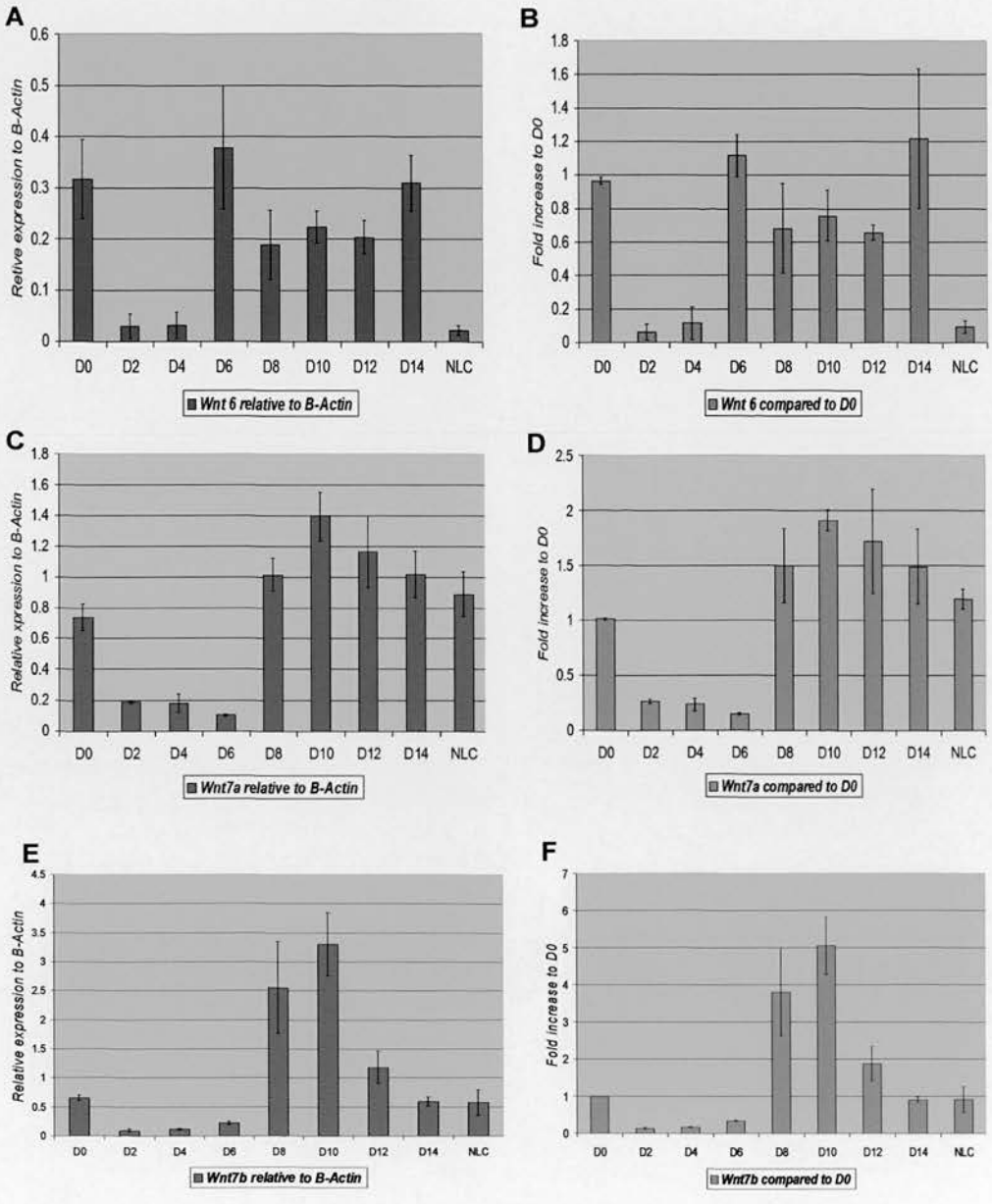

Figure 3.11 : Group B - Wnt Expression profile by qRT-PCR. Group A consists of Wnt genes that were expressed in undifferentiated ES cells (D0) followed by down-regulation of the expression in early stages of neural differentiation process. The expression was then up-regulated either on D6 or D8. (A, C and E) Expression of *Wnt6, Wnt7a* and *Wnt7b* normalized to *ß-Actin*, respectively. (B,D and F) Expression of the respective genes (normalized to *ß-actin*) relative to D0 or undifferentiated ES cells. Standard error bar is the mean ± SEM from three independent experiments.

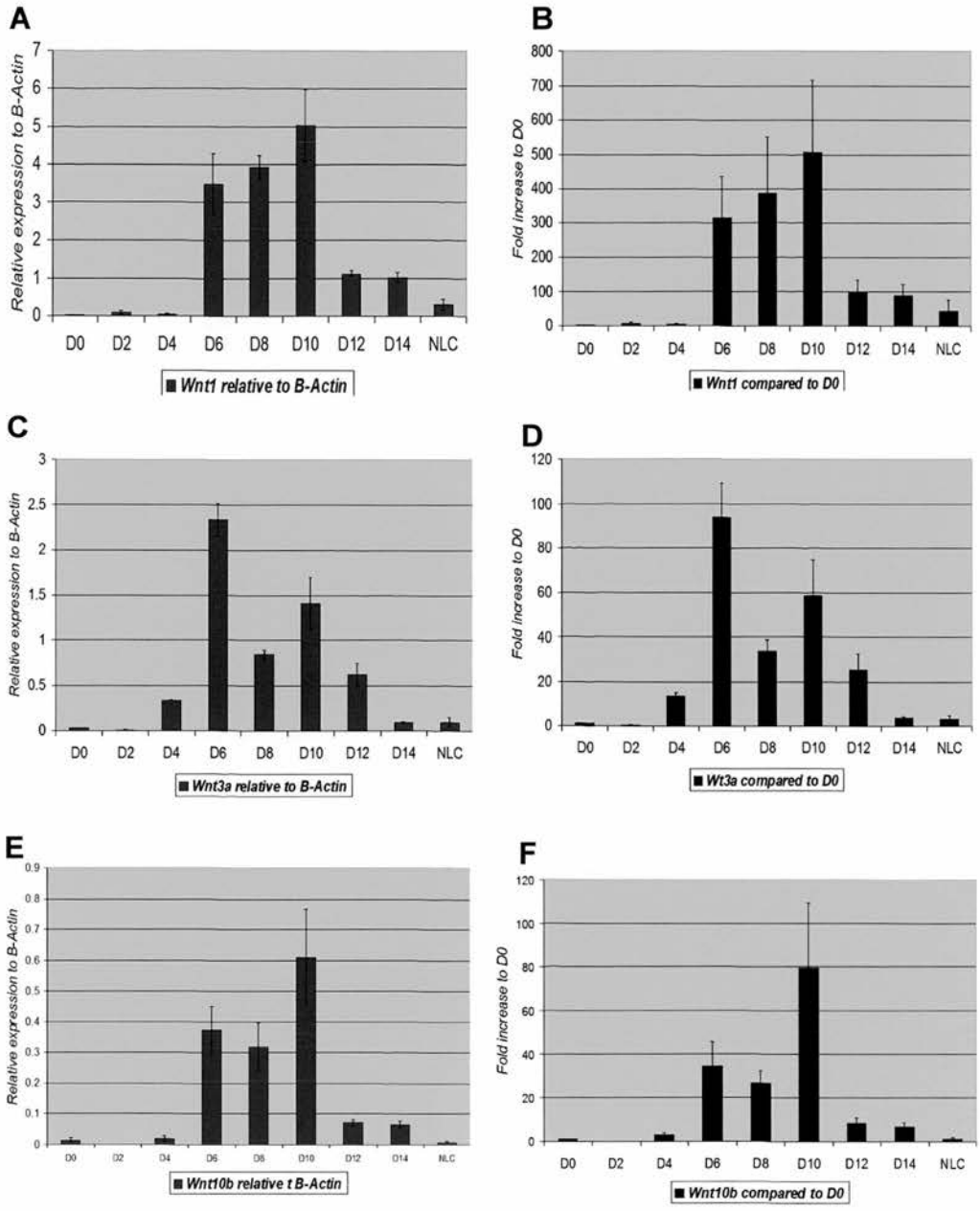

Figure 3.12. : Group C - Wnt Expression profile by qRT-PCR. Quantitative reverse-transcription polymerase reaction (qRT-PCR) was carried out from total RNA extracted from EBs D0-14 and neuron-like cells (NLC). Group C consists of Wnt genes that seem to be RA-induced or up-regulated after the addition of RA. (A, C and E) The expression of *Wnt1, Wnt3a* and *Wnt10b* normalized to ß-Actin, respectively. (B, D and F) ß-Actin normalized expression of *Wnt1, Wnt3a* and *Wnt10b* relative to D0 or undifferentiated ES cells, respectively. Standard error bar is the mean ± SEM from three independent experiments.

expression of these genes was detected in undifferentiated ES cells (D0). Their expression was downregulated in stage 4 EBs (D12-14), which mainly consist of attached EBs with the formation of neurites outgrowth, and stage 5, neuron-like cells (stage 5). The highest expression of *Wnt1* was determined to be on D10 as shown by relative expression to ß-Actin, which is an increase of 500 fold from undifferentiated ES cells (D0). Wnt3*a* was expressed at the highest level on D6 which is an increase of 93 fold as compared to D0. With an increase of almost 80 fold from undifferentiated ES cells, *Wnt10b* reached its maximum expression level on D10. Comparatively, it was also noted that *Wnt1* was highly expressed followed by *Wnt3a* with *Wnt10b* being the lowest expressed gene of this group in this neural differentiation assay. These results demonstrate dynamic gene expression profiles for *Wnt1, 3a* and *10b* with their highest level of expression seen in the highest percentage of cells expressing Sox1-GFP (Figure 3.5 and 3.6).

3.2.6.4 Expression of Group D genes: Wnt2b, -4, -5a, -14 and -11

All genes in this group showed high level of expression at stage 4 (Figure 3.13, Table 3.1). Low level expression of these genes was seen in undifferentiated ES cells (D0) and EBs before the addition of ATRA, on D2 and D4. Their expression was then up-regulated on or after D8. For *Wnt2b, -4* and *-11*, high expression was detected at stage 4 (D10, D12 and D14) which mainly consists of attached EBs (Figure 3.2 and 3.3). However these three genes were expressed at a low level at stage 5 which mainly consists of neuronal cells (Figure 3.4). This most likely indicates that the expression of these genes occurred in non-neural cells since the attached EBs (stage 4) consist of heterogeneous populations as compared to more homogeneous neuronal cells of stage 5. Among the three genes, *Wnt 11* was found to have

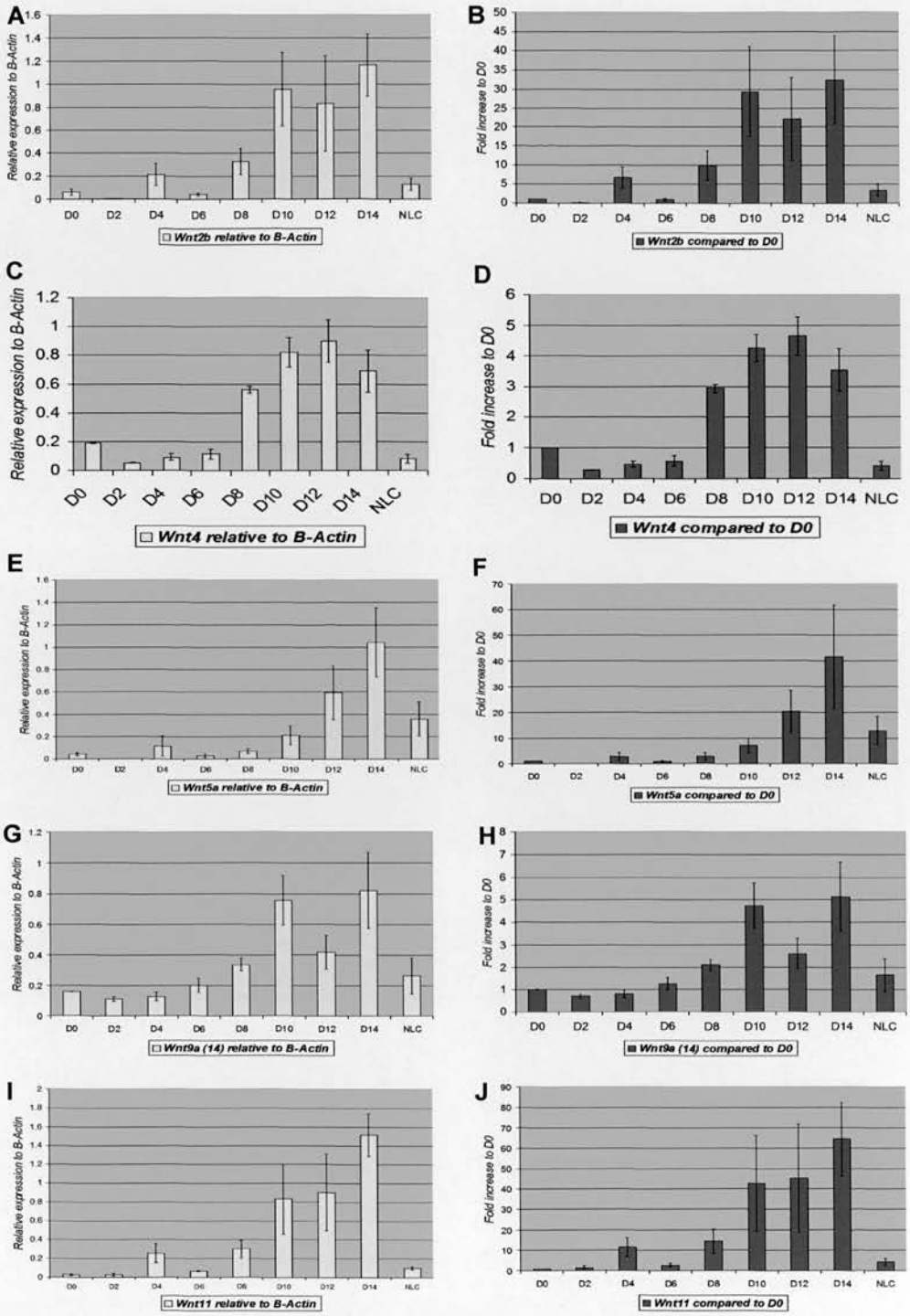

Figure 3.13. : Group D - Wnt Expression profile by qRT-PCR. Group D consists Wnt genes that were up-regulated either on or after D8 EBs. (A, C, E, G and I) Expression of *Wnt2b, Wnt4, Wnt5a, Wnt9a(14)* and *Wnt11* normalized to *ß-Actin*, respectively. (B, D, F, H and J) Expression of the respective genes (normalized to *ß-actin*) relative to D0 or undifferentiated ES cells. Standard error bar is the mean ± SEM from three independent experiments.

the highest increase of expression as compared to D0 (on D14). Its expression was increased 60 fold while *Wnt2b* has an increase of 33 fold from their expression on D0. The highest *Wnt4* expression (on D12) was only 4.5 fold increased compared to its expression on D0.

The other gene in this group, Wnt*5a*, was up-regulated at the very late stage of the differentiation process (D12 and D14 EBs) and also in neuron-like cells population. Its highest expression was detected on D14 with an increase of 40 fold compared to the expression on D0. The gene was also expressed in NLC with an increase of more than 10 fold (Figure 3.13) compared to its expression on D0 which highly suggests that Wnt5a is expressed in neuronal cells. Lastly, group D also includes *Wnt9a* which was upregulated at stage 3 with high expression level detected on D8 onwards including NLC.

3.3 Discussion

3.3.1 Neural differentiation of ES cells

In this study a favoured protocol for differentiating ES cells into the neural lineages that involves the treatment of three dimensional multicellular aggregates, embryoid bodies (EBs), with *all-trans* retinoic acid (ATRA) was applied (Strubing *et al.*, 1995; Fraichard *et al.*, 1995; Bain *et al.*, 1995; Li *et al.*, 1998a). The protocol involves growing the EBs to maturity in the absence of LIF, in the presence of serum, for four days prior to RA treatment for another four days (4-/4+ protocol, Bain *et al.*, 1995). In this protocol, the events occurring during the first 4 days, prior to ATRA treatment, in culture are thought to parallel those occurring between embryonic days 4-6 (E4-6) [Doetschman *et al.*, 1985; Shen and Leder, 1992; Coucouvanis and Martin, 1995; Bielinska *et al.*, 1999; Duncan *et al.*, 1997]. One of the major events

occurring at this stage is the expression of a transcription factor for pluripotent embryonic cells, *Oct-4* (Scholer *et al.*, 1990; Rosnier *et al.*, 1990; Shen and Leder, 1992; Ovitt and Scholer, 1998). In an embryo its expression is downregulated between E5 and E8 (Ovitt and Scholer, 1998). In this study, its expression was also observed in undifferentiated ES cells, which are pluripotent cells, and downregulated as the EBs mature, as previously demonstrated (Shen and Leder, 1992; Niwa *et al.*, 2000).

Upon neural induction, after the addition of ATRA, gene expression studies also have indicated that the stages of differentiation in EBs recapitulate that of the embryo (Gottlieb and Huettner, 1999). One of the genes that are expressed during early neural development within approximately one day of the neural plate formation (E8) is *Wnt1* (Wilkinson *et al.*, 1987; McMahon and Bradley, 1990; Thomas and Capecchi, 1990). In our study as well as in Bain *et al.*, 1996, *Wnt1* expression was detected two days after the addition of ATRA.

In addition, the protocol also generated cells expressing *Sox1*-GFP positive cells as previously described (Aubert *et al.*, 2002; Stavridis and Smith, 2003). More than 60% of cells expressing *Sox1*-GFP were detected on D6 and D8 in this study (Figure 3.6). RT-PCR results also showed high expression of *Sox1* being detected on D6 and D8, thus indicating formation of dividing neural precursor cells. A week after plating the dissociated D8 EBs onto an adhesive substratum, positively stained cells for class III ß-tubulin (Figure 3.4) were observed as previously demonstrated (Bain *et al.*, 1995; Li *et al.*, 1998a). The same phenomena were also observed in differentiation of a human teratocarcinoma (NT2) (Pleasure *et al.*, 1992) and D3 ES cell line (Bain

et al., 1995) into neurons using retinoic acid, RA. Besides the expression patterns of *Oct4*, *Wnt1* and *Sox1*, we also observed an upregulation of *Pax6* expression (a homeodomain protein present in neural tube, Novitch *et al.*, 2003), in EBs after ATRA treatment (data not shown) as previously demonstrated (Gajovic *et al.*, 1997; Li *et al.*, 1998a; Bibel *et al.*, 20004). Taken together, the expression patterns of these genes in this study demonstrate that the protocol was successfully carried out in directing the differentiation of mouse ES cells to neural lineage and that the differentiation process may, in part, recapitulate that of the early stage of embryogenesis *in vivo*.

3.3.2 Expression of Wnts and Wnt antagonists

Due to the unavailability of good antibodies against Wnt proteins, analysis for Wnt gene RNA expression profile became the method of choice. Wnt gene RNA expression was identified at a particular time points during the differentiation of mouse ES cells into neurons. The expression level of all 19 mouse Wnt genes were first analysed by RT-PCR. Gene expression level for Wnt genes with interesting expression profiles were then further quantified by qRT-PCR. In this study, expression levels of *Wnt1, -2b, -3a, -4 ,-5a, -6, -7a, -7b, -8a, -9a, -10b* and *-11* from five different stages during neural differentiation of 46C ES cells *in vitro* were quantitatively analysed. Together with these Wnt genes, two Wnt antagonists which have been shown to be involved in the neural differentiation process (Aubert *et al.*, 2002; Diep *et al.*, 2004; Watanabe *et al.*, 2005), *Dkk1* and *sFRP2*, were also subjected to qRT-PCR analysis.

Expression profile for each of the 19 Wnt genes was monitored at five different stages. As the formation of EBs contains all three primary germ

layers (Weiss and Orkin, 1996; Rathjen and Rathjen, 2002), it is very important to note that they give rise to highly heterogeneous cell populations for each stage. Stage 1 (D0) consists of cells which mainly are *Oct4* positive and *Sox1* negative, indicating that the majority of the cells are undifferentiated ES cells. Stage 2 (D2 and D4) consists of the cells of immature EBs before the addition of ATRA that are *Sox1* negative with downregulation of *Oct4* expression. Being exposed to ATRA, at stage 3 (D6 and D8) most cells expressed high level of *Sox1* and very minute expression of *Oct4* indicating the majority of cells might be neural precursor cells (NPCs). After the withdrawal of RA and grown in high density of EBs, most EBs at stage 4 (D10, D12 and D14) were attached to the dish with the formation of neurite growth. The majority of the cells in this population are both *Oct4* and *Sox1* negative indicating the absence of pluripotent cells and NPCs. Finally, containing many ß-tubulin positive cells, stage 5 is highly occupied by neuronal cells. It seems that stage 5 and 4 contain a proportion of neuronal cells, even though cells at stage 4 are more heterogenous with more types of non-neuronal cells.

3.3.2.1 Expression of Wnts and Wnt antagonists at Stage 1

The first stage of neural differentiation process in this study involves the propagation of undifferentiated ES cells. These cells, that are pluripotent, are originally harvested from preimplantation state, specifically the ICM of the blastocyst in the mouse embryo day 3.5-4.5. A good proliferative state of these uncommitted ES cells, which are maintained in the presence of LIF, is essential in directing the differentiation process into enriched neural lineage (Bibel *et al.*, 2004). However, even in the present of LIF, spontaneous differentiation of the cells might also occur (Stavridis and Smith, 2003).

Comparison of Wnt gene expression in the ES cells *in vitro* to that of the ICM in the mouse embryo may therefore provide some information regarding the probable function of a particular Wnt gene in maintaining the pluripontentiality of ES cells *in vitro*. Activation of Wnt signalling has been shown to be sufficient in maintaining the pluripotency of mouse ES cells (Sato *et al.*, 2004). Besides that localization of ß-catenin in the nucleus of the ICM has also been demonstrated (Wang *et al.*, 2004) which indicates the activation of canonical Wnt pathway in these cells.

In the present study, a high level expression of *Wnt5b, -6, -7a -7b, -8a* and *-16* was detected by RT-PCR at this stage. A low level expression of *Wnt3, -4, -5a, -9a, -9b, -10* and *-11* was also detected by RT-PCR as well as by qRT-PCR, except for *Wnt3* which was not analysed by this method. Interestingly, expression of most of these genes, in particular *Wnt3, -3a, -4, -5a, -5b, -6, -7a, -7b, -10a* and *-11*, has also been detected at RNA level in the mouse blastocyst by other studies (Llyod *et al.*, 2003; Mohamed *et al.*, 2004; Hamatani *et al.*, *et al.*, 2004; Wang *et al.*, 2004; Kemp *et al.*, 2005). Among the studies, the most striking one is the recent study by Kemp *et al.*, 2005 that showed *Wnt7b*, among other genes, to be highly expressed in the whole blastocyst (E3.5 embryo) including the ICM as showed by qRT-PCR and whole-mount in situ hybridisation. Interestingly, *Wnt7b* was also highly expressed in our undifferentiated ES cells as indicated by RT-PCR and qRT-PCR (Figure 3.8 and 3.11). The expression of *Wnt7b* hence may indicate its probable function in maintaining the pluripotentiality of ES cells. Besides that, they also detected high expression of *Wnt1, -3a, -6, -10b* and *-9a* in the blastocyst. In our study, however, *Wnt6, -7a, -7b* and *-8a* were found to be expressed at high level in undifferentiated ES cells. The high level expression in different

type of Wnt genes detected in both populations may indicate the different role of specific Wnt genes *in vitro* compared to their role *in vivo*. On the other hand this might also indicate that these Wnt genes were expressed in the differentiated cells as a result of spontaneous differentiation that occurred in the cultures.

Multiple gene expression detected in undifferentiated ES cells in this study may also indicate redundant roles or different roles that may be acting through different Wnt pathways. Our qRT-PCR results also reveal the expression of Wnt genes that are known to activate the canonical (*Wnt6, Wnt7a Wnt7b and Wnt8a*) and non-canonical (*Wnt7a*) pathway. Interestingly, a study by Kemler *et al.*, 2004 also has suggested a possible role of Wnt pathways in the development of pre-implantion embryos by acting through ß-catenin independent pathway. The study showed mouse embryo constitutively expressing a stabilized form of ß-catenin did not exhibit localization of the mutated protein in the nuclei of preimplanttaion embryos suggesting the expression of multiple Wnt genes at this stage may indicate the possible functions of certain gene through non-canonical pathway. The expression of multiple Wnts in our study may also suggest the function of certain genes acting through different Wnt pathways.

3.3.2.2 Expression of Wnts and Wnt antagonists at stage 2

Based on gene expression studies, the outer layer of EBs at this stage strongly resembles the visceral endoderm (VE), which is the first layer to form in the postimplantation embryo E.5.5 prior to the start of gastrulation at E6.5 (Bielinska *et al.* 1999; Duncan *et al.*, 1997; Gottlieb and Huettner, 1999). During early gastrulation, the pluripotent epiblast (the ICM) cells are

allocated into the three primary germ layers (ectoderm, mesoderm and definitive endoderm) of the embryo (Loebel *et al.*, 2003), where expression of *Wnt2b, -3,* and *-8a* are highly expressed (Takada *et al.*, 1994; Bouillet *et al.*, 1996; Zakin *et al.*, 1998; Kemp *et al.*, 2005). Migration of the visceral endoderm cells from the distal tip of pre-gastrula embryo to the presumptive anterior side forming the anterior VE was defected in ß-catenin mutant mouse (Huelsken *et al.*, 2000). This may highly suggest the role of canonical Wnt signalling in the process which might explains the expression of these genes at this period. Interestingly enough, these genes were also detected at high level in our study (Figure 3.8) which may signify their role in the process *in vitro*.

In addition, lack of mesoderm has also been demonstrated in *Wnt3*- and *ß-catenin* mutant embryos indicating the role of Wnt signalling in axis formation. Therefore, expression of *Wnt3* and *Wnt8a* are most likely to indicate the presence of mesodermal layer in the EBs at this stage of neural differentiation process. In agreement to this, Brachyury, a gene marker for early mesodermal that is transiently expressed during gastrulation, is also highly expressed around D4 in EBs (Rohwedel *et al.*, 1994,1998a,b, 1999). The very strong Wnt antagonists, *Dkk1* and *sFRP2* were also observed in this study. Interestingly, expression of Dkk1 has also been found in the anterior VE (Pearce *et al.*, 1999; Zakin *et al.*, 2000), which highly explains the high expression level of the gene in our study. Even though analysis of *Dkk1* mutant phenotypes did not reveal its requirement for the formation of the head at the early gastrulation stage in mouse embryo (Mukhopadhyay *et al.*, 2001), study in zebrafish has demonstrated a crucial function for *Dkk1* for specification of the anterior nervous system and axial mesendedorm

(Hashimoto *et al.*, 2000). In another study, a member of sFRP family, *tlc*, has also showed the requirement of this gene for the initial formation of the anterior brain in zebrafish (Houart *et al.*, 1998, 2002). In frog, another Wnt antagonist, *Cerberus*, has been found to antagonize Wnt signalling and expressed in the endoderm region that is equivalent to the mouse anterior VE (reviewed in Shibata *et al.*, 2000). These studies therefore demonstrate the important of inhibitory of Wnt signalling in the initial patterning of the anterior brain, which might explain the probable function of *Dkk1* and *sFRP2* in our cultures.

On the other hand, overexpression of *Dkk1* has also been shown to promote anterior neuroectoderm in zebrafish indicating Wnt inhibitory effect on the formation of neuroectoderm. Overexpression of *sFRP* also has been shown to promote the formation of neural progenitors in ES cells (Aubet *et al.*, 2002). The high expression of these two genes therefore may highly indicate the inhibitory effect on Wnt signalling at this stage of neural differentiation process in this study. In addition, expression of neurectodermal markers, *Pax6* and *Mash1*, have also been shown to be expressed during early stages of EBs development as early as day one (Rohwedel *et al.*, 2001) indicating the formation of neuroectodermal cells at this stage. With the possible inhibitory effect showed by the expression of Wnt antagonists, Dkk1 and sFRP2, at this stage, it is therefore reasonable to suggest that this might explain the smaller number of Wnt genes that were highly expressed at this stage. Hence this might suggest the possible role of Wnt signalling in inhibiting the differentiation of ES cells to NPCs *in vitro*. Out of 12 genes that were screened by qRT-PCR, only four genes were highly expressed at this stage.

3.3.2.3 Expression of Wnts and Wnt antagonists upon neural induction

Stages 3, 4 and 5 in the differentiation process involved the enhancement of neural lineage by ATRA treatment. Previous study has shown that differentiation rate for neuronal cells increased 100% after the induction by ATRA compared to only 15-30% of spontaneous neuronal differentiation frequency in cultured EBs (Strubing *et al.*, 1995). In addition, the application of ATRA at high concentrations (10^{-6} to 10^{-7} M) not only significantly increased neuronal differentiation but also repressed mesodermal differentiation (Bain *et al.*, 1995, 1996; Fraichard *et al.*, 1995; Strubing *et al.*, 1995). In a study where RA-treated EBs were transplanted into a chick neural tube, the authors found that RA appears to restrict the ES-cell derived progenitors to the CNS fate (Plactha *et al.*, 2004). RA-treated EBs also have been shown to generate a variety of neural cells including excitatory and inhibitory neurons and glial (Fraichard *et al.*, 1995; Strubing *et al.*, 1995; Finley *et al.*, 1996). However, RA is believed to have posteriorizing effect during neural development (Blumberg *et al.*, 1997). It has been used to induce posteriorization of ES-cell-derived NPCs (Barberi *et al.*, 2003) and differentiation into motorneurons (Wichterle *et al.*, 2002) and interneurons (Renoncourt *et al.*, 1998). On the other hand, with suitable concentration of ATRA and a good proliferative state of the starting uncommitted ES cells, Bibel *et al.*, 2004 have manage to induce cortical pyramidal neurons. These results therefore imply that RA-treated EBs are able to induce the formation of different type of neurons present in the CNS *in vitro*.

Previous studies have demonstrated the CNS as the primary regions for the expression of numerous Wnt genes (Wilkinson *et al.*, 1987; Roelink and

Nusse, 1991; McMahon *et al.*, 1992a,b; Salinas and Nusse, 1992; Parr *et al.*, 1993) which suggest that Wnt signalling plays significant roles in the early development of the CNS *in vivo*. Numerous dynamic expressions of Wnt genes also were detected upon neural induction in this study which highly suggests the importance of Wnt signalling in neural development of ES cells *in vitro*.

A study by Chenn and Walsh, 2002 has suggested the regulation of *ß-catenin* on the proliferation of neural stem cells. In their study, progenitor cells that were constitutively expressing a stabilized form of ß-catenin produced high number of NPCs suggesting a role of canonical Wnt pathway in proliferation of neural progenitors in the mouse embryo brain. Interestingly, we discovered that expression of *Wnt1, -3a, -7a, -7b, and -10b,* which are known to activate canonical Wnt pathway, was upregulated at stage 3 (D6 and D8 EBs) which consists mainly of NPCs. The expression of these genes therefore may highly signify their role in maintaining or stimulating the proliferation of NPCs *in vitro*. In agreement to this, expression of these genes were also detected at the early stage of neural tube development *in vivo* (Parr *et al.*, 1993) which highly to suggest that the neural differentiation in EBs recapitulates that of the embryo. *Wnt1 and Wnt3a* also have been shown to promote cell proliferation in the neural tube (Dickinson *et al.*, 1994; Ikeya *et al.*, 1997). A recent study involving overexpression of *Wnt7a* in neural progenitor cells also showed an early defect in neurulation during E8.5 and E10.5 embryos (Shariatmadari *et al.*, 2005). They observed a striking disruption of adherens junctions which resulted in incomplete cranial and spinal neurulation, and interestingly the defect was found to be activated through non-canonical Wnt signalling. These studies hence might highly

suggest the important function of these Wnt genes in ensuring the proper formation of neural tube hence on the proper development of the CNS through the activation of both non- and canonical pathways.

In contrast to the study by Chenn and Walsh, 2002, a study by Muroyama and colleagues (2004) on the role of *Wnt3a* on the expansion of the number of neurosphere-forming neural stem cells derived from the telencephalon of E11.5 mouse embryos *in vitro* suggested the opposite. In the study, the authors discovered that treatment with Wnt3a conditioned medium on the dissociated telencephalic cells decreased the number of newly-formed neurospheres in culture condition. High expression of *Wnt3a* in NPCs in our culture therefore may suggest a function of the gene that agrees with Chen and Walsh. The agreement might indicate that the proliferation process of NPCs in our culture recapitulates the proliferation process *in vivo*. Further examination on effect of overexpressing Wnt3a during neural differentiation process of ES cells in culture would lead us to some explanation regarding this matter.

As development proceeds, more Wnt genes were highly expressed at stage 4 especially at the beginning of the stage (D10 and D12) compared to the late period of stage 4 (D14) and stage 5. We found *Wnt2b, -4, -5a, -9a* and *-11* in addition to *Wnt1, -3a, -7a* and *-7b* to be highly expressed at stage 4, while Wnt1, -5a, -7a, -7b and -9a were highly expressed in the cells at stage 5. It is believed that these genes were highly expressed in neuronal cells since the formation of neurites growth was observed at these stages. Various studies have implicated the roles of Wnt genes in promoting differentiation of neural stem cells/progenitor cells *in vivo*. In a study by Israsena *et al.*, 2004, the

authors discovered that overexpression of ß-catenin or of a constitutively active form of ß-catenin from E14 neural progenitors from lateral and medial ganglionic eminence significantly increased the number of ß-tubulin neurons and significantly decreased the number of nestin cells. In agreement to the study, another study also showed that overexpression of a stabilized form of ß-catenin together with overexpression of Wnt7a in NPCs prepared from the dorsal cerebral cortex of mouse embryos at E11.5 also induced neuronal differentiation (Hirabayashi *et al.*, 2004). These studies therefore suggested a significant role of canonical Wnt signalling in promoting neuronal differentiation of NPCs. The study is supported by work by Muroyama and colleagues which demonstrated the function of *Wnt3a* in promoting neuronal differentiation of neural stem cells harvested from E11.5 telencephalic cells in culture (Muroyama *et al.*, 2004). Besides that the group also showed the important role of Wnt signalling in neuronal specification of the dorsal spinal cord (Muroyama *et al.*, 2002). Taken together, these studies clearly suggest the important role of Wnt signalling, particularly the canonical Wnt pathway in promoting differentiation of NPCs into neurons. Hence, this may significantly implies the function of those highly expressed Wnt genes in our culture, especially *Wnt3a and Wnt7a,* in promoting the differentiation of NPCs into neurons. Functional analysis such as overexpression of these genes at this point might reveal their role regarding this matter.

3.4 Conclusion

This study has revealed the expression of numerous Wnt genes with interesting dynamic patterns during neural differentiation process of ES cell in culture. We have also shown that the expression pattern of most genes temporally agrees with the expression pattern of Wnt genes during early

development of the CNS in the embryo. We also have categorized the expression pattern of the 12 Wnt genes screened by qRT-PCR into 4 groups (Table 3.1) and identified the pathways that are known to be activated by the genes. We also discovered that Wnt antagonist, Dkk1 and sFRP2 were highly expressed at all stages upon development of EBs. However, there are limitations from what can be learned from the analysis in this study.

The analysis was only done based on the RNA harvested from a complex structure of EBs, which contain highly heterogeneous cells. The expression of all genes was displayed relative to ß-actin which is highly expressed in most cells in the EBs. Therefore, the relative expression may not all be presenting the actual RNA expression of particular functional gene especially if the particular gene is only expressed in a few localized cells in the EBs. The RNA expression from this gene would be misidentified since its relative expression would be very small. Therefore the analysis could not tell us where exactly the cells are expressed.

Wnts are secreted proteins which act extracellularly. Our analysis which only based on RNA expression therefore does not give the information on the functional properties of each expressed gene at particular stage during the differentiation process. The gene expression also does not lead us the information of which Wnt pathway is actually active even though the analysis does give us the idea that different pathways might be involved during the process.

In summary, the analysis, however, does give us the information on which of the Wnt genes that are highly expressed during the process. Upon neural

induction, the study has highly suggested the probable function of *Wnt1, -3a, -6, 7a* and *7b* in maintaining or promoting the proliferation of NPCs (stage 3) while *Wnt5a* and *Wnt9a* in addition to *Wnt1, -3a, 6, 7a* and *7b* may have certain function in neuronal differentiation of NPCs or ES cells in vitro. Manipulation of Wnt signalling through both pathways by overexpression of these particular genes or inhibition of the pathway by overexpression of Wnt anatagonist at specific time point during the process might lead us some answers.

Chapter 4: Characterization of Inducible and Reporter Gene Expression Systems in ES cells

4.1 Introduction

4.1.1 ES cells inducible expression system

As described in chapter 3, many Wnt genes show dynamic RNA expression profiles during neural differentiation *in vitro*, suggesting the possibility that Wnts may have regulatory roles in this process. Specifically, the activity of Wnt signals may be stage-dependent. Unfortunately, due to the nature of Wnt proteins, the use of their soluble proteins is almost impossible. To date, only purification of soluble Wnt3a protein has ever been used which is in a study to determine the effect of Wnt signalling on self-renewal of haematopoietic stem cells (Willert *et al.*, 2003). Therefore, a system that is able to activate or inactivate the genes in a temporally or spatially controlled manner would be useful in testing their functional properties. Here an inducible expression system would be a valuable tool.

Not many ES cells conditional expression vectors used in previous studies have reported the ability of the system to induce the expression of the transgene in undifferentiated ES cells as well as their differentiated derivatives *in vitro* (Whyatt *et al.*, 1993; Zhang *et al.*, 1996; Niwa *et al.*, 2000). In this chapter, we report the generation of an inducible expression system in ES cells that allows for further analysis on the functional properties of Wnts at specific time points during differentiation of ES cells. A conditional gene expression system involving *Cre/loxP* site-specific recombination was used. The system has proven to be very useful not only in activating or deactivating specific genes of interest in a spatiotemporally controlled

manner but also useful for elucidating a complete picture of gene function, especially the genes with multiple roles at different times and in different population of cells. Therefore the system offers great advantages for us in conducting further analysis on the functional properties of specific Wnt genes and Wnt antagonist during neural differentiation assay *in vitro*.

We have constructed five plasmids carrying *Wnt1*-HA, *Wnt3a, Wnt5a, Wnt7a* and *Dkk1* and stably-transfected Cre-expressing ES cells with each of them. In this chapter, characterization of these stable integrants will be presented, particularly, the ability of the system to tightly control the expression of these genes in undifferentiated ES cells and in their differentiated derivatives *in vitro*.

4.1.2 Wnt reporter system

Analysis of RNA expression does not tell us which cells are expressing Wnts, and perhaps more importantly which cells are actually responding to Wnt signal. Therefore, it would be useful to have a system that allows for a direct visualization of specific cells that are responding to Wnt signals at a particular time point and in specific cell population. Existing tools for Wnt reporter gene expression such as TOP-FLASH (Korinek *et al.*, 1997), TOP-GAL (DasGupta and Fuchs, 1999) and BAT-GAL (Maretto *et al.*, 2003), which rely on ß-catenin-mediated activation of a reporter gene, have limitations in providing a direct detection of Wnt signals. Detection of LacZ/ß-galactosidase in TOP-GAL and BAT-GAL requires the use of chemical substrate for histological staining such as X-gal that requires the cells to be fixed. Similarly, TOP-FLASH also requires a subsequent analysis in detecting the activity of luciferase which actually relies on the activity of a

control substance such as Renilla. On the other hand, TOP-dGFP (Dorsky *et al.*, 2002) even though is allowing for direct visualization of the signal, it does not permit the visualization of Wnt signal in GFP-expressing cells, which is commonly used in fluorescent protein knock-in cells.

In this study, red fluorescent protein (RFP) was used as a reporter gene, which was activated in response to canonical Wnt signals. The system not only allows for direct visualization of cells that are responding to canonical Wnt signals is but also useful in distinguishing the expression of RFP and GFP (or other GFP spectral variant expressing cells such as ECFP and EYFP) due to its different wavelength spectrum and genetic origin from GFP (Long *et al.*, 2005). The system allows us to examine the cells that are responding to only canonical Wnt signals during neural differentiation assay and at the same time permits us to monitor Wnt response in neural precursor cells (NPC) by using *Sox1*-GFP knock-in ES cells (46C, Chapter 3). In this chapter, the reliability of reporter gene expression in HEK-293 and ES cells will be evaluated. Finally, the system was used to monitor the specific cells that were responding to Wnt signals during neural differentiation of 46C ES cells in culture.

4.2 Results

4.2.1 Tamoxifen-controlled Inducible Expression in ES cells

Our aim for this part of study was to generate an inducible expression system that would be active not only in ES cells but also upon differentiation. We had identified the best available candidate system (Srinivas *et al.*, 2001) and attempted to adopt it for our purposes (Appendix E). This was, however, unsuccessful for technical reasons. The plasmid contains multiple

direct repeats and despite extensive efforts, recombination always made plasmid construction impossible. We therefore adopted an alternative system. A binary system that applied the Cre/*loxP*-based strategy for an inducible gene expression system was then generated (Figure 4.1). The first part of the system is a ubiquitous Cre-ER^{T2} expressing ES cell line, R26CT2S (Grotewold, unpublished). The cre is fused to a mutated ligand-binding domain (LBD) of a human oestrogen receptor (ER^{T2}) and targeted into the ROSA26 locus, which is constitutively active both in un- and differentiated ES cells. As a result of specific point mutations in the LBD, treatment with tamoxifen or synthetic 4'-hydroxytamoxifen (4'-OHT) highly activates Cre expression but not by endogenous oestrogen normally present in the serum used in culture medium (Feil *et al.*, 1997; Indra *et al.*, 1999). The inducibility of cre-recombinase was tested in driving the expression of GFP in a stably-transfected CAG-floxed-Nanog-IRES-*pac*pASTOP-cassette upstream of enhanced GFP (eGFP) coding region in R26CT2S cells (Figure 4.2A, the experiment was carried out by Lars Grotewold). The expression of GFP was observed upon excision of the floxed cassette upon treatment with 4'-OHT (Figure 4.2B). The ability of this cell line, R26CT2S, to drive 4'-OHT-dependent expression of any genes was applied in this study.

The second part of the system involves an inducible expression vector, pCAG-floxed-*neo*pA, which is transfected into R26CT2S cells to generate stable clones (Figure 4.1). The vector pCAG-floxed-*neo*pA contains CAG (a chicken-beta actin promoter associated with cytomegalovirus immediate-early enhancer)-floxed-*neo*-stop sequence upstream of a cloning site followed by an internal ribosome entry site (IRES) to puromycin N-acetyltransferase (*Pac*) [Figure 4.1A]. Exposure to 4'-OHT results in Cre-mediated deletion of

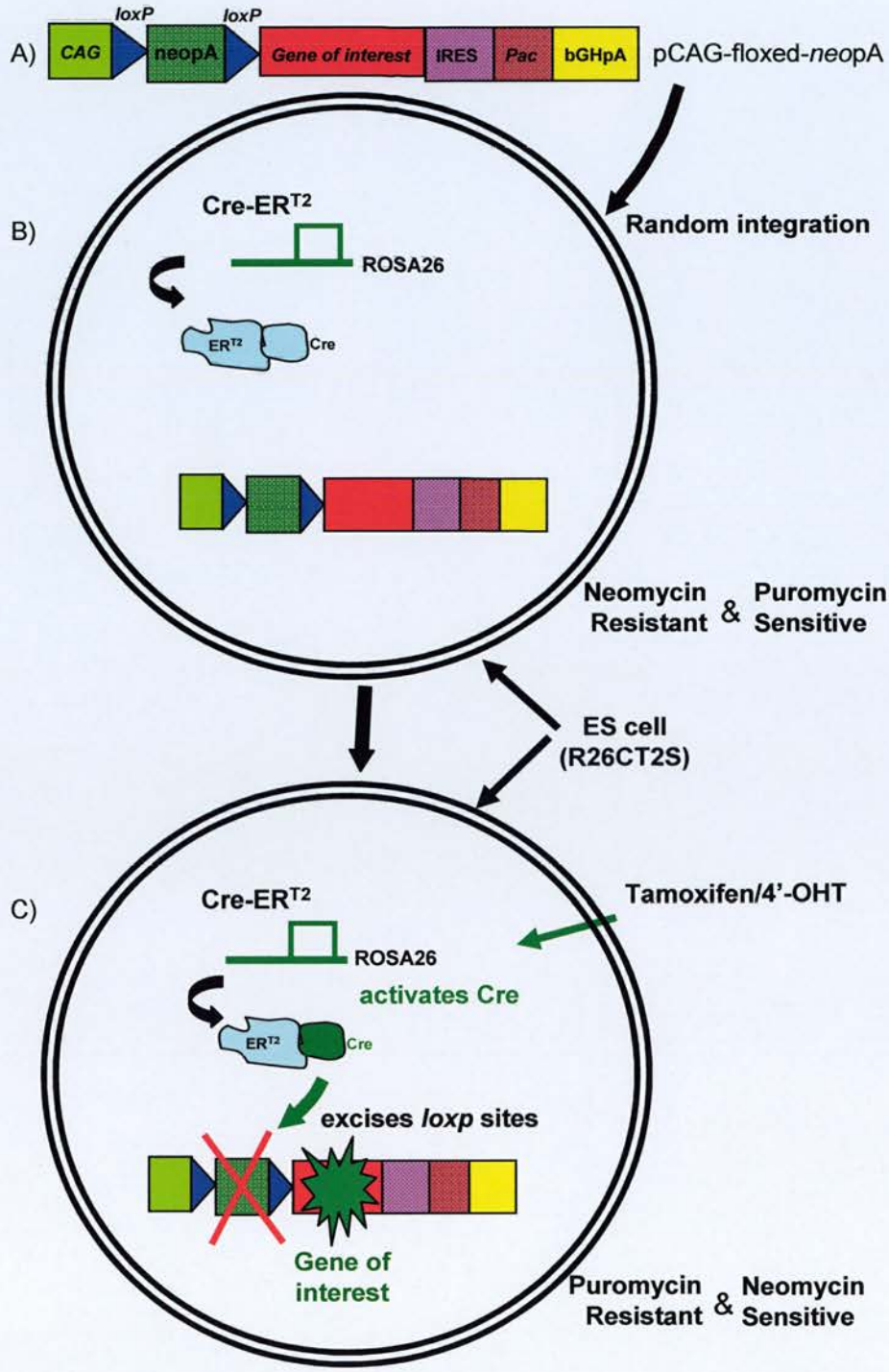

Figure 4.1: Schematic representation of tamoxifen-controlled inducible expression in ES cells. pCAG-floxed-*neo*pA vector carrying a gene of interest (A) is stably transfected into R26CT2S cells (B) by GeneJuice (Novagen) which then makes them resistant to neomycin (G418). Upon treatment with tamoxifen (4'-OHT), Cre-ER^{T2} is activated which then excises the floxed-*neo*-stop cassette (C). The CAG promoter subsequently drives the expression of downstream genes, the gene of interest and the *pac* gene. As a result, the cells become resistant to puromycin.

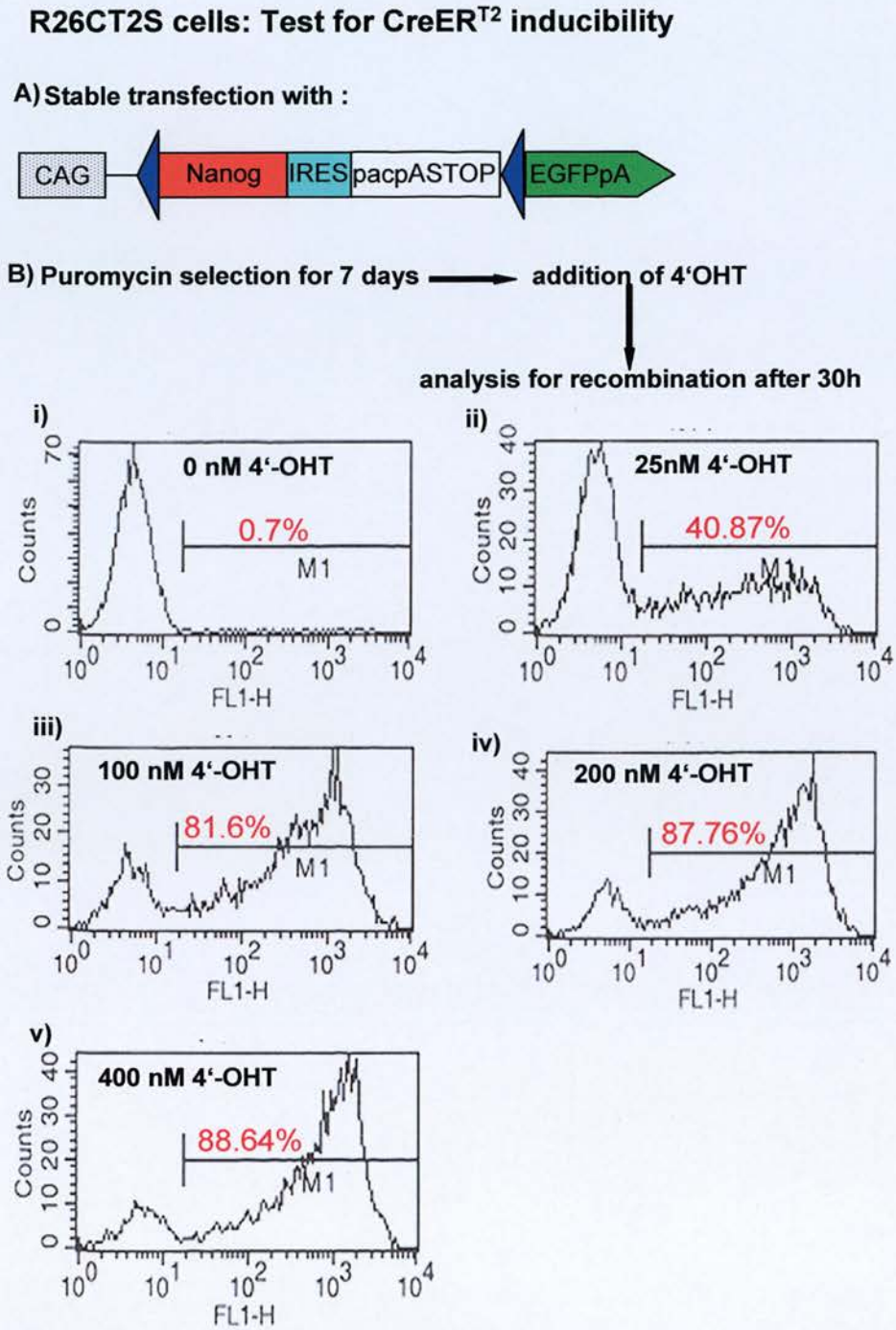

Figure 4.2: Inducibility test for Cre-ER^{T2} was done on stably-transfected R26CT2S cells with pCAG-floxed plasmid (A). B) After selection in puromycin, the clone was treated with different doses of 4'-OHT for 30 hours. The analysis for recombination was then done by FACS. The percentage of cells expressing GFP after treatment with 0 (B-i), 25 (B-ii), 100 (B-iii), 200 (B-iv) and 400 nM of 4'-OHT (B-v) were presented, indicating the efficiency of cre-mediated recombination by 4'-OHT. Diagram and data are from Lars Grotewold, unpublished.

the *neo*-stop cassette and activation of downstream genes (Figure 4.1C). As a consequence, the cells become neomycin (G418) sensitive but are resistant to puromycin. Hence, stable transfection of this plasmid vector into the ubiquitous Cre-ER^{T2} expressing ES cell line, R26CT2S, allows us to tightly control the expression of selected Wnt genes and Wnt antagonists in undifferentiated and differentiated ES cells at any desired time point during neural differentiation process.

4.2.1.1 Generation of stably-transfected pCAG-floxed-*neo*pA ES ell lines

Based on the RNA expression profiles demonstrated in chapter 3, four Wnt genes and one Wnt antagonist, *Dkk1*, were chosen to generate transgenic ES cell lines. For canonical or ß-catenin/Wnt signalling pathway, *Wnt 1* and *Wnt3a* were chosen. *Wnt5a* was chosen as a representative of the Ca^{2+} pathway. Finally, *Wnt7a* which can activate both pathways was also included in the list. To antagonize the endogenous Wnt gene activities, we decided to use *Dkk1*.

In generating pCAG-floxed-*neo*pA vector plasmid carrying these genes, a variety of different transitional vectors were used in order to find the appropriate restriction endonuclease sites (*Xho*I and *Sal*I) as the vector only has one cloning site, *Xho*I (for details in construction of these plamids, refer to Appendix B). *Sal*I was used as it generates compatible 5'-overhangs with *Xho*I. Fortunately, in contrast to pBigT and p9.8 Pac/Asc vectors (Appendix E), pCAG-floxed-*neo*pA vector was much easier to handle and the cloning activities were more straightforward.

4.2.1.1.1 *pCAG-floxed-neopA-Wnt1-HA ES cell line*

Due to the unavailability of a good antibody for Wnt1, we decided to use a haemagglutinin (HA) antigen epitope tagged-*Wnt1*. No negative effect of an HA epitope tag on Wnt1 has ever been reported. In order to generate the pCAG-floxed-*neo*pA carrying *Wnt1*-HA, a 1.3 kb *Wnt1*-HA fragment was excised from *Wnt1*-HA/pBSIIKS$^-$ plasmid (Shimizu *et al.*, 1997) by digestion with *Asp* 718 and *Xba*I prior to cloning into *Asp*718-*Xba*I digested pGEM3zf(+) vector. As a result, a plasmid carrying two *Sal*I sites flanking the *Wnt1*-HA sequence was created. The *Wnt1*-HA fragment used encodes a portion of *Wnt1* 5'UTR upstream of the gene's open reading frame (ORF) immediately followed by the HA sequence. Subsequently, the *Wnt1*-HA fragment was excised by *Sal*I digestion and cloned into the *Xho*I site of a 7.8 kb pCAG-floxed-*neo*pA vector, generating a 9.2 kb pCAG-floxed-*neo*pA-*Wnt1*-HA plasmid (Figure 4.3). Screening for all correct plasmids at each step was done by restriction enzyme digestion (as described in chapter 2 and appendix B). The nucleotide sequence at both of the junctions between the insert and the vector of the correct clone carrying pCAG-floxed-neopA-*Wnt1*-HA was also sequenced.

R26CT2S ES cells were then stably-transfected with the plasmid as described in chapter 2. However, upon induction with 4'-OHT, not all of the clones expressed *Wnt1* when screened by qRT-PCR. Consequently, we decided to test the stability and integrity of the construct by selecting a few of the G418 resistant clones in 1 μg/ml of puromycin (as described in chapter 2) after the clones were treated with 0.5 μM of 4'-OHT. Only clones carrying a stably integrated construct would survive puromycin selection upon excision of the *neo*-stop cassette by 4'-OHT. Out of 6 clones, only two clones survived

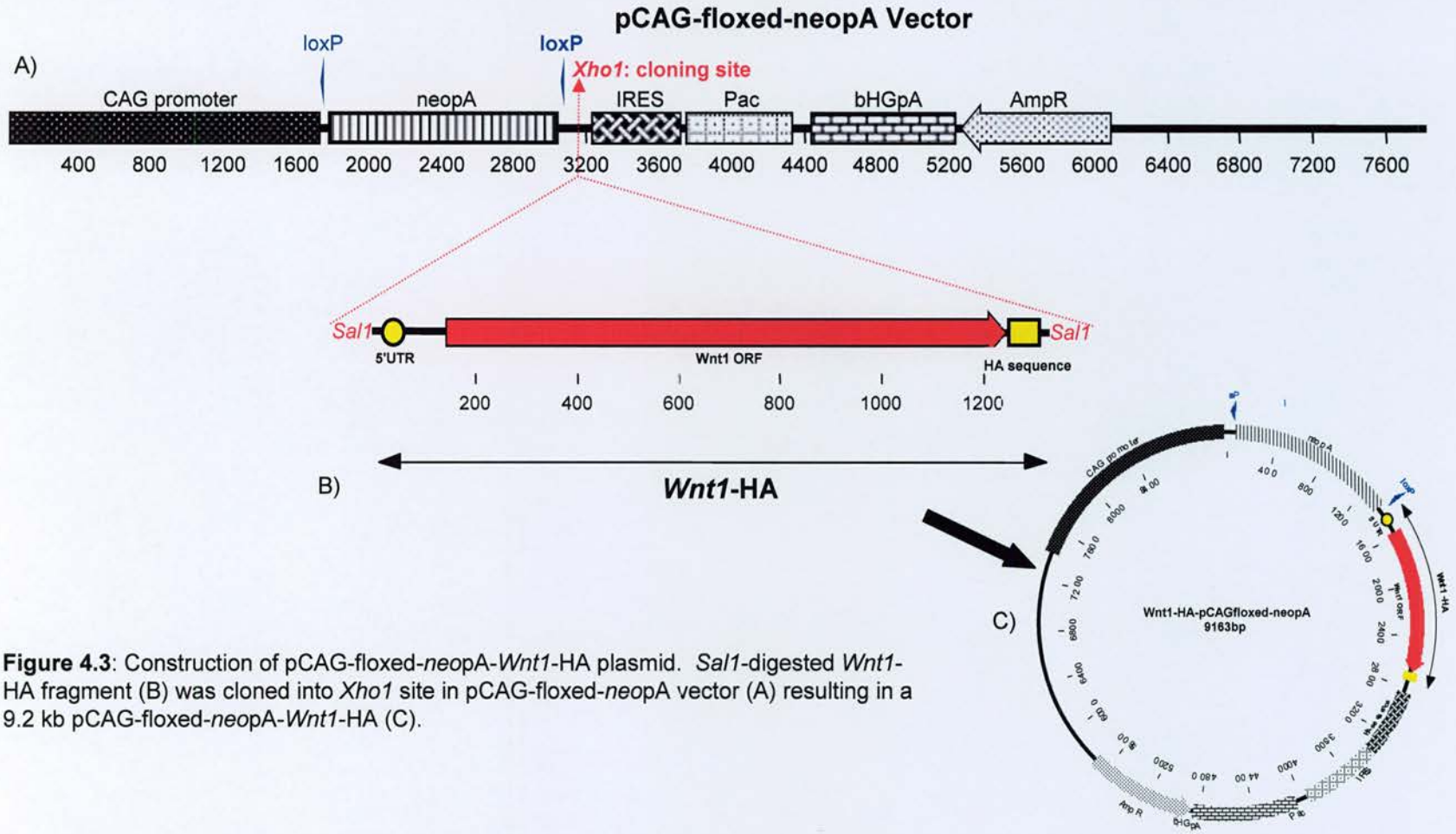

Figure 4.3: Construction of pCAG-floxed-*neo*pA-*Wnt1*-HA plasmid. *Sal1*-digested *Wnt1*-HA fragment (B) was cloned into *Xho1* site in pCAG-floxed-*neo*pA vector (A) resulting in a 9.2 kb pCAG-floxed-*neo*pA-*Wnt1*-HA (C).

puromycin selection which were then referred to as pCAG-*Wnt1*-HA-Tp or constitutively overexpressing *Wnt1*-HA clones. 4'-OHT-untreated cell lines, which were neomycin (G418) resistant, were called CAG-floxed-*neo*pA-*Wnt1*-HA ES cell lines.

4.2.1.1.2 *pCAG-floxed-neopA-Dkk1 ES cell line*

In generating pCAG-floxed-*neo*pA carrying *Dkk1*, *Dkk1* cDNA (0.9 kb) was released from Dkk1/pGEM-T Easy plasmid (a gift from Sarah Millar, University of Pennsylvania) upon digestion with *BamH*I and cloned into *BamH*I site of pBlueScript II KS(+) plasmid. The generated plasmid was then degested with *Asp*718 and *Xba*I prior to subclone into *Asp*718 and *Xba*I sites of pGEM3zf(+) vector. Subsequently, a 0.9 kb *Dkk1* cDNA was excised from this plasmid upon digested with *Sal*1 and cloned into *Xho*1 site of pCAG-floxed-*neo*pA vector (Figure 4.4), resulting in the final 8.7 kb pCAG-floxed-*neo*pA-*Dkk1* plasmid. The correct plasmids for each of the cloning step were screened by restriction enzyme digestions (appendix B). The nucleotide sequence at both of the junctions between the insert and the vector of the correct clones carrying pCAG-floxed-*neo*pA-*Dkk1* was also sequenced.

Screening for stably-transfected R26CT2S cells with pCAG-floxed-*neo*pA-*Dkk1* was conducted as described above. Out of 6 clones that survived G418, only two were resistant to puromycin upon exposure to 4'-OHT. We named these clones pCAG-*Dkk1*-Tp for constitutively expressing Dkk1, and their 4'-OHT-untreated cell lines, which were neomycin (G418) resistant, were called CAG-floxed-*neo*pA-Dkk1 ES cell lines.

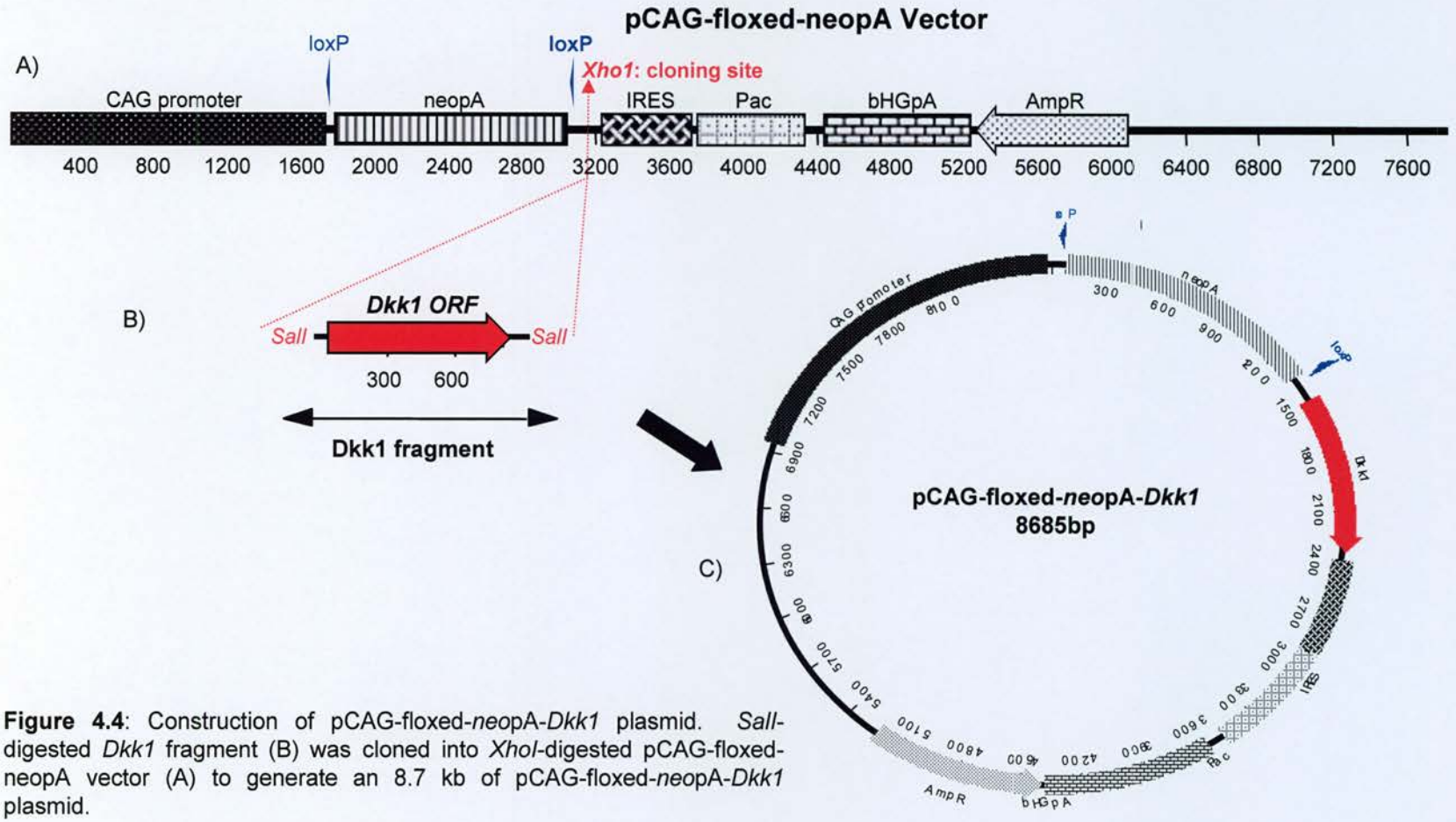

Figure 4.4: Construction of pCAG-floxed-*neo*pA-*Dkk1* plasmid. *Sal*I-digested *Dkk1* fragment (B) was cloned into *Xho*I-digested pCAG-floxed-neopA vector (A) to generate an 8.7 kb of pCAG-floxed-*neo*pA-*Dkk1* plasmid.

4.2.1.1.3 *pCAG-floxed-neopA-Wnt3a ES cell line*

Due to a recent report on the negative effect of HA epitope tag on expression of *Wnt7a* (Hirabayashi *et al.*, 2004), we decided to use untagged-Wnt3a for the construction of transgenic *Wnt3a* ES cell lines despite the unavailability of a good mouse Wnt3a antibody. Unlike for *Wnt1*-HA and *Dkk1*, a different transitional vector was used. We began with excision of 1.5 kb Wnt3a transcript from pCDNA5FRT plasmid by *EcoR*I digestion prior to cloning the transcript into an *EcoR*I site of a transitional vector, pDsRed2-1. A plasmid carrying *Xho*I and *Sal*I sites flanking the Wnt3a transcript was thereby generated. Subsequently, the 1.5 kb insert containing the *Wnt3a* fragment was excised by *Sal*I-*Xho*I digestion and cloned into the *Xho*I site of the 7.8 kb pCAG-floxed-*neo*pA vector, generating a 9.3 kb pCAG-floxed-*neo*pA-*Wnt3a* plasmid (Figure 4.5). Screening for all correct plasmids at every step was done by restriction enzyme digestion (as described in chapter 2 and appendix B).

Screening for stably-transfected R26CT2S with pCAG-floxed-*neo*pA-*Wnt3a* began with selection in G418 (chapter 2). The clones were subsequently screened by selection in puromycin after being treated with various concentrations of 4'-OHT, as described in chapter 2. Out of 11 clones, only 4 survived puromycin selection. These were named CAG-*Wnt3a*-Tp ES cell lines. Their 4'-OHT-untreated cell lines, which were neomycin (G418) resistant, were named CAG-floxed-*neo*pA-*Wnt3a* ES cell lines

4.2.1.1.4 *pCAG-floxed-neopA-Wnt5a ES cell line*

A more direct strategy was applied in constructing pCAG-floxed-*neo*pA-*Wnt5a* plasmid. In generating the plasmid, a 2.5 kb of *Wnt5a* cDNA was

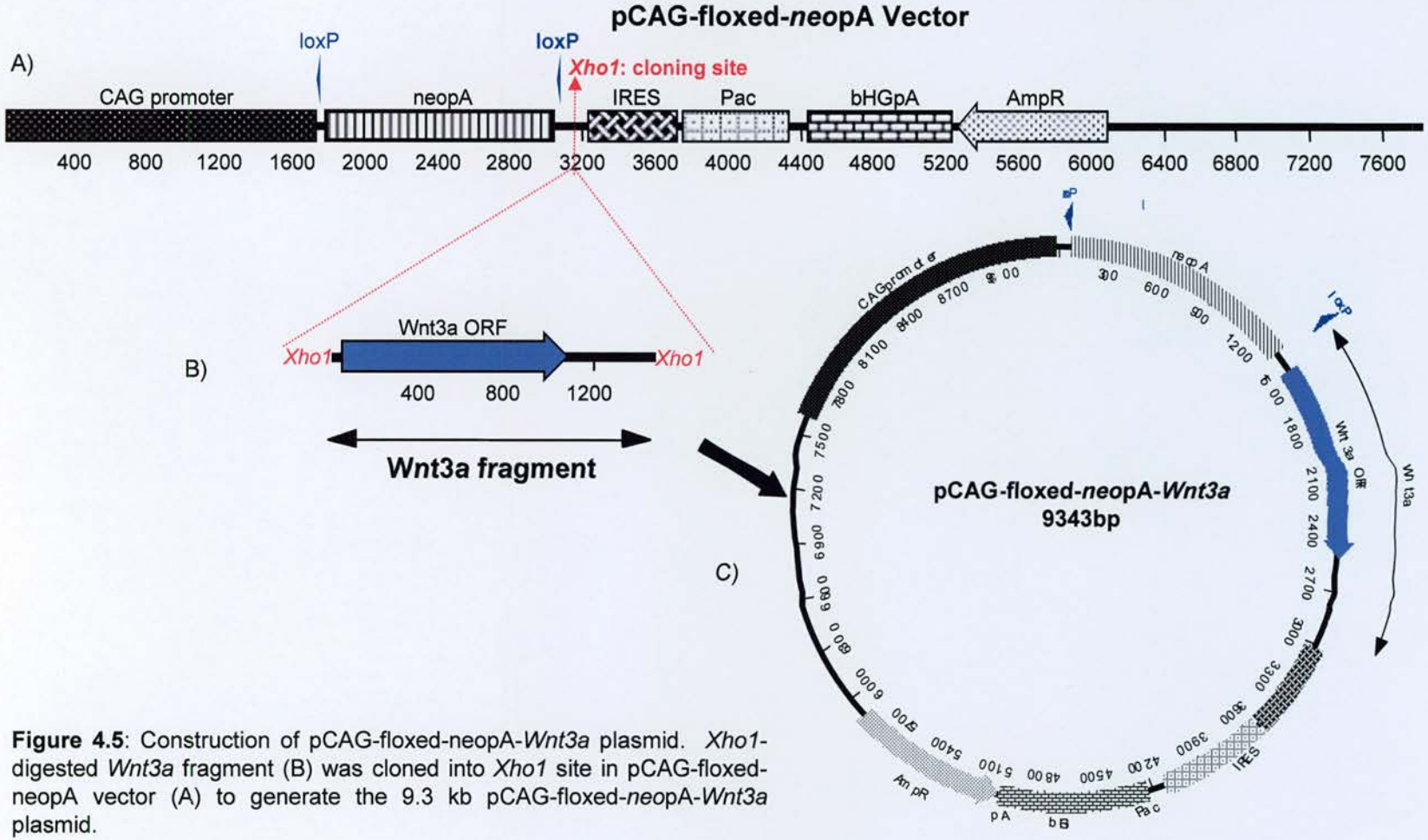

Figure 4.5: Construction of pCAG-floxed-neopA-*Wnt3a* plasmid. *Xho1*-digested *Wnt3a* fragment (B) was cloned into *Xho1* site in pCAG-floxed-neopA vector (A) to generate the 9.3 kb pCAG-floxed-*neo*pA-*Wnt3a* plasmid.

excised from pCMV.SPORT6 (Mammalian Gene Collection 3493095) by digestion with *Sal*I and *Xho*I prior to directly cloning the insert into pCAG-floxed-neopA at the unique *Xho*I site. As a result, a 10.2 kb pCAG-floxed-neopA-*Wnt5a* was produced. The 2.5 kb insert contained a part of *Wnt5a* 5'UTR, a complete *Wnt5a* ORF and a portion of *Wnt5a* 3'UTR (Figure 4.6). Clones carrying the correct plasmid were screened by restriction enzyme digestion (Appendix B).

Screening for stably-transfected R26CT2S with pCAG-floxed-*neo*pA-*Wnt5a* began with selection in G418 (chapter 2) followed by procedures as described above. Out of eight clones that survived G418 (8 out of 18), only one clone survived puromycin upon deletion of *neo*-stop cassette by 4'-OHT. This puromycin resistant clone was referred to as CAG-*Wnt5a*-Tp ES cell line. Its 4'-OHT-untreated cell line, which was neomycin (G418) resistant, was named CAG-floxed-*neo*pA-*Wnt5a* ES cell line.

4.2.1.1.5 *pCAG-floxed-neopA-Wnt7a ES cell line*

In generating the pCAG-floxed-*neo*pA-*Wnt7a*, we began with digestion of pYx-Asc/*Wnt7a* (Mammalian Gene Collection 6415801) with *EcoR*I to release a 1.7 kb fragment encompassing *Wnt7a* cDNA. The 1.7 kb *EcoR*I fragment was subsequently cloned into pDsRed2-1 at the *EcoR*I site to generate a plasmid carrying *XhoI* and *Sal*I sites flanking the *Wnt7a* cDNA. The resulting plasmid was then digested with *XhoI* and *Sal*I, and the 1.7 kb *XhoI-Sal*I fragment containing the Wnt7a coding region was cloned into the *XhoI* site in pCAG-floxed-*neo*pA (Figure 4.7). As a result, a 9.5 kb pCAG-floxed-*neo*pA-*Wnt7a* was generated. Screening for all plasmids at each cloning step was done by restriction enzyme digestion (Appendix B).

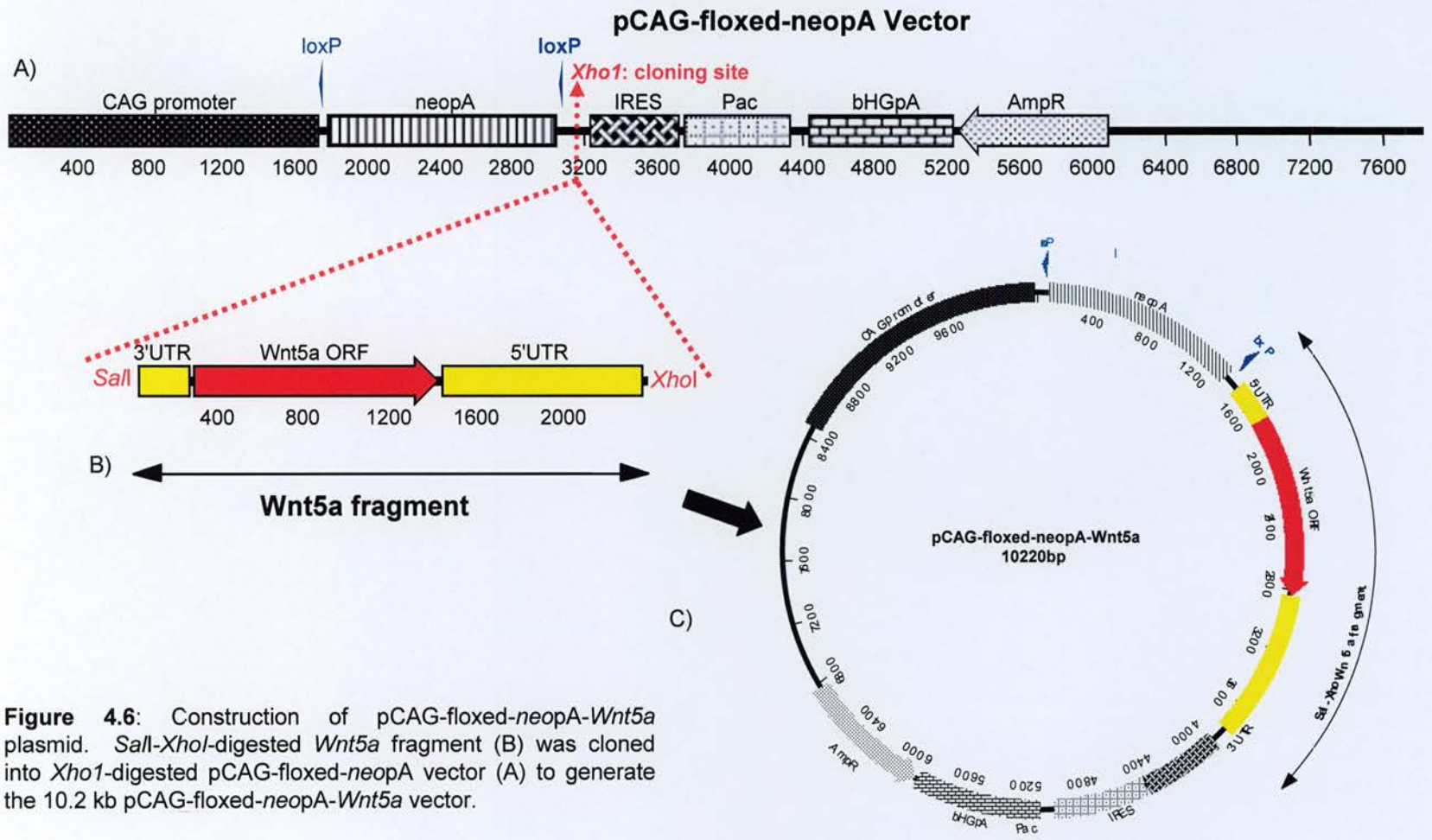

Figure 4.6: Construction of pCAG-floxed-*neo*pA-*Wnt5a* plasmid. *SalI*-*XhoI*-digested *Wnt5a* fragment (B) was cloned into *Xho1*-digested pCAG-floxed-*neo*pA vector (A) to generate the 10.2 kb pCAG-floxed-*neo*pA-*Wnt5a* vector.

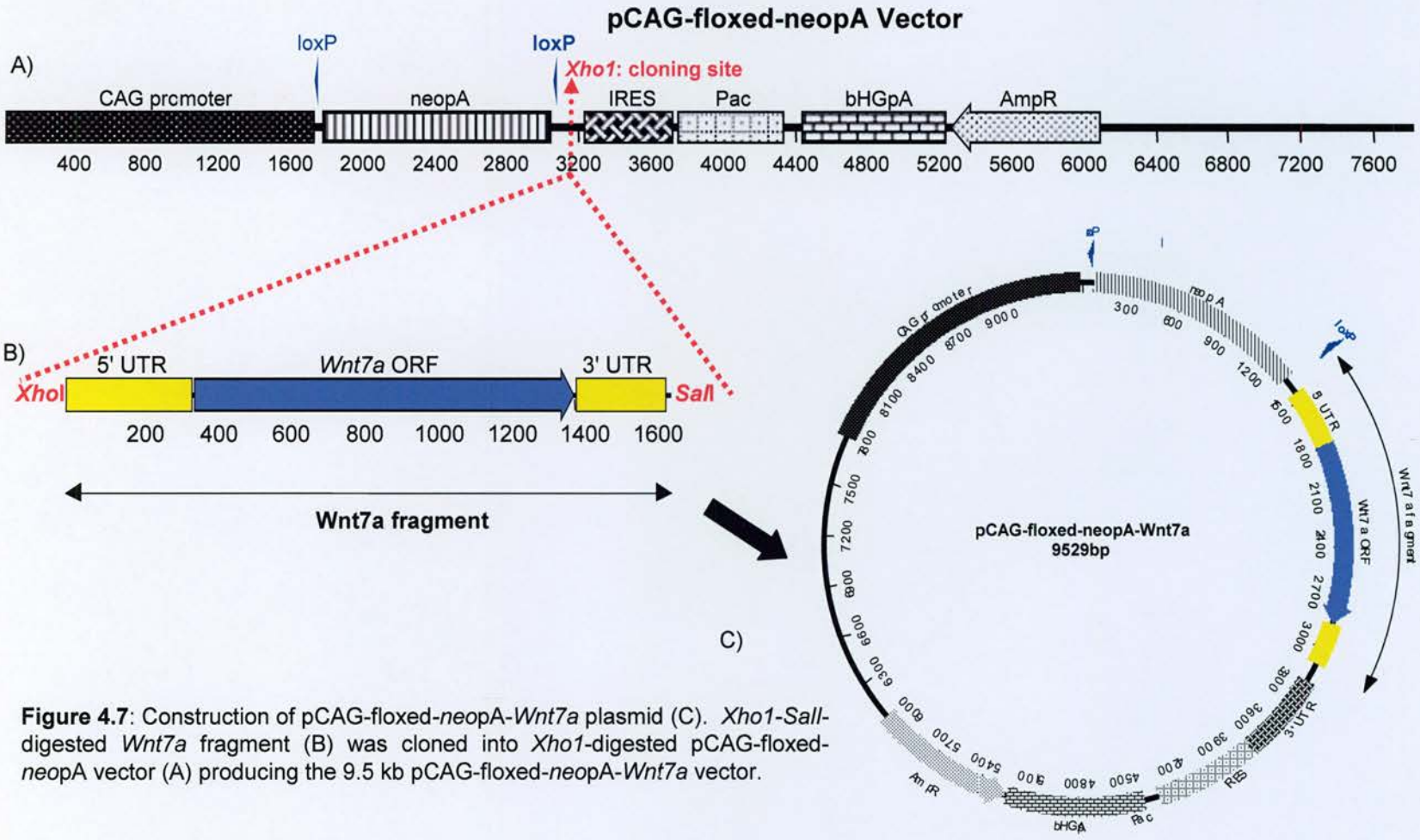

Figure 4.7: Construction of pCAG-floxed-*neo*pA-*Wnt7a* plasmid (C). *Xho1-Sal*I-digested *Wnt7a* fragment (B) was cloned into *Xho1*-digested pCAG-floxed-*neo*pA vector (A) producing the 9.5 kb pCAG-floxed-*neo*pA-*Wnt7a* vector.

Screening for the integrity of stably-transfected R26CT2S with pCAG-floxed-*neo*pA-*Wnt7a* was done as described above. After 4'-OHT treatment, five out of 15 clones that survived G418 were resistant to puromycin. These puromycin resistant clones were referred to as CAG-*Wnt7a*-Tp ES cell lines, while their 4'-OHT-untreated cell lines, which were neomycin (G418) resistant, were named CAG-floxed-*neo*pA-*Wnt7a* ES cell lines.

4.2.1.2 Characterization of transgenic ES cell lines

4.2.1.2.1 Functionality of transgenes

To examine the functionality of pCAG-floxed-*neo*pA-*Wnt1*-HA construct and the ability of the R26CT2S ES cell line in regulating the expression of *Wnt1*-HA in response to 4'-OHT, we performed immunocytochemistry (ICC) on CAG-*Wnt1*-HA-Tp ES cells using an anti-HA antibody. Approximately 80% of the cells expressed Wnt1-HA both in the presence and the absence of LIF (Figure 4.8B,C). Expression of Wnt1-HA was not detected in 4'-OHT-untreated CAG-floxed-*neo*pA-*Wnt1*-HA ES cells (Figure 4.8A). Western blot analysis also showed the appropriate band size (~48 kDa) of HA-tagged Wnt1 protein (Figure 4.10F).

We also looked at protein expression of Wnt7a and Dkk1 in CAG-*Wnt7a*-Tp and CAG-*Dkk1*-Tp cells by ICC. The results clearly show the respective protein expression both in the presence and the absence of LIF (Figure 4.8D-I). These results demonstrate the functionality and stability of the tamoxifen-dependent Cre-mediated activation of transgenes in all of stably-transfected clones for Wnt1-HA, Wnt7a and Dkk1.

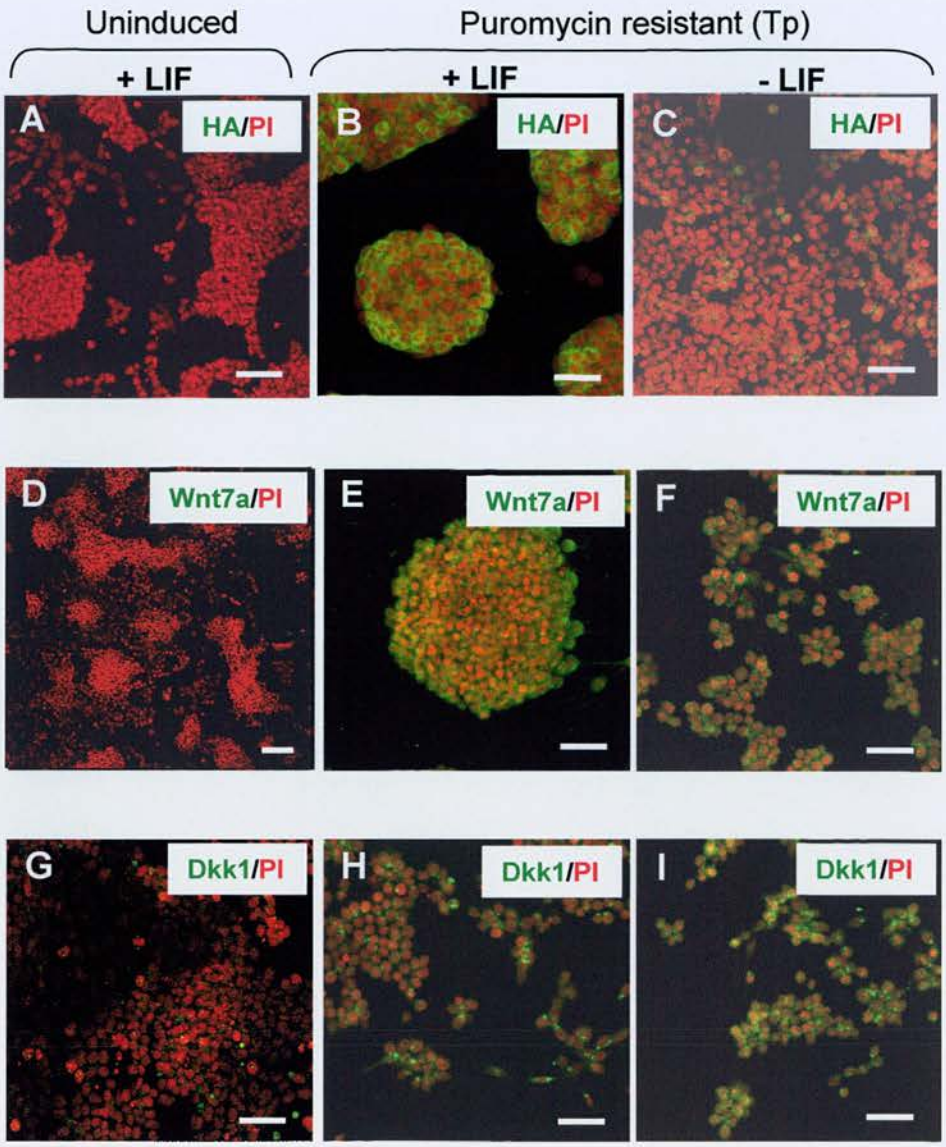

Figure 4.8: Functionality of inducible expression vectors. Expression of Wnt1-HA (B,C), Wnt7a (E,F) and Dkk1 (H,I) from constitutively expressing *Wnt1*-HA, *Wnt7a* and *Dkk1* transfectants, respectively, in the presence (B,E,H) and the absence (C,F,I) of LIF. No expression of these proteins were detected in the respective uninduced cells (A,D,G). Scale bar is 50 μm.

4.2.1.2.2 Inducibility in ES cells

We wanted to see whether 4'-OHT would have any effect in inducing *Wnt1* and Dkk1 expression in the parental line, R26CT2S ES, cells stably-transfected with pCAG-floxed-*neo*pA vector. RNA expression for both genes was determined by qRT-PCR on day 2 of culture after treatment with 400 nM of 4'-OHT for 16, 24 and 48 hours (Figure 4.9A). No significant increase of either Wnt1 or Dkk1 was observed in all treatment conditions for CAG-floxed-neopA ES cell lines. These results indicate that treatment with 4'-OHT does not have any effect in inducing the expression of either Wnt1 or Dkk1 in this cell line.

Time- and dose-dependent experiment was then carried out with two of CAG-floxed-*neo*pA-*Wnt1*-HA and CAG-floxed-*neo*pA-*Dkk1* ES cell clones that were shown to be resistant to puromycin in order to find the optimal conditions for induction of transgene expression. For the Wnt1-HA transgenic ES cell line, we treated the clones with 200, 400, 500 and 1000 nM of 4'-OHT for 24 and 48 hours (Figure 4.9B). In this assay, the ES cells were cultured at 2-4 x 10^5 cells in a well of 6-well plate in the presence of LIF and treated as described above. After two days in culture, the cells were harvested, total RNA was extracted and the expression of *Wnt1* was quantitatively determined by qRT-PCR. Expression of *Wnt1* was also determined by qRT-PCR from CAG-*Wnt1*-HA-Tp ES cells for comparison (Figure 4.9B). Each clone has a different response towards 4'-OHT, even though 48 hour-treatment with every dose of 4'-OHT produced a higher level of *Wnt1* expression than the 24-hour-treament. After 2 days of culture, , a strong activation of *Wnt1* expression (200 fold) for clone 1 was observed after treatment with 400 nM of 4'-OHT for 48 hours, while the highest level

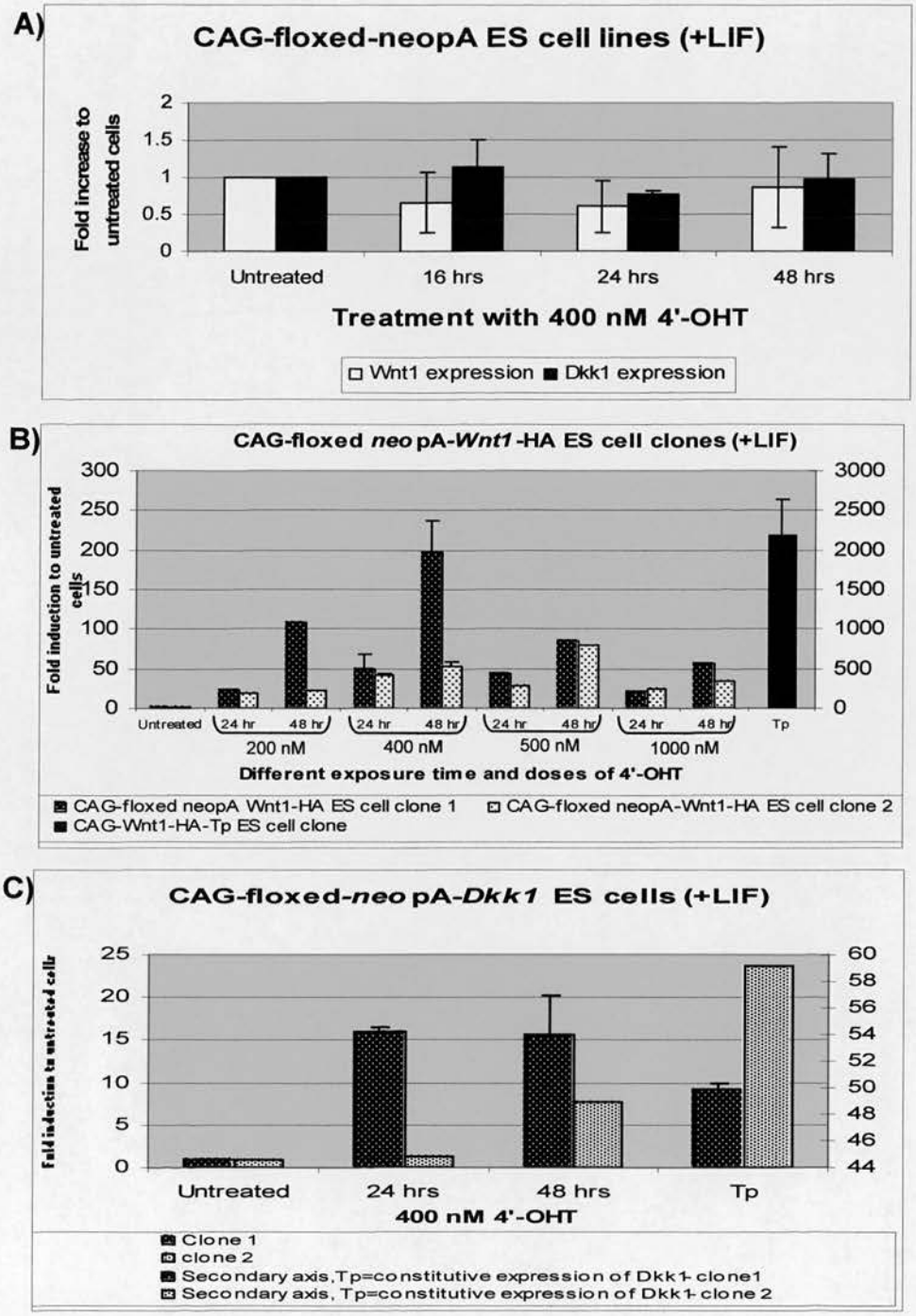

Figure 4.9: Quantitative analysis of *Wnt1 and Dkk1* overexpression by qRT-PCR. A) 4'-OHT treatment does not affect the induction of either *Wnt1* or *Dkk1* expression in R26CT2S stably-transfected with pCAG-floxed-neopA vector. (B) Quantitative expression of *Wnt1* (B) and *Dkk1* (C) from their respective undifferentiated CAG-floxed-*neo*pA-*Wnt1*-HA and CAG-floxed-*neo*pA-*Dkk1* clones after two days grown in the presence of LIF treated with various time and concentrations of 4'-OHT. Overexpression of *Wnt1* (B, Tp-secondary axis) *and Dkk1* (C, Tp-secondary axis) from CAG-*Wnt1*-HA-Tp and CAG-*Dkk1*-Tp ES cells, respectively, was also quantitavely determined. The error bars show mean ± standard deviations from 3 independent experiments.

of *Wnt1* expression for clone 2 (70-fold) was achieved after treatment with 500 nM for 48 hours. In every experiment the overexpression of Wnt1 was never observed in untreated CAG-floxed-*neo*pA-*Wnt1*-HA ES cells indicating a complete repression of *Wnt1*-HA transcription downstream the floxed *neo*-stop cassette in the absence of 4'-OHT. Hence, in this study, the highest level of *Wnt1* expression for undifferentiated ES cells was achieved at 48 hours after 48-hour-treatment with 400 nM of 4'-OHT for clone 1 and after 48-hour-treatment with 500 nM of 4'-OHT for clone 2.

However, the level of induced *Wnt1* expression achieved was far less than the expression level of *Wnt1* produced by the CAG-*Wnt1*-HA-Tp ES cell clone 1, which was constitutively expressing *Wnt1*-HA (Figure 4.9B). About 10-fold increase was observed from these constitutively expressing *Wnt1*-HA cells (about 2000-fold) when compared to the highest level of the induced *Wnt1* expression (of clone 1, 200-fold). The selection by puromycin after 4'-OHT treatment therefore has efficiently eliminated those cells that have incorporated truncated plasmid in CAG-floxed-*neo*pA-*Wnt1*-HA ES cells.

Induction of Wnt1-HA protein expression in undifferentiated CAG-floxed-*neo*pA-*Wnt1*-HA ES cells after treatment with 400 nM 4'-OHT was detected at low level by ICC using an anti-HA antibody (Figure 4.10). A very low level of expression of Wnt1-HA was also detected by western blot analysis when the cells were treated with 500 nM of 4'-OHT for 48 hours (Figure 4.10). These results, albeit producing low level of transgene expression, show that the conditional gene expression system managed to activate the expression of transgene protein in undifferentiated ES cells.

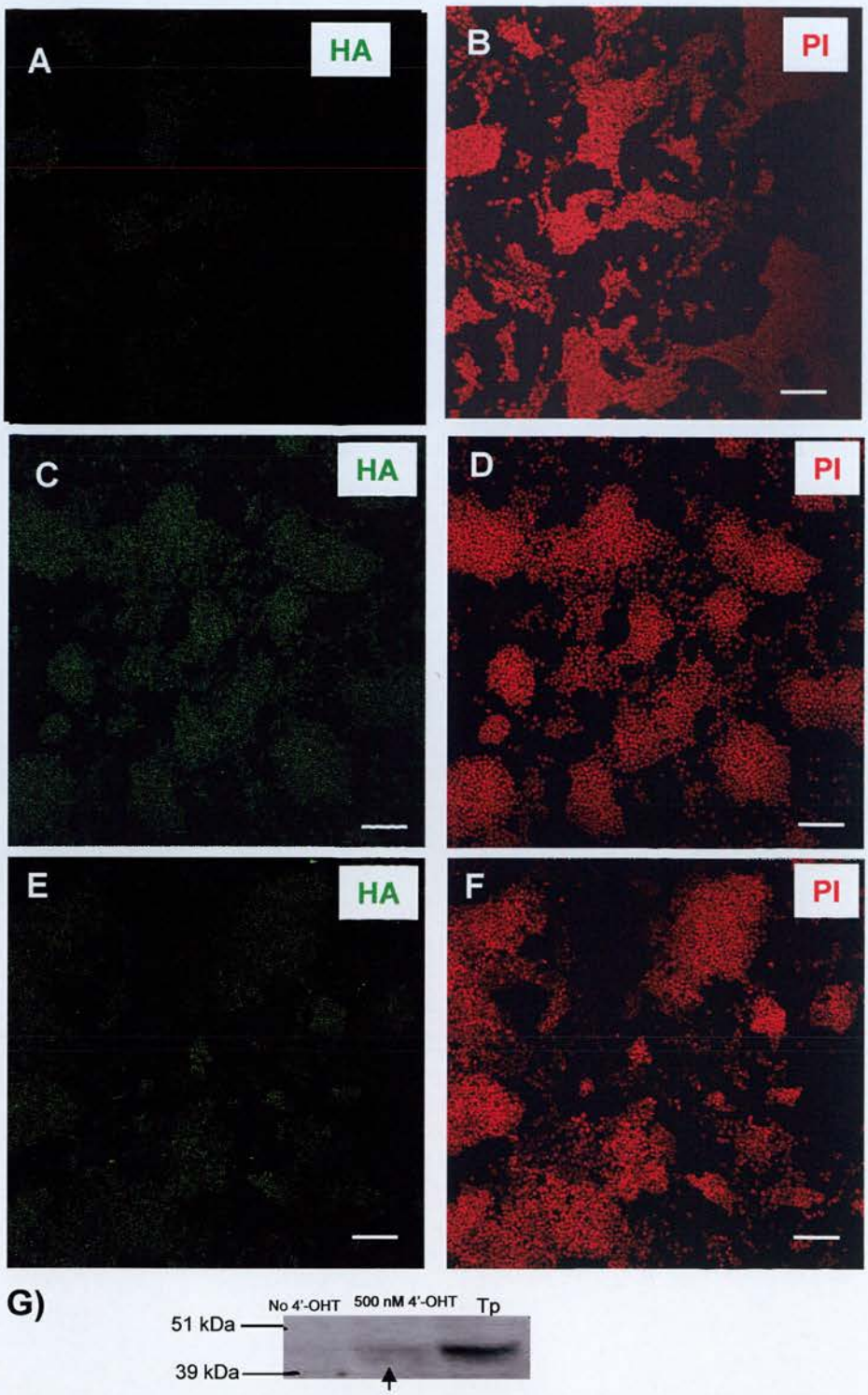

Figure 4.10: Inducibility of pCAG-floxed-*neo*pA-*Wnt1*-HA in undifferentiated ES cells. Protein expression of Wnt1-HA induced by 400 nM 4'OHT for 48 hours on clone 1 (C, D) and clone 2 (E, F) by immunocytochemistry against HA. (A, B) Untreated cells. (A, C, E) anti-HA, (B, D, F) nuclei staining with propidium iodide (PI). G) A very low level expression of Wnt1-HA (an arrow) from clone 1 after treatment with 500 nm 4'-OHT for 48 hours compared to high level expression of the protein from constitutively expressed Wnt1-HA (Tp) cells. Scale bar is 100 μm.

For Dkk1 transgenic ES cell line clones, it was observed that the highest expression of Dkk1 after 2 days in culture was achieved after treatment with 400 nM of 4'-OHT for 48 hours for both treated clones (Figure 4.9C). A different activation level of Dkk1 was observed from each clone. As high as 20-fold increase of *Dkk1* expression was seen from clone 1 whereas less that 10-fold induction was observed from clone 2 after treatment with 400 nM of 4'-OHT for 48 hours.

Similar to *Wnt1*-HA transgene, the induced expression of *Dkk1* from both clones was less than the expression level of Dkk1 from constitutively expressing *Dkk1* cells, CAG-*Dkk1*-Tp ES cells. A difference of 2.5- to 6-fold was determined between the induced and constitutively expressed cells from clone 1 and 2, respectively. No activation of Dkk1 expression was observed in untreated clones when compared to expression from in line cells as well as stably-transfected ES cells with pCAG-floxed-*neo*pA. Taken together, these results clearly show that treatment with 4'-OHT results in inducible expression of the transgenes.

Due to technical problems with western blotting and the unavailability of a good Dkk1 antibody, we were unable to detect any protein expression in either induced or constitutively expressing *Dkk1* cells. However, the RNA expression of Dkk1 in induced and constitutively expressed cells demonstrated the ability of the system to activate the transcriptional activity of the transgene in undifferentiated ES cells.

In summary, it is observed that our constructs for Wnt1-HA and Dkk1 transgenes are working and, after two days in culture, giving the highest

inducible expression of the transgenes after treatment with 400 nM 4'-OHT for 48 hours in undifferentiated ES cells.

4.2.1.2.3 Inducibility in EBs

In order to activate the expression of each transgenes during neural differentiation, for future application, we also conducted a time- and dose-response assay in differentiated transgenic ES cell lines. The cells were grown for two days (D2) in the absence of LIF to promote the formation of EBs before treatment with 200, 500, 800 and 1000 nM of 4'-OHT for 48 hours (Figure 4.11). On D4, the EBs were harvested for RNA extraction and the expression of *Wnt1* was quantitatively determined by qRT-PCR.

From two independent experiments, a strong activation of *Wnt1* expression (about 25-fold) on day 4 EBs (D4 EBs) was observed after treatment with 800 nM of 4'-OHT (Figure 4.11). Higher concentration of 4'-OHT (to 1000 nM) decreased the expression level of Wnt1 to 20-fold when compared to the untreated cells. The overall induction of *Wnt1* expression in these differentiated ES cells (D4 EBs) was lower than that of the induction in undifferentiated ES cells. However, *Wnt1* expression in the CAG-*Wnt1*-HA-Tp EBs was still higher (about 4-fold) than the highest induced expression level from the CAG-floxed-*neo*pA-*Wnt1*-HA EBs.

To our surprise, the maximum induction level of *Dkk1* expression from D4 EBs was quite similar to the maximum induction level in undifferentiated ES cells (Figure 4.11). From two independent experiments, a strong activation of *Dkk1* expression (15-fold), by qRT-PCR, from D4 EBs was observed after treatment with 800 nM 4'-OHT for 48 hours. A higher concentration of 4'-

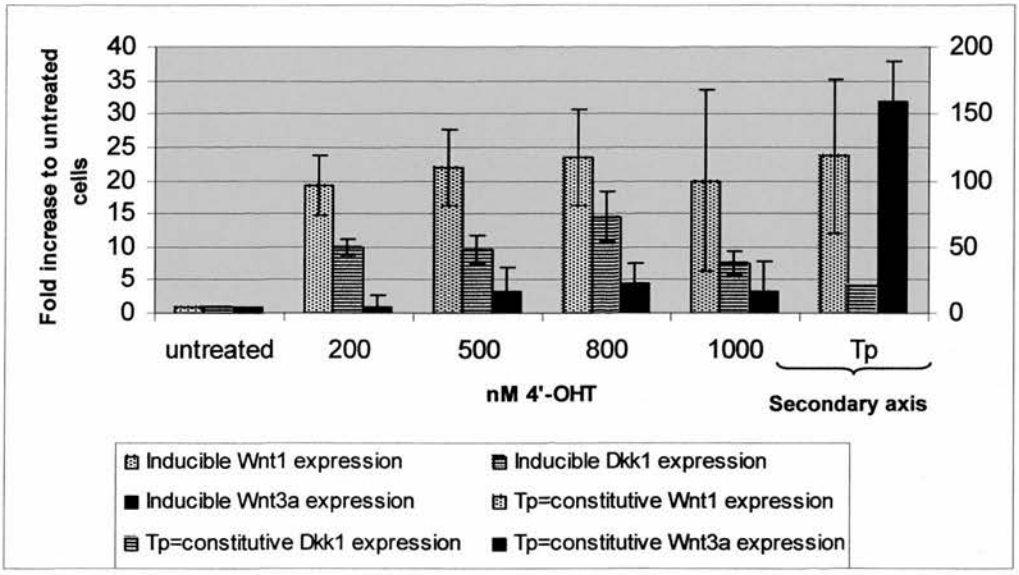

Figure 4.11: Dose- and time-dependent activation of Wnt1, Dkk1 and Wnt3a expression in their respective transgenic ES cell lines. RNA expression was quantitatively analysed by qRT-PCR from RNA harvested on D4 EBs, grown in the absence of LIF, after treatment with 200, 500, 800 and 1000 nM 4'-OHT for 48 hours. Overexpression of each transgene in D4 EBs from each constitutively expressing transgenic lines was also quantitatively determined (Tp-secondary axis). The error bars are mean ± the range from 2 independent experiments.

OHT (1000 nM 4'-OHT) decreased the level of Dkk1 expression down to less than 10-fold. Only a slight reduction in the expression of *Dkk1* of D4 EBs from CAG-*Dkk1*-Tp cells was seen as compared to the induced expression of *Dkk1* from CAG-floxed-*neo*pA-*Dkk1* cells after treatment with all the doses of 4'-OHT.

Due to limitation of time, we only conducted time- and dose-dependent assay for differentiated CAG-floxed-neopA-Wnt3a ES cells. The assay was carried out as described for *Wnt1*-HA and *Dkk1* transgenic ES cell lines. An activation of 5-fold was observed from D4 EBs of CAG-floxed-*neo*pA-*Wnt3a* cells after treatment with 800 nM of 4'-OHT for 48 hours (Figure 4.11). Similar to previously mentioned transgenic ES cell lines, higher expression of Wnt3a (20-fold) was seen from constitutively expressed Wnt3a cells when compared to the induced Wnt3a expression. These results show the ability of the system to induce the expression of Wnt3a.

Taken together, these results show that the activity of each construct is maintained upon differentiation and that they are able to induce transgene expression after treatment with 4'-OHT. Treatment with 800 nM 4'-OHT for 48 hours was found to be the optimal conditions for induction of Wnt1, Dkk1 and Wnt3a transgenes in EBs in our system.

4.2.2 TCF Driving Red Fluorescent protein-reporter ES cell line (TOP-Red2)

Although expression of Wnt genes indicates their possible function during neural differentiation of ES cells, it does not formally demonstrate that Wnt signalling is active. We built a reporter construct which directly reports

canonical Wnt signalling by activating red fluorescent protein (RFP). RFP expression is driven under the control of a promoter that contains multiple LEF/TCF consensus binding motifs upstream from a cFos minimal promoter. The transgene, TOP-Red2, is a derivative of TOPFLASH (TCF binding sites driving luciferase) whose expression is dependent on the formation of nuclear TCF/LEF-ß-catenin complexes (Korinek *et al.*, 1998). TOPFLASH is a well established method of quantifying canonical Wnt signalling. Induction of *Wnt1* in C57MG cells has been shown to increase luciferase activity which indicates the activation of TCF reporter construct in response to Wnt signal (Korinek *et al.*, 1998).

A fragment containing the multiple LEF/TCF-binding sites was excised from pTOPFLASH vector (a gift from Prof Hans Clevers, Korinek *et al.*, 1997) and inserted upstream of the DsRed2 coding region in pDsRed2-1 vector. pDsRed2-1 is a promoterless vector that encodes *Discosoma sp.* red fluorescent protein or DsRed (Matz *et al.*, 1999). DsRed2 is a DsRed variant which contains six amino acids substitutions that allow more rapid maturation of red fluorescent protein (Yarbrough *et al.*, 2001). According to the manufacturer (Clontech), red emitting cells can be detected by fluorescence microscope within 24 hours of transfection. In addition, cells expressing DsRed2 exhibit the same growth characteristic and morphology as non-transfected control cells (BD living colors™ User manual volume II, BD Biosciences).

Therefore, by using the system, we should be able to directly observe cells that are actively responding to canonical Wnt signals during neural differentiation assay, specifically in testing our hypothesis that Wnts may

inhibit the formation of NPC but may also be promoting the differentiation of these cells into neurons. The expression of TOP-Red2 during differentiation would be helpful in confirming the activity of Wnt genes during the process as had been suggested by the genes RNA expression profiles. Furthermore, the availability of *Sox1*-GFP knock-in ES cells (46C ES cell, chapter 3), which express GFP in NPC, has given us the opportunity to specifically monitor Wnt responsive cells in neural precursor cells (NPC) as well as other cells throughout the whole process of neural differentiation of ES cells *in vitro*.

4.2.2.1 Construction of the pTOP-Red2 vector

In constructing the pTopRed vector, a 276 bp of *Xba*I-digested fragment from TOPFLASH (Tcf Optimal Luciferase reporter construct) plasmid was first cloned into a transitional vector [pBSIIKS(+)], due to limited cloning sites, prior to cloning into a pDs-Red2-1 vector (Figure 4.12). The nucleotide sequence of the TCF binding sites and the cFos promoter was confirmed by sequencing the TOPFLASH plasmid using TF1-SF and LuciTF-SS primers (Appendix C). Subsequently, the Top/pBSIIKS(+) plasmid was digested with *Sac*I and *EcoR*I to excise the Top fragment and cloned into the *Sac*I and *EcoR*I sites in pDsRed2-1 vector to generate pTopRed vector. Screening for the correct plasmids was done by restriction enzyme digestions (Appendix E). HEK 293 and ES cell lines were then transiently- and stably-transfected with the vector and also the pDsRed2-1 vector, respectively, as described in chapter 2. The pDsRed2-1 vector also contains a *neo*mycin-resistance cassette (*Neo*^{r}) which allows for selection of stably transfected eukaryotic cells using G418, and kanamycin resistance gene for selection using kanamycin in *E. coli*.

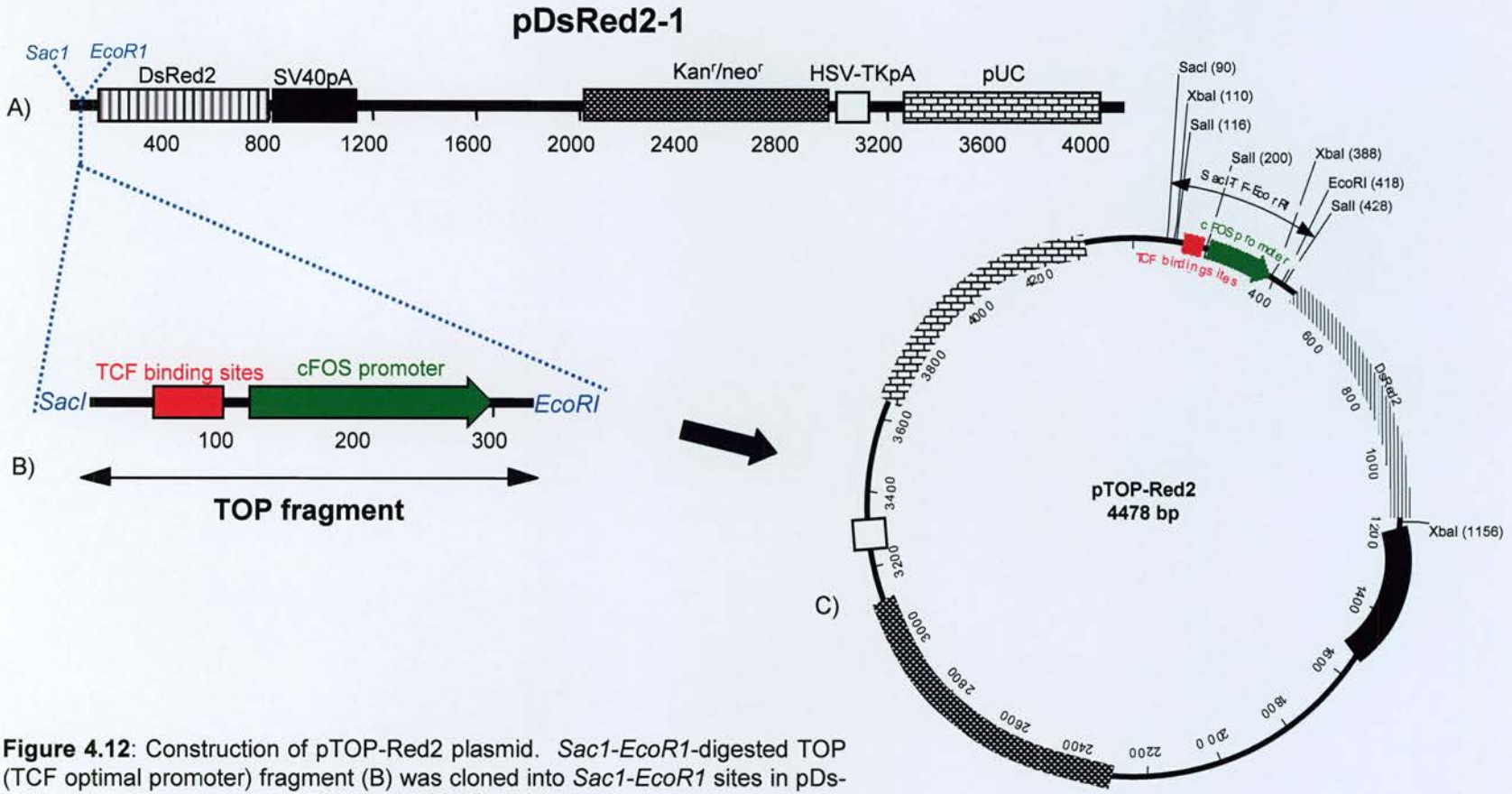

Figure 4.12: Construction of pTOP-Red2 plasmid. *Sac1-EcoR1*-digested TOP (TCF optimal promoter) fragment (B) was cloned into *Sac1-EcoR1* sites in pDs-Red vector (A) generating a 4.5 kb of pTOP-Red2 plasmid.

4.2.2.2 Characterization of pTOP-Red2

In order to evaluate the ability of the pTOP-Red2 vector to respond to canonical Wnt signalling, we transiently introduced the vector into *Wnt1*-HA-expressing HEK 293 cells (*Wnt1*-HA-HEK-TopRed cells) and HEK 293 cells (HEK-TopRed cells). These cells were also transiently transfected with the control vector, pDsRed2-1. Analysis of *Wnt1*-HA-HEK-TopRed cells revealed a slow rate of DsRed2 maturation. In the presence of constitutive expression of *Wnt1*, only a small number of cells expressing RFP was detected 48 hours post-transfection (data not shown). More RFP was detected 72 hours post-transfection (Figure 4.13B). In addition, no cells expressing RFP were detected in the HEK-TOP-Red2 cells as well as in HEK 293 cells harbouring pDsRed2-1 or pDsRed2-1-transfected *Wnt1*-HA-expressing HEK 293 cells (Figure 4.13C, D). These results therefore indicate the absence of leaky expression from cFos promoter. The small number of cells expressing RFP in *Wnt1*-HA-HEK-TopRed, however, was most likely due to low number of cells expressing *Wnt1*-HA in the stably-transfected-*Wnt1*-HA HEK 293 cells. Nevertheless, these results demonstrate the ability of the pTOP-Red2 in driving the expression of RFP in the presence of Wnt signals.

Based on these results, we then decided to use constitutively expressing *Wnt1*-HA (CAG-*Wnt1*-HA-Tp) and *Wnt3a* (CAG-*Wnt3a*-Tp) ES cell lines to further analyse the functionality of TOP-Red2. These cells were transiently transfected with pTopRed and pDsRed2-1. A reasonable number of cells expressing RFP were observed 48 hours post-transfection (approximately 25%) with more of these cells being observed after 72 hours of transfection (approximately 40%, Figure 4.14A). No RFP expression was observed in

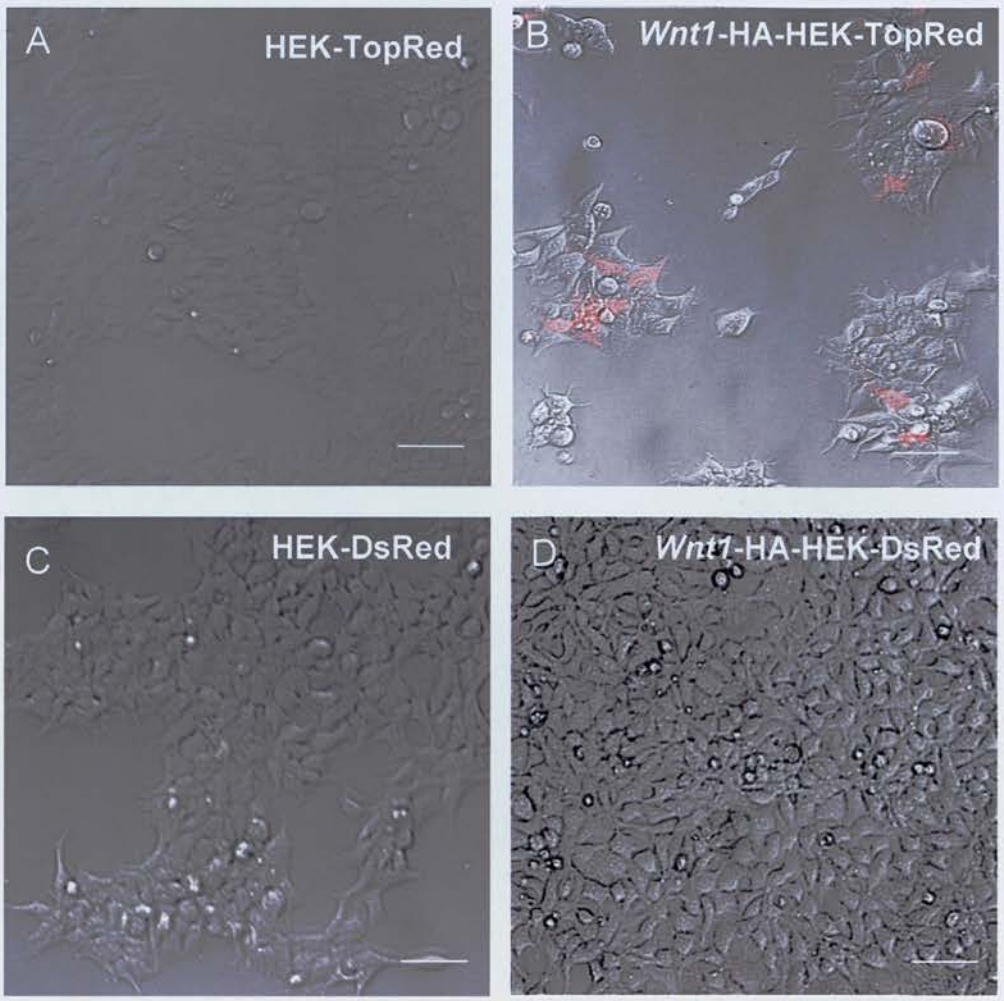

Figure 4.13: Transient transfection of HEK 293 and Wnt1-HA-HEK 293 cells with pTOP-Red2 and pDsRed2-1. Expression of RFP was not detected in HEK 293 transfected with pTOP-Red2 (A) and DsRed2-1 (C), and also in Wnt1-HA overexpressing HEK 293 cells transfected with pDsRed2-1 (D). The expression of RFP was detected in Wnt1-HA expressing HEK 293 cells 3 days post-transfection indicating the ability of pTopRed in expressing the RFP in the presence of Wnt signals. Scale bar is 50 µm.

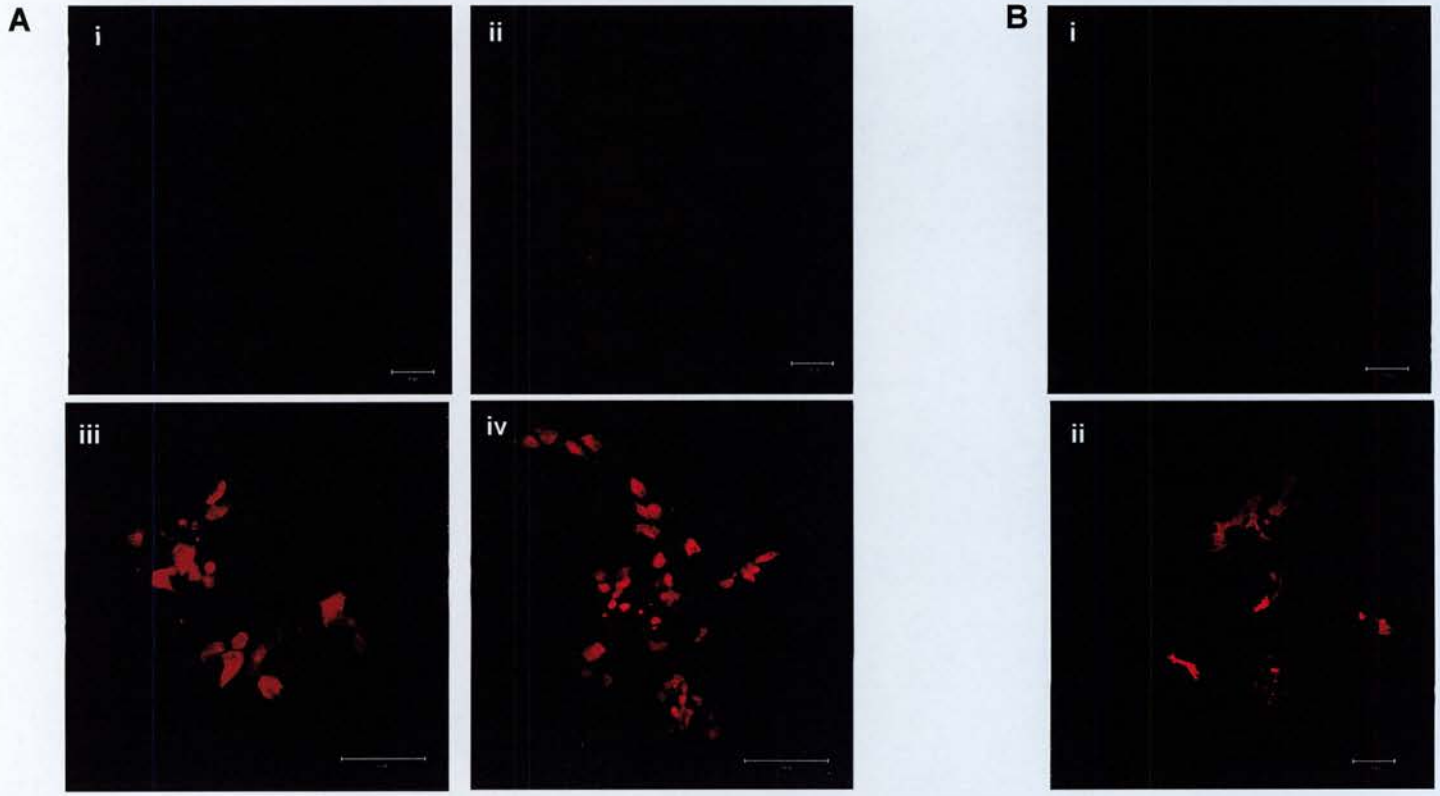

Figure 4.14: Induction of TOP-Red2 expression in ES cells. A) Expression of RFP from transiently transfected pDsRed2-1 (i,ii) and pTOP-Red2 (iii,iv) into constitutively expressing *Wnt3a* (i, iii) and *Wnt1-HA (*ii, iv) ES cells. 72 hours after transfection, no RFP was detected in cel s transfected with pDsRed (i, ii) for both cell lines. The expression of RFP was observed in cells transfected with pTOP-Red2 72 hours post-transfection for both constitutively expressing Wnt3a (iii) and Wnt1-HA (iv) cells. B) Functionality of pTOP-Red2 in response to treatment with 10mM LiCl on R26CT2S cells for 20 hours. After two days in culture, no expression of RFP was obse ved in the untreated cells (i) compared to the presence of RFP expression in the cells treated with LiCl (ii). Scale bar is 100 µm.

pDsRed2-1-transfected cells. In addition, we also tested the functionality of the construct in response to LiCl that mimics Wnt signalling. Non-Wnt-expressing ES cells (R26CT2S) were treated with 10mM LiCl for 20 hours before visualizing the expression of TOP-Red2. After two days in culture, expression of RFP was observed in the cells treated with LiCl but not in untreated cells (Figure 4.14B). Taken together, these results demonstrate the ability of TOP-Red2 in inducing the expression of RFP in ES cells and as a reporter gene in response to Wnt signals.

4.2.2.3 Detection of Wnt responsive cells in EBs during neural differentiation process of ES cells *in vitro*

In order to monitor the cells that were actually responding to endogenous Wnt signals during neural differentiation assay, stably transfected-pTopRed (46C-TR) and –pDsRed2-1 (46C-Ds) 46C ES cells were generated by selection using G418. Out of 20 clones that were picked, only 7 clones survived the selection and were screened for their ability to induce RFP expression in the presence of Wnts. The screening was conducted by treating the clones with 5-20 mM of lithium chloride (LiCl). Based on the screening, we found 10mM LiCl was the optimal concentration to activate reporter gene expression (data not shown). Two clones of each 46C-TR and 46C-Ds ES cells were chosen and subjected to neural differentiation process through the formation of EBs followed by the addition of ATRA (4-/4+ protocol). A positive control condition was also included, in which the clone was treated with 10 mM LiCl on D0 for 48 hours. 46C-Ds cells were used to represent negative control condition.

On D4, a small number of EBs expressing RFP were observed in the positive control cells but not in the LiCl-untreated 46C-TR and 46C-Ds cells (data not shown). The GFP expression was not observed (as expected) at this stage. These results most likely indicate the absence of Wnt signals at D4 of neural differentiation process.

On D6, very few EBs expressing faint RFP were detected from the LiCl-untreated 46C-TR cells (Figure 4.15A) while the positive control cells continued expressing RFP (data not shown). No RFP expression was observed in the 46C-Ds cells. As expected, at this stage, almost all of the EBs in all culture conditions expressed GFP, indicating the presence of neural precursor cells.

Due to technical problem, analysis on the RFP and GFP expression of the positive and negative control cells was done on D7 instead of D6 EBs. On D7, expression of GFP was observed from both 46C-Ds and LiCl-treated 46C-TR cells (Figure 4.16). No RFP expression was observed in the negative control cells indicating the specificity of TOP-Red in response to Wnt signal. To our surprise, higher level of red fluorescence was observed from the positive control cells indicating the stability of the integrated pTOP-Red2 construct upon differentiation.

On D8, more EBs expressing RFP were detected in the LiCl-untreated 46C-TR cells (Figure 4.15B). Unlike D6 EBs, higher levels of fluorescence were observed in these cells. At this stage, almost all EBs were still expressing GFP even though the percentage of cells expressing GFP in each EBs was reduced. Expression of RFP alone, however, was never observed in any EBs

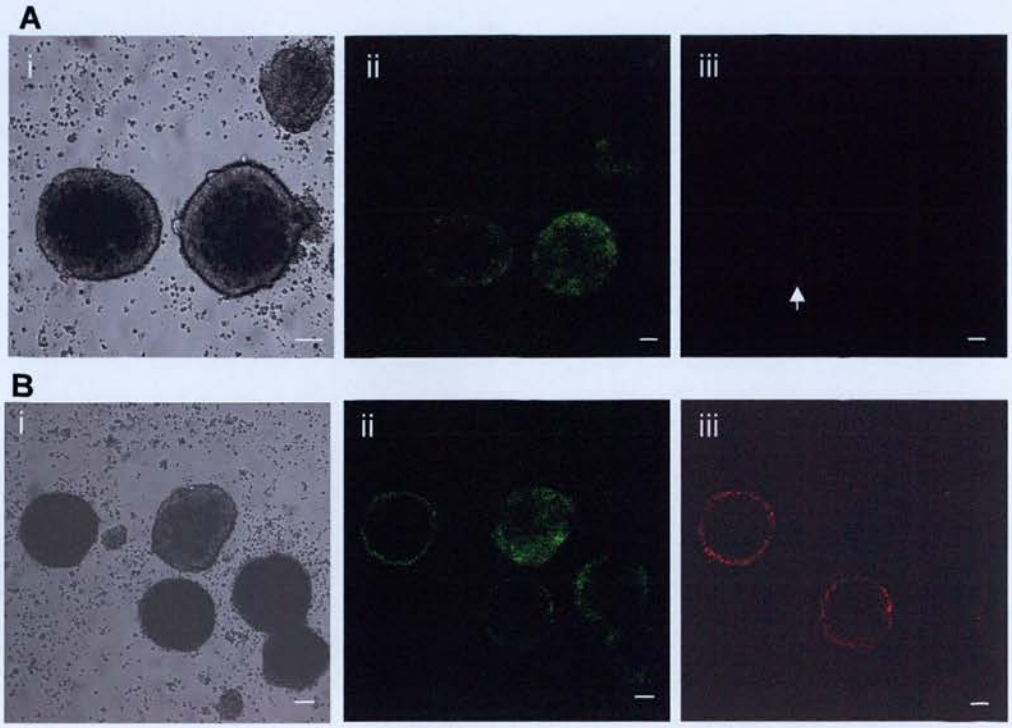

Figure 4.15: Expression of RFP and GFP in stably-transfected 46C ES cells (46C-TR) with pTOP-Red2. A and B are the EBs on D6 and D8 of neural differentiation process of 46C-TR cells, respectively. The expression of GFP was observed in all EBs both on D6 (A, ii) and D8 (B, ii) EBs. A very faint expression of RFP was observed on D6 EBs (A,iii, arrow). More EBs expressing brighter expression of RFP were observed on D8 EBs (B, iii). Ai, Bi show the bright field of the respective EBs. This is most likely to indicate the late presence of Wnt signals during neural differentiation process of ES cells *in vitro*. Scale bar is 50 μm.

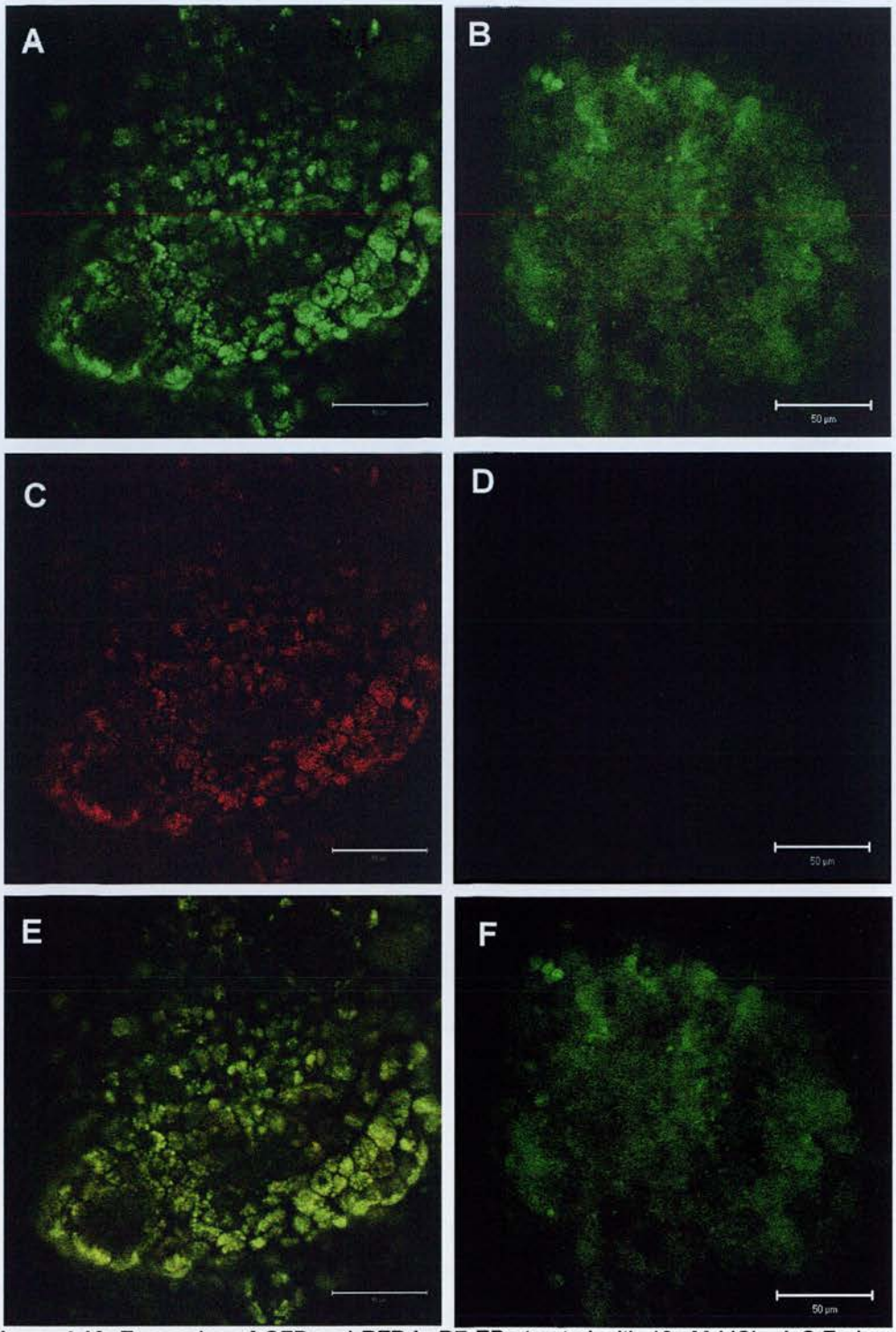

Figure 4.16: Expression of GFP and RFP in D7 EBs treated with 10mM LiCl. A,C,E show EBs derived from stably-transfected 46C cells with pTOP-Red2 (46C-TR). B,D,F show EBs derived from stably-transfected 46C cells with empty pDs-Red2-1 vector (46C-Ds). Both cell lines expressed GFP (A,B) showing $Sox1^{GFP}$ expression. Treatement with LiCl results in expression of RFP expression (C) in 46C-TR cells but not in 46C-Ds cells (D), clearly indicating that the Wnt responsive (pTOP-Red2) construct is working. E,F show the merge between RFP and GFP. Scale bar is 50 µM.

(Figure 4.15). Interestingly, co-localization of these proteins seemed to occur in the EBs that have less number of cells expressing GFP (Figure 4.18B ii, iii).

We were then still interested to locate the cells that were only expressing RFP in the EBs. We optically sectioned two selected EBs (5μm/stack) and discovered that RFP expression was always co-localized with GFP, but clearly no expression of RFP alone was ever detected (Figure 4.17). However, the expression of GFP alone could be observed (Figure 4.17C). Unfortunately, due to slow maturation of DsRed2 as described before, the exact time for the presence of Wnt signals could not be determined. However, it might be worth noting that the expression of RFP, albeit at a very low level of fluorescence and in very few number of EBs, was first detected on D6 of neural differentiation assay.

4.3 Discussion

4.3.1 Inducible ES cell expression system

Combining two techniques, *Cre/loxP*-based genetic recombination and ligand-dependent activation of Cre, we have generated transgenic ES cell lines that allow for the temporal control of expression and activity of Wnt genes and a Wnt antagonist. Using this system, expression of *Wnt1-HA*, *Dkk1*, and *Wnt3a* from respective transgenic ES cell lines, driven by a strong promoter, CAG, have been achieved in response to a nondetrimental dose of the synthetic oestrogen, 4'-OHT.

Our system was characterized by the activation of the transgene both in undifferentiated and differentiated ES cells indicating the stability of the integrant and its transcriptional activity in ES cells as well as upon

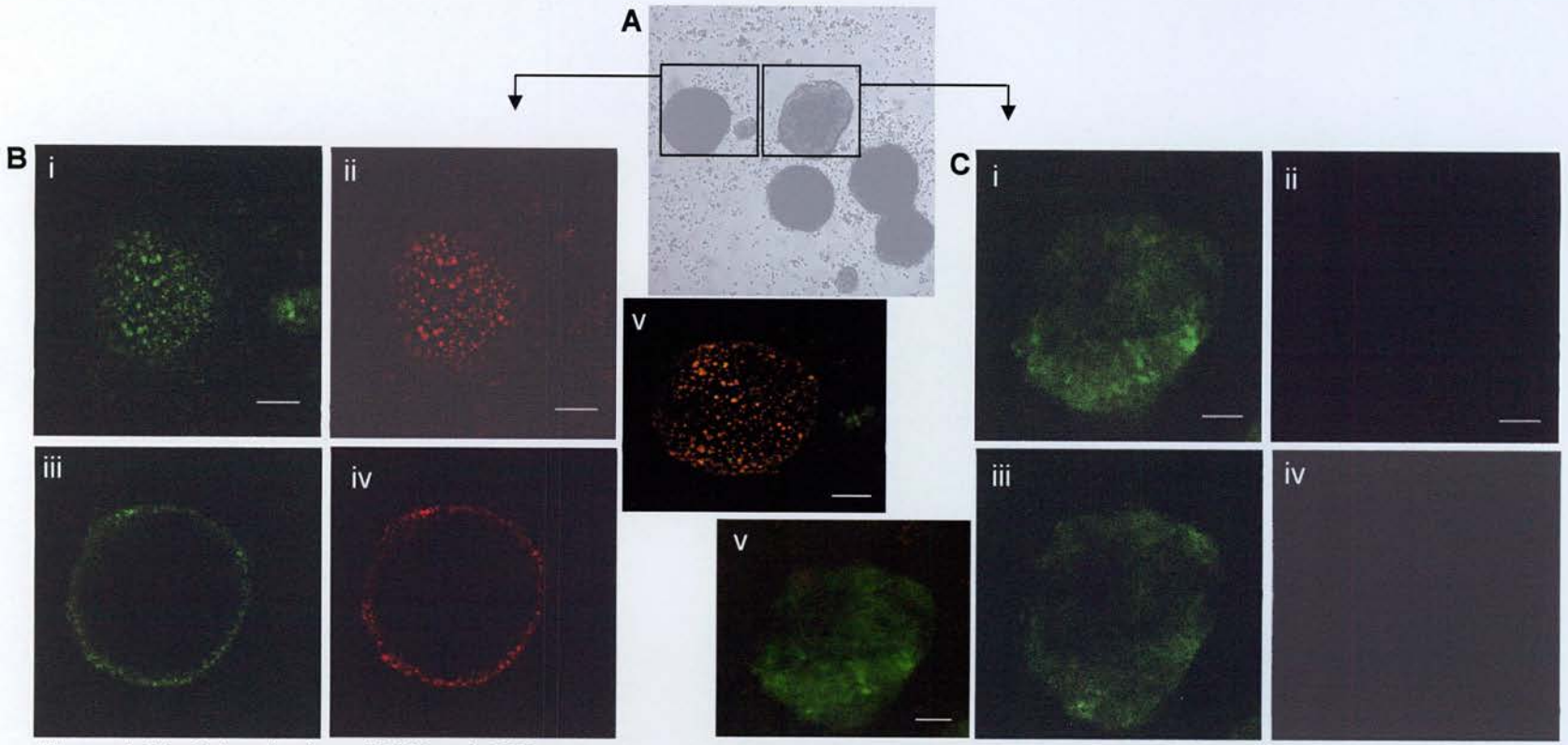

Figure 4.17: Colocalization of RFP and GFP expression on D8 EBs of 46C-TR cells. Optical dissection (5 µm/stack) on selected D8 EBs (A, bright field) of neural differentiation assay revealed colocalization of RFP and GFP. EB with only GFP expression was observed (C) but the expression of RFP alone was never observed (B). i and ii show the green and red fluorescent field, rspectively, of the second stack of the optical section. iii and iv show the green and red fluorescent field, rspectively, of the seventh stack of the optical section of the selected EBs. v shows the overlay for both EBs. Scale bar is 50 µm.

differentiation. In agreement with a previous study in which tamoxifen-regulated expression of human alkaline phosphatase in differentiated derivatives was lower than that of undifferentiated ES cells (Vallier *et al.*, 2001), the same phenomenon was also observed in our system. The system however is also capable of producing about the same induction level of transgene expression in undifferentiated ES cells and their differentiated derivatives. The high expression of the transgene in differentiated derivatives of ES cells is most likely due to the strong CAG promoter, which has been shown to be capable of maintaining strong transcriptional activity upon prolonged culture (Kosuga *et al.*, 2000; MacKay *et al.*, 2005). The promoter which consists of a human CMV immediate-early enhancer, a chicken ß-actin transcription start site together with intron sequences from rabbit ß-globin, has been shown to produce high level of gene expression in numerous *in vivo* studies (Miyazaki *et al.*, 1989; Niwa *et al.*, 1991; Nitta *et al.*, 2005).

The system also produced very low background activity of Cre-ER^{T2} (almost not detected) indicating an efficient repression of the genes downstream of the floxed-*neo*-stop cassette in the absence of 4'-OHT. The repression is most likely due to the selectable gene marker (*neo*^{r}) and the multiple polyadenylation sites for strong termination sequence inserted between the *loxP* sites in the pCAG-floxed-*neo*pA. Selection in G418 would eliminate the cells that spontaneously delete the floxed-*neo*pA cassette because of background activity of Cre-ER^{T2}, and the strong termination sequence would prevent the leakiness of transgene expression prior to treatment with 4'-OHT.

With double selection marker cassettes (floxed-*neo*pA and IRES-*pac*), our system also provides a more reliable screening method for transgenic clones with high inducing transgene activity. Puromycin selection after treatment with 4'-OHT on clones that survived neomycin (G418) selection positively selects the clones with full length expression construct; the most stable and integrated clones. The IRES-*pac* coding region downstream of the gene of interest inserted in the pCAG-floxed-*neo*pA vector allows for the selection in puromycin upon excision of the floxed-*neo*-stop cassette. The puromycin selection thus is able to eliminate the clones with truncated coding region of the gene of interest as only intact integrated clones survive the selection.

Induction of transgene expression is highly sensitive to 4'-OHT. We have observed the induction of expression following the treatment with as low as 200 nM of 4'-OHT after as short as 10 hour-treatment (data not shown). The sensitivity of the system is probably a result of the use of Cre-ER^{T2} recombinase that has been shown to be more sensitive to 4'-OHT induction than the original Cre-ER^{TM} (Feil *et al.*, 1997; Indra *et al.*, 1999; Vallier *et al.*, 2000). Besides being able to induce the expression of the transgene in a temporally controlled manner, the system also offers the production of constitutively expressing transgenic ES cells whenever required. One of the biggest problems with constitutive expression of Wnt genes and some other genes is the selective growth advantage of untransfected cells or cells that are spontaneously lost Wnt expression over cell expressing Wnts resulting in elimination of the cells which are constitutively expressing Wnt upon prolonged culture. As opposed to conventional approach, our system therefore offers greater advantage in that it is continuously capable of producing constitutive gene expression whenever required. The cells that

are constitutively expressing the gene of interest are easily selected by puromycin.

The transgenic ES cell lines established will be very useful for inducing ectopic expression of the genes at any specific time point during neural differentiation assay *in vitro*, thus allowing us to examine the consequences of overexpression during the process. We have demonstrated the ability of these cell lines in inducing the expression of transgene in undifferentiated ES cells and, more importantly, in differentiated derivatives of ES cells *in vitro*. Additionally, the production levels of transgene expression upon treatment with 4'-OHT should be enough for a biological effect to occur as has been shown in previous studies such as in the effect of forced expression of *sFRP2* on differentiation of 46C cells (Aubert *et al.*, 2002). The study showed the amplification of both endogeneous and introduced *sFRP2* sequences by RT-PCR where the production levels of the amplified gene were similar to our RT-PCR results for our induced transgene expression (data not shown). The system thus gives us the opportunity to examine the effects of overexpressing Wnt genes, specifically *Wnt1* and *Wnt3a*, on neural development in *vitro*. In addition, the effect of inhibiting Wnt signalling, by overexpression of *Dkk1*, during neural differentiation process could also be analysed.

4.3.2 Wnt responsive reporter gene expression system (TOP-Red2)

In this part of study, we have generated a Wnt responsive red fluorescent reporter gene expression in ES cells (TOP-Red2). The expression of the RFP was driven by the binding activity of multiple LEF/TCF binding sites in response to the presence of Wnt signals or activation of canonical Wnt

signalling. TOP-Red2 was found to be stably-integrated into the genome in undifferentiated and differentiated ES cells.

The system offers two advantages. First, it offers a direct visualization of the fluorescent protein in the living cells that are actually responding to Wnt signals, thus avoiding the use of other substrates in analysing the presence of the signal as required in other reporter gene system. For example, the use of vital substrates needed to visualize ß-galactosidase in *LacZ* reporter system or the use of Renilla plasmid in detecting the luciferase activity in Luciferase reporter system (such as TOPFLASH). Second, it allows for the detection of co-localization of proteins using spectrally different fluorochomes. RFP which is spectrally distinct form GFP and its blue, cyan and yellow variants would therefore be useful as an additional indicator.

However, the system which uses DsRed2 as the RFP has some drawbacks. Despite attempts in improving the problems with slow and incomplete maturation, and obligate tetramerization (Baird *et al.*, 2000; Verkhusha *et al.*, 2001a,b; Terskikh *et al.*, 2002) with DsRed, we found that the new version of DsRed, DsRed2, still has these problems. We believe that the system is still able to monitor the cells that are responding to Wnt signals but not the time point of the occurrence. A recent Ds-Red-derived monomeric RFP1 (mRFP1) has been shown to reduce these problems. A study by Long *et al.*, 2005 has shown the ability of mRFP1 to produce high levels expression of monomer RFP that are constitutively maintained in ES cells *in vitro* and in transgenic mice. Hence, a better TOP-Red2 might be produced if mRFP1 were to be used instead of DsRed2.

In this limited study, we discovered that only cells at the late stages of neural differentiation process were most likely to respond to canonical Wnt signal activity. However, the system was not able to exactly indicate the time for the occurrence of the signals. Nevertheless, this may suggest the presence of Wnt activity during late stages of neural differentiation process of ES cells *in vitro*.

Chapter 5: Manipulation of Wnt signalling during neural differentiation of mouse ES cells *in vitro*

5.1 Introduction

Based on numerous studies, Wnt signalling is now known to regulate multiple functions during animal development especially during the development of the CNS (Chapter 1). A number of *in vivo* and *ex vivo* studies of mouse embryos have strongly suggested the activity of Wnt to be stage-dependent, in which depending on the cell-intrinsic properties at a particular time point during neural development switches its role from, for example, promoting cell proliferation to cell differentiation (Chapter 1). Several *in vitro* studies also have implicated different roles of Wnts during neural differentiation of ES cells. It has been observed that Wnt signalling seems to inhibit the differentiation of these cells into neural precursor cells (Aubert *et al.*, 2002; Kielman *et al.*, 2002; Haegele *et al.*, 2003) and may also stimulate the formation of neurons from these precursor cells (Hirabayashi *et al.*, 2004; Muroyama *et al.*, 2002, 2004; Watanabe *et al.*, 2005). In accordance to this, our results (Chapter 3) also demonstrated some interesting dynamic RNA expression profiles for a number of Wnt genes, which might indicate functional properties of the genes during neural differentiation. However due to the nature of Wnt, isolation of an active form of its protein has been extremely difficult and only recently being managed to be purified (Willert *et al.*, 2003). Only purified Wnt3a and Wnt5a-HA have ever been used (Schulte *et al.*, 2005). Other *in vivo* studies in mouse embryos are mostly done by injecting the mouse ventricles with retroviruses overexpressing the Wnt gene of interest (Viti *et al.*, 2003; Hirabayashi *et al.*, 2004). Most *in vitro* studies in analysing the functions of Wnt genes during mouse neural development

used Wnt conditioned medium (Castelo-Branco *et al.*, 2003) or recently purified Wnt5a (Schulte *et al.*, 2005) treated on selected mouse embryo explants.

Studies involving analysis of Wnt function during neural differentiation of ES cells *in vitro* mostly used Wnt conditioned medium (CM, Haegele *et al.*, 2003; Watanabe *et al.*, 2005;) or constitutive overexpression of a particular Wnt gene (Aubert *et al.*, 2002). Unfortunately, Wnt CM does not represent the whole effect of purified active form of Wnt protein since other extracellular factors contained in the medium may underscore the function of Wnt compared to if the purified Wnt protein is used (Willert *et al.*, 2003). Willert and colleagues (2003) have discovered that Wnt3a CM promotes differentiation of HSCs while purified Wnt3a protein stimulates self-renewal of these cells. Constitutive overexpression of Wnt, on the other hand, does not allow for temporal function of Wnt at a specific time point to be analysed. Hence evaluation of stage-dependent Wnt function is hampered.

Here an inducible ES system would be an invaluable tool in monitoring the effect of inducing or deleting specific Wnt gene in a temporally-controlled manner in culture conditions. In accordance to this, we have established an ES cell inducible system (chapter 4) that would allow us to directly test the hypothesis that Wnt signalling may inhibit the differentiation of ES cells into NPCs and then may also function in stimulating the differentiation of these NPCs into neurons. The system offers a greater advantage compared to previous studies such as the study by Aubert *et al.*, 2003 which only analysed the effect of constitutive expression of *Wnt1* during neural differentiation of ES cells. Our system, as far as the study is concerned, is the first system to

be described that uses a tightly controlled overexpression of Wnt in a temporally-controlled manner in analysing its effects during neural differentiation of ES cells.

By using the system, this study was aimed to examine the effects of stimulating or inhibiting Wnt signalling at specific time points during neural differentiation of ES cells in culture. Based on the expression profiles determined in previous chapter and due to time limitations, we were able to overexpress only two Wnt genes (*Wnt1* and *Wnt3a)* and one Wnt antagonist *(Dkk1)* during the differentiation process. The neural differentiation process was carried through the formation of EBs and RA induction (4-/4+ protocol, Bain *et al.,* 1995; Li *et al.,* 1998a). Specifically the aims were to see whether activation of Wnt signalling by overexpressing a particular Wnt gene (*Wnt1* or *Wnt3a*) or inhibiting certain Wnts activities, specifically the canonical Wnt signalling by overexpressing Wnt antagonist, Dkk1, at a specific time point during the process would lead to the inhibition or promotion of the differentiation processes. This was targeted to see whether the formation of NPCs and neurons were inhibited or stimulated in the cultures stimulated by RA through the formation of EBs.

Induction of these genes at different time points during the process was conducted using the optimized inducible ES cell system as described in chapter 4. The ubiquitous Cre-expressing ES cell line, R26CT2S, was stably-transfected with a pCAG-floxed-*neo*pA vector carrying the gene of interest or empty vector. We have established stably-transfected *Wnt1*-HA (CAG-floxed-*neo*pA-*Wnt1*-HA), *Wnt3a* (CAG-floxed-*neo*pA-*Wnt3a*), *Dkk1* (CAG-floxed-*neo*pA-*Dkk1*) and empty vector (CAG-floxed-*neo*pA) ES cell clones.

The transgene was induced at three time points (Figure 5.1). At the first time point, the gene expression was induced in undifferentiated ES cell clones by treatment with 500 nM 4'-OHT for 2 days prior to selecting the cell expressing the particular gene in 1.0 μg/ml puromycin (as described in Chapter 4). This puromycin resistant ES cell line is constitutively expressing the particular transgene. The second point of induction took place on D2 and finally, the third induction point was on D7 of neural differentiation process and exposed for 48 hours. As described in the previous chapter, the highest RNA expression of transgenes in EBs was detected after 48 hours of treatment with 4'-OHT. Treatment with 4'-OHT on D2-4 of neural differentiation process therefore was presumed to give enough time for the expression of the particular transgene to give any cellular effect on Wnt signalling during early stages of the process particularly prior to the formation of NPCs (before the addition of RA, Figure 5.1). In addition, treatment of 4'-OHT on D7-9 was intended to give enough time for the expression of transgene to have effects on Wnt signalling at late stages of the process specifically after the addition of RA, during the presence NPCs.

In summary, the effect of overexpressing Wnt gene and Wnt antagonist at the early stages of the process should give us the opportunity to examine the ability of the early stage EBs of neural differentiation process to differentiate into NPCs and later on the ability of these precursors to differentiate into neurons. The effect of overexpressing the genes at the late stages of the process, in addition, gives us the opportunity to analyse the ability of NPCs to form neurons. Moreover, constitutive expression of the transgene gives us the opportunity to analyse the ability of ES cells to differentiate into NPCs and later on the ability of these precursors to differentiate into neurons.

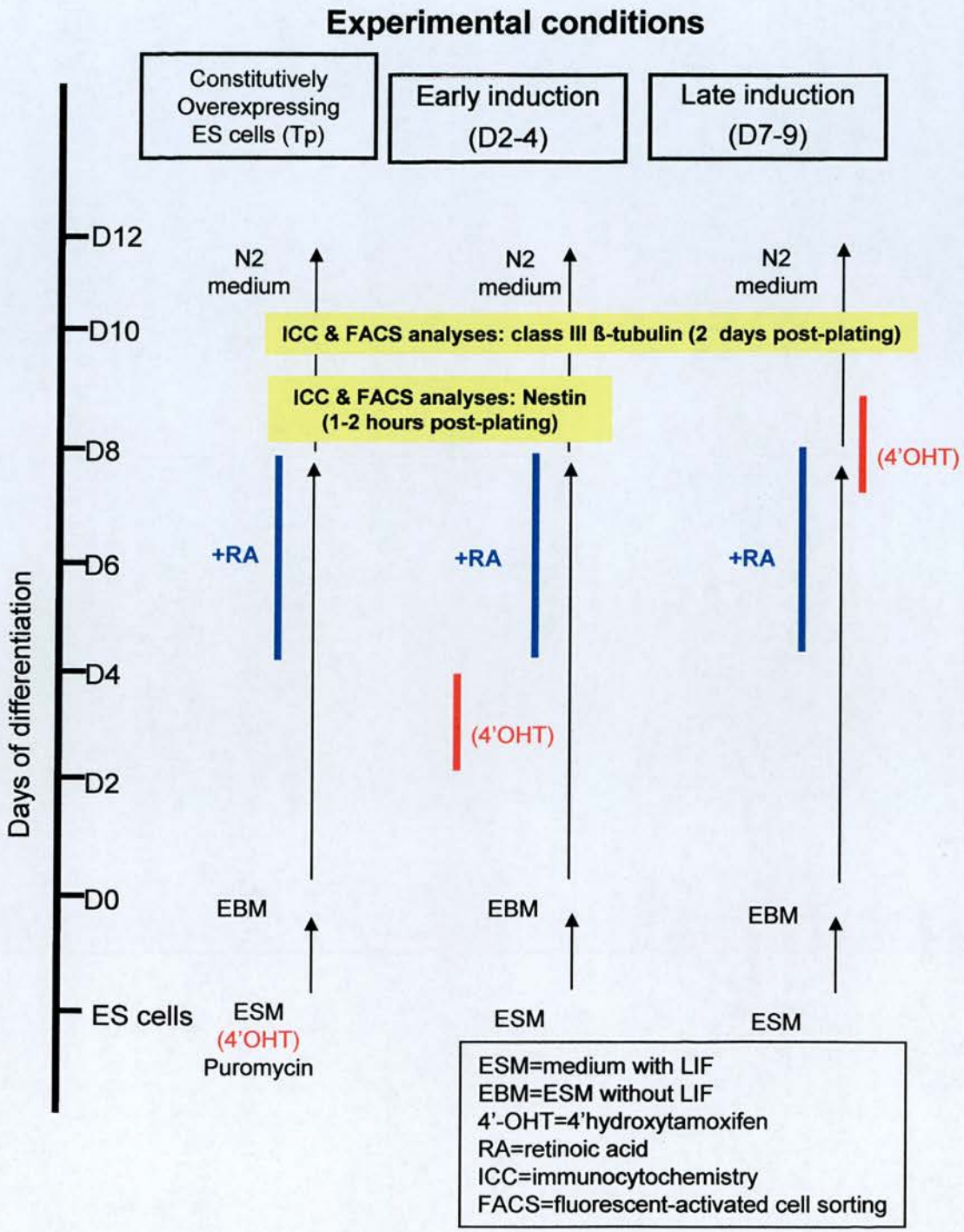

Figure 5.1: Schematic representation of neural differentiation assay of ES cells *in vitro*. Temporal sequence of all induction for *Wnt1*, *Wnt3a* and *Dkk1* overexpression by treatment with 4'-OHT (as indicated in red). Analysis for the formation of NPCs is done 1-2 hours post-plating by ICC and FACS using Nestin. The formation of neurons is analyzed by ICC and FACS using class III ß-tubulin, 2 days post-plating.

5.2 Results

5.2.1 Effects of 4′-OHT on ES cells during neural differentiation

To examine the potential cytotoxic effect of 800 nM 4′-hydroxytamoxifen (4′-OHT) on the cells during neural differentiation process, CAG-floxed-*neo*pA ES cell line was used. The ability of these cells to differentiate into NPCs was compared between non-treated and treated EBs on D2-4 with 800 nM 4′-OHT (Figure 5.2). Neural induction was then followed by adding 1.0 μM *all-trans* retinoic acid (ATRA) into the EB culture medium for four days (D4-8) prior to dissociation of D8 EBs onto PDL/laminin-coated plates and grown in DMEM-F12/N2 medium. 1-2 hours post-plating the cells were either fixed in 4% PFA for immunocytochemistry or trypsinized for FACS analysis. Both sets of cells were stained with a marker for uncommitted neural precursor cells, nestin. As compared to non-treated cells, treatment with tamoxifen on D2 EBs did not affect the ability of CAG-floxed-*neo*pA ES cells to differentiate into NPCs (Figure 5.2). In agreement with this, FACS profiles also show no significant difference in the percentage of the cells expressing nestin (Figure 5.2D, H) between non- and treated cells. There was also no significant difference between the percentage of nestin positive cells between FACS analysed and manually counted results (Figure 5.3A, C). In addition, there was no significant difference between the number of nestin non-expressing cells between non- and treated cells (Figure 5.3B, C), indicating that tamoxifen does not affect the survival of either non- or neural cells in culture. Thus, tamoxifen at a concentration of 800 nM does not affect the ability of EBs to form neural precursor cells in the presence of RA *in vitro*, in other

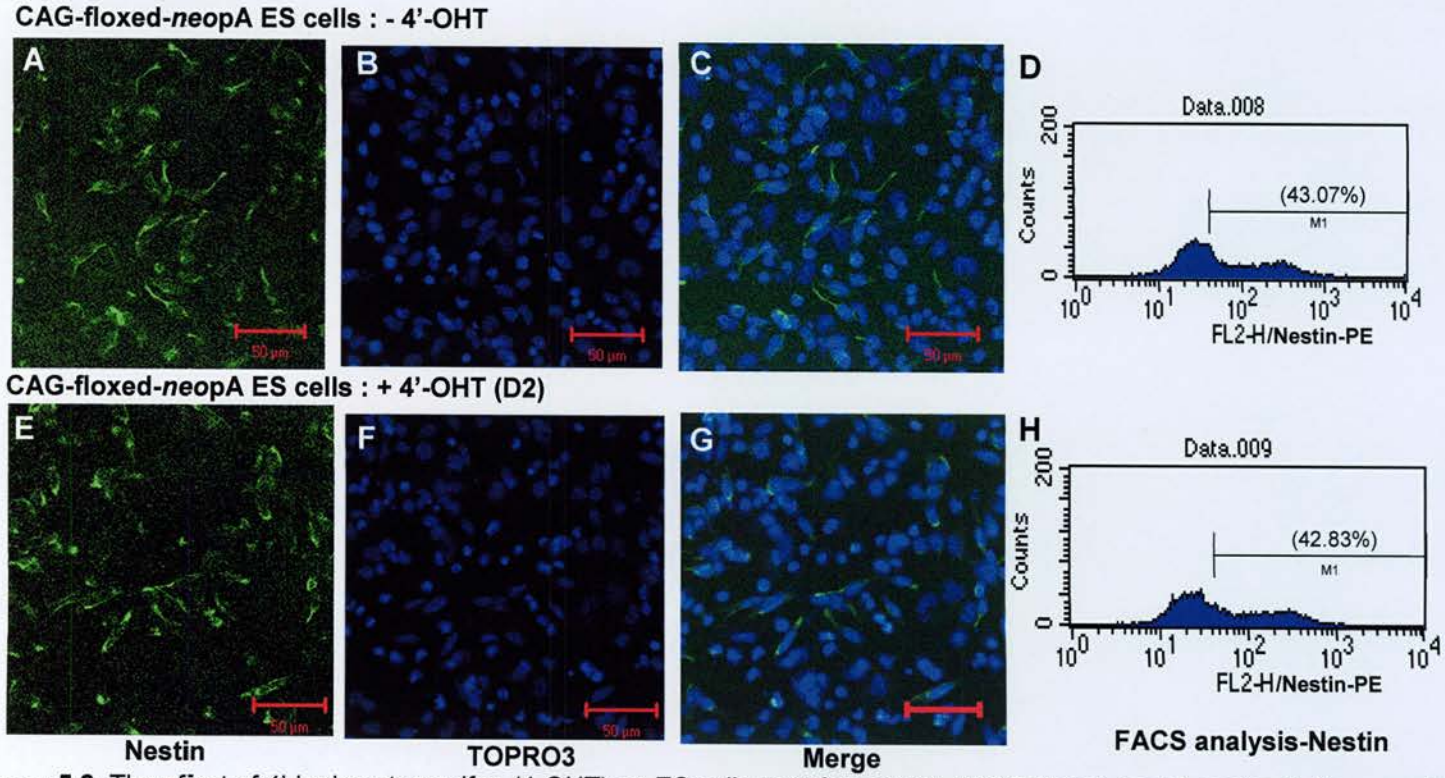

Figure 5.2: The effect of 4'-hydroxytamoxifen (4-OHT) on ES cells transfected with pCAG-floxed-*neo*pA vector during neural differentiation process (CAG-floxed-*neo*pA cells). CAG-floxed-*neo*pA ES cells were treated with 800 nM 4'-OHT on D2 for 48 hours, and their ability to differentiate into npc was compared to the non-treated cells. The EBs were dissociated on D8 before being plated on PDL/laminin plates. The cells were then stained for intermediate filament protein, nestin for NPCs after 1-2 hours post-plating. A,E are nestin immunocytochemistry (ICC) for non- and treated cells, respectively. D,H are FACS profiles for nestin staining for non-treated and treated cells, respectively. The percentage of nestin expressing cells is shown in parentheses. B,F are cells stained with TOPRO3 while C,G are the merge images for the respective treatment. Note that both results, ICC and FACS, demonstrate that treatment with tamoxifen at 800 nM does not have any effect on the ability of the cells to differentiate into NPCs. Scale bar is 50 µm.

A)

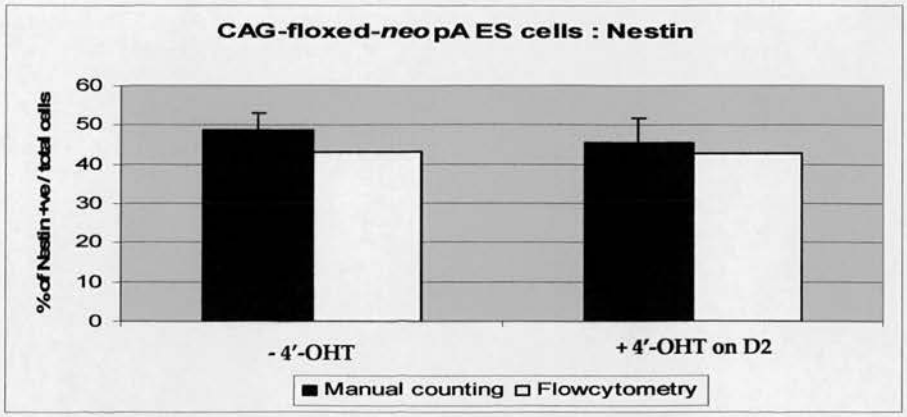

B)

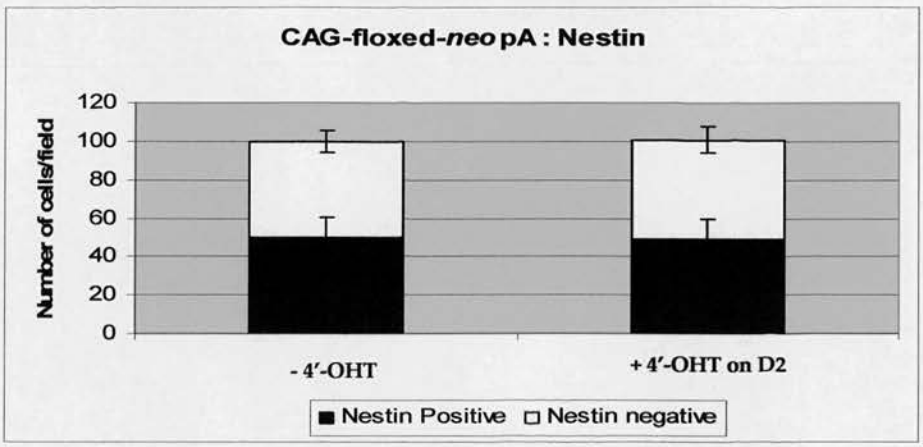

C)

CAG-floxed-*neo*pA	Nestin positive cells (± SEM)	Nestin negative cells (± SEM)	% of Nestin positive (± SEM)	Total cell	Flowcytomety (% positive cells)
- 4'-OHT	50.17 ± 9.99	49.83 ± 5.65	48.83 ± 4.37	600	43.07
+ 4'-OHT on D2	48.83 ± 11.09	52.17 ± 6.53	45.53 ± 6.38	606	42.83

Figure 5.3: Quantification of nestin expressing cells from 4'-OHT non- and treated CAG-floxed-*neo*pA ES cells. The cells stained for nestin as shown in Figure 5.2 were counted, plotted and tabulated. A) The percentage of nestin positive cells over total number of cells were manually counted and analysed by FACS. Results from both analyses were then plotted. The results demonstrate that tamoxifen does not affect the percentage of nestin positive cells for both conditions. B) Average cell number of nestin positive and negative cells per field was counted and compared between non- and treated cells. The results clearly show that tamoxifen at 800 nM does not effect the survival of nestin positive and negative cells during neural differentiation process of ES cells *in vitro*. C) Data for A and B were tabulated. Error bars are mean ± SEM (n=6 fields) from single experiment with duplicate wells. Tamoxifen at a concentration of 800 nM does not seem to have any effect on the ability of ES cells to differentiate into NPCs and also the survival of non-neural precursor cells.

words, 4'-OHT neither promotes nor inhibits the differentiation of ES cells into NPCs.

We were then interested to know whether tamoxifen treatment affected the ability of CAG-floxed-*neo*pA cells to differentiate into neurons when the cells were treated on D2 and also on D7 during neural differentiation assay. After dissociation on D8, the cells were stained for neuronal marker, class III ß-tubulin, 48 hours post-plating. Immunocytochemistry (ICC) with ß-tubulin shows no significant difference on the ability of non- and treated cells to differentiate into ß-tubulin positive cells (Figure 5.4 A, D, G). In addition, tamoxifen also does not affect the survival of ß-tubulin negative cells (Figure 5.4 B, C, E, F, H, I). For quantification, total cells and cells stained with ß-tubulin were manually counted, plotted (Figure 5.5A, B) and tabulated (Figure 5.5C). The percentage of ß-tubulin positive cells was about the same with no significant different between non- and treated cells (Figure 5.5A, C). Similar to ICC with nestin, there was no significant difference between ß-tubulin negative and positive cells per field beween non- and treated cells (Figure 5.5 B, C), indicating that tamoxifen does not affect the survival of non- and neuronal cells. Taken together, these results show that tamoxifen at 800 nM does not affect the ability of CAG-floxed-*neo*pA ES cells to differentiate into NPCs (nestin-expressing cells) or neuronal cells (ß-tubulin-expressing cells). It also has no affect on the survival of both non- or neural and non- or neuronal cells. The same phenomenon was observed when the experiment was repeated using another clone of CAG-floxed-*neo*pA cells (data not shown). Therefore, 800 nM 4'-OHT does not seem to have any cytotoxity effect on neural and neuronal differentiation process through the formation of EBs in the presence of RA.

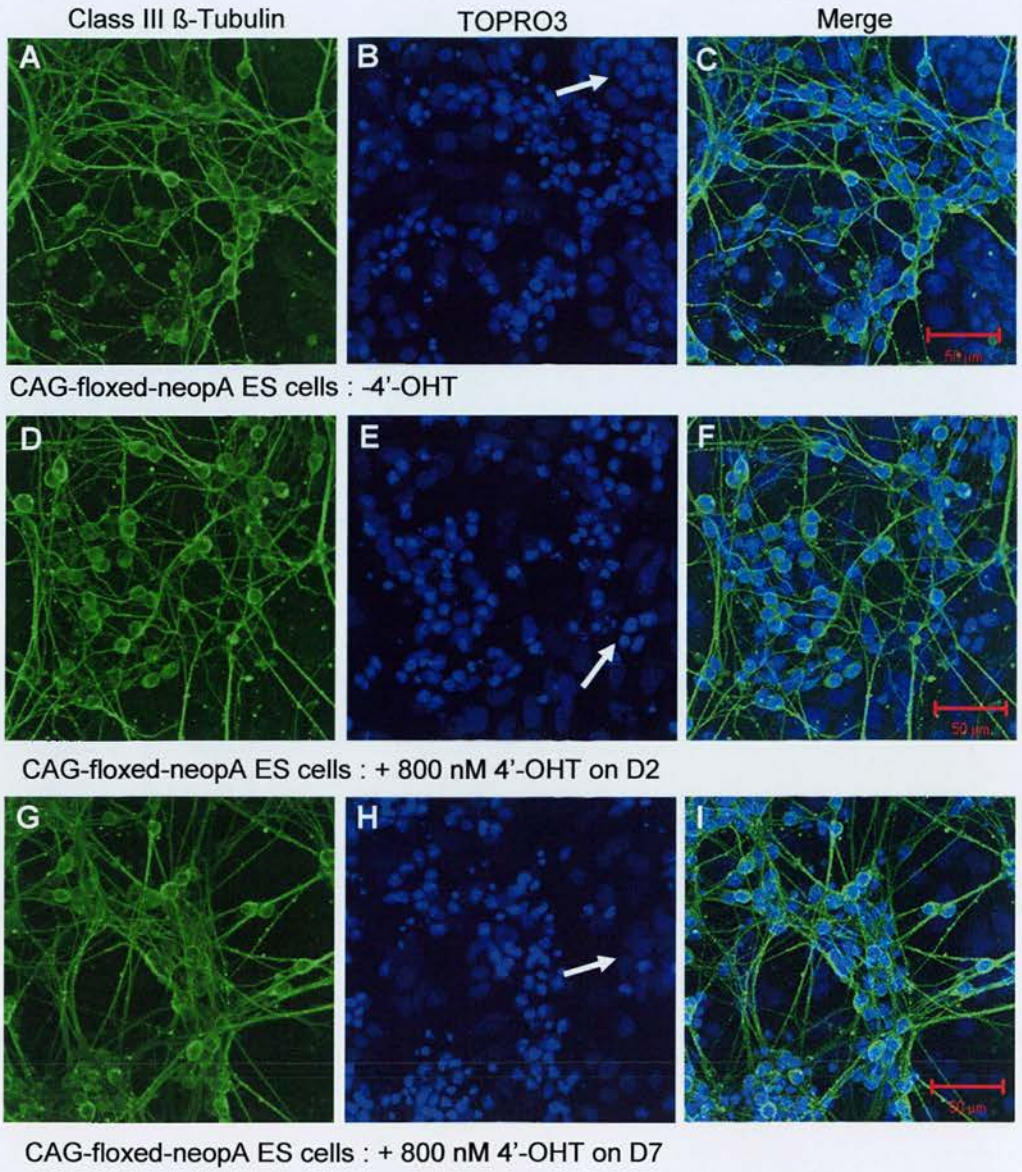

Figure 5.4: The effect of 4'-OHT on R26CT2S cells stably-transfected with pCAG-floxed-*neo*pA on the formation of neurons *in vitro*. D8 EBs were trypsinized and plated on PDL/laminin-coated plate before the cells were stained for neuronal marker, class III ß-Tubulin, 48 hours post plating. A, D and G show immunocytochemistry with class III ß-Tubulin for non-treated cells, cells treated with 800 nM tamoxifen on D2 and on D7, respectively. Nuclei stained with TOPRO3 for each respective treatment is shown in B, E and H. C, F and I show the merge between TOPRO3 and class III ß-Tubulin for each respective treatment. Tamoxifen at 800 nM does not have any effect on the formation and survival of both non- and neuronal cells. White arrows indicate the ß-tubulin negative cells. Scale bar is 50 µm.

A)

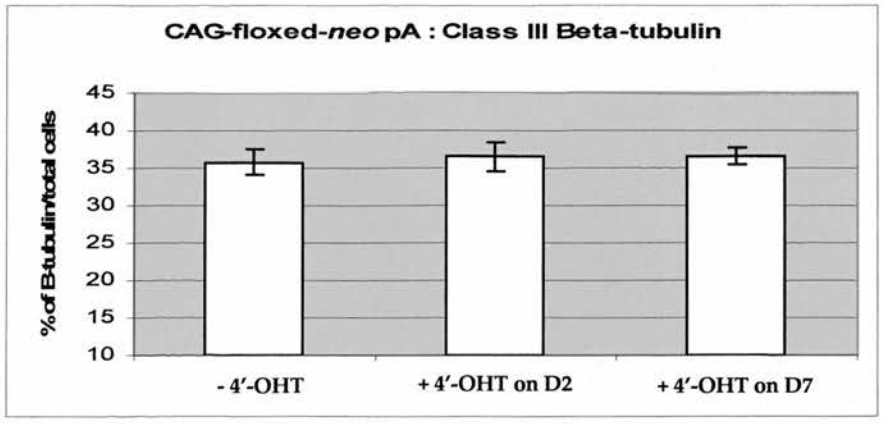

B)

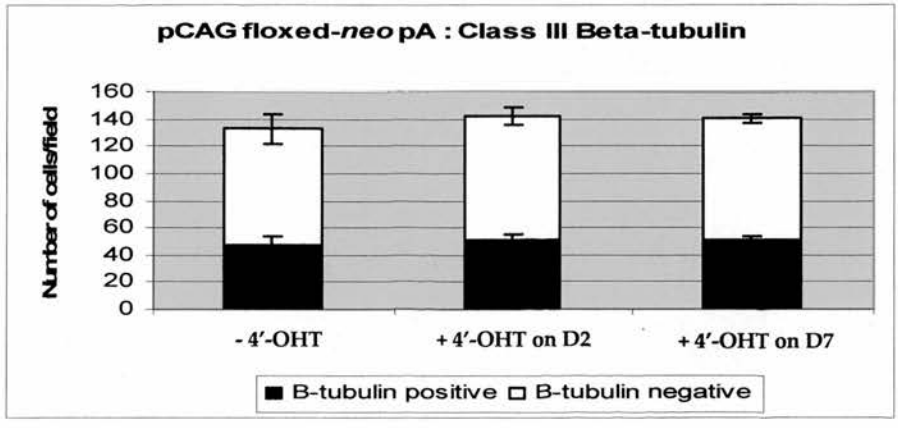

C)

CAG-floxed-*neo*pA	B-tubulin positive cells (± SEM)	B-tubulin negative cells (± SEM)	% of B-tubulin positive (± SEM)	Total cell score
- 4'-OHT	47.62 ± 6.18	85.00 ± 10.42	35.79 ± 1.73	1061
+ 4'-OHT (D2)	51.62 ± 3.36	90.87 ± 6.62	36.49 ± 1.96	1140
+ 4'-OHT (D7)	51.25 ± 1.94	89.12 ± 2.91	36.52 ± 1.12	1123

Figure 5.5: Quantification analysis of ß-tubulin expression in untreated and treated (on D2 and D7) CAG-floxed-*neo*pA ES cells. The cells stained for ß-tubulin 2 days post-plating were manually counted. Percentage of ß-tubulin positive cells were plotted (A) and tabulated (C). Total number of ß-tubulin positive and negative cells per field were also plotted (B) and tabulated (C). There was no significant difference on the formation of neurons between non- and treated cells. Error bar is the mean ± standard error of mean (SEM, n=8 fields) from single experiment with duplicate wells.

5.2.2 Effects of *Wnt1*-HA overexpression during neural differentiation of ES cells

To examine the effect of overexpressing *Wnt1* on neural differentiation of ES cells *in vitro,* stably-transfected Cre-expressing ES cells (R26CT2S) with pCAG-floxed-*Wnt1*-HA construct (CAG-floxed-*neo*pA-*Wnt1*-HA ES cells) were used. In this part of study, we wanted to determine the effect of inducing *Wnt1*-HA at early stages of differentiation (on D2-4 EBs, just before the addition of ATRA) as well as constitutive expression of *Wnt1*-HA on the formation of NPCs and neurons. We also wanted to know the capability of the cells overexpressing *Wnt1*-HA during the late stages (on D7-9 EBs) of differentiation process to differentiate into neurons. Wnt1-HA was induced by treating CAG-floxed-*neo*pA-*Wnt1*-HA cells at indicated time points with 800 nM 4'-OHT for 48 hours. In all cases, dissociated D8 EBs were plated at a density of 3 x 10^5 cells/cm^2. The formation of NPCs was determined by the presence of cells expressing nestin, while neuronal cells were confirmed by the presence of the class III ß-tubulin-expressing cells. In all cases, the number of cells expressing these antibodies was manually counted and the percentage of the positive cells expressing the antibody was calculated. In some cases the percentage of positive cells expressing these antibodies were confirmed by FACS analysis. Results from three independent experiments on two separate clones of CAG-floxed-*neo*pA-*Wnt1*-HA ES cells will be presented.

5.2.2.1 Constitutive expression of *Wnt1*-HA

1-2 hours post-plating, most cells expressing nestin have a spindle-shaped morphology in untreated CAG-floxed-*neo*pA-*Wnt1*-HA cells (Figure 5.6A, D)

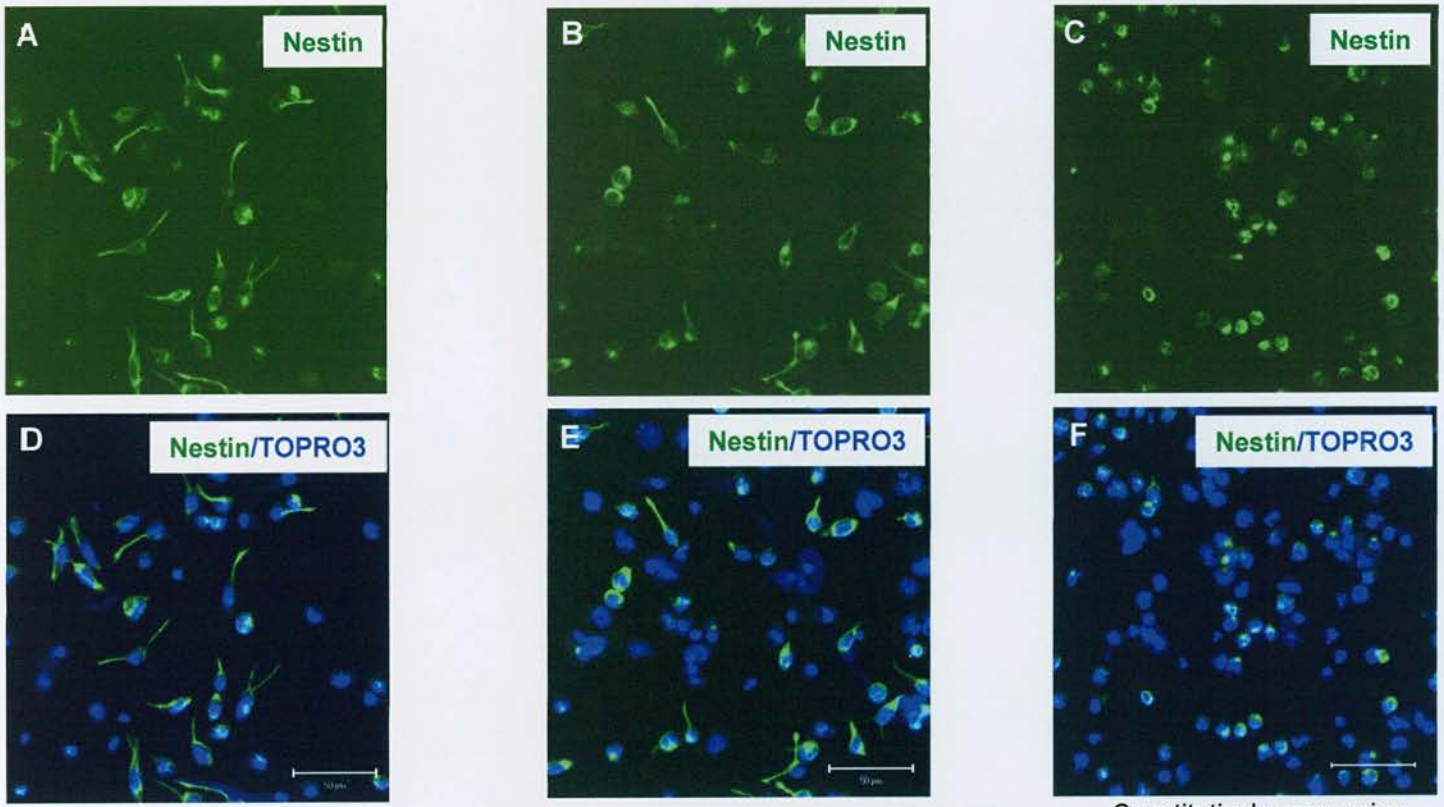

Figure 5.6: Nestin expression in *Wnt1*-HA expressing ES cell lines. Cre-expressing ES cell line (R26CT2S) was stably transfected with pCAG-floxed-*neo*pA-*Wnt1*-HA construct. ICC was carried out for intermediate filament protein, nestin, after 1-2 hours post plating on the cells treated with A) no 4'-OHT or B) 4'-OHT on D2, and C) constitutively expressing *Wnt1*-HA cells. D, E and F show the merge between nuclei staining with TOPRO3 and Nestin for each respective treatment. Scale bar is 50 µm.

as shown by ICC results. However the number of nestin-expressing cells was reduced in the cells constitutively expressing *Wnt1*-HA with no appearance of the spindle-shaped morphology (Figure 5.6C, F). In agreement with this, FACS profiles also demonstrates a lower percentage of cells expressing nestin in these cells compared to untreated cells (Figure 5.7C,G). ICC results also show a significant decrease in the percentage of nestin-expressing cells as well as the number of nestin-positive cells per field compared to Wnt1-HA non-overexpressing cells (control, Figure 5.8A,C,E).

A number of *in vivo* and *in vitro* studies have suggested the role of *Wnt1* in promoting the proliferation rate of precursor cells during the development of mouse embryonic brain (McMahon and Bradley, 1990; Thomas and Capecchi, 1990; Castelo-Branco, *et al.*, 2003; Panhuysen *et al.*, 2004). We were interested to see if the same phenomenon would be observed in our system. We wanted to examine whether the number of nestin-expressing cells would be increased 24 hours after plating the dissociated D8 EBs on PDL/laminin-coated plates. To our surprise, after 24 hours post-plating, both FACS (Figure 5.7D,H) and ICC results demonstrate an increase of nestin-expressing cells in *Wnt1*-HA constitutively expressing cells compared to the control cells (Figure 5.8).

A significant reduction of ß-tubulin expressing cells was observed after 48 hours post-plating from these cells compared to that of the control cells as analysed by ICC and FACS (Figure 5.9, 5.10). Interestingly, as observed by Aubert and colleagues (2002), we also found that constitutive expression of *Wnt1*-HA directed the differentiation of ES cells into non-neuronal cells and inhibited the formation of neurons (Figure 5.9K, 5.10K,L). A different type of

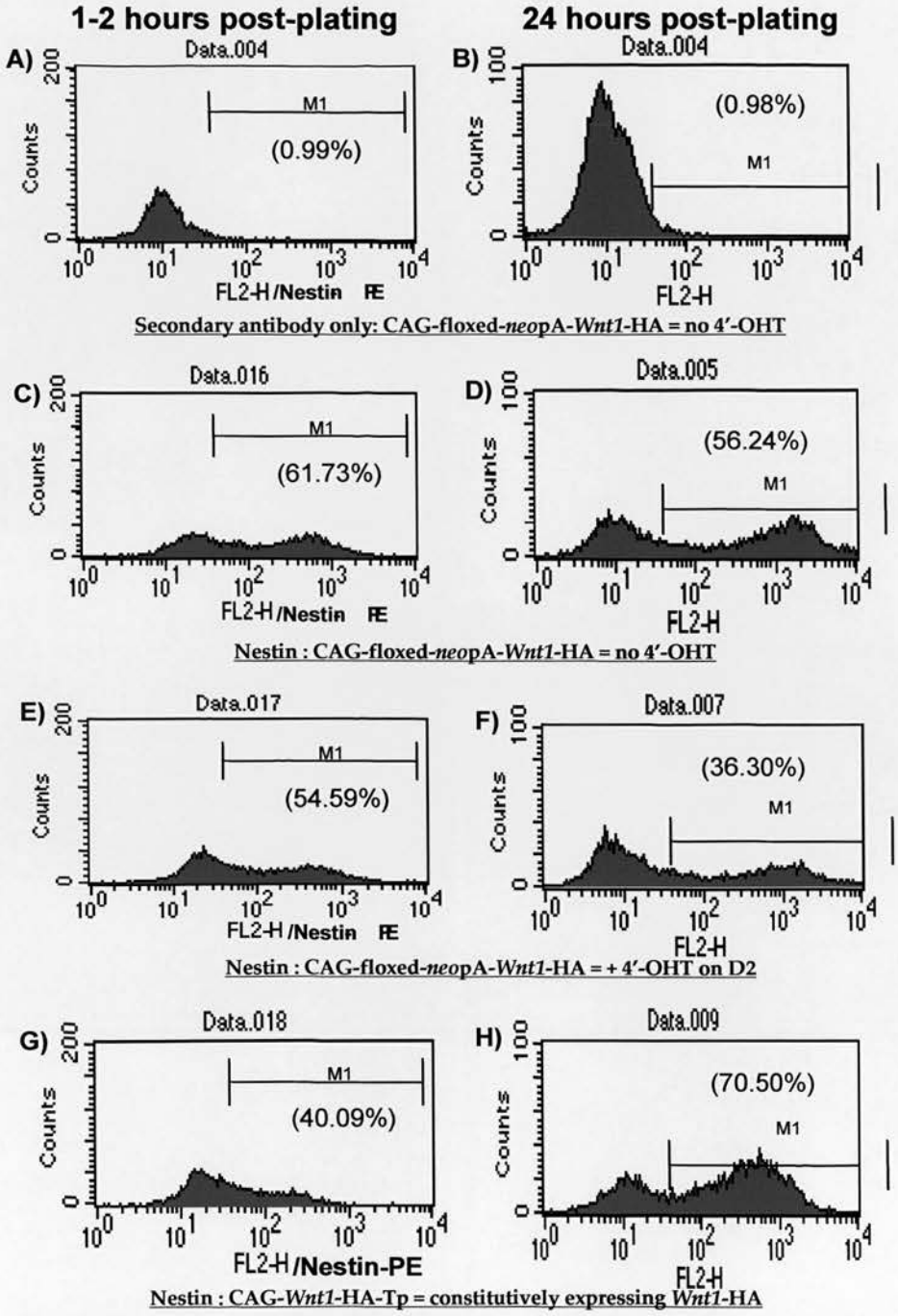

Figure 5.7: FACS analysis on *Wnt1*-HA expressing cell lines stained for nestin 1-2 (A,C,E,G) and 24 (B,D,F,H) hours post plating. (A, B) Non-treated CAG-floxed-*neo*pA-*Wnt1*-HA cells stained with only secondary antibody (PE). This acts as control cells for setting up the M1 gate. (C,D) untreated CAG-floxed-*neo*pA-*Wnt1*-HA cells, (E,F) the cells treated with 800 nM 4'-OHT on D2 and (G,H) constitutively expressing *Wnt1*-HA cells (CAG-*Wnt1*-HA-Tp). The percentage of nestin positive cells is shown in parentheses.

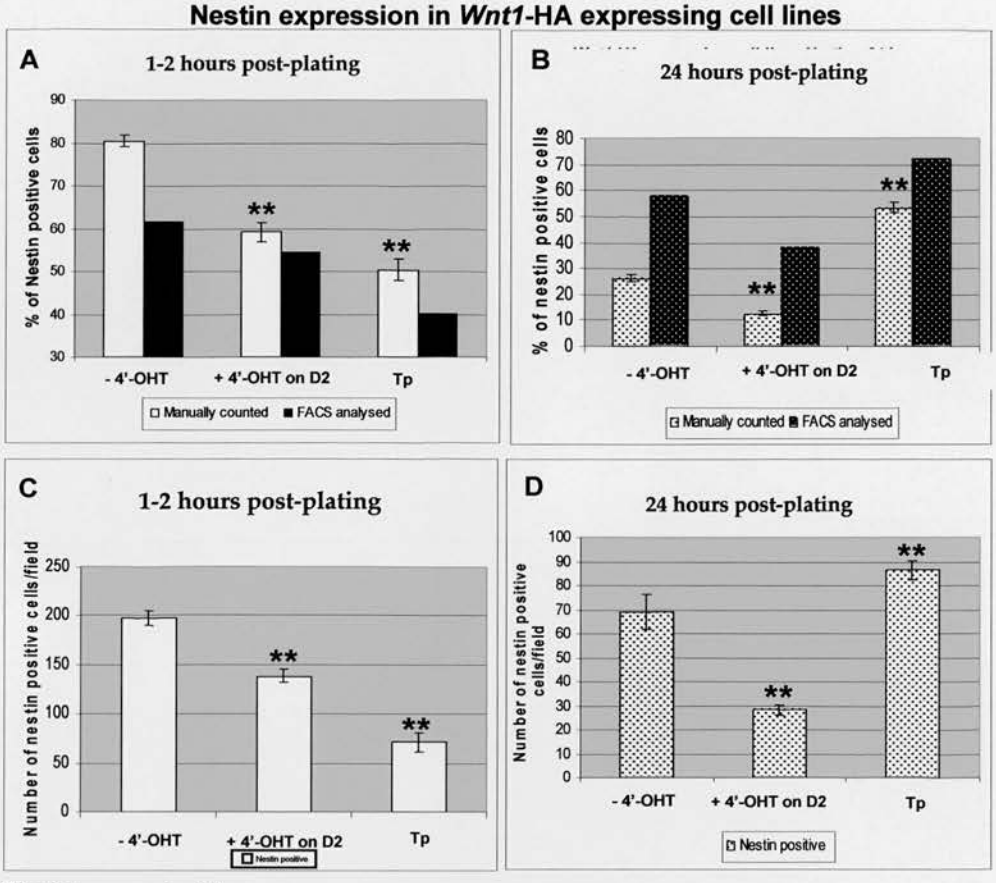

E) 1-2 hours post-plating

Wnt1-HA expressing cell lines	Number of nestin positive cells/field (1-2 hours post plating) (± SEM)	% of nestin positive (manual counting, 1-2 hours post plating) (± SEM)	Total cell score	FACS data 1-2 hours post plating (± SEM)
- 4'-OHT	197.5 ± 7.75	80.54 ± 1.25	3915	61.73
+ 4'-OHT on D2	138.12 ± 6.57	59.22 ± 2.23	3892	54.59
Constitutively expressing Wnt1-HA (Tp)	71.17 ± 10.22	50.36 ± 2.60	828	40.09

F) 24 hours post-plating

Wnt1-HA expressing cell lines	Average nestin positive cells/field (± SEM)	% of nestin positive cells 24 hours post plating (± SEM)	Total cell score	FACS data
- 4'-OHT	69.125 ± 7.09	26.34 ± 1.60	6019	56.24
+ 4'-OHT on D2	28.25 ± 2.11	12.64 ± 0.94	5467	36.30
Constitutively expressing Wnt1-HA (Tp)	86.46 ± 3.76	53.56 ± 2.15	3909	70.50

Figure 5.8: Quantitative analysis of Nestin expression of *Wnt1*-HA expressing lines from ICC by manual counting and FACS 1-2 (A,C,E) and 24 (B,D,F) hours post-plating. Percentage (A,B) and number (C,D) of Nestin positive cells from CAG-floxed-*neo*pA-*Wnt1*-HA cells treated with no 4'-OHT and 800 nM 4'-OHT on D2, and CAG-Wnt1-HA-Tp cells. (E,F) tabulated data of results from A-D. Manually counted results for NPCs (Nestin) 1-2 and 24 hours post plating were from three independent experiment from two clones (n=8 fileds) and single independent experiment with duplicate wells (n=21 fields), respectively. FACS results were from single independent experiment from one clone. ** indicates highly significant to non-induced, T-test $p<0.001$. Error bar is the mean ± standard error of mean, SEM.

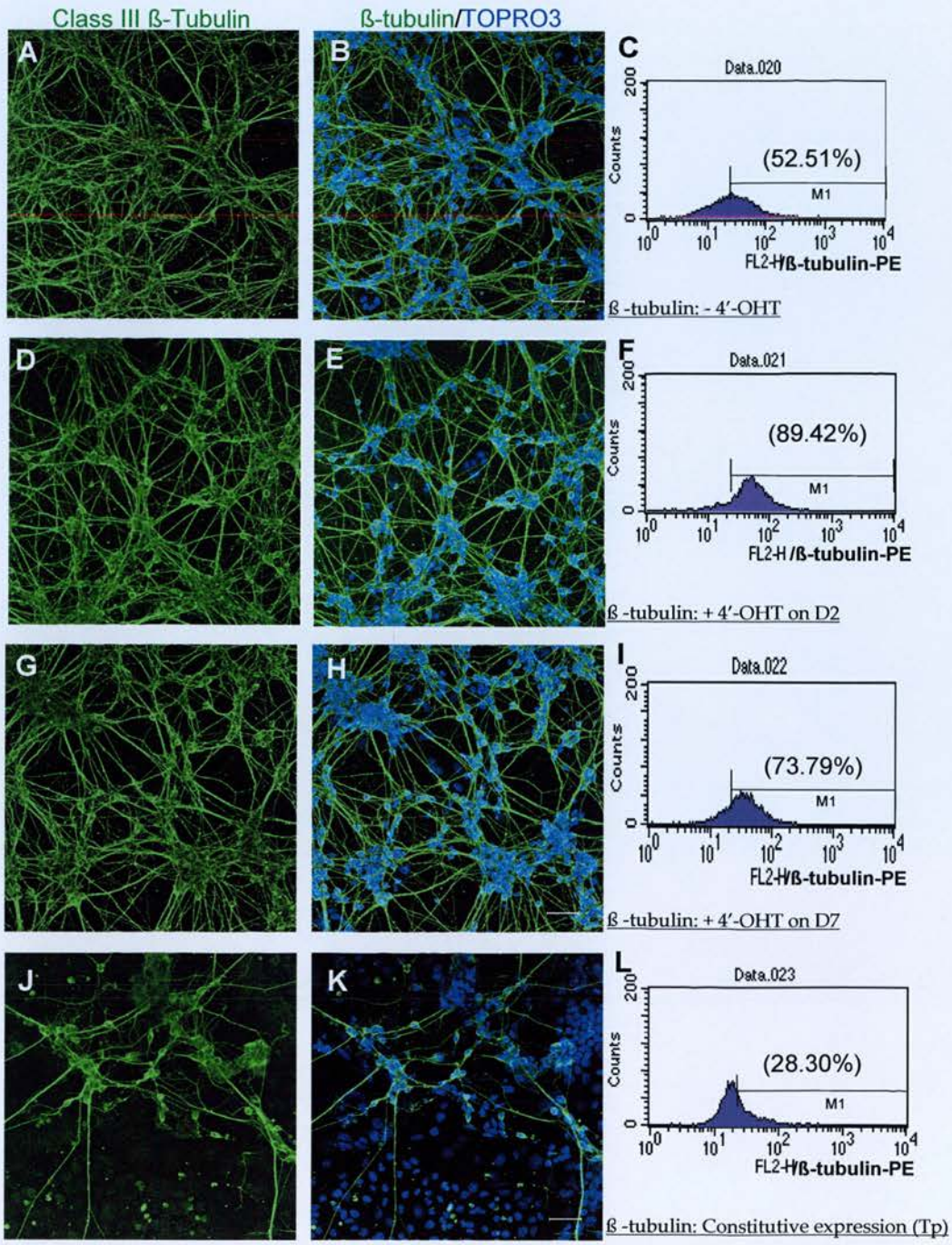

Figure 5.9: ß-tubulin expression in *Wnt1*-HA expressing cells. The effect of overexpressing *Wnt1*-HA on D2 (D,E,F) and D7 (G,H,I), and constitutively overexpressing *Wnt1*-HA (J,K,L) compared to uninduced (A,B,C) cells was analysed by ICC (A,B,D,E,G,H,J,K) and FACS (C,F,I,L). D8 EBs were trypsinized and plated on PDL/laminin-coated plates in N2 medium before the cells were stained for neuronal marker, class III ß-Tubulin, 48 hours post plating. A, D, G and J show immunocytochemistry with class III ß-Tubulin. Merge of ß-tubulin staining and nuclei stained with TOPRO3 for each respective treatment is shown in B, E, H and K. Scale bar is 50 µm.

ß-tubulin-negative cells was observed when compared to the ß-tubulin-negative cells formed from untreated cells (the control cells, Figure 5.10B,K, cells in circle and rectangular shape). Quantitative analysis also revealed a significant decrease in the percentage of ß-tubulin positive cells as well as the number of ß-tubulin-expressing cells per field from these cells (Figure 5.11). Interestingly enough, neural differentiation of these cells (CAG-Wnt1-HA-Tp) also led to the similar formation of non-neuronal cells or ß-tubulin-negative cells even in the absence of RA (Figure 5.12J-L) compared to that of the control cells as well as early and late induction of cultures without RA treatment (Figure 5.12A-I).

In summary, constitutive expression of *Wnt1*-HA during the differentiation process may inhibit the formation of NPCs. Constitutive expression of *Wnt1*-HA also may inhibit neuronal differentiation of ES cells into neurons.

5.2.2.2 Overexpression of *Wnt1*-HA at early stages

The formation of nestin-expressing cells was reduced in the cells where the overexpression of *Wnt1*-HA was induced at the early stages of neural differentiation process when analysed 1-2 hours post-plating. The number of cells with spindle-shaped morphology was also decreased (Figure 5.6B,E). Unlike constitutive expression of *Wnt1*-HA, overexpression of *Wnt1*-HA induced at the early stages of the process did not seem to increase the number of nestin-expressing cells when analysed 24 hours post-plating (Figure 5.7E,F; 5.8). However, the analysis revealed a significant decrease in the percentage of nestin positive cells as well as the number of nestin positive

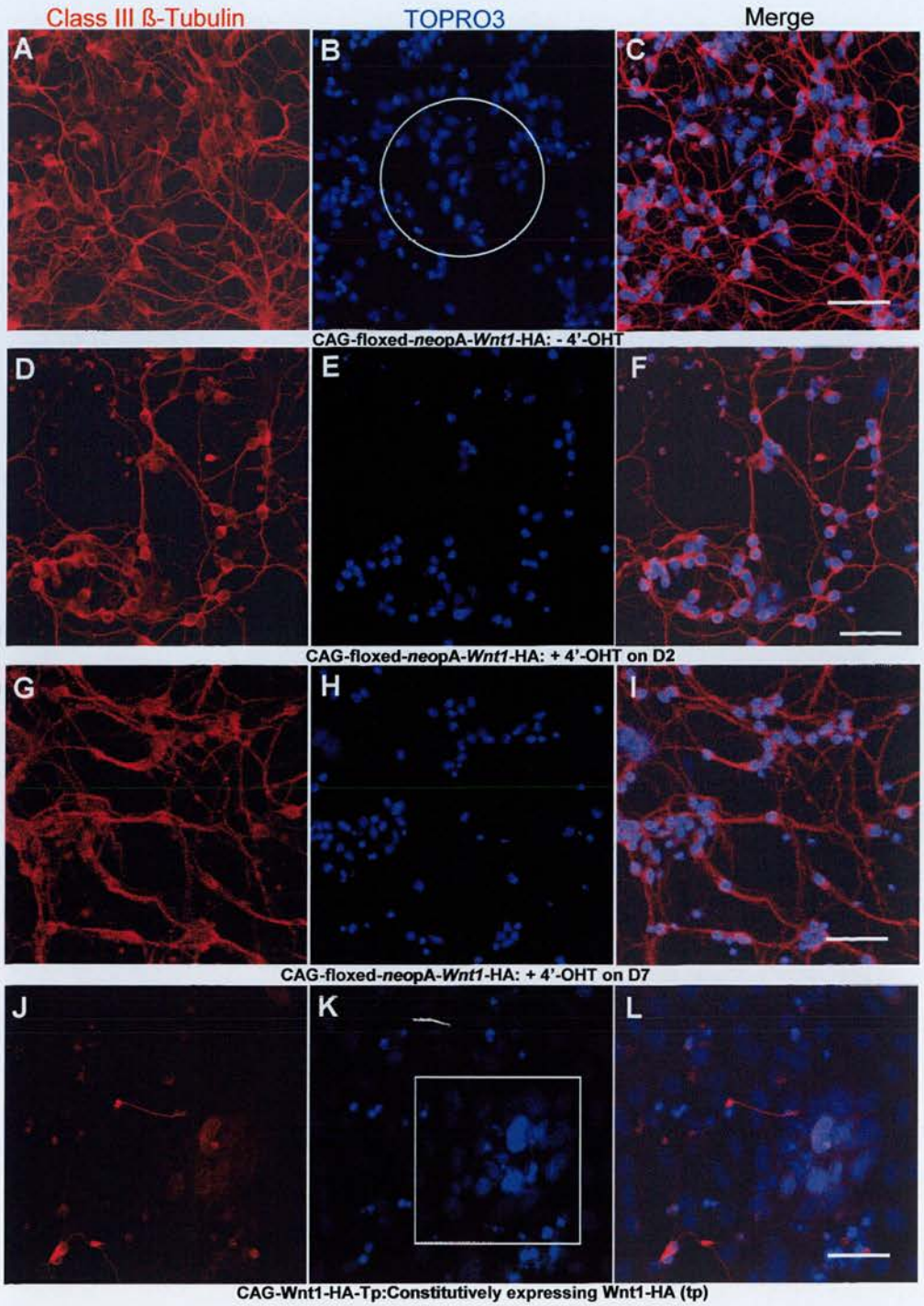

Figure 5.10: The effect of overexpressing Wnt1-HA on the formation of non-neural cells. W1-HA expressing lines were subjected to neural differentiation and stained for class III ß-Tubulin as described before (Figure 5.12). A, D, G and J show ICC with class III ß-Tubulin for CAG-floxed-*neo*pA-*Wnt1*-HA cells without 4'-OHT treatment (AB,C) and the cells after treatment with 800 nM 4'-OHT on D2 (D,E,F) and on D7 (G,H,I), and constitutively overexpressing *Wnt1*-HA CAG-Wnt1-HA-Tp cells (J,K,L). Nuclei stained with TOPRO3 for each respective treatment is shown in B,E,H,K. C,F,I,L show the merge between TOPRO3 and class III ß-Tubulin for each respective treatment. Scale bar is 50 µm. Note the presence of less ß-Tubulin negative cells in cells treated with 4'-OHT on D2 (E,F) and D7 (H,I) compared to untreated cells (B,C). Cells in circle showing non-neural cells present in non-induced cells for comparison. Cells in rectangular shape showing different morphology formed in Wnt1-HA-overexpressed cells.

A)

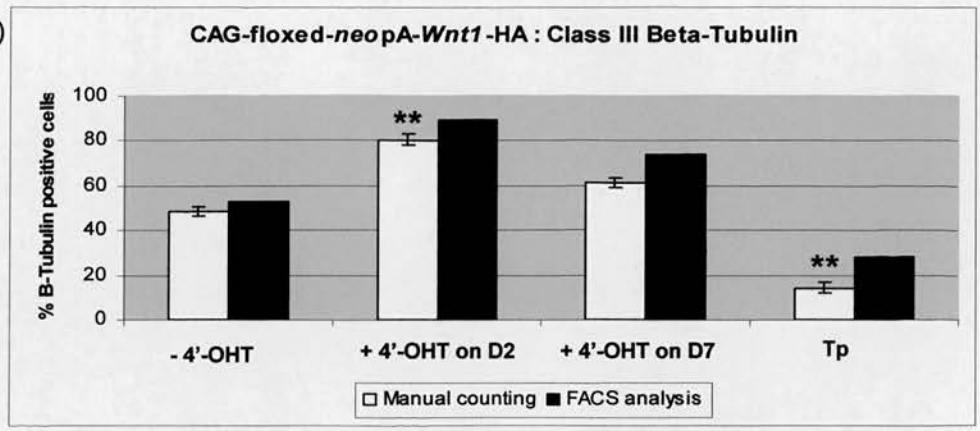

B)

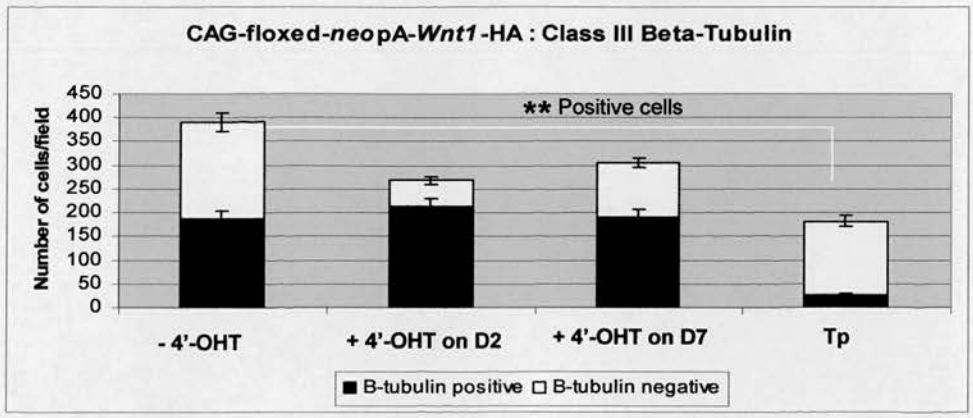

C)

CAG-floxed-*neo*pA-*Wnt1*-HA clones	FACS analysed (± SEM)	B -tubulin positive cells (± SEM)	B -tubulin negative cells (± SEM)	% of B -tubulin positive (± SEM)	Total cell score
- 4'-OHT	52.51	186.75 ± 15.27	202.85 ± 19.75	48.69 ± 2.31	7792
+ 4'-OHT on D2	89.42	214.05 ± 15.68	54.32 ± 7.45	80.37 ± 2.38	5099
+ 4'-OHT on D7	73.79	189.95 ± 17.43	115.79 ± 9.65	61.05 ± 2.09	5809
Constitutively expressing *Wnt1*-HA (Tp)	28.30	24.75 ± 3.81	156.83 ± 11.95	14.37 ± 2.31	2179

Figure 5.11: Quantification analysis on the expression of class III ß-tubulin in *Wnt1*-HA expressing cell lines by ICC. After each indicated treatment, no 4'-OHT, 800 nM 4'-OHT on D2 and D7, and constitutively expressing *Wnt1*-HA (Tp), the cells stained for ß-tubulin 2 days post-plating were manually counted and analysed by FACS. Percentage of ß-tubulin positive cells were plotted (A) and tabulated (C). ß-tubulin positive and negative cells were also plotted (B) and tabulated (C). Error bar is the mean ± standard error of mean (SEM, n=20 fields) from three independent experiment with duplicate wells. ** indicates highly significant to non-treated cells, T-test, $p<0.001$. Note the agreement between manually counted and FACS analysed results.

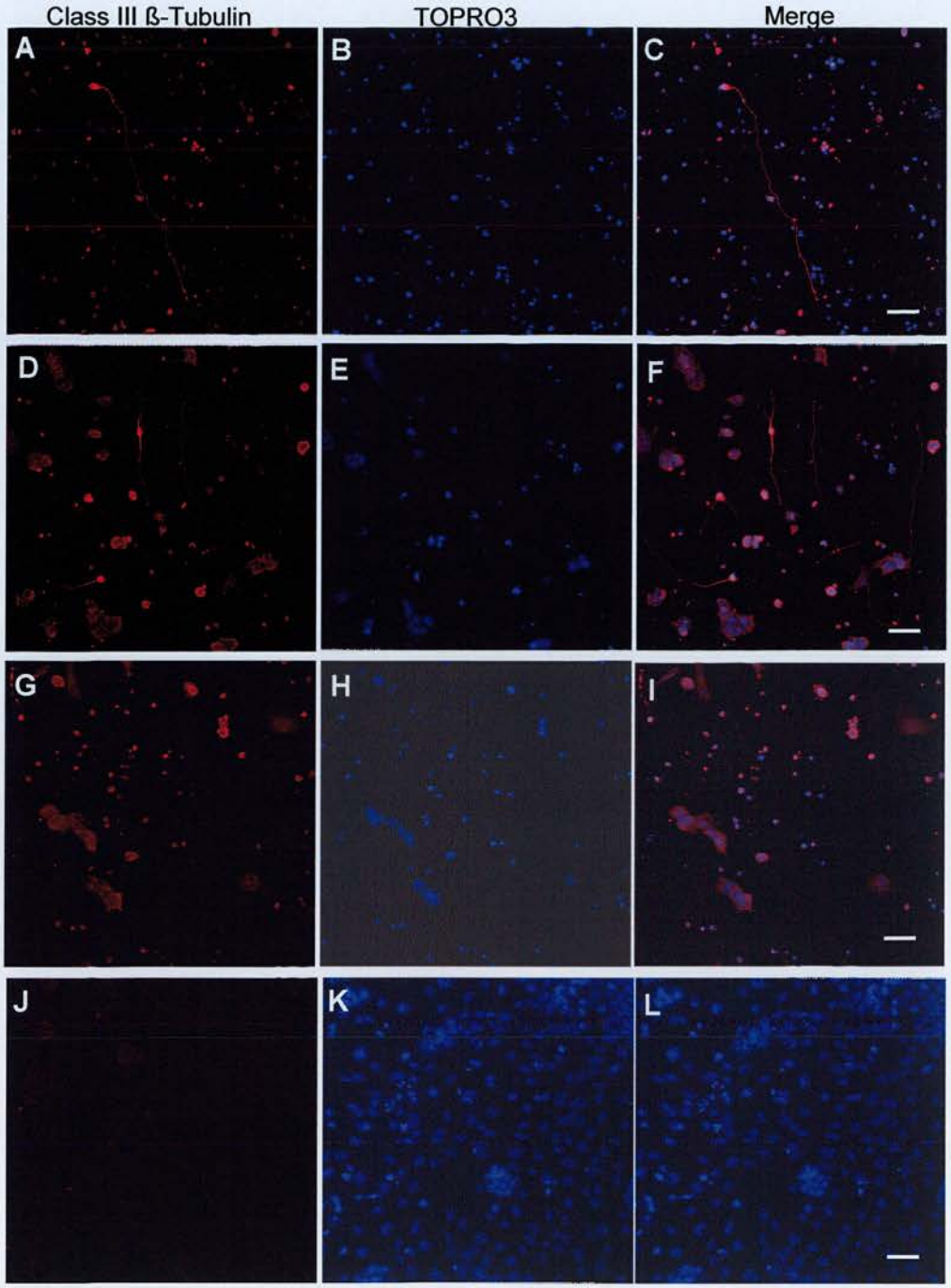

Figure 5.12: Effect of overexpressing *Wnt1*-HA in neural differentiation process without retinoic acid (RA). Untreated CAG-floxed-*neo*pA-*Wnt1*-HA cells together with the cells treated with 800 nM 4'-OHT on D2 and D7, and CAG-Wnt1-HA-Tp cells were subjected to neural differentiation in the absence of RA. In all conditions the formation of proper neurons was hampered. A,D,G,J show immunocytochemistry with class III ß-Tubulin, 48 hours post-plating, for each treatment conditions, respectively. Nuclei stained with TOPRO3 for each respective treatment is shown in B,E,H,K. C,F,I,L show the merge between TOPRO3 and class III ß-Tubulin for each respective treatment. Scale bar is 50 µm. Note the formation of non-neural cells as observed in constitutively expressing *Wnt1*-HA (CAG-*Wnt1*-HA-Tp) cells in the presence of RA (Figure 5.12 and 5.13).

cells per field when analysed at 1-2 and 24 hours post-plating compared to that of the control cells (Figure 5.8).

Analysis of the expression of ß-tubulin in these cells 48 hours post-plating revealed a significant increase in the percentage of ß-tubulin-positive cells (Figure 5.11A) but only a slight increase in the average formation of ß-tubulin-positive cells per field (Figure 5.11B) when compared to that of control cells. A great decrease of non-neural cells was also observed in these cells (Figure 5.11B) which resulted in the increase of the percentage of ß-tubulin positive cells. In other words, fewer ß-tubulin-negative cells were observed in these cells compared to that of the control cells (Figure 5.9D,E; Figure 5.10D,E,F). FACS analysis demonstrated the same phenomenon, the percentage of ß-tubulin-positive cells was higher in the cells when *Wnt1*-HA was induced on D2 (Figure 5.9F, 5.11A).

In summary, overexpression of *Wnt1*-HA induced on D2 may inhibit the formation of NPCs. The number of neurons formed as determined by the expression of ß-tubulin increased slightly with significant increase in the percentage of ß-tubulin-positive cells hence the presence of overexpressing Wnt1-HA cells during the late stages of the differentiation process of ES cells may enhance the percentage of neurons formed at the expense of non-neuronal cells.

5.2.2.3 Overexpression of *Wnt1*-HA at late stages

When the overexpression of *Wnt1*-HA was induced at late stages of the differentiation process (on D7-9), the percentage of ß-tubulin-positive cells

increased significantly while the number of ß-tubulin-positive cells increased slightly compared to that of the control cells, as demonstrated by ICC and FACS analysis (Figure 5.9G,H,I) 48 hours post-plating. Similar to the overexpression of *Wnt1*-HA at early stage, overexpression at the late stage significantly decreased the number of ß-tubulin-negative cells (Figure 5.11B) which explained the higher percentage of ß-tubulin-positive cells in the culture as compared to the expression of ß-tubulin in the control cells. Figure 5.10G,H,I clearly show the absence of ß-tubulin-negative cells when *Wnt1*-HA was overexpressed at the late stage of the differentiation process.

In summary, overexpression of *Wnt1*-HA at late stages of the neural differentiation process of ES cells may enhance the percentage of ß-tubulin-positive cells at the expense of non-neuronal cells (ß-tubulin-negative cells).

5.2.3 Effects of *Wnt3a* overexpression during neural differentiation of ES cells

To examine the effect of overexpressing *Wnt3a* on neural differentiation of ES cells, CAG-floxed-*neo*pA-*Wnt3a* ES cells was used. Due to limitations of time, results from a single experiment with duplicate wells will be presented. Albeit preliminary, they were interesting observations with potential for expansion. *Wnt3a* was induced by activation of Cre-recombinase with 750 nM tamoxifen on D2 and D7 EBs for 48 hours. ES cells constitutively expressing *Wnt3a* (CAG-*Wnt3a*-Tp) were also used. The analysis of the effects of overexpressing *Wnt3a* on neural differentiation of ES cells was carried out as described for that of Wnt1-HA overexpression.

5.2.3.1 Constitutive overexpression of *Wnt3a*

Unlike constitutive expression of *Wnt1*-HA, more nestin-expressing cells with the spindle-shaped morphology were observed in CAG-*Wnt3a*-Tp cells even though the total number of cells expressing nestin was actually reduced in these cells (Figure 5.13G,H,I) when compared to that of the 4'-OHT-untreated CAG-floxed-*neo*pA-*Wnt3a* cells (control cells). In agreement with this, FACS profiles on the cells expressing nestin in these cells also revealed the same phenomenon (Figure 5.14 F). In addition, quantitative analysis also demonstrates that the percentage of nestin positive cells as well as the total number of nestin positive cells per field decreased significantly when *Wnt3a* was constitutively overexpressed (Figure 5.15).

Constitutive overexpression of *Wnt3a* also resulted in a decreased percentage of cells expressing ß-tubulin as demonstrated by FACS analysis (Figure 5.16L; Figure 5.17A,C) compared to that of the control cells. Unfortunately, due to technical problems in the binding specificity of the secondary antibody, we had to discard the quantification analysis from ICC (Figure 5.16 J,K). However, it was clear that the formation of neuron-like cells was inhibited in these cells.

In summary, constitutive overexpression of Wnt 3a may inhibit the formation of NPCs and may also perturb the ability of ES cells to differentiate into neurons.

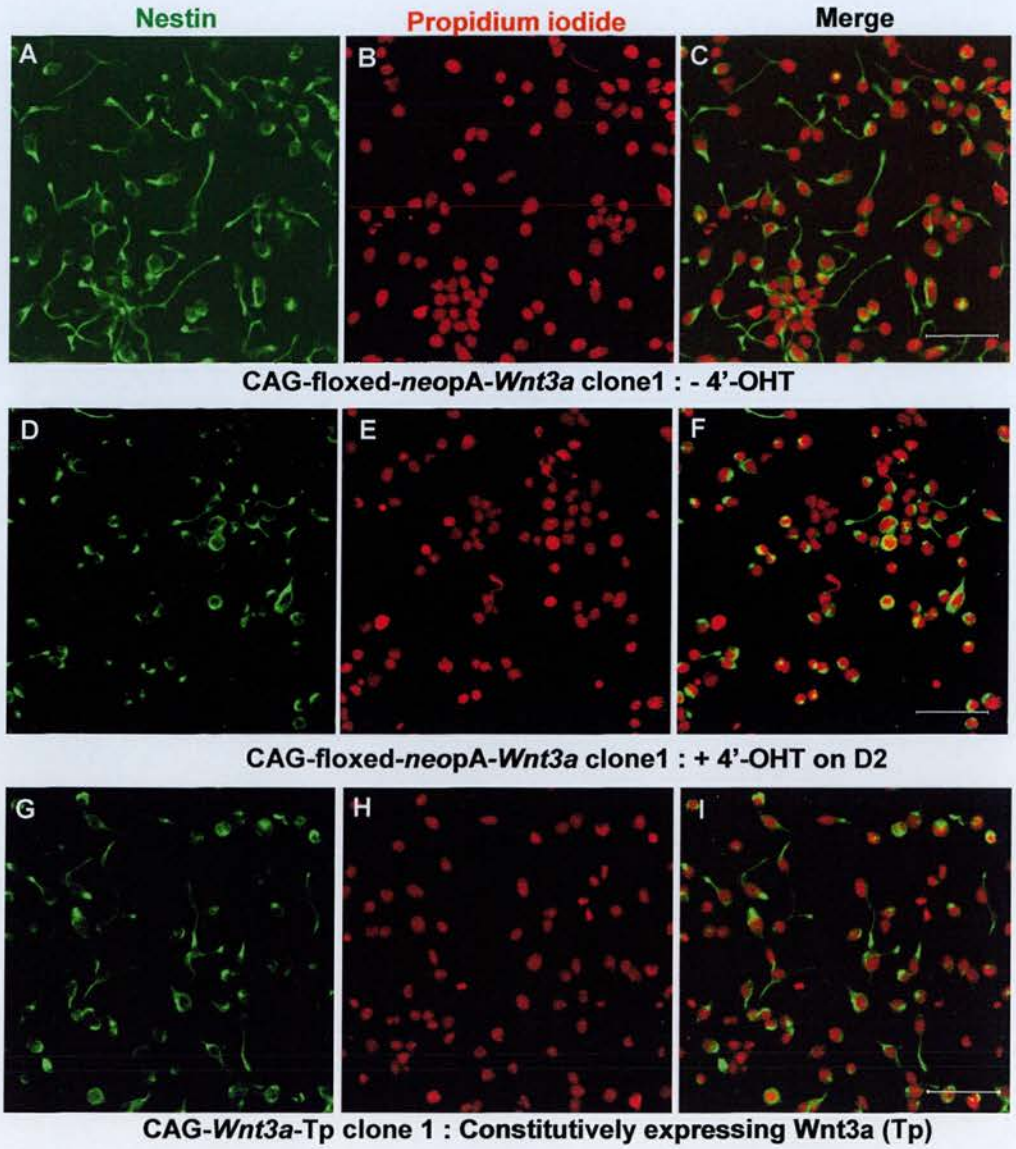

Figure 5.13: Expression of Nestin in *Wnt3a*-expressing ES cell lines. ICC was carried out for intermediate filament protein, Nestin, 1-2 hours post plating on CAG-floxed-*neo*pA-*Wnt3a* cells treated with (A,B,C) no 4'-OHT or (D,E,F) with 750 nM 4'-OHT on D2, and (G,H,I) constitutively expressing *Wnt3a*-HA (CAG-*Wnt3a*-Tp) cells. (B,E,H) nuclei staining with propidium iodide (PI) and (C,F,I) the merge between nuclei staining with PI and Nestin for each respective treatment. Scale bar is 50 μm.

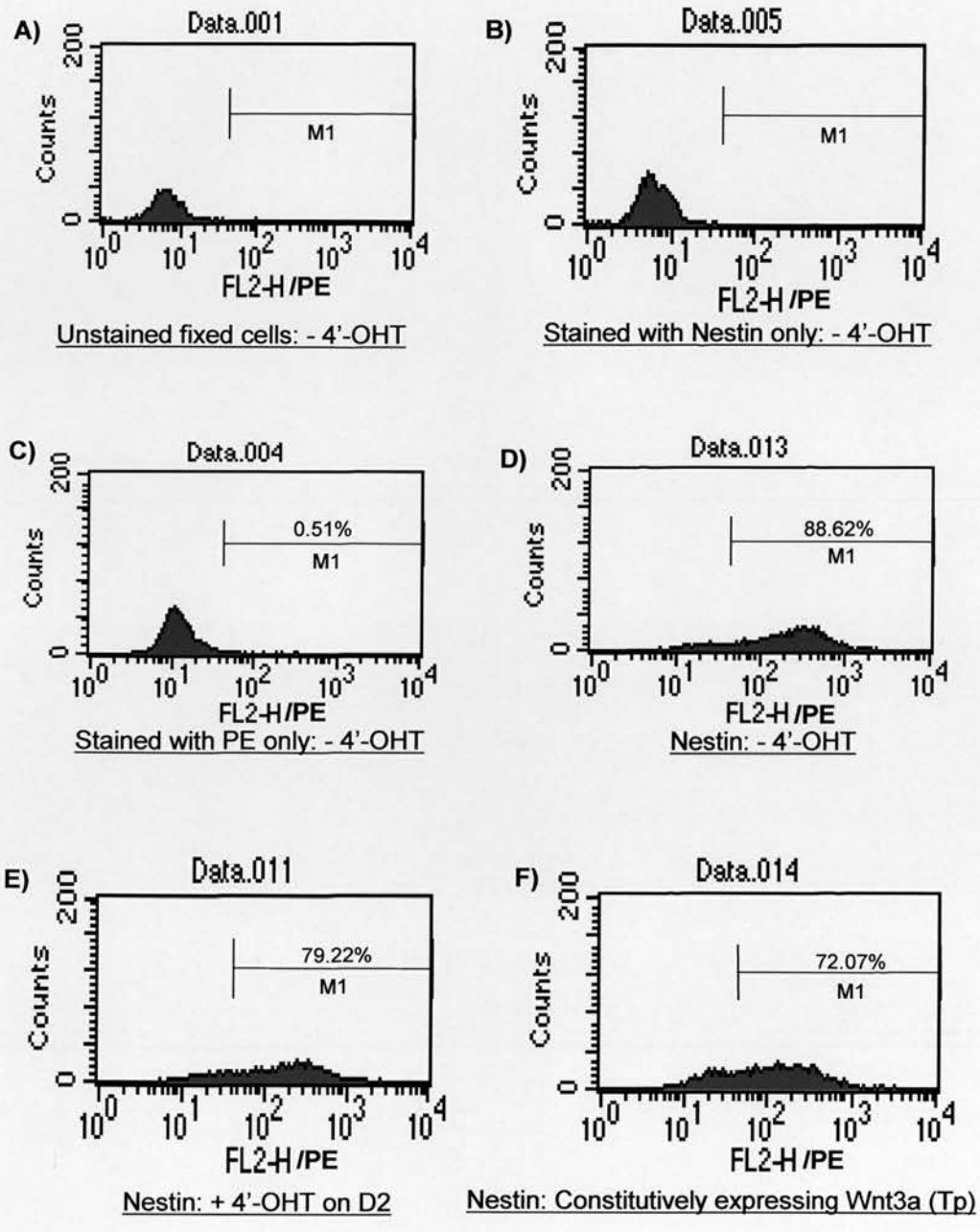

Figure 5.14: FACS analysis on CAG-floxed-*neo*pA-*Wnt3a* cells stained for nestin 1-2 hours post plating. A, B and C are untreated CAG-floxed-*neo*pA-*Wnt3a* cells that were either unstained, stained with primary antibody only or stained with secondary antibody only, as controls used to setup the M1 gate. D, E and F are the FACS profiles for nestin staining for non-treated CAG-floxed-*neo*pA-*Wnt3a* cells, the cells treated with 750 nM 4'-OHT on D2 and constitutively expressing *Wnt3a* (CAG-*Wnt3a*-Tp) cells, respectively. The percentage of nestin positive cells is shown in parentheses.

A)

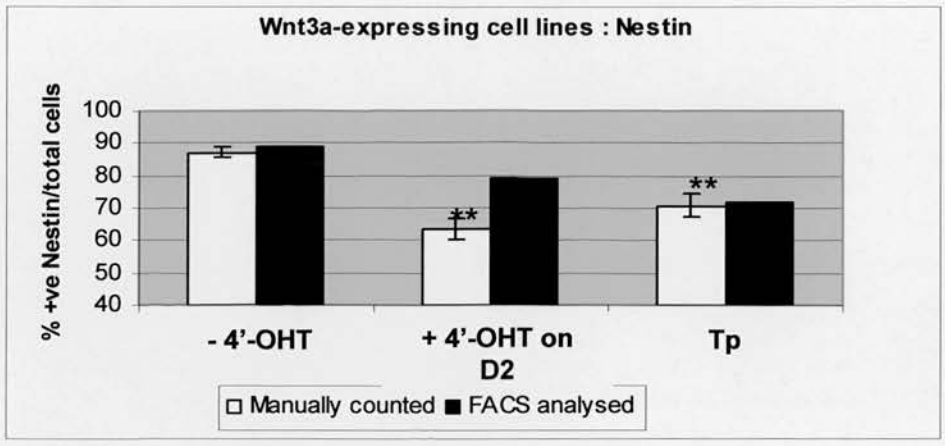

B)

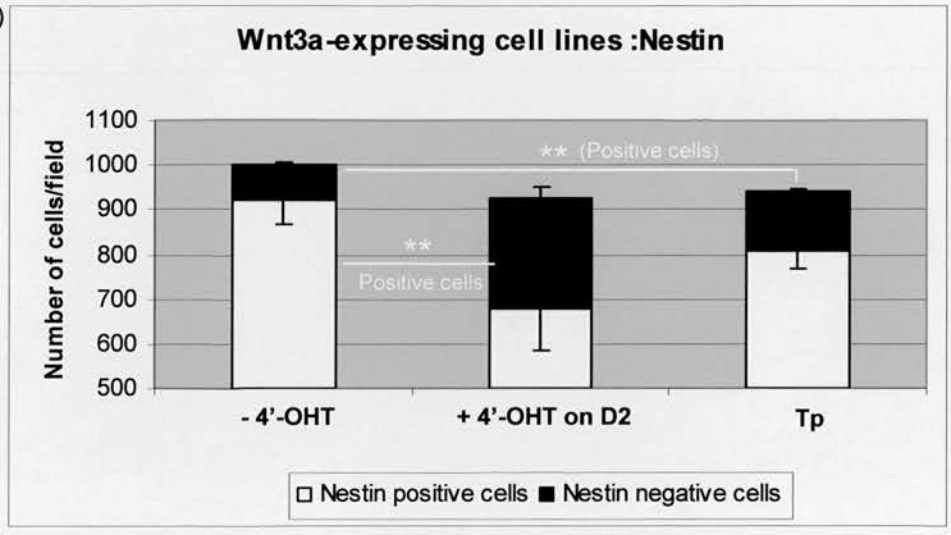

C)

Wnt3a-expressing lines	% of Nestin positive (± SEM)	Total cell	FACS (% positive cells)
- 4'-OHT	87.25 ± 1.57	7958	88.62
+ 4'-OHT on D2	63.64 ± 3.11	7311	79.22
Constitutively expressing Wnt3a (Tp)	70.93 ± 3.83	9566	72.07

Figure 5.15: Quantification of nestin expression in *Wnt3a*-expressing cells. The analysis was done on untreated CAG-floxed-*neo*pA-*Wnt3a* cells or the cells treated with 4'-OHT on D2 and constitutively overexpressing Wnt3a (CAG-*Wnt3a*-Tp) cells at 1-2 hours post plating. A) Percentage of nestin positive cells counted manually (ICC from 4-well plate) and analysed by FACS. Note both results demonstrate decrease in percentage of nestin positive cells in the presence of Wnt3a. B) Number of nestin positive cells per field. Note the number of nestin positive cells were decreased when treated with *Wnt3a*. C) Tabulated data of results from A and B. Manually counted results for npc 1-2 post plating were from single experiment with duplicate wells. FACS results were from single experiment from one clone. ** indicates highly significant to non-treated cells, T-test, $p<0.001$. Error bar is the mean ± standard error of mean, SEM (n=7 fields).

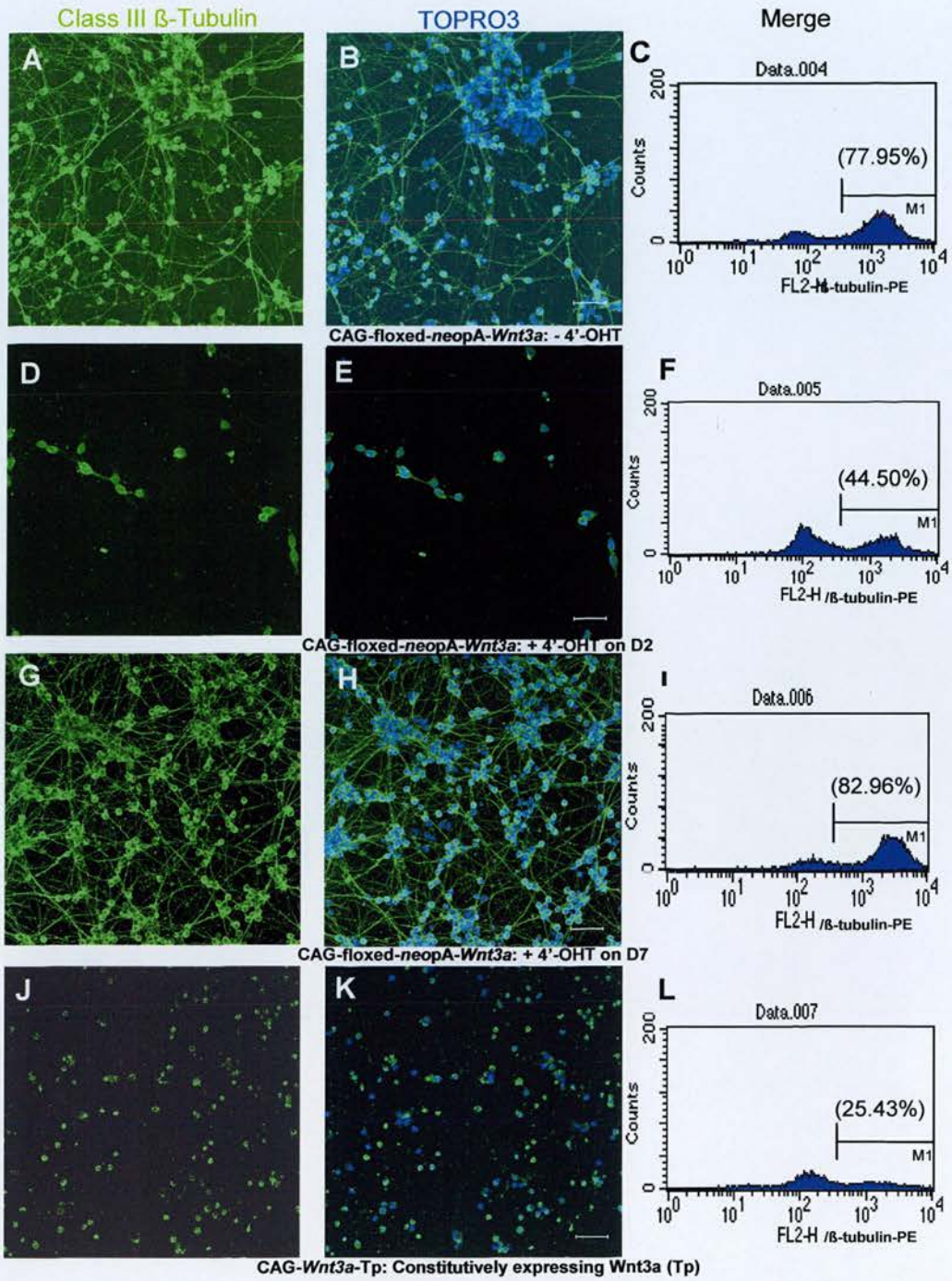

Figure 5.16: Class III ß-tubulin expression in Wnt3a-overexpresing cell lines. Neural differentiation was carried out as described previously. ICC and FACS analyses were done on CAG-floxed-*neo*pA-*Wnt3a* treated with no 4'-OHT (A,B,C), with 750 nM 4'-OHT on D2 (D,E,F) and D7 (G,H,I), and on CAG-*Wnt3a*-Tp cells (J,K,L) two days post-plating for neuronal marker, class III ß-Tubulin. A,D,G,J show staining with class III ß-Tubulin, B,E,H,K. show the merge between TOPRO3 and class III ß-Tubulin and C,F,I,L show the FACS profiles of the cells in each respective treatment. Scale bar, 50 µM.

A)

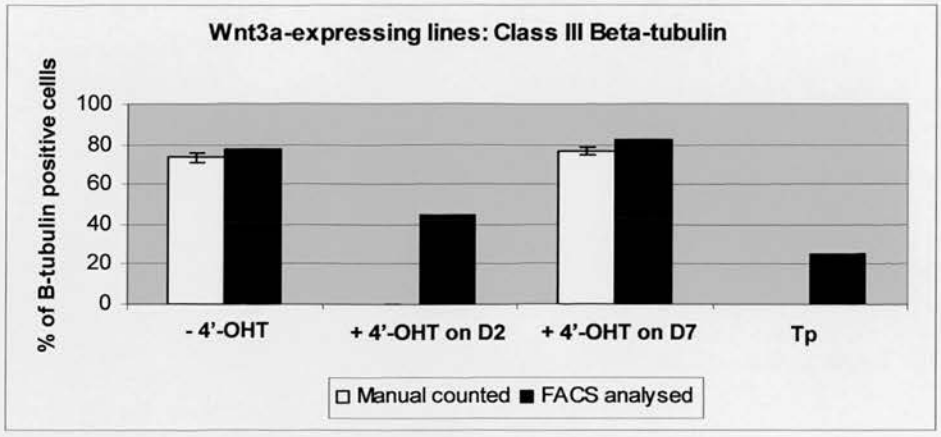

B)

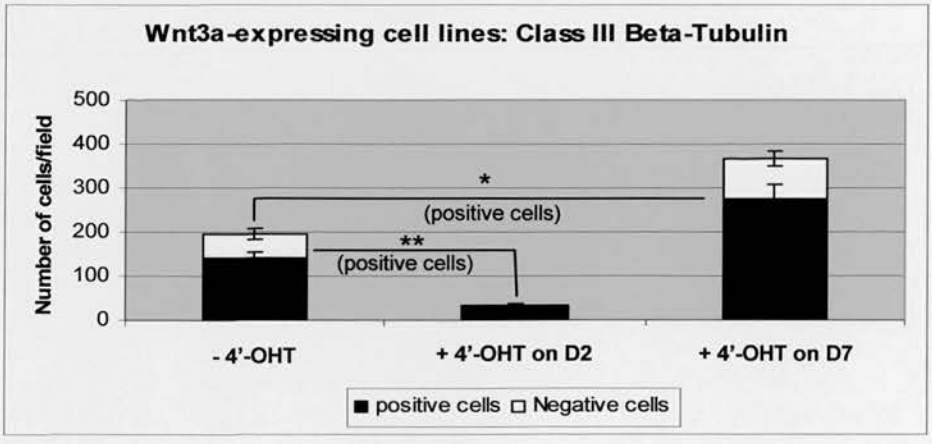

C)

*Wnt3*a-expressing lines	ß-tubulin positive cells (± SEM)	ß -tubulin negative cells (± SEM)	% of ß -tubulin positive (± SEM)	Total cell score	FACS data
Non -treated	140.5 ± 13.15	54. 67 ± 11.13	73.35 ± 2.32	1171	77.95
Treated on D2 EBs	28.67 ± 5.37	5.83 ± 3.39	-	207	44.50
Treated on D7 EBs	277 ± 29.89	90 ± 17.20	76.73 ± 2.30	2202	82.96
Constitutive expression of Wnt3a (Tp)	-	-	-	-	25.43

Figure 5.17: Quantification of ß-tubulin expression in Wnt3a-expressing cell lines. The analysis was done on CAG-floxed-*neo*pA-*Wnt3a* cells with treatment as indicated above and on CAG-*Wnt3a*-Tp cells. Percentage of positive cells were plotted (A) and tabulated (C). ß-tubulin positive and negative cells were also plotted (B) and tabulated (C). ** indicates highly significant to non-treated cells, T-test, $p<0.001$. * indicates highly significant to non-treated cells, T-test, $p<0.005$. Error bar is the mean ± standard error of mean (SEM, n=6 fields) from single experiment with duplicate wells.

5.2.3.2 Induction of *Wnt3a* overexpression at early stage

A significant decrease in the percentage of nestin-positive cells as well as the number of nestin positive cells per field was observed when the overexpression of *Wnt3a* was induced on D2 of the differentiation process as demonstrated by ICC (Figure 5,13 D,E,F; Figure 5.15) and FACS (Figure5.14 E, 5.15 A) analyses 1-2 hours post-plating, when compared to that of the control cells and also of the cells that constitutively overexpressing *Wnt3a*. In addition, the spindle-shaped morphology was still observed in a few cells that were expressing nestin (Figure 5.13D,F).

48 hours post-plating, the number of ß-tubulin-expressing cells per field was significantly decreased as observed from ICC (Figure 5.16D,E,F) in these cells. Unfortunately due to a technical problem, quantitative analysis of this result had to be discarded since for unknown reasons, the ß-tubulin-negative cells were lost during the ICC procedure. Fortunately, FACS analysis reliably demonstrates that the percentage of ß-tubulin-expressing cells was reduced when compared to that of the control cells (Figure 5.16 F; Figure 5.17A).

In summary, overexpression of *Wnt3a* induced on D2 of the neural differentiation process may inhibit the formation of NPCs. The formation of neurons may also be inhibited from these cells.

5.2.3.3 Induction of *Wnt3a* overexpression at late stage

In constrast to *Wnt1*-HA, the induction of *Wnt3a* expression on D7 significantly increased the formation of ß-tubulin-positive cells (Figure 5.16

G,H). Supporting this, FACS analysis agreed with the ICC result, overexpression of *Wnt3a* at late stage of the process increased the percentage of cells expressing ß-tubulin (Figure 5.16I, 5.17A). The number of ß-tubulin-expressing cells was also increased significantly (Figure 5.17B) even though the percentage of ß-tubulin-positive cells only increased slightly compared to that of the control cells as quantitatively analysed from ICC results (Figure 5.17A).

In summary, overexpression of Wnt3a during the late stages of neural differentiation of ES cells may promote the formation of neurons.

5.2.4 Effects of *Dkk1* overexpression during neural differentiation of ES cells

As discussed in chapter 3, a number of Wnts are expressed during neural differentiation of ES cells. Hence, it is always difficult to be clear about the effects of overexpressing a single Wnt gene during the process. In constrast, by overexpressing *Dkk1*, which is presently known to antagonise the canonical Wnt signalling, we hoped to be able to block activity of multiple Wnts, specifically the ones that are involved in activating the canonical pathway. A dynamic RNA expression profile for *Dkk1* during neural differentiation process has also been observed. To examine the functional properties of the gene in the process, CAG-floxed-*neo*pA*Dkk1* ES cells were used. Similar procedures, as described for *Wnt1*-HA and *Wnt3a*, were carried out in order to analyse the effects of overexpressing *Dkk1* during the process, except for FACS analysis. Due to a technical problem, the FACS analysis had to be discarded. *Dkk1* expression was induced with 800 nM 4'-

OHT on D2 and D7 for 48 hours. Results from two independent experiments using one CAG-floxed-*neo*pA-*Dkk1* ES cells will be presented.

5.2.4.1 Constitutive overexpression of *Dkk1*

Similar to constitutive overexpression of *Wnt1*-HA, 1-2 hours post-plating a significant decrease of nestin-expressing cells with spindle-shaped morphology was observed in cultured cells constitutively overexpressing *Dkk1* (Figure 5.18 G,H,I) compared to the control cells. Quantitative analysis from ICC also revealed a significant decrease in the percentage as well as the total number of nestin-positive cells per field in these cells compared to that of the control cells (Figure 5.19). Interestingly, constitutive overexpression of Dkk1 did not seem to affect the viability of nestin-negative cells as compared to the control cells (Figure 5.19B).

A recent study by a group of Japanese researchers demonstrates that treatment with Dkk1 protein into ES cell cultures directs the differentiation of the cells into telencephalic precursor cells, as determined by an increase of a transcription factor Foxg1 expression, which is specifically expressed in the VZ and SVZ of the telencephalon (Watanabe *et al.*, 2005). We were also interested to see if constitutive overexpression of *Dkk1* would affect the expression of *Foxg1* in our cultures, unlike in Watanabe *et al.*'s culture condition, in the presence of RA. In the presence of RA, more than 50% of the cells in this condition from all selected field analysed expressed Foxg1 (Figure 5.20G,H,I). Interestingly, a number of these cells only expressed Foxg1 but not nestin (Figure 5.20H,I, arrows). This is likely to explain that the Foxg1-expressing cells has been differentiated since *in vivo* study has

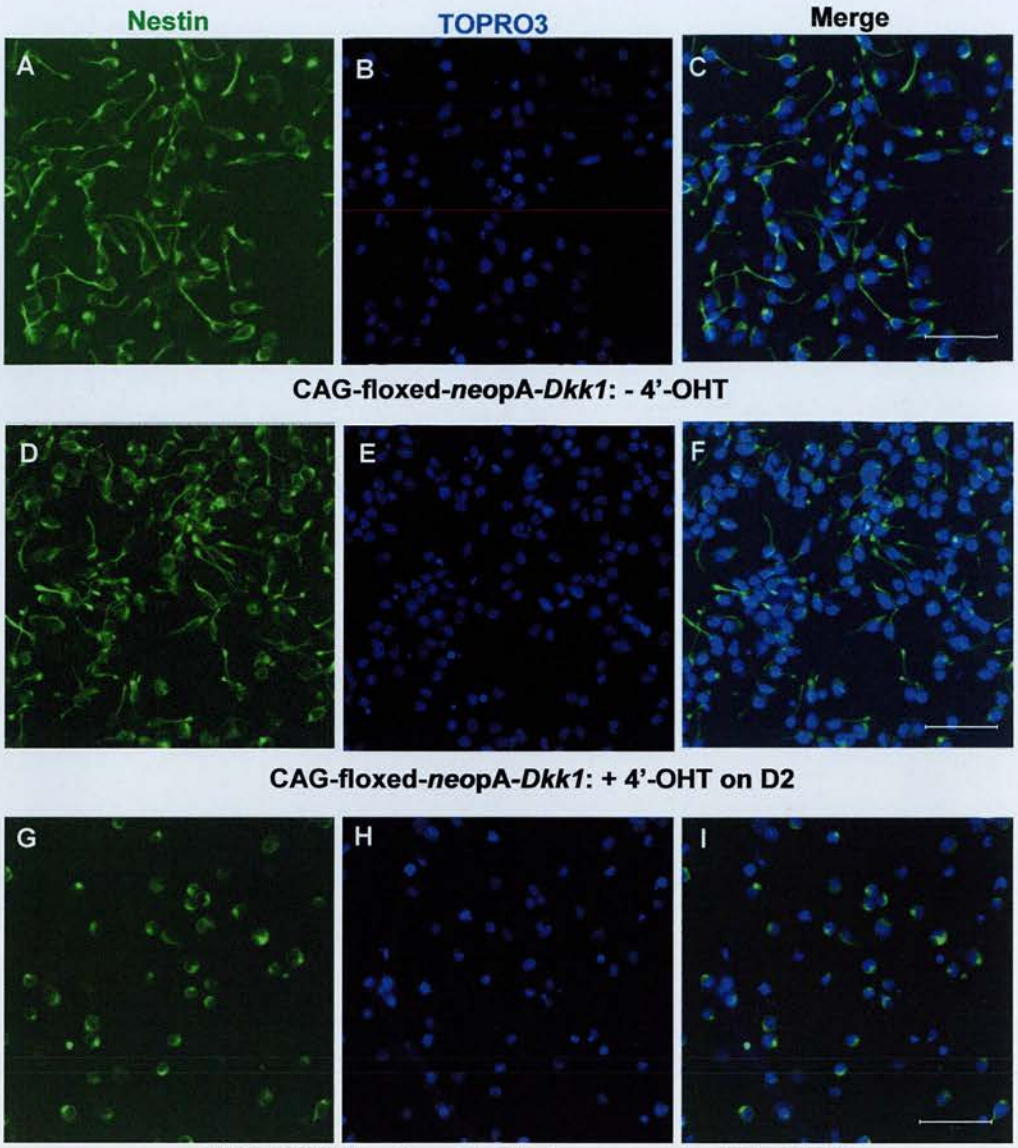

Figure 5.18: Nestin expression in *Dkk1*-expressing ES cell lines. Expression of Nestin in CAG-floxed-*neo*pA-*Dkk1* cells treated with 800 nM 4'-OHT on D2 (D,E,F) and constitutively expressing Dkk1 (CAG-*Dkk1*-Tp) cells (G,H,I) was compared to the un-treated cells (A,B,C). B,E,H show nuclei staining with TOPRO3 while C,F,I are the merged images for each respective treatment. Scale bar is 50 μm.

A)

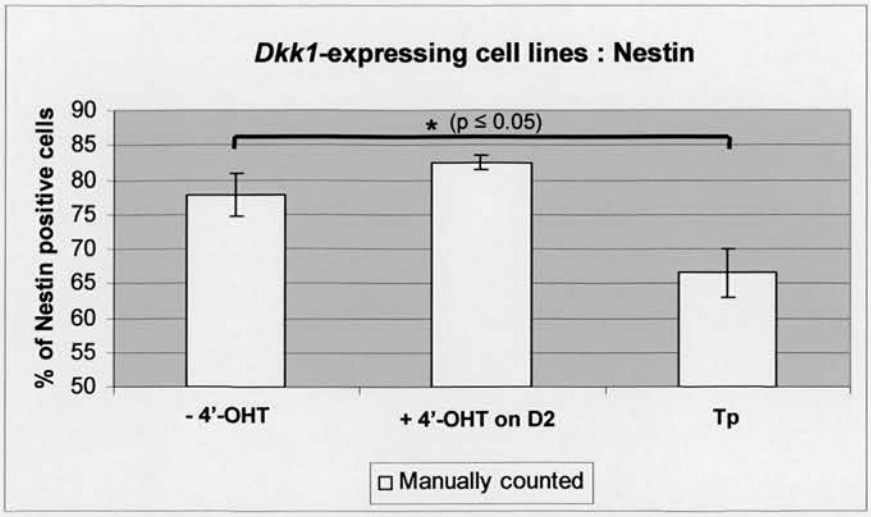

B)

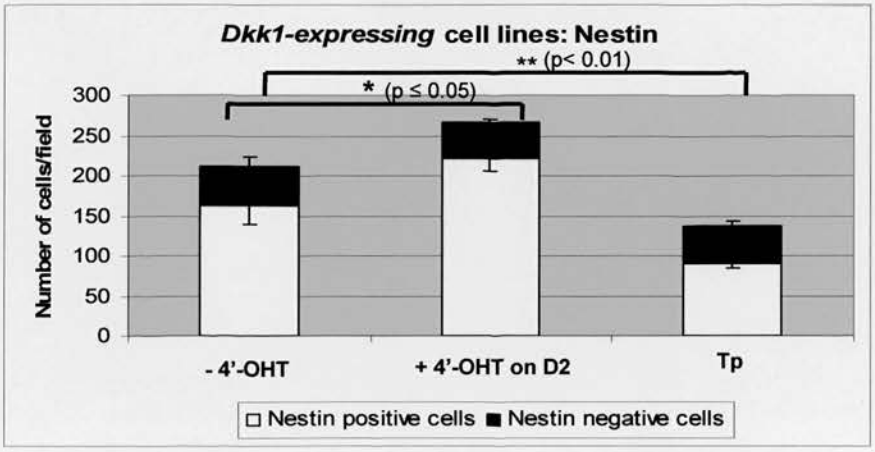

C)

*Dkk*1-expressing cells	Nestin positive cells/field (± SEM)	Nestin negative cells/field (± SEM)	% of Nestin positive (± SEM)	Total cell
- 4'-OHT	162.12 ± 22.36	49.62 ± 12.33	77.71 ± 3.10	1698
+ 4'-OHT on D2	221.37 ± 16.11	46.25 ± 2.73	82.99 ± 1.27	2141
Constitutive expression *Dkk1* (Tp)	89.75 ± 5.76	46.87 ± 6.77	66.50 ± 3.48	1093

Figure 5.19: Quantification of nestin expression in 4'-OHT untreated and treated CAG-floxed-*neo*pA-*Dkk1,* and CAG-*Dkk1*-Tp cells from ICC. (A) Percentage of nestin positive cells counted manually (ICC from 4-well plate). (B) Number of nestin positive cells per field. (C) Tabulated data of results from A and B. Manually counted results for npc 1-2 post plating were from single experiment with duplicate wells. ** indicates highly significant to non-induced, t-test, $p<0.01$. * indicate significant to non-induced, t-test, $p\leq0.05$. Error bar is the mean ± standard error of mean, SEM (n=8 fields).

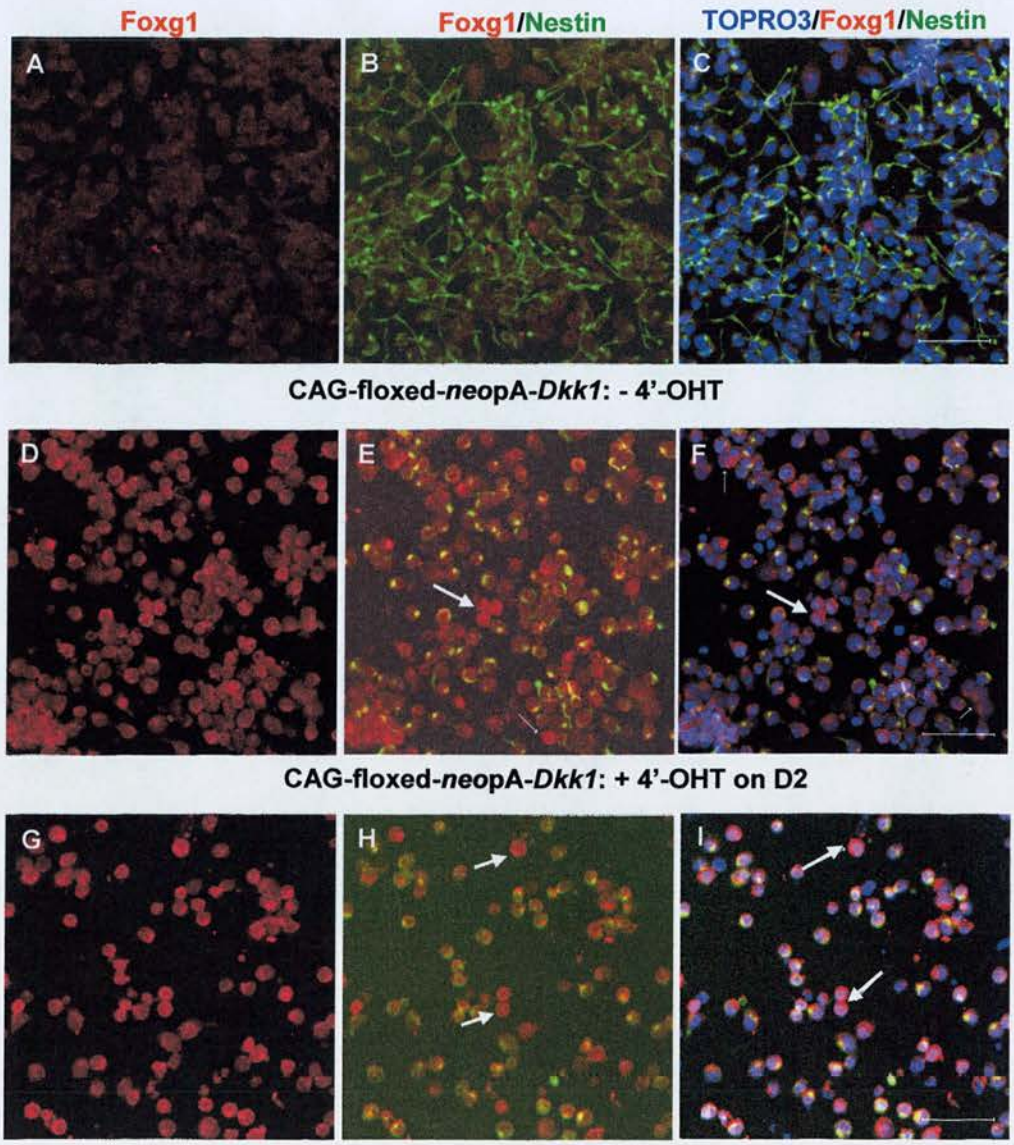

Figure 5.20: Effects of overexpressing *Dkk1* on expression of *Foxg1* during neural differentiation of ES cells. After 1-2 hours post plating, untreated and treated CAG-floxed-*neo*pA-*Dkk1* (with 4'-OHT) and CAG-*Dkk1*-Tp cells were stained for Foxg1. A,D,G show the cells stained for Foxg1. B,E,H show double staining for nestin and Foxg1 for the respective treatments. C, F and I show the merge between TOPRO3, Nestin and Foxg1, for the respective treatments. Arrows point the cells stained for Foxg1 but not nestin (F and I). Scale bar is 50 µm.

shown that differentiated neuronal cells outside the VZ also express the gene. Thus this might explain the reduced number of nestin-expressing cells when *Dkk1* is constitutively expressed. Notably, the majority of these cells expressed Foxg1 both in the cytoplasm and in the nucleus (Figure 5.20I). Quantitative analysis from ICC also show a significant increase in the percentage of Foxg1 positive cells in these cells compared to the control cells (Figure 5.21).

On the other hand, 48 hours post-plating, constitutive overexpression of Dkk1 seemed to inhibit neuronal differentiation of ES cells. Notably, high percentage of non-neuronal cell death was observed resulting in the survival of neuronal cells, although fewer neuronal cells survived, compared to the control cells (Figure 5.22 A,B,C,J,K,L). Consequently, as also revealed by quantitative analysis, a high percentage of ß-tubulin positive cells was observed (Figure 5.23A). The analysis, however, also revealed a significant decrease in the total number of both ß-tubulin-negative and –positive cells per field compared to that of the control cells.

In summary, constitutive overexpression of *Dkk1* may have directed the differentiation of ES cells into more regional specialized type of precursor cells (telencephalic cells). Consequently, it may also result in generation of more specific type of neurons.

5.2.4.2 Induction of *Dkk1* expression at early stage

1-2 hours post-plating, overexpression of *Dkk1* induced at early stages (on D2) of the differentiation process substantially increased the number of

A)

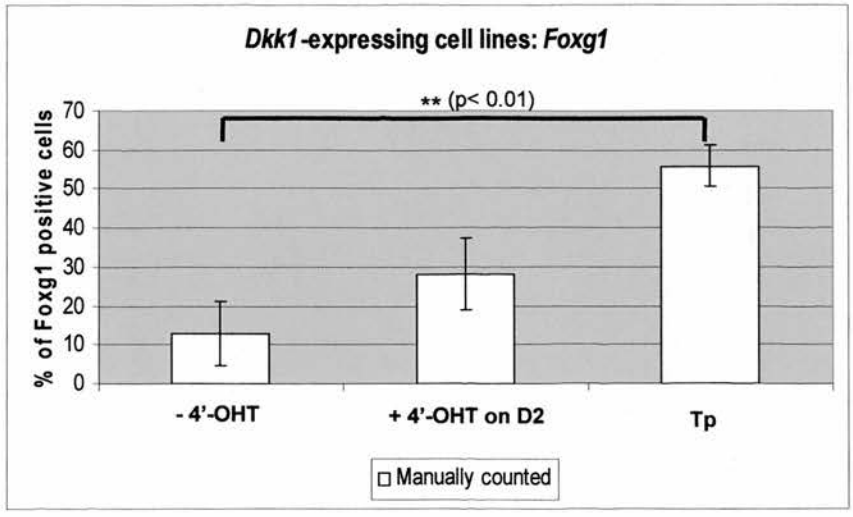

B)

Dkk1 expressing cells	% of Foxg1 positive (± SEM)	Total cell
- 4'-OHT	12.77 ± 8.33	669
+ 4'-OHT on D2	28.22 ± 9.24	650
Constitutive expression of *Dkk1* (Tp)	66.50 ± 3.50	285

Figure 5.21: Quantification of Foxg1expression from untreated and treated CAG-floxed-*neo*pA-*Dkk1* with 4'-OHT and CAG-*Dkk1*-Tp cells. The cells were stained for *Foxg1* 1-2 hours post plating and were manually counted. A) Percentage of Foxg1 positive cells were counted manually (ICC from 4-well plate). B) Tabulated data from A. Results were from single experiment with duplicate wells. ** indicates highly significant to non-induced, t-test, $p<0.01$. Error bar is the mean ± standard error of mean, SEM (n=4 fields).

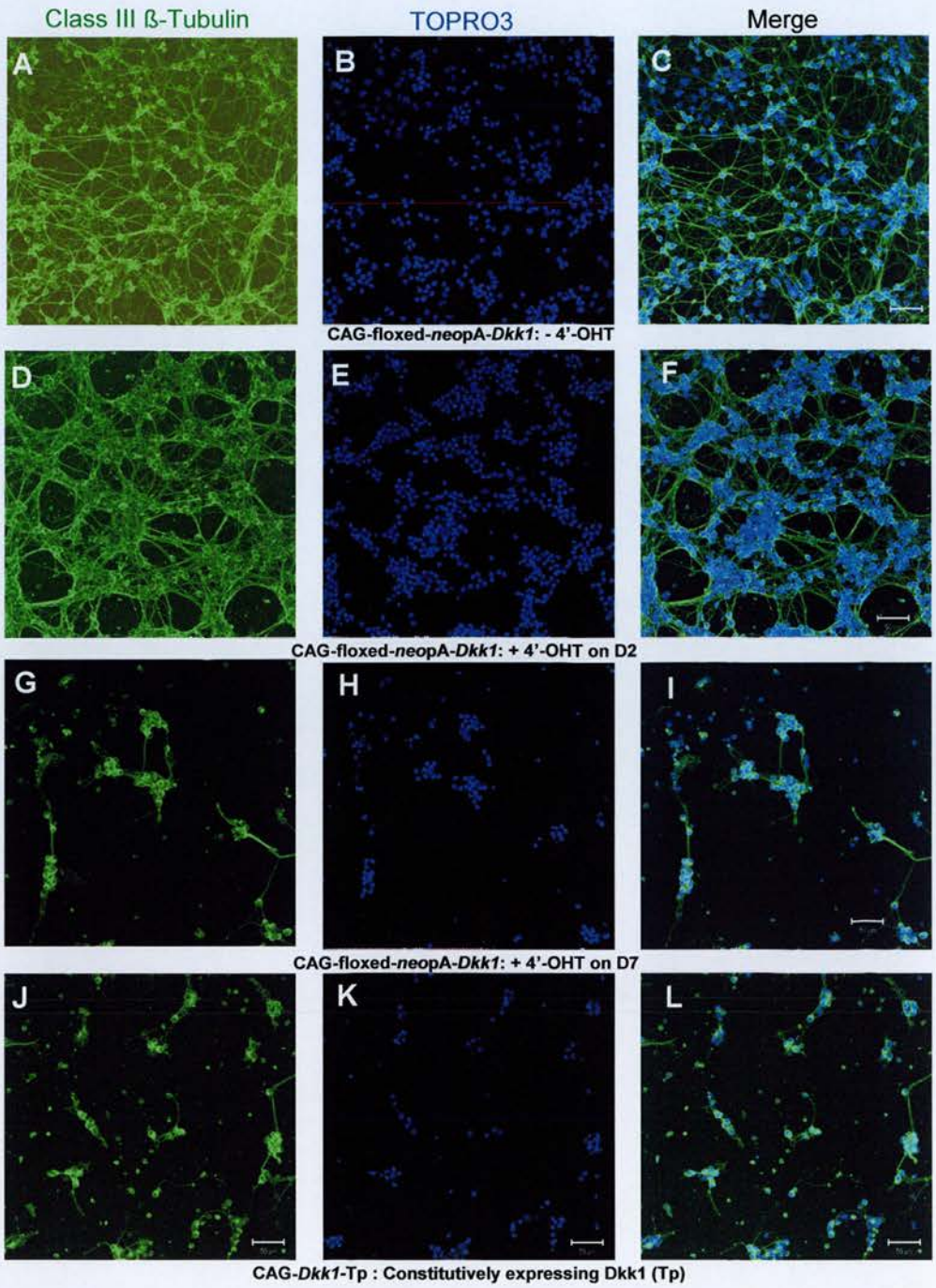

Figure 5.22: Expression of class III ß-Tubulin in *Dkk1*-expressing ES cell lines. Expression of ß-Tubulin in CAG-floxed-*neo*pA-*Dkk1* cells treated with 800 nM 4'-OHT on D2 (D,E,F) and D7 (G,H,I), and constitutively expressing Dkk1 (CAG-*Dkk1*-Tp) cells (J,K,L) were compared to the un-treated cells (A,B,C). B,E,H,K show nuclei staining with TOPRO3 while C,F,I, L show the merged images for each respective treatment. Scale bar is 50 µm.

A)

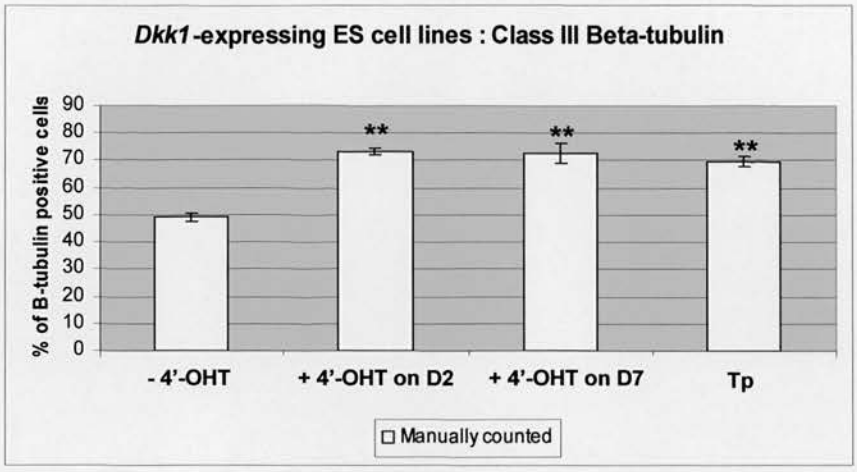

B)

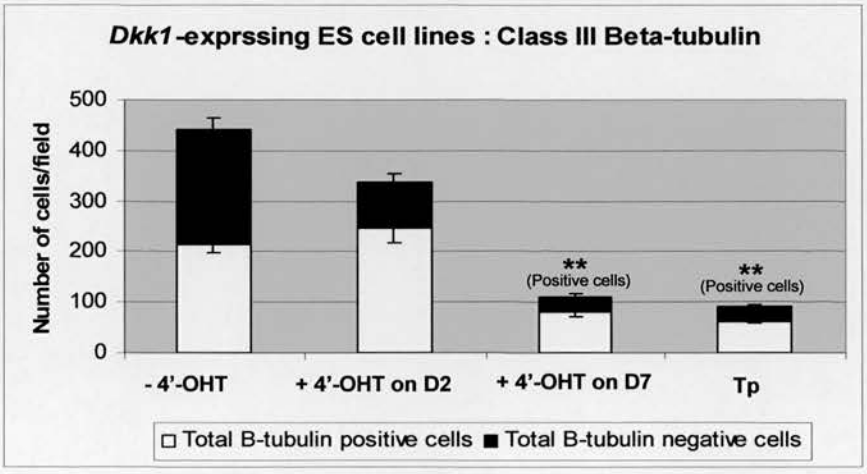

C)

Dkk1-expressing lines	B -tubulin positive cells (± SEM)	B -tubulin negative cells (± SEM)	% of B -tubulin positive (± SEM)	Total cell score
- 4'-OHT	213.5 ± 16.16	226.9 ± 24.88	49.19 ± 1.60	4404
+ 4'-OHT on D2	245.2 ± 29.26	92.9 ±15.72	73.46 ± 1.25	3381
+ 4'-OHT on D7	82.5 ± 10.66	28.8 ± 4.14	72.87 ± 3.76	1113
Constitutive expression of Dkk1 (Tp)	62.6 ± 5.21	27.9 ± 3.25	69.70 ± 1.99	905

Figure 5.23: Quantification analysis of ß-tubulin expression in *Dkk1*-expressing cells. Cells expressing ß-tubulin from CAG-floxed-neopA-Dkk1 treated with no 4'-OHT or treated with 800 nM 4'-OHT on D2 and D7, and CAG-Dkk1-Tp were manually counted. Percentage of positive cells was plotted (A) and tabulated (C). Total number of ß-tubulin positive and negative cells per field were also plotted (B) and tabulated (C). Error bar is the mean ± standard error of mean (SEM, n=10 fields) from two independent experiment with duplicate wells. ** indicates highly significant to non-induced, t-test, $p<0.001$

nestin-expressing cells with spindle-shaped morphology (Figure 5.18D,E,F). This condition significantly increased the number of nestin-positive cells per field and slightly increased the percentage of nestin-positive cells compared to that of the control cells (Figure 5.19).

When the cells were stained for *Foxg1* (1-2 hours post-plating), only a few fields among all selected field analysed displayed expression of this gene. (Figure 5.20D,E,F). In comparison to the control cells, in which no expression of *Foxg1* was ever observed in any of the selected fields, we believe that overexpression of *Dkk1* at early stages of differentiation process may also have some effect on the formation *Foxg1*-expressing cells even though only in small number of cells. Quantitative analysis on the selected field revealed around 30% of the cells expressed Foxg1 (Figure 5.21). Similar to constitutive expression, overexpression of *Dkk1* at this stage also generated cells expressing Foxg1 in the cytoplasm as well as in the nucleus (Figure 5.20F). Unlike constitutive expression, the majority of these cells expressed both nestin and Foxg1 (Figure 5.20E).

As expected, more ß-tubulin-positive cells were observed 48 hours post-plating in this condition (Figure 5.22D,E,F). Quantitative analysis also revealed a significant increase in the percentage of ß-tubulin-expressing cells as well as an increase in the total number of ß-tubulin-positive cells when overexpression of *Dkk1* was induced at early stage (Figure 5.23).

In summary, induction of Dkk1 overexpression at early stages of neural differentiation process may promote differentaion of ES cells into NPCs as well as the formation of neurons.

5.2.4.3 Induction of *Dkk1* expression at late stage

Similar to constitutive overexpression, less number of ß-tubulin-expressing cells with very few number of ß-tubulin-negative cells were observed when the culture was analysed 48 hours post-plating (Figure 5.22 G,H,I). Quantitative analysis from ICC also demonstrates a reduction in the total number of both ß-tubulin-positive and –negative cells per field in this condition compared to the control cells as well as when Dkk1 was overexpressed at early stage (Figure 5.23B). Consequently, a significant increase in the ß-tubulin-positive cells was revealed (Figure 5.23A).

In summary, late induction of *Dkk1* may inhibit differentiation of ES cells into certain type of neurons and may, on the other hand, enhance the percentage of those particular neurons at the expense of non-neuronal cells.

5.3 Discussion

In this study the effects of *Wnt1, Wnt3a and Dkk1* overexpression on neural differentiation process of ES cell *in vitro* were demonstrated. Using an optimized inducible ES cell system (as described in chapter 4), we were able to test the functional properties of these genes, as they have been shown to exhibit dynamic RNA expression profiles (Chapter 3), during neural differentiation process in EB cultures stimulated by RA. More importantly, the system has enabled us to induce the overexpression of each gene in temporally-controlled manner. This is an advantage over previous studies where only constitutive expression of Wnt gene or component of Wnt signalling were used in examining the functions of these genes during neural differentiation of ES cells (Aubert *et al.*, 2002; Kielman *et al.*, Haegele *et al.*,

2003). Specifically, we have analysed the effects of overexpressing each of these genes at the early stages of the differentiation process (D2-4), at the time before neural enrichment by treatment of RA (D6-8) takes place in the EBs, on the ability of these EBs to differentiate into NPCs and also on neuronal differentiation of ES cells. Overexpression of each of these genes was also induced during late stages of the process (D7-9), and its effects on neuronal differentiation of ES cells was also analysed. Together with that, we also monitored the effect of the constitutive overexpression of *Wnt1*-, *Wt3a*- and *Dkk1*. In all cases, due to time limitations, we only managed to show the presence of NPCs by nestin positive cells. Nestin is the intermediate filament protein that marks neuroepithelium but also somatic mesoderm (Lendahl *et al.*, 1990; Sejersen, 1993; Sejersen and Lendahl, 1993Lendahl, 1997; Lee *et al.*, 2000). We have also attempted to monitor the differential expression of Pax6 (a paired-box transcription factor expressed in dividing NPCs throughout embryonic neural tube, Walther and Gruss, 1991; Tanabe and Jessell, 1996) and RC2 (marker for radial glial cells) between non- and induced cells, however failed to do so due to technical problems. Therefore, our analysis on the presence of NPCs was dependent on nestin expression. We presumed the comparison to the percentage of nestin positive cells in the control cells would be enough to indicate the effect of Wnt genes or *Dkk1* on the formation of precursor cells, even may not all be NPCs. The formation of neurons was indicated only by the expression of class III ß-tubulin, which marks post mitotic neurons.

Using the inducible system, our study has demonstrated the stage-specific effect of Wnt signalling as well as their multiple functions during neural differentiation process (Figure 5.24) as previously discussed (reviewed by

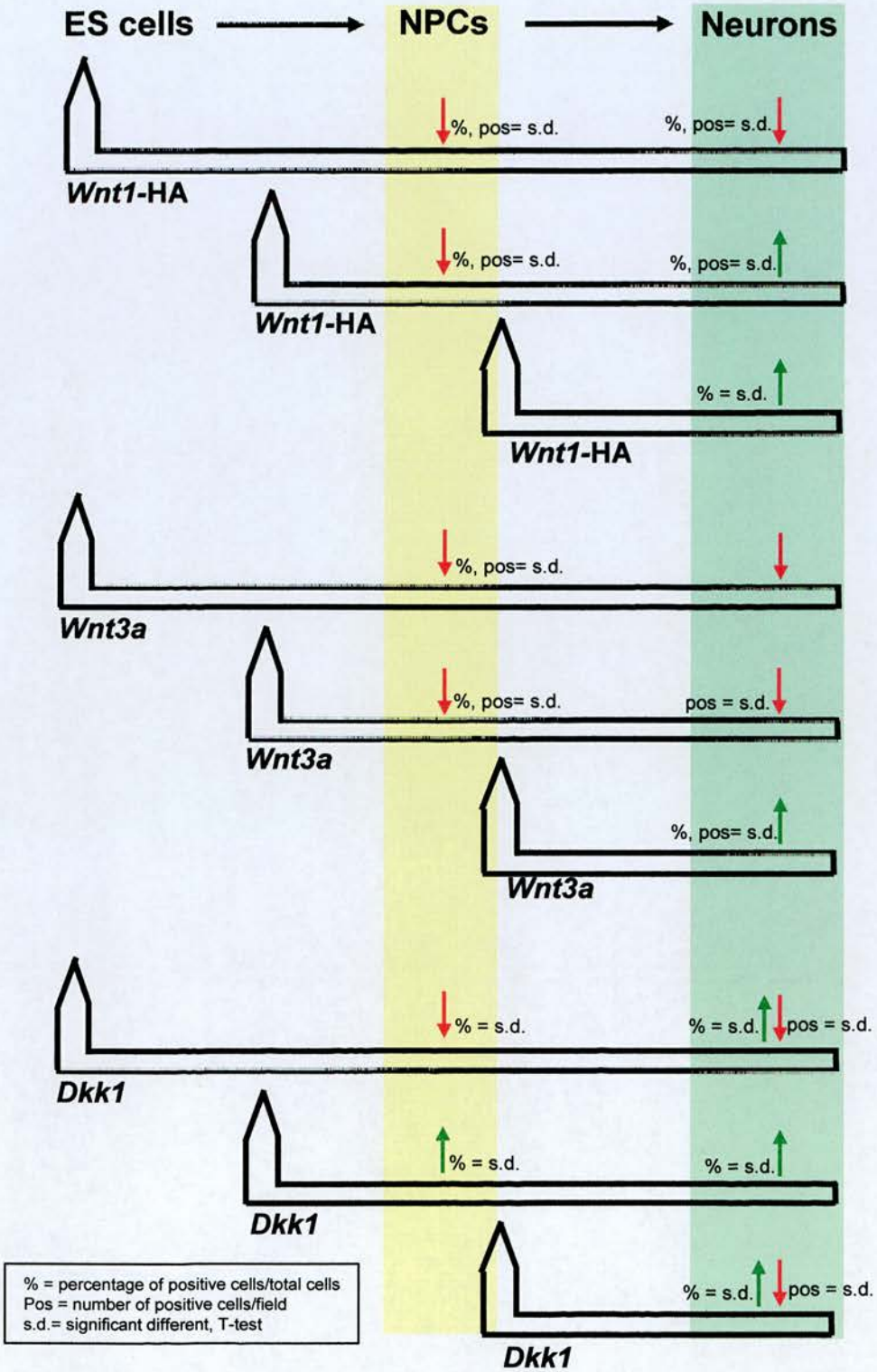

Figure 5.24: Summary of the observations made on the effects of overexpression of *Wnt1*-HA, *Wnt3a* and *Dkk1* on neural differentiation of ES cells at the indicated time point of induction. The arrows indicate an increase ↑ or a decrease ↓ in the formation of NPCs or neurons as determined by the expression of nestin or class III ß-tubulin, respectively.

Patapoutian and Reichardt, 2000; Kleber and Sommer, 2004; Wang and Wynshaw-Boris, 2004). Most of the *in vivo* and *in vitro* studies described point to the roles of Wnt signalling in cell-fate determination especially in instructing cell proliferation or differentiation in ensuring proper development of the vertebrate CNS or neural lineage specification of ES cells (also described in Chapter 1-references therein). One general observation made is that inhibition of Wnt signalling is required during the early patterning of neural tube (around E6.5 mouse embryo) and during later stages of its development requires the activity of Wnt signalling (after E8). In addition, many studies also have strongly suggested the involvement of Wnt in promoting proliferation of precursor cells during early stage of brain development, and during later stage of the development, Wnt has been implicated in promoting the formation of neurons (Dickinson *et al.*, 1994; Chenn and Walsh, 2002; Muroyama *et al.*, 2002; Castelo-Branco *et al.* 2003; Hirabayashi *et al.*, 2004; Panhuysen *et al.*, 2004; Schulte *et al.*, 2005). Based on these studies, we have analysed the effect of stimulating and inhibiting Wnt signalling on neural differentiation of ES cells.

5.3.1 The effects of stimulating Wnt signalling

In the present study, Wnt signalling was stimulated by overexpressing *Wnt1*-HA and *Wnt3a*. The inducible system allowed us to induce the overexpression of these genes at three specific time points. Hence permitting us to examine the stage-dependent effect of Wnt activity, as being described *in vivo*, in culture conditions. The effect of stimulating Wnt activity at the early stage of development *in vivo* was recapitulated by inducing the expression of these genes on D2-4, the stage which is believed to be similar to

that of E4-6 of mouse embryo (as discussed in chapter 3). Its effects on the ability of EBs to differentiate into NPCs and neurons together under the influence of RA was evaluated. Additionaly, inducing the expression of these genes on D7-9 may recapitulate the stimulation of Wnt activity at late stages of mouse embryo, and gave us the opportunity to analyse its effect on the ability of the NPCs to differentiate into neurons. Constitutive overexpression, on the other hand, may recapitulate the effect of Wnt activity during preimplantationn stage of mouse embryo, and led us to the analysis of constitutively overexpressing these genes on the ability of ES cells to differentiate into NPCs and neurons.

5.3.1.1 Wnts inhibit the formation of NPCs

Our limited study discovered that constitutive and early induction of overexpression of *Wnt1* and *Wnt3a* in ES cells significantly inhibited the formation of NPCs. Recent study on ES cells *in vitro* by Aubert and colleagues (2002) has shown that constitutive overexpression of *Wnt1* suppressed neural differentiation of ES cells in response to RA. We also have repeated their work in using *Wnt1*-constitutively overexpressing ES cells. In our work, however, constitutively expressed *Wnt1*-HA was used instead of non-tagged *Wnt1* construct. The same results were observed indicating no effect of HA epitope-tagged on *Wnt1* expression. By contrast, Hirabayashi and colleagues (2004) discovered that HA epitope tag interfered with the activity of *Wnt7a* in their work. Thus, to be on the safe side, we have used non-tagged *Wnt3a* and *Dkk1* in our study.

Other studies have found that stimulation of Wnt signalling inhibits the formation NPCs from ES cells. In study by Haegele *et al.* (2003), expression

of nestin and Sox1 were reduced in APC-deficient (component of Wnt signalling) and ß-catenin-overexpressed ES cells *in vitro,* suggesting Wnt signalling in inhibition of NPCs. Another study with APC-mutated ES cells also showed inhibition of neural lineages *in vivo* and *in vitro* (Kielman *et al.,* 2002). Taken together these studies and our studies strongly suggest the inhibition role of Wnt signalling in differentiation of ES cells into NPCs.

In addition, treatment of Wnt3a protein into early stages of RA- and serum-free EB cultures also suppressed the number of cells expressing Sox1, a marker for NPCs (Watanabe *et al.,* 2005). In agreement to that, our study also shows that exposure of Wnt3a on the early stages of EBs and ES cells, even though in the presence of serum and RA, inhibit the formation of NPCs. The study by Watanabe and co-workers and our study suggest that Wnt signalling could work independent of serum and RA to inhibit neural differentiation of ES cells.

Although many studies have shown the effect of Wnt signalling, especially through the canonical pathway, in inhibiting neural differentiation, many studies have also demonstrated its role in enhancing proliferation of NPCs. Expansion of cortical precursor cell number was observed in cells with expression of a stabilized form of ß-catenin (Chenn and Walsh, 2002). Similarly, the same phenomenon was observed in this study where constitutively overexpressing *Wnt1*-HA cells significantly produced higher number of nestin positive cells after 24 hours post-plating suggesting the role of *Wnt1* in promoting proliferation of nestin-positive cells. Immunostaining with marker for proliferating neural precursor cells, such as Sox1, or cell proliferation assay with BrdU labelling on these nestin-positive cells would

have confirmed this. However, we believe nestin was also marking non-NPCs in these cells. Previous study has suggested that overexpression of Wnt signals led to differentiation of non-neural cells (Haegele *et al.*, 2003). Hence, immunostaining with appropriate markers for non-neural cells would have led us to some explanations. This might also indicate the role of Wnts in differentiation into non-neural lineage despite of neural enrichment of RA. On the other hand, induction of *Wnt1*-HA overexpression on D2 did not increase the number of nestin-expressing cells 24 hours post-plating. Thus, the different effect on the proliferation of nestin-expressing cells from these two conditions may strongly suggest the stage-dependence of Wnt activity during neural differentiation process. It is most likely to signify the communication between components of the molecular mechanisms of Wnt signalling, specifically Wnt/ß-catenin, in ES cells. Recent study has demonstrated that convergence of Wnt/ß-catenin and LIF on STAT3 delays differentiation of ES cells in the presence of serum (Hao *et al.*, 2006). This might explain our observations on the initial low number of nestin-positive cells in constitutively overexpressing *Wnt1*-HA cells when analysed 1-2 hours post-plating, but later increased its number 24 hours post-plating. Thus, immunostaining these cells with a marker for undifferentiated ES cells 1-2 post-plating may explain the situation.

5.3.1.2 Late stage Wnts promote the formation of neurons

We also observed an increase of ß-tubulin-expressing cells when both *Wnt1*-HA and *Wnt3a* were overexpressed at late stage of neural differentiation. Similar phenomena have been demonstrated when comparing the effect of ectopic expression of a stabilized form of ß-catenin on different stages of

mouse neocortex development (Hirabayashi *et al.*, 2004). In the study, more neurons were produced from older aged neocortex in response to the expression of stabilized ß-catenin. This study may suggest stimulation of canonical Wnt signalling during late stages of neural differentiation stimulates neuron formation. Indeed, late induction of *Wnt1*-HA and *Wnt3a* overexpression, which are known to activate the canonical pathway, significantly increased in the percentage of ß-tubulin-expressing cells. The same results were observed when Wnt3a conditioned medium (CM) was added into newly formed neurospheres from dissociated telencephalon of mouse embryo day 11.5 (Muroyama *et al.*, 2004). In addition, their study showed enhanced neuronal differentiation when dissociated neurospheres plated on adhesive substratum was treated with Wnt3a CM. Similar results were observed in our study. Late induction of *Wnt3a* during neural process promoted differentiation of ES cells into neurons. The results also indicate that the pCAG-floxed-*neo*pA-*Wnt3a* construct is inducible and capable of expressing Wnt3a with the same functional activity as Wnt3a CM.

In addition, an increase of the number of neurons was observed when Wnt1-HA overexpression was induced on D2. Not only that we also discovered that the percentage was enhanced as a result of positive selection on neuronal cells and elimination of ß-tubulin-negative cells. On the contrary to *Wnt1*, our results showed inhibition of neuronal differentiation when *Wnt3a* was induced at early stages of neural differentiation. This may imply functional stage-specifity of individual Wnt gene in addition to their redundant function during differentiation process.

Forced differentiation to non-neural lineage in constitutively overexpressing *Wnt1*-HA cells in this study was clearly seen with the reduced percentage of class III ß-tubulin-expressing cells two days post-plating. With this result, we have confirmed the study by Aubert *et al.* (2002). In addition to their study, we also discovered non-neural differentiation from these cells in the absence of RA. This might indicate the role of *Wnt1* in cell fate decision during differentiation of ES cells *in vitro*.

5.3.2 The effects of inhibiting Wnt signalling

In this study, Wnt signalling was inhibited by overexpressing *Dkk1* at the specific time points as described above. *Dkk1* is believed to inhibit canonical Wnt signalling pathway (Semenov *et al.*, 2001). At early stages of developing mouse embryo, inhibition of Wnt by Dkk1 expression is required for proper patterning of vertebrate axis (Glinka *et al.*, 1998; Hashimoto *et al.*, 2000; Mukhopadhyay *et al.*, 2001). Overexpression of this gene has resulted in embryos with enlarged heads (Glinka *et al.*, 1998; Hashimoto *et al.*, 2000). Indeed, an increased number of NPCs and also ß-tubulin-positive cells observed when overexpression of Dkk1 was induced on D2 suggesting that Wnt signalling is inhibiting neural differentiation of ES cells. It may also indicate that the developmental process *in vivo* has been recapitulated in culture condition as overexpression of Dkk1 *in vivo* has been shown to enlarge embryos head in zebrafish and *Xenopus* (Glinka *et al.*, 1998; Hashimoto *et al.*, 2000) when injected at early stage of development. A study by Watanabe and colleagues (2005) also demonstrated that treatment with Dkk1 protein into their EB cultures increasesd the formation of Sox1-positive cells as well as Foxg1-expressing cells. In accordance to this, exposure to

overexpression of Dkk1 in ES cells as well as in early-stage EBs also increased the formation of Foxg1-expressing cells in our culture, even in the presence of RA. This may indicate that overexpression of Dkk1 at these specific stages overrides the caudalizing effect of RA. However, the reduced number of nestin-positive cells in *Dkk1*-constitutively expressed ES cells in our system may indicate the antagonistic effect of *Dkk1* on other Wnt signalling pathway. A recent study has shown that Dkk1 could activate the noncanonical PCP-like pathway (Pandur *et al.*, 2002). Through other pathway, overexpression of Dkk1 in ES cells may have promote the Wnt activity acting through the canonical pathway and inhibit neural differentiation of ES cells as observed in this study and previous studies.

Overexpression of Dkk1 during late stages of neural differentiation significantly increased the percentage of ß-tubulin-expressing cells while the total number of positive cells per field was reduced significantly. This highly suggests that overexpression of Dkk1 is blocking Wnt signals which is required in promoting the formation of neurons. It may also indicate that overexpression of Dkk1 during the late culture period has specifically select the differentiation into a specific type of neuron. Indeed, when Watanabe and colleagues (2005) treated their culture with Dkk1 during late stages of neural differentiation, less number of Pax6-expressing cells was detected in their Foxg1-positive cells, indicating that inhibition of Wnt activity through overexpression of Dkk1 has perturbed the differentiation into certain type of neurons. Alternatively, the reduced number of neurons in *Dkk1*-overexpressing ES cells might also be due to its proapoptotic activity (Shou *et al.*, 2002). These results, therefore, demonstrate that the specific induction time is critical for the role played by *Dkk1* during neural differentiation.

Early induction of *Dkk1* overexpression seems to promote neuronal differentiation while late induction seems to inhibit formation of neurons. However, the presence of *Dkk1* in ES cells which seems to have similar effect as inducing overexpression of *Dkk1* during late stages on the formation of neurons highly suggest the complexity of Wnt signaling as well as the role played by Dkk1 during the process.

5.4 Conclusion

In summary, using an inducible system we have analyzed the effects of stimulating and inhibiting Wnt signalling by overexpressing Wnt (*Wnt1*-HA and *Wnt3a*) and Wnt antagonist (*Dkk1*), respectively, at specific time points during neural differentiation of ES cells in culture conditions; in the presence of serum and RA. Taken together, the results generally indicate the role of Wnt signalling in inhibiting differentiation of ES cells in to NPCs, but also promoting the differentiation into neurons, when induced at particular time. Stage-specific effect of Wnt signalling was demonstrated. Early induction of *Wnt1* and *Wnt3a* overexpression resulted in inhibition of NPCs, while early induction of *Dkk1* overexpression promoted the formation of NPCs. Exposure to overexpression of Wnt1 and Wnt3a during late period of culture promoted neuron formation, and decreased the number of neurons when the culture was exposed to overexpression of Dkk1 during that stage. Constitutive expression of all genes during the process, interestingly, decreased the formation of NPCs as well as neurons. These results, hence, demonstrate the complexity of the roles played by Wnt signalling during neural differentiation of ES cells *in vitro* as it is *in vivo*.

Chapter 6: Final Discussion

6.1 Conditional activation and inhibition of Wnt signalling during neural differentiation of ES cells.

In an effort to understand the roles of Wnt signalling during neural differentiation of ES cells, we began by screening the expression profiles of all 19 Wnt genes during the process. Results from RT-PCR as well as qRT-PCR demonstrated the expression of almost all Wnt genes with a few genes exhibiting interesting dynamic RNA expression pattern, suggesting possible functions of the gene in the process. However, heterogeneity of cell population of EBs does not identify the specific cell type(s) in which the Wnts are expressed. Analysis of RNA expression from $Sox1^{GFP}$-positive cells versus the negative cells would have given us some closer explanations. This could have been carried out by using homogeneous GFP-positive and –negative cells sorted by FACS. Differential expression from these sorted populations as well as from population of stage 1 (undifferentiated ES cells) and stage 2 (young EBs before neural enrichment by RA) of neural differentiation would tell us more specifically the Wnt genes and Wnt antagonists that are actually expressed during neural lineage commitment. Expression of TOP-Red2, despite its technical limitations, also suggested involvement of the canonical Wnt activity particularly during the late stage, which is an agreement with most of Wnt RNA expression profiles. Functional analysis of selected Wnt genes and Wnt antagonist was then carried out with a focus on the roles of Wnt signalling in inhibiting differentiation of ES cells into NPCs and stimulating differentiation of NPCs into neurons as our hypothesis using an inducible expression system.

Using an inducible expression system in ES cells, we have discovered that Wnt signalling plays broader functions than just affecting cell proliferation and differentiation in cell fate determination during different stages of neural differentiation of ES cells. The system has allowed us to examine in more detail the function of Wnt activity, as proposed by Aubert and colleagues (2002), in inhibiting or stimulating neural determination of ES cells. Constitutive overexpression of *Wnt1* and *Wnt3a* seem to inhibit the ability of ES cells to differentiate into NPCs and neurons when analysed 1-2 hours after plating on PDL/laminin-coated plates (Figure 5.24), suggesting inhibition of Wnt signalling may be required to stimulate the production of NPCs. On the other hand, constitutive overexpression of *Dkk1* tells a different story. Instead of promoting the generation of nestin-positive cells, a higher percentage of Foxg1-positive cells with fewer cells expressing nestin were observed. This may indicate that inhibition of Wnt activity, specifically of the canonical pathway, does not stimulate the production of NPCs but instead directs the differentiation of ES cells into more region specific cells. Additionally, the inhibition of Wnt signalling may positively regulate cell cycle exit which might explain the decreased number of nestin-positive but higher number of Foxg1-nestin cells. A high percentage of ß-tubulin-positive with lower number of ß-tubulin-negative cells observed may also suggest positive selective towards neuronal cells rather than non-neuronal cells.

Inhibition of Wnt signalling by overexpressing Dkk1 induced at early stages of differentiation stimulated the generation of NPCs and also neurons, implying the inhibition effect of Wnt signalling in the process. In agreement

with this, overexpression of Wnt1 and Wnt3a induced at early stages inhibit the differentiation of ES cells into NPCs. These results indicate that early stage of this process may be the critical time point where stimulation or inhibition of Wnt signalling will influence cell-fate decision. Similarly, the significant increase of ß-tubulin-positive cells seen when Wnt signalling is stimulated by overexpressing Wnt1 and Wnt3a at late period of differentiation may also indicate that this time point is important in promoting differentiation of ES cells into neurons.

In summary, in an effort to understand the functions of Wnt signalling during neural differentiation of ES cells, we began this study by showing the presence of RNA expression (RT-PCR and qRT-PCR) of Wnt genes and Wnt antagonists during the process. Based on the expression profiles in addition to expression of Wnt reporter gene (TOP-Red2), it is believed that the regulation of Wnt activity during this process is highly stage-dependent. Finally we have examined the effects of stimulating and inhibiting, particularly the canonical Wnt signalling, by overexpressing Wnt1 and Wnt3a, and Dkk1 at three different time points. Using the inducible system, we discovered that Wnt signalling might plays multiple complex functions during neural differentiation of ES cells.

6.2 Limitations of study and future work

One major drawback of this study is the limited set of markers used for NPCs and neurons. The study only used nestin as a marker for NPCs which

in broader terms may not only represent proliferating neural precursors. Dahlstrand *et al.* (1994) found that there are few exceptions to the expression of nestin that marks the proliferating CNS progenitor cells. There are a few differentiated regions of the CNS (the intermediate zone of E15.5 telencephalon) and cells of non-CNS origin (muscle cells) that expressed nestin were detected in the study. Therefore, in addition to nestin, the use of other markers for neural progenitors particularly the SRY-related transcription factor Sox1 (marks dividing neural progenitors and neuroepithelium of the neural plate, Pevny *et al.*, 1998) and the paired-box transcription factor Pax6 (expressed mainly in the ventral region of the neural tube, Walther and Gruss, 1991) might be useful in confirming the presence of NPCs or nestin-positve non-neural precursor cells.

One of the main functions proposed by this study is the role of Wnt signalling in inhibition of differentiation of ES cells into NPCs. There are many factors that might contribute to the decreased in the number of NPCs or specifically nestin-expressing cells when Wnt gene is overexpressed or the increased of these cells whenever Wnt signalling is inhibited. This could be due to changes in mitotic rate, cell survival or proapoptotic factor, or cell fate choice on whether to re-enter cell cycle or to differentiate. One way of addressing these possibilities is by looking at the proliferation or death rate of these cells in response to stimulation or inhibition of Wnt signalling at various specific time points.

This study also found that Wnt signalling might be stimulating the formation of neurons. A variety of distinct neuronal cell types is generated during development of mammalian CNS and have been reproduced *in vitro* using

various protocols from ES cells. Several extracellular factors such as platelet-derived growth factor, PDGF (Erlandsson *et al.*, 2001), insulin growth factor 1 (Arsenijevic and Weiss, 1998), brain-derived neurotrophic factor (Ahmed *et al.*, 1995), bone morphogenetic protein (Li *et al.*, 1998b) have been implicated during neurogenesis *in vivo*, and RA, FGF, EGF and BMP have been demonstrated to be involved in neural development of ES cells *in vitro* (Ying *et al.*, 2003a; Irioka *et al.*, 2005; Watanabe *et al.*, 2005; Conti *et al.*, 2005). It will be interesting to determine which types of neurons are generated upon activation or inhibition of Wnt signalling and also to examine the interactions of this pathway to these factors, particularly, in the generation of regional specific neurons.

Wnt also has been implicated to play a role in the self-renewal of ES cells (Sato *et al.*, 2004). The decrease in the formation of neurons when Wnt1 and Wnt3a were overexpressed in ES cells might suggest the effects of overexpressing Wnts on self renewal of ES cells that might result in inhibition of differentiation process of the cells. It therefore would be interesting to examine the effects of overexpressing Wnts as well as Dkks on this mechanism.

Over the years, considerable progress has been made in understand the role of Wnt signalling especially during development *in vivo*. Progressive evident is pointing to probable functions of this signalling molecule during differentiation of ES cells in culture conditions. Multiple functions of Wnt signalling addressed in this study demonstrate the complexity of Wnt signal transduction mechanisms. One of the biggest problems with Wnt signalling is the understanding the interaction of Fzd/Wnt interaction and the role of

specific Wnt gene in activating the different pathways. Inducible expression system may provide invaluable tool especially in trying to unravel the function of particular gene that is directly or indirectly involves in this process.

References

Aberle, H., Bauer, A., Stappert, J., Kispert, A. and Kemler, R. (1997). beta-catenin is a target for the ubiquitin-proteasome pathway. *Embo J* **16**, 3797-804.

Ahmed, S., Reynolds, B.A. and Weiss S. (1995). BDNF enhances the differentiation but not the survival of CNS stem cell-derived neuronal precursors. *J Neurosci* **15**(8),5765-78.

Alonso, L. and Fuchs, E. (2003). Stem cells in the skin: waste not, Wnt not. *Genes Dev* **17**, 1189-200.

Amit, S., Hatzubai, A., Birman, Y., Andersen, J. S., Ben-Shushan, E., Mann, M., Ben-Neriah, Y. and Alkalay, I. (2002). Axin-mediated CKI phosphorylation of beta-catenin at Ser 45: a molecular switch for the Wnt pathway. *Genes Dev* **16**, 1066-76.

Arsenijevic, Y. and Weiss, S. (1998). Insulin-like growth factor-I is a differentiation factor for postmitotic CNS stem cell-derived neuronal precursors: distinct actions from those of brain-derived neurotrophic factor. *J Neurosci* **18**(6):2118-28. Review.

Arsenijevic, Y., Weiss, S., Schneider, B., Aebischer, P. (2001). Insulin-like growth factor-I is necessary for neural stem cell proliferation and demonstrates distinct actions of epidermal growth factor and fibroblast growth factor-2. *J Neurosci* **21**(18), 7194-202.

Aubert, J., Dunstan, H., Chambers, I. and Smith, A. (2002). Functional gene screening in embryonic stem cells implicates Wnt antagonism in neural differentiation. *Nat Biotechnol* **20**, 1240-5.

Aubert, J., Stavridis, M. P., Tweedie, S., O'Reilly, M., Vierlinger, K., Li, M., Ghazal, P., Pratt, T., Mason, J. O., Roy, D. et al. (2003). Screening for mammalian neural genes via fluorescence-activated cell sorter purification of neural precursors from Sox1-gfp knock-in mice. *Proc Natl Acad Sci U S A* **100 Suppl 1**, 11836-41.

Axelrod, J. (1984). Neuroscience advances. *Science* **225**, 1253.

Backman, M., Machon, O., Mygland, L., van den Bout, C. J., Zhong, W., Taketo, M. M. and Krauss, S. (2005). Effects of canonical Wnt signaling on dorso-ventral specification of the mouse telencephalon. *Dev Biol* **279**, 155-68.

Bafico, A., Gazit, A., Pramila, T., Finch, P. W., Yaniv, A. and Aaronson, S. A. (1999). Interaction of frizzled related protein (FRP) with Wnt ligands and the frizzled receptor suggests alternative mechanisms for FRP inhibition of Wnt signaling. *J Biol Chem* **274**, 16180-7.

Bafico, A., Liu, G., Yaniv, A., Gazit, A. and Aaronson, S. A. (2001). Novel mechanism of Wnt signalling inhibition mediated by Dickkopf-1 interaction with LRP6/Arrow. *Nat Cell Biol* **3**, 683-6.

Bagutti, C., Wobus, A. M., Fassler, R. and Watt, F. M. (1996). Differentiation of embryonal stem cells into keratinocytes: comparison of wild-type and beta 1 integrin-deficient cells. *Dev Biol* **179**, 184-96.

Bagutti, C., Hutter, C., Chiquet-Ehrismann, R., Fassler, R. and Watt, F. M. (2001). Dermal fibroblast-derived growth factors restore the ability of beta(1) integrin-deficient embryonal stem cells to differentiate into keratinocytes. *Dev Biol* **231**, 321-33.

Bain, G., Kitchens, D., Yao, M., Huettner, J. E. and Gottlieb, D. I. (1995). Embryonic stem cells express neuronal properties in vitro. *Dev Biol* **168**, 342-57.

Bain, G., Ray, W. J., Yao, M. and Gottlieb, D. I. (1996). Retinoic acid promotes neural and represses mesodermal gene expression in mouse embryonic stem cells in culture. *Biochem Biophys Res Commun* **223**, 691-4.

Baird, G. S., Zacharias, D. A. and Tsien, R. Y. (2000). Biochemistry, mutagenesis, and oligomerization of DsRed, a red fluorescent protein from coral. *Proc Natl Acad Sci U S A* **97**, 11984-9.

Barberi, T., Klivenyi, P., Calingasan, N. Y., Lee, H., Kawamata, H., Loonam, K., Perrier, A. L., Bruses, J., Rubio, M. E., Topf, N. et al. (2003). Neural subtype specification of fertilization and nuclear transfer embryonic stem cells and application in parkinsonian mice. *Nat Biotechnol* **21**, 1200-7.

Baron, M. (2001). Induction of embryonic hematopoietic and endothelial stem/progenitor cells by hedgehog-mediated signals. *Differentiation* **68**, 175-85.

Beddington, R. S. (1994). Induction of a second neural axis by the mouse node. *Development* **120**, 613-20.

Behrens, J., von Kries, J. P., Kuhl, M., Bruhn, L., Wedlich, D., Grosschedl, R. and Birchmeier, W. (1996). Functional interaction of beta-catenin with the transcription factor LEF-1. *Nature* **382**, 638-42.

Belo, J. A., Bouwmeester, T., Leyns, L., Kertesz, N., Gallo, M., Follettie, M. and De Robertis, E. M. (1997). Cerberus-like is a secreted factor with neutralizing activity expressed in the anterior primitive endoderm of the mouse gastrula. *Mech Dev* **68**, 45-57.

Bhanot, P., Brink, M., Samos, C. H., Hsieh, J. C., Wang, Y., Macke, J. P., Andrew, D., Nathans, J. and Nusse, R. (1996). A new member of the frizzled family from Drosophila functions as a Wingless receptor. *Nature* **382**, 225-30.

Bhanot, P., Fish, M., Jemison, J. A., Nusse, R., Nathans, J. and Cadigan, K. M. (1999). Frizzled and Dfrizzled-2 function as redundant receptors for Wingless during Drosophila embryonic development. *Development* **126**, 4175-86.

Bibel, M., Richter, J., Schrenk, K., Tucker, K. L., Staiger, V., Korte, M., Goetz, M. and Barde, Y. A. (2004). Differentiation of mouse embryonic stem cells into a defined neuronal lineage. *Nat Neurosci* **7**, 1003-9.

Bielinska, M., Narita, N. and Wilson, D. B. (1999). Distinct roles for visceral endoderm during embryonic mouse development. *Int J Dev Biol* **43**, 183-205.

Billon, N., Jolicoeur, C., Ying, Q. L., Smith, A. and Raff, M. (2002). Normal timing of oligodendrocyte development from genetically engineered, lineage-selectable mouse ES cells. *J Cell Sci* **115**, 3657-65.

Bjorklund, L. M., Sanchez-Pernaute, R., Chung, S., Andersson, T., Chen, I. Y., McNaught, K. S., Brownell, A. L., Jenkins, B. G., Wahlestedt, C., Kim, K. S. et al. (2002). Embryonic stem cells develop into functional dopaminergic neurons after transplantation in a Parkinson rat model. *Proc Natl Acad Sci U S A* **99**, 2344-9.

Blumberg, B. (1997). An essential role for retinoid signaling in anteroposterior neural specification and neuronal differentiation. *Semin Cell Dev Biol* **8**, 417-28.

Blyszczuk, P., Asbrand, C., Rozzo, A., Kania, G., St-Onge, L., Rupnik, M. and Wobus, A. M. (2004). Embryonic stem cells differentiate into insulin-producing cells without selection of nestin-expressing cells. *Int J Dev Biol* **48**, 1095-104.

Blyszczuk, P. and Wobus, A. M. (2004). Stem cells and pancreatic differentiation in vitro. *J Biotechnol* **113**, 3-13.

Boheler, K. R., Czyz, J., Tweedie, D., Yang, H. T., Anisimov, S. V. and Wobus, A. M. (2002). Differentiation of pluripotent embryonic stem cells into cardiomyocytes. *Circ Res* **91**, 189-201.

Boudjelal, M., Taneja, R., Matsubara, S., Bouillet, P., Dolle, P. and Chambon, P. (1997). Overexpression of Stra13, a novel retinoic acid-inducible gene of the basic helix-

loop-helix family, inhibits mesodermal and promotes neuronal differentiation of P19 cells. *Genes Dev* **11**, 2052-65.

Bouillet, P., Oulad-Abdelghani, M., Vicaire, S., Garnier, J. M., Schuhbaur, B., Dolle, P. and Chambon, P. (1995). Efficient cloning of cDNAs of retinoic acid-responsive genes in P19 embryonal carcinoma cells and characterization of a novel mouse gene, Stra1 (mouse LERK-2/Eplg2). *Dev Biol* **170**, 420-33.

Bouillet, P., Oulad-Abdelghani, M., Ward, S. J., Bronner, S., Chambon, P. and Dolle, P. (1996). A new mouse member of the Wnt gene family, mWnt-8, is expressed during early embryogenesis and is ectopically induced by retinoic acid. *Mech Dev* **58**, 141-52.

Bradley, R. S. and Brown, A. M. (1990). The proto-oncogene int-1 encodes a secreted protein associated with the extracellular matrix. *Embo J* **9**, 1569-75.

Brewster, R. and Dahmane, N. (1999). Getting a-head of the organizer: anterior-posterior patterning of the forebrain. *Bioessays* **21**, 631-6.

Brook, F. A. and Gardner, R. L. (1997). The origin and efficient derivation of embryonic stem cells in the mouse. *Proc Natl Acad Sci U S A* **94**, 5709-12.

Brott, B. K. and Sokol, S. Y. (2002). Regulation of Wnt/LRP signaling by distinct domains of Dickkopf proteins. *Mol Cell Biol* **22**, 6100-10.

Brown, J. D. and Moon, R. T. (1998). Wnt signaling: why is everything so negative? *Curr Opin Cell Biol* **10**, 182-7.

Brustle, O., Jones, K. N., Learish, R. D., Karram, K., Choudhary, K., Wiestler, O. D., Duncan, I. D. and McKay, R. D. (1999). Embryonic stem cell-derived glial precursors: a source of myelinating transplants. *Science* **285**, 754-6.

Burdon, T., Chambers, I., Stracey, C., Niwa, H. and Smith, A. (1999). Signaling mechanisms regulating self-renewal and differentiation of pluripotent embryonic stem cells. *Cells Tissues Organs* **165**, 131-43.

Burdon, T., Smith, A. and Savatier, P. (2002). Signalling, cell cycle and pluripotency in embryonic stem cells. *Trends Cell Biol* **12**, 432-8.

Buttery, L. D., Bourne, S., Xynos, J. D., Wood, H., Hughes, F. J., Hughes, S. P., Episkopou, V. and Polak, J. M. (2001). Differentiation of osteoblasts and in vitro bone formation from murine embryonic stem cells. *Tissue Eng* **7**, 89-99.

Cabrera, C. V., Alonso, M. C., Johnston, P., Phillips, R. G. and Lawrence, P. A. (1987). Phenocopies induced with antisense RNA identify the wingless gene. *Cell* **50**, 659-63.

Campbell, K. (2003). Dorsal-ventral patterning in the mammalian telencephalon. *Curr Opin Neurobiol* **13**, 50-6.

Caricasole, A., Ferraro, T., Iacovelli, L., Barletta, E., Caruso, A., Melchiorri, D., Terstappen, G. C. and Nicoletti, F. (2003). Functional characterization of WNT7A signaling in PC12 cells: interaction with A FZD5 x LRP6 receptor complex and modulation by Dickkopf proteins. *J Biol Chem* **278**, 37024-31.

Castelo-Branco, G., Wagner, J., Rodriguez, F. J., Kele, J., Sousa, K., Rawal, N., Pasolli, H. A., Fuchs, E., Kitajewski, J. and Arenas, E. (2003). Differential regulation of midbrain dopaminergic neuron development by Wnt-1, Wnt-3a, and Wnt-5a. *Proc Natl Acad Sci U S A* **100**, 12747-52.

Castelo-Branco, G., Rawal, N. and Arenas, E. (2004). GSK-3beta inhibition/beta-catenin stabilization in ventral midbrain precursors increases differentiation into dopamine neurons. *J Cell Sci* **117**, 5731-7.

Cavaleri, F. and Scholer, H. R. (2003). Nanog: a new recruit to the embryonic stem cell orchestra. *Cell* **113**, 551-2.

Cavallo, R. A., Cox, R. T., Moline, M. M., Roose, J., Polevoy, G. A., Clevers, H., Peifer, M. and Bejsovec, A. (1998). Drosophila Tcf and Groucho interact to repress Wingless signalling activity. *Nature* **395**, 604-8.

Chambers, I., Colby, D., Robertson, M., Nichols, J., Lee, S., Tweedie, S. and Smith, A. (2003). Functional expression cloning of Nanog, a pluripotency sustaining factor in embryonic stem cells. *Cell* **113**, 643-55.

Chen, G., Fernandez, J., Mische, S. and Courey, A. J. (1999). A functional interaction between the histone deacetylase Rpd3 and the corepressor groucho in Drosophila development. *Genes Dev* **13**, 2218-30.

Chenn, A. and Walsh, C. A. (2002). Regulation of cerebral cortical size by control of cell cycle exit in neural precursors. *Science* **297**, 365-9.

Chenn, A. and Walsh, C. A. (2003). Increased neuronal production, enlarged forebrains and cytoarchitectural distortions in ß-catenin overexpressin transgenic mice. *Cereberal cortex* **13**, 599-606.

Ciani, L. and Salinas, P. C. (2005). WNTS in the vertebrate nervous system: from patterning to neuronal connectivity. *Nat Rev Neurosci* **6**, 351-62.

Cliffe, A., Hamada, F. and Bienz, M. (2003). A role of Dishevelled in relocating Axin to the plasma membrane during wingless signaling. *Curr Biol* **13**, 960-6.

Corcoran, J., So, P. L. and Maden, M. (2002). Absence of retinoids can induce motoneuron disease in the adult rat and a retinoid defect is present in motoneuron disease patients. *J Cell Sci* **115**, 4735-41.

Cox, R. T., Pai, L. M., Miller, J. R., Orsulic, S., Stein, J., McCormick, C. A., Audeh, Y., Wang, W., Moon, R. T. and Peifer, M. (1999). Membrane-tethered Drosophila Armadillo cannot transduce Wingless signal on its own. *Development* **126**, 1327-35.

Cox, W. G. and Hemmati-Brivanlou, A. (1995). Caudalization of neural fate by tissue recombination and bFGF. *Development* **121**, 4349-58.

Conti, L., Pollard, S. M., Gorba, T., Reitano, E., Toselli, M., Biella, G., Sun, Y., Sanzone, S., Ying, Q. L., Cattaneo, E. et al. (2005). Niche-independent symmetrical self-renewal of a mammalian tissue stem cell. *PLoS Biol* **3**, e283.

Coucouvanis, E. and Martin, G. R. (1995). Signals for death and survival: a two-step mechanism for cavitation in the vertebrate embryo. *Cell* **83**, 279-87.

Coucouvanis, E. C., Martin, G. R. and Nadeau, J. H. (1995). Genetic approaches for studying programmed cell death during development of the laboratory mouse. *Methods Cell Biol* **46**, 387-440.

Cumberledge, S. and Reichsman, F. (1997). Glycosaminoglycans and WNTs: just a spoonful of sugar helps the signal go down. *Trends Genet* **13**, 421-3.

Dabdoub, A., Donohue, M. J., Brennan, A., Wolf, V., Montcouquiol, M., Sassoon, D. A., Hseih, J. C., Rubin, J. S., Salinas, P. C. and Kelley, M. W. (2003). Wnt signaling mediates reorientation of outer hair cell stereociliary bundles in the mammalian cochlea. *Development* **130**, 2375-84.

Dahlstrand, J., Lardelli, M. and Lendahl, U. (1994). Nestin mRNA expression correlates with the central nervous system progenitor cells state in many, but not all, regions of developing central nervous system. *Dev Brain Res* **84**, 109-129.

Dahlstrand, J., Lardelli, M. and Lendahl, U. (1995). Nestin mRNA expression correlates with the central nervous system progenitor cell state in many, but not all, regions of developing central nervous system. *Brain Res Dev Brain Res* **84**, 109-29.

Dani, C. (1999). Embryonic stem cell-derived adipogenesis. *Cells Tissues Organs* **165**, 173-80.

Daniels, D. L. and Weis, W. I. (2002). ICAT inhibits beta-catenin binding to Tcf/Lef-family transcription factors and the general coactivator p300 using independent structural modules. *Mol Cell* **10**, 573-84.

Danielian, P. S., Muccino, D., Rowitch, D. H., Michael, S. K. and McMahon, A. P. (1998). Modification of gene activity in mouse embryos in utero by a tamoxifen-inducible form of Cre recombinase. *Curr Biol* **8**, 1323-6. **DasGupta, R. and Fuchs, E.** (1999). Multiple roles for activated LEF/TCF transcription complexes during hair follicle development and differentiation. *Development* **126**, 4557-68.

Davidson, G., Mao, B., del Barco Barrantes, I. and Niehrs, C. (2002). Kremen proteins interact with Dickkopf1 to regulate anteroposterior CNS patterning. *Development* **129**, 5587-96.

Dhoot, G. K., Gustafsson, M. K., Ai, X., Sun, W., Standiford, D. M. and Emerson, C. P., Jr. (2001). Regulation of Wnt signaling and embryo patterning by an extracellular sulfatase. *Science* **293**, 1663-6.

Dickinson, M. E., Krumlauf, R. and McMahon, A. P. (1994). Evidence for a mitogenic effect of Wnt-1 in the developing mammalian central nervous system. *Development* **120**, 1453-71.

Doetschman, T. C., Eistetter, H., Katz, M., Schmidt, W. and Kemler, R. (1985). The in vitro development of blastocyst-derived embryonic stem cell lines: formation of visceral yolk sac, blood islands and myocardium. *J Embryol Exp Morphol* **87**, 27-45.

Dorsky, R. I., Sheldahl, L. C. and Moon, R. T. (2002). A transgenic Lef1/beta-catenin-dependent reporter is expressed in spatially restricted domains throughout zebrafish development. *Dev Biol* **241**, 229-37.

Dorsky, R. I., Sheldahl, L. C. and Moon, R. T. (2002). A transgenic Lef1/beta-catenin-dependent reporter is expressed in spatially restricted domains throughout zebrafish development. *Dev Biol* **241**, 229-37.

Dorsky, R. I., Itoh, M., Moon, R. T. and Chitnis, A. (2003). Two tcf3 genes cooperate to pattern the zebrafish brain. *Development* **130**, 1937-47.

Drab, M., Haller, H., Bychkov, R., Erdmann, B., Lindschau, C., Haase, H., Morano, I., Luft, F. C. and Wobus, A. M. (1997). From totipotent embryonic stem cells to spontaneously contracting smooth muscle cells: a retinoic acid and db-cAMP in vitro differentiation model. *Faseb J* **11**, 905-15.

Du, S. J., Purcell, S. M., Christian, J. L., McGrew, L. L. and Moon, R. T. (1995). Identification of distinct classes and functional domains of Wnts through expression of wild-type and chimeric proteins in Xenopus embryos. *Mol Cell Biol* **15**, 2625-34.

Du, Z.W. and Zhang, S.C. (2004). Neural differentiation from embryonic stem cells:Which way? *Stem cells Dev* **13**, 372-381.

Duncan, S. A., Nagy, A. and Chan, W. (1997). Murine gastrulation requires HNF-4 regulated gene expression in the visceral endoderm: tetraploid rescue of Hnf-4(-/-) embryos. *Development* **124**, 279-87.

Duncan, S. A., Zhong, Z., Wen, Z. and Darnell, J. E., Jr. (1997). STAT signaling is active during early mammalian development. *Dev Dyn* **208**, 190-8.

Durston, A. J., Timmermans, J. P., Hage, W. J., Hendriks, H. F., de Vries, N. J., Heideveld, M. and Nieuwkoop, P. D. (1989). Retinoic acid causes an anteroposterior transformation in the developing central nervous system. *Nature* **340**, 140-4.

Edlund, T. and Jessell, T. M. (1999). Progression from extrinsic to intrinsic signaling in cell fate specification: a view from the nervous system. *Cell* **96**, 211-24.

Eiges, R. and Benvenisty, N. (2002). A molecular view on pluripotent stem cells. *FEBS Lett* **529**, 135-41.

Eistetter, H. R. (1988). A mouse pluripotent embryonal stem cell line stage-specifically regulates expression of homeo-box containing DNA sequences during differentiation in vitro. *Eur J Cell Biol* **45**, 315-21.

Ericson, J., Morton, S., Kawakami, A., Roelink, H. and Jessell, T. M. (1996). Two critical periods of Sonic Hedgehog signaling required for the specification of motor neuron identity. *Cell* **87**, 661-73.

Erlandsson, A., Enarsson, M. and Forsberg-Nilsson, K. (2001). Immature neurons from CNS stem cells proliferate in response to platelet-derived growth factor. *J Neurosci* **21**(10):3483-91.

Ernst, M., Novak, U., Nicholson, S. E., Layton, J. E. and Dunn, A. R. (1999). The carboxyl-terminal domains of gp130-related cytokine receptors are necessary for suppressing embryonic stem cell differentiation. Involvement of STAT3. *J Biol Chem* **274**, 9729-37.

Evans, M. J. and Kaufman, M. H. (1981). Establishment in culture of pluripotential cells from mouse embryos. *Nature* **292**, 154-6.

Fairchild, P. J., Brook, F. A., Gardner, R. L., Graca, L., Strong, V., Tone, Y., Tone, M., Nolan, K. F. and Waldmann, H. (2000). Directed differentiation of dendritic cells from mouse embryonic stem cells. *Curr Biol* **10**, 1515-8.

Fairchild, P. J., Nolan, K. F., Cartland, S. and Waldmann, H. (2005). Embryonic stem cells: a novel source of dendritic cells for clinical applications. *Int Immunopharmacol* **5**, 13-21.

Farr, G. H., 3rd, Ferkey, D. M., Yost, C., Pierce, S. B., Weaver, C. and Kimelman, D. (2000). Interaction among GSK-3, GBP, axin, and APC in Xenopus axis specification. *J Cell Biol* **148**, 691-702.

Feil, R., Brocard, J., Mascrez, B., LeMeur, M., Metzger, D. and Chambon, P. (1996). Ligand-activated site-specific recombination in mice. *Proc Natl Acad Sci U S A* **93**, 10887-90.

Feil, R., Wagner, J., Metzger, D. and Chambon, P. (1997). Regulation of Cre recombinase activity by mutated estrogen receptor ligand-binding domains. *Biochem Biophys Res Commun* **237**, 752-7.

Feraud, O., Cao, Y. and Vittet, D. (2001). Embryonic stem cell-derived embryoid bodies development in collagen gels recapitulates sprouting angiogenesis. *Lab Invest* **81**, 1669-81.

Feraud, O., Prandini, M. H. and Vittet, D. (2003). Vasculogenesis and angiogenesis from in vitro differentiation of mouse embryonic stem cells. *Methods Enzymol* **365**, 214-28.

Finley, M. F., Kulkarni, N. and Huettner, J. E. (1996). Synapse formation and establishment of neuronal polarity by P19 embryonic carcinoma cells and embryonic stem cells. *J Neurosci* **16**, 1056-65.

Flores-Saaib, R. D. and Courey, A. J. (2000). Analysis of Groucho-histone interactions suggests mechanistic similarities between Groucho- and Tup1-mediated repression. *Nucleic Acids Res* **28**, 4189-96.

Foley, A. C., Skromne, I. and Stern, C. D. (2000). Reconciling different models of forebrain induction and patterning: a dual role for the hypoblast. *Development* **127**, 3839-54.

Fraichard, A., Chassande, O., Bilbaut, G., Dehay, C., Savatier, P. and Samarut, J. (1995). In vitro differentiation of embryonic stem cells into glial cells and functional neurons. *J Cell Sci* **108 (Pt 10)**, 3181-8.

Fuhrmann, G., Chung, A. C., Jackson, K. J., Hummelke, G., Baniahmad, A., Sutter, J., Sylvester, I., Scholer, H. R. and Cooney, A. J. (2001). Mouse germline restriction of Oct4 expression by germ cell nuclear factor. *Dev Cell* **1**, 377-87.

Fujikura, J., Yamato, E., Yonemura, S., Hosoda, K., Masui, S., Nakao, K., Miyazaki Ji, J. and Niwa, H. (2002). Differentiation of embryonic stem cells is induced by GATA factors. *Genes Dev* **16**, 784-9.

Gajovic, S., St-Onge, L., Yokota, Y. and Gruss, P. (1997). Retinoic acid mediates Pax6 expression during in vitro differentiation of embryonic stem cells. *Differentiation* **62**, 187-92.

Galceran, J., Farinas, I., Depew, M. J., Clevers, H. and Grosschedl, R. (1999). Wnt3a-/--like phenotype and limb deficiency in Lef1(-/-)Tcf1(-/-) mice. *Genes Dev* **13**, 709-17.

Galceran, J., Miyashita-Lin, E. M., Devaney, E., Rubenstein, J. L. and Grosschedl, R. (2000). Hippocampus development and generation of dentate gyrus granule cells is regulated by LEF1. *Development* **127**, 469-82.

Gavin, B. J., McMahon, J. A. and McMahon, A. P. (1990). Expression of multiple novel Wnt-1/int-1-related genes during fetal and adult mouse development. *Genes Dev* **4**, 2319-32.

Glinka, A., Wu, W., Delius, H., Monaghan, A. P., Blumenstock, C. and Niehrs, C. (1998). Dickkopf-1 is a member of a new family of secreted proteins and functions in head induction. *Nature* **391**, 357-62.

Gofflot, F., Hall, M. and Morriss-Kay, G. M. (1997). Genetic patterning of the developing mouse tail at the time of posterior neuropore closure. *Dev Dyn* **210**, 431-45.

Gofflot, F., Hall, M. and Morriss-Kay, G. M. (1998). Genetic patterning of the posterior neuropore region of curly tail mouse embryos: deficiency of Wnt5a expression. *Int J Dev Biol* **42**, 637-44.

Gottlieb, D. I. and Huettner, J. E. (1999). An in vitro pathway from embryonic stem cells to neurons and glia. *Cells Tissues Organs* **165**, 165-72.

Graham, T. A., Ferkey, D. M., Mao, F., Kimelman, D. and Xu, W. (2001). Tcf4 can specifically recognize beta-catenin using alternative conformations. *Nat Struct Biol* **8**, 1048-52.

Gratsch, T. E. and O'Shea, K. S. (2002). Noggin and chordin have distinct activities in promoting lineage commitment of mouse embryonic stem (ES) cells. *Dev Biol* **245**, 83-94.

Grove, E. A., Tole, S., Limon, J., Yip, L. and Ragsdale, C. W. (1998). The hem of the embryonic cerebral cortex is defined by the expression of multiple Wnt genes and is compromised in Gli3-deficient mice. *Development* **125**, 2315-25.

Gualandris, A., Annes, J. P., Arese, M., Noguera, I., Jurukovski, V. and Rifkin, D. B. (2000). The latent transforming growth factor-beta-binding protein-1 promotes in vitro differentiation of embryonic stem cells into endothelium. *Mol Biol Cell* **11**, 4295-308.

Gutierrez-Ramos, J. C. and Palacios, R. (1992). In vitro differentiation of embryonic stem cells into lymphocyte precursors able to generate T and B lymphocytes in vivo. *Proc Natl Acad Sci U S A* **89**, 9171-5.

Hadjantonakis, A. and Papaioannou, V. (2001). The stem cells of early embryos. *Differentiation* **68**, 159-66.

Haegele, L., Ingold, B., Naumann, H., Tabatabai, G., Ledermann, B. and Brandner, S. (2003). Wnt signalling inhibits neural differentiation of embryonic stem cells by controlling bone morphogenetic protein expression. *Mol Cell Neurosci* **24**, 696-708.

Hall, A. C., Lucas, F. R. and Salinas, P. C. (2000). Axonal remodeling and synaptic differentiation in the cerebellum is regulated by WNT-7a signaling. *Cell* **100**, 525-35.

Hamatani, T., Carter, M. G., Sharov, A. A. and Ko, M. S. (2004). Dynamics of global gene expression changes during mouse preimplantation development. *Dev Cell* **6**, 117-31.

Hamazaki, T., Iiboshi, Y., Oka, M., Papst, P. J., Meacham, A. M., Zon, L. I. and Terada, N. (2001). Hepatic maturation in differentiating embryonic stem cells in vitro. *FEBS Lett* **497**, 15-9.

Hao, J., Li, T. G., Qi, X., Zhao, D. F. and Zhao, G. Q. (2006). WNT/beta-catenin pathway up-regulates Stat3 and converges on LIF to prevent differentiation of mouse embryonic stem cells. *Dev Biol* **290**, 81-91.

Hart, M. J., de los Santos, R., Albert, I. N., Rubinfeld, B. and Polakis, P. (1998). Downregulation of beta-catenin by human Axin and its association with the APC tumor suppressor, beta-catenin and GSK3 beta. *Curr Biol* **8**, 573-81.

Hashimoto, H., Itoh, M., Yamanaka, Y., Yamashita, S., Shimizu, T., Solnica-Krezel, L., Hibi, M. and Hirano, T. (2000). Zebrafish Dkk1 functions in forebrain specification and axial mesendoderm formation. *Dev Biol* **217**, 138-52.

Hawley, S. H., Wunnenberg-Stapleton, K., Hashimoto, C., Laurent, M. N., Watabe, T., Blumberg, B. W. and Cho, K. W. (1995). Disruption of BMP signals in embryonic Xenopus ectoderm leads to direct neural induction. *Genes Dev* **9**, 2923-35.

Hayashi, S., Yamane, T., Miyamoto, A., Hemmi, H., Tagaya, H., Tanio, Y., Kanda, H., Yamazaki, H. and Kunisada, T. (1998). Commitment and differentiation of stem cells to the osteoclast lineage. *Biochem Cell Biol* **76**, 911-22.

Hecht, A., Vleminckx, K., Stemmler, M. P., van Roy, F. and Kemler, R. (2000). The p300/CBP acetyltransferases function as transcriptional coactivators of beta-catenin in vertebrates. *Embo J* **19**, 1839-50.

Hegert, C., Kramer, J., Hargus, G., Muller, J., Guan, K., Wobus, A. M., Muller, P. K. and Rohwedel, J. (2002). Differentiation plasticity of chondrocytes derived from mouse embryonic stem cells. *J Cell Sci* **115**, 4617-28.

Heisenberg, C. P., Tada, M., Rauch, G. J., Saude, L., Concha, M. L., Geisler, R., Stemple, D. L., Smith, J. C. and Wilson, S. W. (2000). Silberblick/Wnt11 mediates convergent extension movements during zebrafish gastrulation. *Nature* **405**, 76-81.

Hemmi, H., Okuyama, H., Yamane, T., Nishikawa, S., Nakano, T., Yamazaki, H., Kunisada, T. and Hayashi, S. (2001). Temporal and spatial localization of osteoclasts in colonies from embryonic stem cells. *Biochem Biophys Res Commun* **280**, 526-34.

Hirabayashi, Y., Itoh, Y., Tabata, H., Nakajima, K., Akiyama, T., Masuyama, N. and Gotoh, Y. (2004). The Wnt/beta-catenin pathway directs neuronal differentiation of cortical neural precursor cells. *Development* **131**, 2791-801.

Hitoshi, S., Tropepe, V., Ekker, M. and van der Kooy, D. (2002). Neural stem cell lineages are regionally specified, but not committed, within distinct compartments of the developing brain. *Development* **129**, 233-44.

Hoang, B. H., Thomas, J. T., Abdul-Karim, F. W., Correia, K. M., Conlon, R. A., Luyten, F. P. and Ballock, R. T. (1998). Expression pattern of two Frizzled-related genes, Frzb-1 and Sfrp-1, during mouse embryogenesis suggests a role for modulating action of Wnt family members. *Dev Dyn* **212**, 364-72.

Hori, Y., Rulifson, I. C., Tsai, B. C., Heit, J. J., Cahoy, J. D. and Kim, S. K. (2002). Growth inhibitors promote differentiation of insulin-producing tissue from embryonic stem cells. *Proc Natl Acad Sci U S A* **99**, 16105-10.

Houart, C., Westerfield, M. and Wilson, S. W. (1998). A small population of anterior cells patterns the forebrain during zebrafish gastrulation. *Nature* **391**, 788-92.

Houart, C., Caneparo, L., Heisenberg, C., Barth, K., Take-Uchi, M. and Wilson, S. (2002). Establishment of the telencephalon during gastrulation by local antagonism of Wnt signaling. *Neuron* **35**, 255-65.

Huelsken, J., Vogel, R., Brinkmann, V., Erdmann, B., Birchmeier, C. and Birchmeier, W. (2000). Requirement for beta-catenin in anterior-posterior axis formation in mice. *J Cell Biol* **148**, 567-78.

Hsieh, J. C., Kodjabachian, L., Rebbert, M. L., Rattner, A., Smallwood, P. M., Samos, C. H., Nusse, R., Dawid, I. B. and Nathans, J. (1999). A new secreted protein that binds to Wnt proteins and inhibits their activities. *Nature* **398**, 431-6.

Huelsken, J., Vogel, R., Brinkmann, V., Erdmann, B., Birchmeier, C. and Birchmeier, W. (2000). Requirement for beta-catenin in anterior-posterior axis formation in mice. *J Cell Biol* **148**, 567-78.

Ikeya, M., Lee, S. M., Johnson, J. E., McMahon, A. P. and Takada, S. (1997). Wnt signalling required for expansion of neural crest and CNS progenitors. *Nature* **389**, 966-70.

Ille, F. and Sommer, L. (2005). Wnt signaling: multiple functions in neural development. *Cell Mol Life Sci* **62**, 1100-8.

Indra, A. K., Warot, X., Brocard, J., Bornert, J. M., Xiao, J. H., Chambon, P. and Metzger, D. (1999). Temporally-controlled site-specific mutagenesis in the basal layer of the epidermis: comparison of the recombinase activity of the tamoxifen-inducible Cre-ER(T) and Cre-ER(T2) recombinases. *Nucleic Acids Res* **27**, 4324-7.

Irioka, T., Watanabe, K., Mizusawa, H., Mizuseki, K. and Sasai, Y. (2005). Distinct effects of caudalizing factors on regional specification of embryonic stem cell-derived neural precursors. *Brain Res Dev Brain Res* **154**(1), 63-70.

Ishikawa, T. O., Tamai, Y., Li, Q., Oshima, M. and Taketo, M. M. (2003). Requirement for tumor suppressor Apc in the morphogenesis of anterior and ventral mouse embryo. *Dev Biol* **253**, 230-46.

Israsena, N., Hu, M., Fu, W., Kan, L. and Kessler, J.,A. (2004). The presence of FGF2 signaling determines whether beta-catenin exerts effects on proliferation or neuronal differentiation of neural stem cells. *Dev Biol* **268**(1), 220-31.

Jessell, T. M. (2000). Neuronal specification in the spinal cord: inductive signals and transcriptional codes. *Nat Rev Genet* **1**, 20-9.

Jones-Villeneuve, E. M., McBurney, M. W., Rogers, K. A. and Kalnins, V. I. (1982). Retinoic acid induces embryonal carcinoma cells to differentiate into neurons and glial cells. *J Cell Biol* **94**, 253-62.

Jones, E. A., Tosh, D., Wilson, D. I., Lindsay, S. and Forrester, L. M. (2002). Hepatic differentiation of murine embryonic stem cells. *Exp Cell Res* **272**, 15-22.

Kan, L., Israsena, N., Zhang, Z., Hu, M., Zhao, L. R., Jalali, A., Sahni, V. and Kessler, J. A. (2004). Sox1 acts through multiple independent pathways to promote neurogenesis. *Dev Biol* **269**, 580-94.

Kawano, Y. and Kypta, R. (2003). Secreted antagonists of the Wnt signalling pathway. *J Cell Sci* **116**, 2627-34.

Kawasaki, H., Mizuseki, K., Nishikawa, S., Kaneko, S., Kuwana, Y., Nakanishi, S., Nishikawa, S. I. and Sasai, Y. (2000). Induction of midbrain dopaminergic neurons from ES cells by stromal cell-derived inducing activity. *Neuron* **28**, 31-40.

Kawasaki, H., Mizuseki, K. and Sasai, Y. (2002a). Selective neural induction from ES cells by stromal cell-derived inducing activity and its potential therapeutic application in Parkinson's disease. *Methods Mol Biol* **185**, 217-27.

Kawasaki, H., Suemori, H., Mizuseki, K., Watanabe, K., Urano, F., Ichinose, H., Haruta, M., Takahashi, M., Yoshikawa, K., Nishikawa, S. et al. (2002b). Generation of dopaminergic neurons and pigmented epithelia from primate ES cells by stromal cell-derived inducing activity. *Proc Natl Acad Sci U S A* **99**, 1580-5.

Keller, G., Kennedy, M., Papayannopoulou, T. and Wiles, M. V. (1993). Hematopoietic commitment during embryonic stem cell differentiation in culture. *Mol Cell Biol* **13**, 473-86.

Kelly, O. G., Pinson, K. I. and Skarnes, W. C. (2004). The Wnt co-receptors Lrp5 and Lrp6 are essential for gastrulation in mice. *Development* **131**, 2803-15.

Kemler, R., Hierholzer, A., Kanzler, B., Kuppig, S., Hansen, K., Taketo, M. M., de Vries, W. N., Knowles, B. B. and Solter, D. (2004). Stabilization of beta-catenin in the mouse zygote leads to premature epithelial-mesenchymal transition in the epiblast. *Development* **131**, 5817-24.

Kemp, C., Willems, E., Abdo, S., Lambiv, L. and Leyns, L. (2005). Expression of all Wnt genes and their secreted antagonists during mouse blastocyst and postimplantation development. *Dev Dyn*.

Kengaku, M., Capdevila, J., Rodriguez-Esteban, C., De La Pena, J., Johnson, R. L., Belmonte, J. C. and Tabin, C. J. (1998). Distinct WNT pathways regulating AER formation and dorsoventral polarity in the chick limb bud. *Science* **280**, 1274-7.

Kennedy, M., Firpo, M., Choi, K., Wall, C., Robertson, S., Kabrun, N. and Keller, G. (1997). A common precursor for primitive erythropoiesis and definitive haematopoiesis. *Nature* **386**, 488-93.

Kielman, M. F., Rindapaa, M., Gaspar, C., van Poppel, N., Breukel, C., van Leeuwen, S., Taketo, M. M., Roberts, S., Smits, R. and Fodde, R. (2002). Apc modulates embryonic stem-cell differentiation by controlling the dosage of beta-catenin signaling. *Nat Genet* **32**, 594-605.

Kim, T. E., Lee, H. S., Lee, Y. B., Hong, S. H., Lee, Y. S., Ichinose, H., Kim, S. U. and Lee, M. A. (2003). Sonic hedgehog and FGF8 collaborate to induce dopaminergic phenotypes in the Nurr1-overexpressing neural stem cell. *Biochem Biophys Res Commun* **305**, 1040-8.

Kishida, S., Yamamoto, H., Ikeda, S., Kishida, M., Sakamoto, I., Koyama, S. and Kikuchi, A. (1998). Axin, a negative regulator of the wnt signaling pathway, directly interacts with adenomatous polyposis coli and regulates the stabilization of beta-catenin. *J Biol Chem* **273**, 10823-6.

Kitagawa, M., Hatakeyama, S., Shirane, M., Matsumoto, M., Ishida, N., Hattori, K., Nakamichi, I., Kikuchi, A., Nakayama, K. and Nakayama, K. (1999). An F-box protein, FWD1, mediates ubiquitin-dependent proteolysis of beta-catenin. *Embo J* **18**, 2401-10.

Kioussi, C., Briata, P., Baek, S. H., Rose, D. W., Hamblet, N. S., Herman, T., Ohgi, K. A., Lin, C., Gleiberman, A., Wang, J. et al. (2002). Identification of a Wnt/Dvl/beta-Catenin --> Pitx2 pathway mediating cell-type-specific proliferation during development. *Cell* **111**, 673-85.

Kleber, M. and Sommer, L. (2004). Wnt signaling and the regulation of stem cell function. *Curr Opin Cell Biol* **16**, 681-7.**Kohn, A. D. and Moon, R. T.** (2005). Wnt and calcium signaling: beta-catenin-independent pathways. *Cell Calcium* **38**, 439-46.

Korinek, V., Barker, N., Morin, P. J., van Wichen, D., de Weger, R., Kinzler, K. W., Vogelstein, B. and Clevers, H. (1997). Constitutive transcriptional activation by a beta-catenin-Tcf complex in APC-/- colon carcinoma. *Science* **275**, 1784-7.

Korinek, V., Barker, N., Willert, K., Molenaar, M., Roose, J., Wagenaar, G., Markman, M., Lamers, W., Destree, O. and Clevers, H. (1998). Two members of the Tcf family implicated in Wnt/beta-catenin signaling during embryogenesis in the mouse. *Mol Cell Biol* **18**, 1248-56.

Kosuga, M., Takahashi, S., Sasaki, K., Li, X. K., Fujino, M., Hamada, H., Suzuki, S., Yamada, M., Matsuo, N. and Okuyama, T. (2000). Adenovirus-mediated gene therapy for mucopolysaccharidosis VII: involvement of cross-correction in wide-

spread distribution of the gene products and long-term effects of CTLA-4Ig coexpression. *Mol Ther* **1**, 406-13.

Kramer, J., Hegert, C., Guan, K., Wobus, A. M., Muller, P. K. and Rohwedel, J. (2000). Embryonic stem cell-derived chondrogenic differentiation in vitro: activation by BMP-2 and BMP-4. *Mech Dev* **92**, 193-205.

Krupnik, V. E., Sharp, J. D., Jiang, C., Robison, K., Chickering, T. W., Amaravadi, L., Brown, D. E., Guyot, D., Mays, G., Leiby, K. et al. (1999). Functional and structural diversity of the human Dickkopf gene family. *Gene* **238**, 301-13.

Krylova, O., Herreros, J., Cleverley, K. E., Ehler, E., Henriquez, J. P., Hughes, S. M. and Salinas, P. C. (2002). WNT-3, expressed by motoneurons, regulates terminal arborization of neurotrophin-3-responsive spinal sensory neurons. *Neuron* **35**, 1043-56.

Kudoh, T., Wilson, S. W. and Dawid, I. B. (2002). Distinct roles for Fgf, Wnt and retinoic acid in posteriorizing the neural ectoderm. *Development* **129**, 4335-46.

Kudoh, T., Concha, M. L., Houart, C., Dawid, I. B. and Wilson, S. W. (2004). Combinatorial Fgf and Bmp signalling patterns the gastrula ectoderm into prospective neural and epidermal domains. *Development* **131**, 3581-92.

Kuhl, M., Sheldahl, L. C., Malbon, C. C. and Moon, R. T. (2000a). Ca(2+)/calmodulin-dependent protein kinase II is stimulated by Wnt and Frizzled homologs and promotes ventral cell fates in Xenopus. *J Biol Chem* **275**, 12701-11.

Kuhl, M., Sheldahl, L. C., Park, M., Miller, J. R. and Moon, R. T. (2000b). The Wnt/Ca2+ pathway: a new vertebrate Wnt signaling pathway takes shape. *Trends Genet* **16**, 279-83.

Kyba, M., Perlingeiro, R. C. and Daley, G. Q. (2002). HoxB4 confers definitive lymphoid-myeloid engraftment potential on embryonic stem cell and yolk sac hematopoietic progenitors. *Cell* **109**, 29-37.

Kyba, M., Perlingeiro, R. C., Hoover, R. R., Lu, C. W., Pierce, J. and Daley, G. Q. (2003). Enhanced hematopoietic differentiation of embryonic stem cells conditionally expressing Stat5. *Proc Natl Acad Sci U S A* **100 Suppl 1**, 11904-10.

Lake, J., Rathjen, J., Remiszewski, J. and Rathjen, P. D. (2000). Reversible programming of pluripotent cell differentiation. *J Cell Sci* **113 (Pt 3)**, 555-66.

Latres, E., Chiaur, D. S. and Pagano, M. (1999). The human F box protein beta-Trcp associates with the Cul1/Skp1 complex and regulates the stability of beta-catenin. *Oncogene* **18**, 849-54.

Lee, K. J. and Jessell, T. M. (1999). The specification of dorsal cell fates in the vertebrate central nervous system. *Annu Rev Neurosci* **22**, 261-94.

Lee, S. K., Kim, J. H., Lee, Y. C., Cheong, J. and Lee, J. W. (2000a). Silencing mediator of retinoic acid and thyroid hormone receptors, as a novel transcriptional corepressor molecule of activating protein-1, nuclear factor-kappaB, and serum response factor. *J Biol Chem* **275**, 12470-4.

Lee, S. M., Tole, S., Grove, E. and McMahon, A. P. (2000b). A local Wnt-3a signal is required for development of the mammalian hippocampus. *Development* **127**, 457-67.

Lee, S. K. and Pfaff, S. L. (2001). Transcriptional networks regulating neuronal identity in the developing spinal cord. *Nat Neurosci* **4 Suppl**, 1183-91.

Leimeister, C., Bach, A. and Gessler, M. (1998). Developmental expression patterns of mouse sFRP genes encoding members of the secreted frizzled related protein family. *Mech Dev* **75**, 29-42.

Lendahl, U. (1997). Gene regulation in the formation of the central nervous system. *Acta Paediatr Suppl* **422**, 8-11.

Lendahl, U., Zimmerman, L. B. and McKay, R. D. (1990). CNS stem cells express a new class of intermediate filament protein. *Cell* **60**, 585-95.

Leon-Quinto, T., Jones, J., Skoudy, A., Burcin, M. and Soria, B. (2004). In vitro directed differentiation of mouse embryonic stem cells into insulin-producing cells. *Diabetologia* **47**, 1442-51.

Lescher, B., Haenig, B. and Kispert, A. (1998). sFRP-2 is a target of the Wnt-4 signaling pathway in the developing metanephric kidney. *Dev Dyn* **213**, 440-51.

Levers, T. E., Edgar, J. M. and Price, D. J. (2001). The fates of cells generated at the end of neurogenesis in developing mouse cortex. *J Neurobiol* **48**, 265-77.

Lewandoski, M. (2001). Conditional control of gene expression in the mouse. *Nat Rev Genet* **2**, 743-55.

Li, M., Pevny, L., Lovell-Badge, R. and Smith, A. (1998a). Generation of purified neural precursors from embryonic stem cells by lineage selection. *Curr Biol* **8**, 971-4.

Li, W., Cogswell, C. A. and LoTurco, J. J. (1998b). Neuronal differentiation of precursors in the neocortical ventricular zone is triggered by BMP. *J Neurosci* **18**, 8853-62.

Li, L., Yuan, H., Weaver, C. D., Mao, J., Farr, G. H., 3rd, Sussman, D. J., Jonkers, J., Kimelman, D. and Wu, D. (1999). Axin and Frat1 interact with dvl and GSK, bridging Dvl to GSK in Wnt-mediated regulation of LEF-1. *Embo J* **18**, 4233-40.

Lin, K., Wang, S., Julius, M. A., Kitajewski, J., Moos, M., Jr. and Luyten, F. P. (1997). The cysteine-rich frizzled domain of Frzb-1 is required and sufficient for modulation of Wnt signaling. *Proc Natl Acad Sci U S A* **94**, 11196-200.

Lin, X., Buff, E. M., Perrimon, N. and Michelson, A. M. (1999). Heparan sulfate proteoglycans are essential for FGF receptor signaling during Drosophila embryonic development. *Development* **126**, 3715-23.

Lindmark, H., Rosengren, B., Hurt-Camejo, E. and Bruder, C. E. (2004). Gene expression profiling shows that macrophages derived from mouse embryonic stem cells is an improved in vitro model for studies of vascular disease. *Exp Cell Res* **300**, 335-44.

Littlewood, T.D., Hancock, D.C., Danielian, P.S., Parker, M.G. and Evan, G.I. (1995). A modified oestrogen receptor ligand-binding domain as an improved switch for the regulation of hetrologous proteins. *Nuc Acids Res* **23**, 1686-1690.

Liu, X., Liu, T., Slusarski, D. C., Yang-Snyder, J., Malbon, C. C., Moon, R. T. and Wang, H. (1999a). Activation of a frizzled-2/beta-adrenergic receptor chimera promotes Wnt signaling and differentiation of mouse F9 teratocarcinoma cells via Galphao and Galphat. *Proc Natl Acad Sci U S A* **96**, 14383-8.

Liu, P., Wakamiya, M., Shea, M. J., Albrecht, U., Behringer, R. R. and Bradley, A. (1999b). Requirement for Wnt3 in vertebrate axis formation. *Nat Genet* **22**, 361-5.

Liu, S., Qu, Y., Stewart, T. J., Howard, M. J., Chakrabortty, S., Holekamp, T. F. and McDonald, J. W. (2000). Embryonic stem cells differentiate into oligodendrocytes and myelinate in culture and after spinal cord transplantation. *Proc Natl Acad Sci U S A* **97**, 6126-31.

Lloyd, S., Fleming, T. P. and Collins, J. E. (2003). Expression of Wnt genes during mouse preimplantation development. *Gene Expr Patterns* **3**, 309-12.

Loebel, D. A., Watson, C. M., De Young, R. A. and Tam, P. P. (2003). Lineage choice and differentiation in mouse embryos and embryonic stem cells. *Dev Biol* **264**, 1-14.

Logan, C. Y. and Nusse, R. (2004). The Wnt signaling pathway in development and disease. *Annu Rev Cell Dev Biol* **20**, 781-810.

Loonstra, A., Vooijs, M., Beverloo, H. B., Allak, B. A., van Drunen, E., Kanaar, R., Berns, A. and Jonkers, J. (2001). Growth inhibition and DNA damage induced by Cre recombinase in mammalian cells. *Proc Natl Acad Sci U S A* **98**, 9209-14.

Long, J. Z., Lackan, C. S. and Hadjantonakis, A. K. (2005). Genetic and spectrally distinct in vivo imaging: embryonic stem cells and mice with widespread expression of a monomeric red fluorescent protein. *BMC Biotechnol* **5**, 20.

Lucas, F. R. and Salinas, P. C. (1997). WNT-7a induces axonal remodeling and increases synapsin I levels in cerebellar neurons. *Dev Biol* **192**, 31-44.

Lumelsky, N., Blondel, O., Laeng, P., Velasco, I., Ravin, R. and McKay, R. (2001). Differentiation of embryonic stem cells to insulin-secreting structures similar to pancreatic islets. *Science* **292**, 1389-94.

Lustig, B. and Behrens, J. (2003). The Wnt signaling pathway and its role in tumor development. *J Cancer Res Clin Oncol* **129**, 199-221.

Lyuksyutova, A. I., Lu, C. C., Milanesio, N., King, L. A., Guo, N., Wang, Y., Nathans, J., Tessier-Lavigne, M. and Zou, Y. (2003). Anterior-posterior guidance of commissural axons by Wnt-frizzled signaling. *Science* **302**, 1984-8.

Maden, M. (2000). The role of retinoic acid in embryonic and post-embryonic development. *Proc Nutr Soc* **59**, 65-73.

Maden, M. (2001). Role and distribution of retinoic acid during CNS development. *Int Rev Cytol* **209**, 1-77.

Maden, M. (2002). Retinoic acid and limb regeneration--a personal view. *Int J Dev Biol* **46**, 883-6.

MacKay, G. E., Keighren, M. A., Wilson, L., Pratt, T., Flockhart, J. H., Mason, J. O., Price, D. J. and West, J. D. (2005). Evaluation of the mouse TgTP6.3 tauGFP transgene as a lineage marker in chimeras. *J Anat* **206**, 79-92.

Maltsev, V. A., Rohwedel, J., Hescheler, J. and Wobus, A. M. (1993). Embryonic stem cells differentiate in vitro into cardiomyocytes representing sinusnodal, atrial and ventricular cell types. *Mech Dev* **44**, 41-50.

Mangold, O. (1933). Uber die indiktiosfahighkeit der verschiedenen Bezirke der Neurula von Urodelen. *Naturwissenshaften* **21**, 761-766.

Mao, J., Wang, J., Liu, B., Pan, W., Farr, G. H., 3rd, Flynn, C., Yuan, H., Takada, S., Kimelman, D., Li, L. et al. (2001). Low-density lipoprotein receptor-related protein-5 binds to Axin and regulates the canonical Wnt signaling pathway. *Mol Cell* **7**, 801-9.

Mao, B., Wu, W., Davidson, G., Marhold, J., Li, M., Mechler, B. M., Delius, H., Hoppe, D., Stannek, P., Walter, C. et al. (2002). Kremen proteins are Dickkopf receptors that regulate Wnt/beta-catenin signalling. *Nature* **417**, 664-7.

Mao, B. and Niehrs, C. (2003). Kremen2 modulates Dickkopf2 activity during Wnt/LRP6 signaling. *Gene* **302**, 179-83.

Maretto, S., Cordenonsi, M., Dupont, S., Braghetta, P., Broccoli, V., Hassan, A. B., Volpin, D., Bressan, G. M. and Piccolo, S. (2003). Mapping Wnt/beta-catenin signaling during mouse development and in colorectal tumors. *Proc Natl Acad Sci U S A* **100**, 3299-304.

Matz, M. V., Fradkov, A. F., Labas, Y. A., Savitsky, A. P., Zaraisky, A. G., Markelov, M. L. and Lukyanov, S. A. (1999). Fluorescent proteins from nonbioluminescent Anthozoa species. *Nat Biotechnol* **17**, 969-73.

Martin, G. R. (1981). Isolation of a pluripotent cell line from early mouse embryos cultured in medium conditioned by teratocarcinoma stem cells. *Proc Natl Acad Sci U S A* **78**, 7634-8.

Martynoga, B., Morrison, H., Price, D. J. and Mason, J. O. (2005). Foxg1 is required for specification of ventral telencephalon and region-specific regulation of dorsal telencephalic precursor proliferation and apoptosis. *Dev Biol* **283**, 113-27.

Matsuda, T., Nakamura, T., Nakao, K., Arai, T., Katsuki, M., Heike, T. and Yokota, T. (1999). STAT3 activation is sufficient to maintain an undifferentiated state of mouse embryonic stem cells. *Embo J* **18**, 4261-9.

Mayr, T., Deutsch, U., Kuhl, M., Drexler, H. C., Lottspeich, F., Deutzmann, R., Wedlich, D. and Risau, W. (1997). Fritz: a secreted frizzled-related protein that inhibits Wnt activity. *Mech Dev* **63**, 109-25.

McDonald, J. W., Liu, X. Z., Qu, Y., Liu, S., Mickey, S. K., Turetsky, D., Gottlieb, D. I. and Choi, D. W. (1999). Transplanted embryonic stem cells survive, differentiate and promote recovery in injured rat spinal cord. *Nat Med* **5**, 1410-2.

McGrew, L. L., Lai, C. J. and Moon, R. T. (1995). Specification of the anteroposterior neural axis through synergistic interaction of the Wnt signaling cascade with noggin and follistatin. *Dev Biol* **172**, 337-42.

McGrew, L. L., Hoppler, S. and Moon, R. T. (1997). Wnt and FGF pathways cooperatively pattern anteroposterior neural ectoderm in Xenopus. *Mech Dev* **69**, 105-14.

McMahon, A. P. and Bradley, A. (1990). The Wnt-1 (int-1) proto-oncogene is required for development of a large region of the mouse brain. *Cell* **62**, 1073-85.

McMahon, A. P., Gavin, B. J., Parr, B., Bradley, A. and McMahon, J. A. (1992a). The Wnt family of cell signalling molecules in postimplantation development of the mouse. *Ciba Found Symp* **165**, 199-212; discussion 212-8.

McMahon, A. P., Joyner, A. L., Bradley, A. and McMahon, J. A. (1992b). The midbrain-hindbrain phenotype of Wnt-1-/Wnt-1- mice results from stepwise deletion of engrailed-expressing cells by 9.5 days postcoitum. *Cell* **69**, 581-95.

Megason, S. G. and McMahon, A. P. (2002). A mitogen gradient of dorsal midline Wnts organizes growth in the CNS. *Development* **129**, 2087-98.

Melkonyan, H. S., Chang, W. C., Shapiro, J. P., Mahadevappa, M., Fitzpatrick, P. A., Kiefer, M. C., Tomei, L. D. and Umansky, S. R. (1997). SARPs: a family of secreted apoptosis-related proteins. *Proc Natl Acad Sci U S A* **94**, 13636-41.

Merrill, B.J., Pasolli, H.A., Polak, L., Rendl, M., Garcia-Garcia, M.J., Anderson, K.V. and Fuchs. E. (2004). Tcf3: a transcriptional regulator of axis induction in the early embryo.
Development **131**(2):263-74.

Miller, J. R. (2002). The Wnts. *Genome Biol* **3**, REVIEWS3001.

Miller, L. D., Park, K. S., Guo, Q. M., Alkharouf, N. W., Malek, R. L., Lee, N. H., Liu, E. T. and Cheng, S. Y. (2001). Silencing of Wnt signaling and activation of multiple metabolic pathways in response to thyroid hormone-stimulated cell proliferation. *Mol Cell Biol* **21**, 6626-39.

Mitsui, K., Tokuzawa, Y., Itoh, H., Segawa, K., Murakami, M., Takahashi, K., Maruyama, M., Maeda, M. and Yamanaka, S. (2003). The homeoprotein Nanog is required for maintenance of pluripotency in mouse epiblast and ES cells. *Cell* **113**, 631-42.

Miyazaki, J., Takaki, S., Araki, K., Tashiro, F., Tominaga, A., Takatsu, K. and Yamamura, K. (1989). Expression vector system based on the chicken beta-actin promoter directs efficient production of interleukin-5. *Gene* **79**, 269-77.

Mohamed, O. A., Dufort, D. and Clarke, H. J. (2004). Expression and estradiol regulation of Wnt genes in the mouse blastocyst identify a candidate pathway for embryo-maternal signaling at implantation. *Biol Reprod* **71**, 417-24.

Molenaar, M., van de Wetering, M., Oosterwegel, M., Peterson-Maduro, J., Godsave, S., Korinek, V., Roose, J., Destree, O. and Clevers, H. (1996). XTcf-3 transcription factor mediates beta-catenin-induced axis formation in Xenopus embryos. *Cell* **86**, 391-9.

Moon, R. T. and Miller, J. R. (1997). The APC tumor suppressor protein in development and cancer. *Trends Genet* **13**, 256-8.

Moore, K. B. and Moody, S. A. (1999). Animal-vegetal asymmetries influence the earliest steps in retina fate commitment in Xenopus. *Dev Biol* **212**, 25-41.

Morriss-Kay, G. M. and Sokolova, N. (1996). Embryonic development and pattern formation. *Faseb J* **10**, 961-8.

Mukhopadhyay, M., Shtrom, S., Rodriguez-Esteban, C., Chen, L., Tsukui, T., Gomer, L., Dorward, D. W., Glinka, A., Grinberg, A., Huang, S. P. et al. (2001). Dickkopf1 is required for embryonic head induction and limb morphogenesis in the mouse. *Dev Cell* **1**, 423-34.

Mummery, C., Ward, D., van den Brink, C. E., Bird, S. D., Doevendans, P. A., Opthof, T., Brutel de la Riviere, A., Tertoolen, L., van der Heyden, M. and Pera, M. (2002). Cardiomyocyte differentiation of mouse and human embryonic stem cells. *J Anat* **200**, 233-42.

Munemitsu, S., Albert, I., Rubinfeld, B. and Polakis, P. (1996). Deletion of an amino-terminal sequence beta-catenin in vivo and promotes hyperphosporylation of the adenomatous polyposis coli tumor suppressor protein. *Mol Cell Biol* **16**, 4088-94.

Muroyama, Y., Fujihara, M., Ikeya, M., Kondoh, H. and Takada, S. (2002). Wnt signaling plays an essential role in neuronal specification of the dorsal spinal cord. *Genes Dev* **16**, 548-53.

Muroyama, Y., Kondoh, H. and Takada, S. (2004). Wnt proteins promote neuronal differentiation in neural stem cell culture. *Biochem Biophys Res Commun* **313**, 915-21.

Murray, P. and Edgar, D. (2001). The regulation of embryonic stem cell differentiation by leukaemia inhibitory factor (LIF). *Differentiation* **68**, 227-34.

Muzio, L., DiBenedetto, B., Stoykova, A., Boncinelli, E., Gruss, P. and Mallamaci, A. (2002). Conversion of cerebral cortex into basal ganglia in Emx2(-/-) Pax6(Sey/Sey) double-mutant mice. *Nat Neurosci* **5**, 737-45.

Nagy, A., Gocza, E., Diaz, E. M., Prideaux, V. R., Ivanyi, E., Markkula, M. and Rossant, J. (1990). Embryonic stem cells alone are able to support fetal development in the mouse. *Development* **110**, 815-21.

Nagy, A., Rossant, J., Nagy, R., Abramow-Newerly, W. and Roder, J. C. (1993). Derivation of completely cell culture-derived mice from early-passage embryonic stem cells. *Proc Natl Acad Sci U S A* **90**, 8424-8.

Nakashima, K., Takizawa, T., Ochiai, W., Yanagisawa, M., Hisatsune, T., Nakafuku, M., Miyazono, K., Kishimoto, T., Kageyama, R. and Taga, T. (2001). BMP2-mediated alteration in the developmental pathway of fetal mouse brain cells from neurogenesis to astrocytogenesis. *Proc Natl Acad Sci U S A* **98**, 5868-73.

Nakashima, K., Colamarino, S. and Gage, F. H. (2004). Embryonic stem cells: staying plastic on plastic. *Nat Med* **10**, 23-4.

Nasevicius, A., Hyatt, T. M., Hermanson, S. B. and Ekker, S. C. (2000). Sequence, expression, and location of zebrafish frizzled 10. *Mech Dev* **92**, 311-4.

Nichols, J., Zevnik, B., Anastassiadis, K., Niwa, H., Klewe-Nebenius, D., Chambers, I., Scholer, H. and Smith, A. (1998). Formation of pluripotent stem cells in the mammalian embryo depends on the POU transcription factor Oct4. *Cell* **95**, 379-91.

Niehrs, C. (1999). Head in the WNT: the molecular nature of Spemann's head organizer. *Trends Genet* **15**, 314-9.

Nieuwkoop, P.D., Botternenbrood, E.C., Kremer, A., Bloesma, F.F.S.N., Hoessels, E.L.M.J., Meyer, G. and Verheyen, F.J. (1952). Activation and organization of the central nervous system in amphibians. *J. Exp. Zool.* **120**, 1-108.

Nitta, Y., Kawamoto, S., Halbert, C., Iwata, A., Miller, A. D., Miyazaki, J. and Allen, M. D. (2005). A CMV-actin-globin hybrid promoter improves adeno-associated viral vector gene expression in the arterial wall in vivo. *J Gene Med* **7**, 1348-55.

Niwa, H., Yamamura, K. and Miyazaki, J. (1991). Efficient selection for high-expression transfectants with a novel eukaryotic vector. *Gene* **108**, 193-9.

Niwa, H., Burdon, T., Chambers, I. and Smith, A. (1998). Self-renewal of pluripotent embryonic stem cells is mediated via activation of STAT3. *Genes Dev* **12**, 2048-60.

Niwa, H., Miyazaki, J. and Smith, A. G. (2000). Quantitative expression of Oct-3/4 defines differentiation, dedifferentiation or self-renewal of ES cells. *Nat Genet* **24**, 372-6.

Niwa, H. (2001). Molecular mechanism to maintain stem cell renewal of ES cells. *Cell Struct Funct* **26**, 137-48.

Nornes, H. O. and Carry, M. (1978). Neurogenesis in spinal cord of mouse: an autoradiographic analysis. *Brain Res* **159**, 1-6.

Novitch, B. G., Wichterle, H., Jessell, T. M. and Sockanathan, S. (2003). A requirement for retinoic acid-mediated transcriptional activation in ventral neural patterning and motor neuron specification. *Neuron* **40**, 81-95.

Nusse, R. and Varmus, H. E. (1982). Many tumors induced by the mouse mammary tumor virus contain a provirus integrated in the same region of the host genome. *Cell* **31**, 99-109.

O'Gorman, S., Fox, D. T. and Wahl, G. M. (1991). Recombinase-mediated gene activation and site-specific integration in mammalian cells. *Science* **251**, 1351-5.

Ohtsuka, T., Ishibashi, M., Gradwohl, G., Nakanishi, S., Guillemot, F. and Kageyama, R. (1999). Hes1 and Hes5 as notch effectors in mammalian neuronal differentiation. *Embo J* **18**, 2196-207.

Ohtsuka, T., Sakamoto, M., Guillemot, F. and Kageyama, R. (2001). Roles of the basic helix-loop-helix genes Hes1 and Hes5 in expansion of neural stem cells of the developing brain. *J Biol Chem* **276**, 30467-74.

Okabe, S., Forsberg-Nilsson, K., Spiro, A. C., Segal, M. and McKay, R. D. (1996). Development of neuronal precursor cells and functional postmitotic neurons from embryonic stem cells in vitro. *Mech Dev* **59**, 89-102.

O'Shea, K. S. (2001). Neuronal differentiation of mouse embryonic stem cells: lineage selection and forced differentiation paradigms. *Blood Cells Mol Dis* **27**, 705-12.

Otero, J. J., Fu, W., Kan, L., Cuadra, A. E. and Kessler, J. A. (2004). Beta-catenin signaling is required for neural differentiation of embryonic stem cells. *Development* **131**, 3545-57.

Ovitt, C. E. and Scholer, H. R. (1998). The molecular biology of Oct-4 in the early mouse embryo. *Mol Hum Reprod* **4**, 1021-31.

Pan, G. J., Chang, Z. Y., Scholer, H. R. and Pei, D. (2002). Stem cell pluripotency and transcription factor Oct4. *Cell Res* **12**, 321-9.

Pandur, P., Maurus, D. and Kuhl, M. (2002). Increasingly complex: new players enter the Wnt signaling network. *Bioessays* **24**, 881-4.

Panhuysen, M., Vogt Weisenhorn, D. M., Blanquet, V., Brodski, C., Heinzmann, U., Beisker, W. and Wurst, W. (2004). Effects of Wnt1 signaling on proliferation in the developing mid-/hindbrain region. *Mol Cell Neurosci* **26**, 101-11.

Parr, B. A., Shea, M. J., Vassileva, G. and McMahon, A. P. (1993). Mouse Wnt genes exhibit discrete domains of expression in the early embryonic CNS and limb buds. *Development* **119**, 247-61.

Parr, B. A. and McMahon, A. P. (1994). Wnt genes and vertebrate development. *Curr Opin Genet Dev* **4**, 523-8.

Patapoutian, A. and Reichardt, L. F. (2000). Roles of Wnt proteins in neural development and maintenance. *Curr Opin Neurobiol* **10**, 392-9.

Pelton, T. A., Sharma, S., Schulz, T. C., Rathjen, J. and Rathjen, P. D. (2002). Transient pluripotent cell populations during primitive ectoderm formation: correlation of in vivo and in vitro pluripotent cell development. *J Cell Sci* **115**, 329-39.

Pearce, J. J., Penny, G. and Rossant, J. (1999). A mouse cerberus/Dan-related gene family. *Dev Biol* **209**, 98-110.

Pesce, M., Anastassiadis, K. and Scholer, H. R. (1999). Oct-4: lessons of totipotency from embryonic stem cells. *Cells Tissues Organs* **165**, 144-52.

Pesce, M. and Scholer, H. R. (2000). Oct-4: control of totipotency and germline determination. *Mol Reprod Dev* **55**, 452-7.

Pesce, M. and Scholer, H. R. (2001). Oct-4: gatekeeper in the beginnings of mammalian development. *Stem Cells* **19**, 271-8.

Pevny, L.H., Sockanathan, S., Placzek, M. and Lovell-Badge, R. (1998). A role for SOX1 in neural determination. *Development* **125**(10):1967-78.

Phillips, B. W., Belmonte, N., Vernochet, C., Ailhaud, G. and Dani, C. (2001). Compactin enhances osteogenesis in murine embryonic stem cells. *Biochem Biophys Res Commun* **284**, 478-84.

Pinson, K. I., Brennan, J., Monkley, S., Avery, B. J. and Skarnes, W. C. (2000). An LDL-receptor-related protein mediates Wnt signalling in mice. *Nature* **407**, 535-8.

Plachta, N., Bibel, M., Tucker, K. L. and Barde, Y. A. (2004). Developmental potential of defined neural progenitors derived from mouse embryonic stem cells. *Development* **131**, 5449-56.

Pleasure, S. J. and Lee, V. M. (1993). NTera 2 cells: a human cell line which displays characteristics expected of a human committed neuronal progenitor cell. *J Neurosci Res* **35**, 585-602.

Pleasure, S. J., Page, C. and Lee, V. M. (1992). Pure, postmitotic, polarized human neurons derived from NTera 2 cells provide a system for expressing exogenous proteins in terminally differentiated neurons. *J Neurosci* **12**, 1802-15.

Popperl, H., Schmidt, C., Wilson, V., Hume, C. R., Dodd, J., Krumlauf, R. and Beddington, R. S. (1997). Misexpression of Cwnt8C in the mouse induces an ectopic embryonic axis and causes a truncation of the anterior neuroectoderm. *Development* **124**, 2997-3005.

Pownall, M. E., Isaacs, H. V. and Slack, J. M. (1998). Two phases of Hox gene regulation during early Xenopus development. *Curr Biol* **8**, 673-6.

Pratt, T., Quinn, J. C., Simpson, T. I., West, J. D., Mason, J. O. and Price, D. J. (2002). Disruption of early events in thalamocortical tract formation in mice lacking the transcription factors Pax6 or Foxg1. *J Neurosci* **22**, 8523-31.

Prelle, K., Vassiliev, I. M., Vassilieva, S. G., Wolf, E. and Wobus, A. M. (1999). Establishment of pluripotent cell lines from vertebrate species--present status and future prospects. *Cells Tissues Organs* **165**, 220-36.

Qian, X., Shen, Q., Goderie, S. K., He, W., Capela, A., Davis, A. A. and Temple, S. (2000). Timing of CNS cell generation: a programmed sequence of neuron and glial cell production from isolated murine cortical stem cells. *Neuron* **28**, 69-80.

Rallu, M., Machold, R., Gaiano, N., Corbin, J. G., McMahon, A. P. and Fishell, G. (2002). Dorsoventral patterning is established in the telencephalon of mutants lacking both Gli3 and Hedgehog signaling. *Development* **129**, 4963-74.

Rathjen, J., Lake, J. A., Bettess, M. D., Washington, J. M., Chapman, G. and Rathjen, P. D. (1999). Formation of a primitive ectoderm like cell population, EPL cells, from ES cells in response to biologically derived factors. *J Cell Sci* **112 (Pt 5)**, 601-12.

Rathjen, J. and Rathjen, P. D. (2002). Formation of neural precursor cell populations by differentiation of embryonic stem cells in vitro. *ScientificWorldJournal* **2**, 690-700.

Rathjen, J., Haines, B. P., Hudson, K. M., Nesci, A., Dunn, S. and Rathjen, P. D. (2002). Directed differentiation of pluripotent cells to neural lineages: homogeneous formation and differentiation of a neurectoderm population. *Development* **129**, 2649-61.

Reichsman, F., Smith, L. and Cumberledge, S. (1996). Glycosaminoglycans can modulate extracellular localization of the wingless protein and promote signal transduction. *J Cell Biol* **135**, 819-27.

Renoncourt, Y., Carroll, P., Filippi, P., Arce, V. and Alonso, S. (1998). Neurons derived in vitro from ES cells express homeoproteins characteristic of motoneurons and interneurons. *Mech Dev* **79**, 185-97.

Resnick, J. L., Bixler, L. S., Cheng, L. and Donovan, P. J. (1992). Long-term proliferation of mouse primordial germ cells in culture. *Nature* **359**, 550-1.

Reya, T. (2003). Regulation of hematopoietic stem cell self-renewal. *Recent Prog Horm Res* **58**, 283-95.

Reynolds, B. A. and Weiss, S. (1992). Generation of neurons and astrocytes from isolated cells of the adult mammalian central nervous system. *Science* **255**, 1707-10.

Ridgeway, A. G., Wilton, S. and Skerjanc, I. S. (2000). Myocyte enhancer factor 2C and myogenin up-regulate each other's expression and induce the development of skeletal muscle in P19 cells. *J Biol Chem* **275**, 41-6.

Ringrose, L., Lounnas, V., Ehrlich, L., Buchholz, F., Wade, R. and Stewart, A. F. (1998). Comparative kinetic analysis of FLP and cre recombinases: mathematical models for DNA binding and recombination. *J Mol Biol* **284**, 363-84.

Robb, L. and Begley, C. G. (1996). The helix-loop-helix gene SCL: implicated in T-cell acute lymphoblastic leukaemia and in normal haematopoietic development. *Int J Biochem Cell Biol* **28**, 609-18.

Rodda, S. J., Kavanagh, S. J., Rathjen, J. and Rathjen, P. D. (2002). Embryonic stem cell differentiation and the analysis of mammalian development. *Int J Dev Biol* **46**, 449-58.

Roelink, H. and Nusse, R. (1991). Expression of two members of the Wnt family during mouse development--restricted temporal and spatial patterns in the developing neural tube. *Genes Dev* **5**, 381-8.

Roelink, H., Porter, J. A., Chiang, C., Tanabe, Y., Chang, D. T., Beachy, P. A. and Jessell, T. M. (1995). Floor plate and motor neuron induction by different concentrations of the amino-terminal cleavage product of sonic hedgehog autoproteolysis. *Cell* **81**, 445-55.

Rohwedel, J., Maltsev, V., Bober, E., Arnold, H. H., Hescheler, J. and Wobus, A. M. (1994). Muscle cell differentiation of embryonic stem cells reflects myogenesis in vivo: developmentally regulated expression of myogenic determination genes and functional expression of ionic currents. *Dev Biol* **164**, 87-101.

Rohwedel, J., Guan, K., Zuschratter, W., Jin, S., Ahnert-Hilger, G., Furst, D., Fassler, R. and Wobus, A. M. (1998a). Loss of beta1 integrin function results in a retardation of myogenic, but an acceleration of neuronal, differentiation of embryonic stem cells in vitro. *Dev Biol* **201**, 167-84.

Rohwedel, J., Kleppisch, T., Pich, U., Guan, K., Jin, S., Zuschratter, W., Hopf, C., Hoch, W., Hescheler, J., Witzemann, V. et al. (1998b). Formation of postsynaptic-like

membranes during differentiation of embryonic stem cells in vitro. *Exp Cell Res* **239**, 214-25.

Rohwedel, J., Guan, K. and Wobus, A. M. (1999). Induction of cellular differentiation by retinoic acid in vitro. *Cells Tissues Organs* **165**, 190-202.

Rohwedel, J., Guan, K., Hegert, C. and Wobus, A. M. (2001). Embryonic stem cells as an in vitro model for mutagenicity, cytotoxicity and embryotoxicity studies: present state and future prospects. *Toxicol In Vitro* **15**, 741-53.

Rossant, J., Ciruna, B. and Partanen, J. (1997). FGF signaling in mouse gastrulation and anteroposterior patterning. *Cold Spring Harb Symp Quant Biol* **62**, 127-33.

Rossant, J. and McKerlie, C. (2001). Mouse-based phenogenomics for modelling human disease. *Trends Mol Med* **7**, 502-7.

Rossant, J. and Tam, P. P. (2004). Emerging asymmetry and embryonic patterning in early mouse development. *Dev Cell* **7**, 155-64.

Sacchetti, A., El Sewedy, T., Nasr, A. F. and Alberti, S. (2001). Efficient GFP mutations profoundly affect mRNA transcription and translation rates. *FEBS Lett* **492**, 151-5.

Saint-Jeannet, J. P., He, X., Varmus, H. E. and Dawid, I. B. (1997). Regulation of dorsal fate in the neuraxis by Wnt-1 and Wnt-3a. *Proc Natl Acad Sci U S A* **94**, 13713-8.

Salic, A., Lee, E., Mayer, L. and Kirschner, M. W. (2000). Control of beta-catenin stability: reconstitution of the cytoplasmic steps of the wnt pathway in Xenopus egg extracts. *Mol Cell* **5**, 523-32.

Salinas, P. C. and Nusse, R. (1992). Regional expression of the Wnt-3 gene in the developing mouse forebrain in relationship to diencephalic neuromeres. *Mech Dev* **39**, 151-60.

Sato, N., Meijer, L., Skaltsounis, L., Greengard, P. and Brivanlou, A. H. (2004). Maintenance of pluripotency in human and mouse embryonic stem cells through activation of Wnt signaling by a pharmacological GSK-3-specific inhibitor. *Nat Med* **10**, 55-63.

Sauer, B. and Henderson, N. (1989). Cre-stimulated recombination at loxP-containing DNA sequences placed into the mammalian genome. *Nucleic Acids Res* **17**, 147-61.

Scholer, H. R., Hatzopoulos, A. K., Balling, R., Suzuki, N. and Gruss, P. (1989). A family of octamer-specific proteins present during mouse embryogenesis: evidence for germline-specific expression of an Oct factor. *Embo J* **8**, 2543-50.

Scholer, H. R., Dressler, G. R., Balling, R., Rohdewohld, H. and Gruss, P. (1990). Oct-4: a germline-specific transcription factor mapping to the mouse t-complex. *Embo J* **9**, 2185-95.

Scholer, H. R., Ciesiolka, T. and Gruss, P. (1991). A nexus between Oct-4 and E1A: implications for gene regulation in embryonic stem cells. *Cell* **66**, 291-304.

Schmidt, M. M., Guan, K. and Wobus, A. M. (2001). Lithium influences differentiation and tissue-specific gene expression of mouse embryonic stem (ES) cells in vitro. *Int J Dev Biol* **45**, 421-9.

Schulte, G., Bryja, V., Rawal, N., Castelo-Branco, G., Sousa, K. M. and Arenas, E. (2005). Purified Wnt-5a increases differentiation of midbrain dopaminergic cells and dishevelled phosphorylation. *J Neurochem* **92**, 1550-3.

Schuurmans, C., Armant, O., Nieto, M., Stenman, J. M., Britz, O., Klenin, N., Brown, C., Langevin, L. M., Seibt, J., Tang, H. et al. (2004). Sequential phases of cortical specification involve Neurogenin-dependent and -independent pathways. *Embo J* **23**, 2892-902.

Seidensticker, M. J. and Behrens, J. (2000). Biochemical interactions in the wnt pathway. *Biochim Biophys Acta* **1495**, 168-82.

Sejersen, T. and Lendahl, U. (1993). Transient expression of the intermediate filament nestin during skeletal muscle development. *J Cell Sci* **106 (Pt 4)**, 1291-300.

Semenov, M. V., Tamai, K., Brott, B. K., Kuhl, M., Sokol, S. and He, X. (2001). Head inducer Dickkopf-1 is a ligand for Wnt coreceptor LRP6. *Curr Biol* **11**, 951-61.

Shariatmadari, M., Peyronnet, J., Papachristou, P., Horn, Z., Sousa, K. M., Arenas, E. and Ringstedt, T. (2005). Increased Wnt levels in the neural tube impair the function of adherens junctions during neurulation. *Mol Cell Neurosci* **30**, 437-51.

Sheldahl, L. C., Park, M., Malbon, C. C. and Moon, R. T. (1999). Protein kinase C is differentially stimulated by Wnt and Frizzled homologs in a G-protein-dependent manner. *Curr Biol* **9**, 695-8.

Sheldahl, L. C., Slusarski, D. C., Pandur, P., Miller, J. R., Kuhl, M. and Moon, R. T. (2003). Dishevelled activates Ca2+ flux, PKC, and CamKII in vertebrate embryos. *J Cell Biol* **161**, 769-77.

Shen, M. M. and Leder, P. (1992). Leukemia inhibitory factor is expressed by the preimplantation uterus and selectively blocks primitive ectoderm formation in vitro. *Proc Natl Acad Sci U S A* **89**, 8240-4.

Shibamoto, S., Higano, K., Takada, R., Ito, F., Takeichi, M. and Takada, S. (1998). Cytoskeletal reorganization by soluble Wnt-3a protein signalling. *Genes Cells* **3**, 659-70.

Shibata, M., Ono, H., Hikasa, H., Shinga, J. and Taira, M. (2000). Xenopus crescent encoding a Frizzled-like domain is expressed in the Spemann organizer and pronephros. *Mech Dev* **96**, 243-6.

Shimizu, H., Julius, M. A., Giarre, M., Zheng, Z., Brown, A. M. and Kitajewski, J. (1997). Transformation by Wnt family proteins correlates with regulation of beta-catenin. *Cell Growth Differ* **8**, 1349-58.

Shinya, M., Eschbach, C., Clark, M., Lehrach, H. and Furutani-Seiki, M. (2000). Zebrafish Dkk1, induced by the pre-MBT Wnt signaling, is secreted from the prechordal plate and patterns the anterior neural plate. *Mech Dev* **98**, 3-17.

Shou, J., Ali-Osman, F., Multani, A. S., Pathak, S., Fedi, P. and Srivenugopal, K. S. (2002). Human Dkk-1, a gene encoding a Wnt antagonist, responds to DNA damage and its overexpression sensitizes brain tumor cells to apoptosis following alkylation damage of DNA. *Oncogene* **21**, 878-89.

Slusarski, D. C., Corces, V. G. and Moon, R. T. (1997). Interaction of Wnt and a Frizzled homologue triggers G-protein-linked phosphatidylinositol signalling. *Nature* **390**, 410-3.

Smith, A. (1998). Cell therapy: in search of pluripotency. *Curr Biol* **8**, R802-4.

Smith, A. G. (2001). Embryo-derived stem cells: of mice and men. *Annu Rev Cell Dev Biol* **17**, 435-62.

Smith, E. M. and Blalock, J. E. (1988). A molecular basis for interactions between the immune and neuroendocrine systems. *Int J Neurosci* **38**, 455-64.

Smith, D. K. and Treutlein, H. R. (1998). LIF receptor-gp130 interaction investigated by homology modeling: implications for LIF binding. *Protein Sci* **7**, 886-96.

Smith, A. G., Heath, J. K., Donaldson, D. D., Wong, G. G., Moreau, J., Stahl, M. and Rogers, D. (1988). Inhibition of pluripotential embryonic stem cell differentiation by purified polypeptides. *Nature* **336**, 688-90.

Solter, D. and Knowles, B. B. (1978). Monoclonal antibody defining a stage-specific mouse embryonic antigen (SSEA-1). *Proc Natl Acad Sci U S A* **75**, 5565-9.

Songyang, Z., Fanning, A. S., Fu, C., Xu, J., Marfatia, S. M., Chishti, A. H., Crompton, A., Chan, A. C., Anderson, J. M. and Cantley, L. C. (1997). Recognition of unique carboxyl-terminal motifs by distinct PDZ domains. *Science* **275**, 73-7.

Soria, B. (2001). In-vitro differentiation of pancreatic beta-cells. *Differentiation* **68**, 205-19.

Spemann, H. and Mangold, H. (1924). Uber Induktion von Embryonalanlagen durch Implantation artfremder Organisatoren. Roux's Arch. *EntwMech. Org.* **100**, 599-638.

Srinivas, S., Watanabe, T., Lin, C. S., William, C. M., Tanabe, Y., Jessell, T. M. and Costantini, F. (2001). Cre reporter strains produced by targeted insertion of EYFP and ECFP into the ROSA26 locus. *BMC Dev Biol* **1**, 4.

St-Arnaud, R., Craig, J., McBurney, M. W. and Papkoff, J. (1989). The int-1 proto-oncogene is transcriptionally activated during neuroectodermal differentiation of P19 mouse embryonal carcinoma cells. *Oncogene* **4**, 1077-80.

Stavridis, M. P. and Smith, A. G. (2003). Neural differentiation of mouse embryonic stem cells. *Biochem Soc Trans* **31**, 45-9.

Stern, C. D. (2005). Neural induction: old problem, new findings, yet more questions. *Development* **132**, 2007-21.

Stewart, C. L. (1994). The role of leukemia inhibitory factor (LIF) and other cytokines in regulating implantation in mammals. *Ann N Y Acad Sci* **734**, 157-65.

Srinivas, S., Watanabe, T., Lin, C.S., William, C.M., Tanabe, Y., Jessell, T.M. and Costantini, F. (2001). Cre reporter strains produced by targeted insertion of EYFP and ECFP into the ROSA26 locus. *BMC Dev Biol* **1**:4. Epub Mar 27. 2001.

Stavridis, M.P. and Smith, A.G. (2003). Neural differentiation of mouse embryonic stem cells. *Biochem Soc Trans* **31**(Pt 1):45-9.

Stern, C. D. (2001). Initial patterning of the central nervous system: how many organizers? *Nat Rev Neurosci* **2**, 92-8.

Stern, C.D. (2004). The chick embryo--past, present and future as a model system in developmental biology. *Mech Dev.* 121(9),1011-3.

Stern, C.D. (2005). Neural induction: old problem, new findings, yet more questions. *Develop* **132**(9), 2007-21.

Stewart, C. L., Kaspar, P., Brunet, L. J., Bhatt, H., Gadi, I., Kontgen, F. and Abbondanzo, S. J. (1992). Blastocyst implantation depends on maternal expression of leukaemia inhibitory factor. *Nature* **359**, 76-9.

Strubing, C., Ahnert-Hilger, G., Shan, J., Wiedenmann, B., Hescheler, J. and Wobus, A. M. (1995). Differentiation of pluripotent embryonic stem cells into the neuronal lineage in vitro gives rise to mature inhibitory and excitatory neurons. *Mech Dev* **53**, 275-87.

Suda, J., Suda, T. and Ogawa, M. (1984). Analysis of differentiation of mouse hemopoietic stem cells in culture by sequential replating of paired progenitors. *Blood* **64**, 393-9.

Suda, Y., Suzuki, M., Ikawa, Y. and Aizawa, S. (1987). Mouse embryonic stem cells exhibit indefinite proliferative potential. *J Cell Physiol* **133**, 197-201.

Sumanas, S., Strege, P., Heasman, J. and Ekker, S. C. (2000). The putative wnt receptor Xenopus frizzled-7 functions upstream of beta-catenin in vertebrate dorsoventral mesoderm patterning. *Development* **127**, 1981-90.

Tago, K., Nakamura, T., Nishita, M., Hyodo, J., Nagai, S., Murata, Y., Adachi, S., Ohwada, S., Morishita, Y., Shibuya, H. et al. (2000). Inhibition of Wnt signaling by ICAT, a novel beta-catenin-interacting protein. *Genes Dev* **14**, 1741-9.

Takada, S., Stark, K. L., Shea, M. J., Vassileva, G., McMahon, J. A. and McMahon, A. P. (1994). Wnt-3a regulates somite and tailbud formation in the mouse embryo. *Genes Dev* **8**, 174-89.

Takemaru, K. I. and Moon, R. T. (2000). The transcriptional coactivator CBP interacts with beta-catenin to activate gene expression. *J Cell Biol* **149**, 249-54.

Takemaru, K., Yamaguchi, S., Lee, Y. S., Zhang, Y., Carthew, R. W. and Moon, R. T. (2003). Chibby, a nuclear beta-catenin-associated antagonist of the Wnt/Wingless pathway. *Nature* **422**, 905-9.

Tam, P. P. and Behringer, R. R. (1997). Mouse gastrulation: the formation of a mammalian body plan. *Mech Dev* **68**, 3-25.

Tam, P. P. and Steiner, K. A. (1999). Anterior patterning by synergistic activity of the early gastrula organizer and the anterior germ layer tissues of the mouse embryo. *Development* **126**, 5171-9.

Tam, P. P., Williams, E. A. and Chan, W. Y. (1993). Gastrulation in the mouse embryo: ultrastructural and molecular aspects of germ layer morphogenesis. *Microsc Res Tech* **26**, 301-28.

Tamai, K., Semenov, M., Kato, Y., Spokony, R., Liu, C., Katsuyama, Y., Hess, F., Saint-Jeannet, J. P. and He, X. (2000). LDL-receptor-related proteins in Wnt signal transduction. *Nature* **407**, 530-5.

Tanabe, Y. and Jessell, T. M. (1996). Diversity and pattern in the developing spinal cord. *Science* **274**, 1115-23.

Tanabe, Y., Roelink, H. and Jessell, T. M. (1995). Induction of motor neurons by Sonic hedgehog is independent of floor plate differentiation. *Curr Biol* **5**, 651-8.

Tamai, K., Zeng, X., Liu, C., Zhang, X., Harada, Y., Chang, Z. and He, X. (2004). A mechanism for Wnt coreceptor activation. *Mol Cell* **13**, 149-56.

Terskikh, A. V., Fradkov, A. F., Zaraisky, A. G., Kajava, A. V. and Angres, B. (2002). Analysis of DsRed Mutants. Space around the fluorophore accelerates fluorescence development. *J Biol Chem* **277**, 7633-6.

Temple, S. (2003). Embryonic stem cell self-renewal, analyzed. *Cell* **115**, 247-8.

Thomas, K. R. and Capecchi, M. R. (1990). Targeted disruption of the murine int-1 proto-oncogene resulting in severe abnormalities in midbrain and cerebellar development. *Nature* **346**, 847-50.

Thomas, P., Brickman, J. M., Popperl, H., Krumlauf, R. and Beddington, R. S. (1997). Axis duplication and anterior identity in the mouse embryo. *Cold Spring Harb Symp Quant Biol* **62**, 115-25.

Thomson, J. A., Marshall, V. S. and Trojanowski, J. Q. (1998). Neural differentiation of rhesus embryonic stem cells. *Apmis* **106**, 149-56; discussion 156-7.

Tolwinski, N. S. and Wieschaus, E. (2004). Rethinking WNT signaling. *Trends Genet* **20**, 177-81.

Tropepe, V., Hitoshi, S., Sirard, C., Mak, T. W., Rossant, J. and van der Kooy, D. (2001). Direct neural fate specification from embryonic stem cells: a primitive mammalian neural stem cell stage acquired through a default mechanism. *Neuron* **30**, 65-78.

Tropepe, V., Li, S., Dickinson, A., Gamse, J. T. and Sive, H. L. (2006). Identification of a BMP inhibitor-responsive promoter module required for expression of the early neural gene zic1. *Dev Biol* **289**, 517-29.

Tsai, M., Wedemeyer, J., Ganiatsas, S., Tam, S. Y., Zon, L. I. and Galli, S. J. (2000). In vivo immunological function of mast cells derived from embryonic stem cells: an approach for the rapid analysis of even embryonic lethal mutations in adult mice in vivo. *Proc Natl Acad Sci U S A* **97**, 9186-90.

Uren, A., Reichsman, F., Anest, V., Taylor, W. G., Muraiso, K., Bottaro, D. P., Cumberledge, S. and Rubin, J. S. (2000). Secreted frizzled-related protein-1 binds

directly to Wingless and is a biphasic modulator of Wnt signaling. *J Biol Chem* **275**, 4374-82.

Vallier, L., Mancip, J., Markossian, S., Lukaszewicz, A., Dehay, C., Metzger, D., Chambon, P., Samarut, J. and Savatier, P. (2001). An efficient system for conditional gene expression in embryonic stem cells and in their in vitro and in vivo differentiated derivatives. *Proc Natl Acad Sci U S A* **98**, 2467-72.

van de Wetering, M., Cavallo, R., Dooijes, D., van Beest, M., van Es, J., Loureiro, J., Ypma, A., Hursh, D., Jones, T., Bejsovec, A. et al. (1997). Armadillo coactivates transcription driven by the product of the Drosophila segment polarity gene dTCF. *Cell* **88**, 789-99.

Van der Weyden, L., Adams, D.J. and Bradley, L. (2002). Tools for targeted manipulation of the mouse genome. *Physiol Genomics* **11**, 133-164.

van Es, J. H., Barker, N. and Clevers, H. (2003). You Wnt some, you lose some: oncogenes in the Wnt signaling pathway. *Curr Opin Genet Dev* **13**, 28-33.

van Leeuwen, F., Samos, C. H. and Nusse, R. (1994). Biological activity of soluble wingless protein in cultured Drosophila imaginal disc cells. *Nature* **368**, 342-4.

Veeman, M. T., Slusarski, D. C., Kaykas, A., Louie, S. H. and Moon, R. T. (2003). Zebrafish prickle, a modulator of noncanonical Wnt/Fz signaling, regulates gastrulation movements. *Curr Biol* **13**, 680-5.

Verkhusha, V. V., Akovbian, N. A., Efremenko, E. N., Varfolomeyev, S. D. and Vrzheshch, P. V. (2001a). Kinetic analysis of maturation and denaturation of DsRed, a coral-derived red fluorescent protein. *Biochemistry (Mosc)* **66**, 1342-51.

Verkhusha, V. V., Otsuna, H., Awasaki, T., Oda, H., Tsukita, S. and Ito, K. (2001b). An enhanced mutant of red fluorescent protein DsRed for double labeling and developmental timer of neural fiber bundle formation. *J Biol Chem* **276**, 29621-4.

Viti, J., Gulacsi, A. and Lillien, L. (2003). Wnt regulation of progenitor maturation in the cortex depends on Shh or fibroblast growth factor 2. *J Neurosci* **23**, 5919-27.

Wallingford, J. B., Rowning, B. A., Vogeli, K. M., Rothbacher, U., Fraser, S. E. and Harland, R. M. (2000). Dishevelled controls cell polarity during Xenopus gastrulation. *Nature* **405**, 81-5.

Wallingford, J. B. and Harland, R. M. (2001). Xenopus Dishevelled signaling regulates both neural and mesodermal convergent extension: parallel forces elongating the body axis. *Development* **128**, 2581-92.

Walther, C. and Gruss, P. (1991). Pax-6, a murine paired box gene, is expressed in the developing CNS. *Development* **113**, 1435-49.

Wang, J. and Wynshaw-Boris, A. (2004). The canonical Wnt pathway in early mammalian embryogenesis and stem cell maintenance/differentiation. *Curr Opin Genet Dev* **14**, 533-9.

Wang, Q. T., Piotrowska, K., Ciemerych, M. A., Milenkovic, L., Scott, M. P., Davis, R. W. and Zernicka-Goetz, M. (2004). A genome-wide study of gene activity reveals developmental signaling pathways in the preimplantation mouse embryo. *Dev Cell* **6**, 133-44.

Watabe, T., Nishihara, A., Mishima, K., Yamashita, J., Shimizu, K., Miyazawa, K., Nishikawa, S. and Miyazono, K. (2003). TGF-beta receptor kinase inhibitor enhances growth and integrity of embryonic stem cell-derived endothelial cells. *J Cell Biol* **163**, 1303-11.

Watanabe, K., Kamiya, D., Nishiyama, A., Katayama, T., Nozaki, S., Kawasaki, H., Watanabe, Y., Mizuseki, K. and Sasai, Y. (2005). Directed differentiation of telencephalic precursors from embryonic stem cells. *Nat Neurosci* **8**, 288-96.

Wehrli, M., Dougan, S. T., Caldwell, K., O'Keefe, L., Schwartz, S., Vaizel-Ohayon, D., Schejter, E., Tomlinson, A. and DiNardo, S. (2000). arrow encodes an LDL-receptor-related protein essential for Wingless signalling. *Nature* **407**, 527-30.

Weiss, M. J. and Orkin, S. H. (1996). In vitro differentiation of murine embryonic stem cells. New approaches to old problems. *J Clin Invest* **97**, 591-5.

Westfall, T. A., Hjertos, B. and Slusarski, D. C. (2003). Requirement for intracellular calcium modulation in zebrafish dorsal-ventral patterning. *Dev Biol* **259**, 380-91.

Whyatt, L. M., Duwel, A., Smith, A. G. and Rathjen, P. D. (1993). The responsiveness of embryonic stem cells to alpha and beta interferons provides the basis of an inducible expression system for analysis of developmental control genes. *Mol Cell Biol* **13**, 7971-6.

Whyatt, L. M. and Rathjen, P. D. (2001). Interferon-inducible ES cell expression systems. *Methods Mol Biol* **158**, 301-18.

Wichterle, H., Lieberam, I., Porter, J. A. and Jessell, T. M. (2002). Directed differentiation of embryonic stem cells into motor neurons. *Cell* **110**, 385-97.

Wiles, M. V. (1993). Embryonic stem cell differentiation in vitro. *Methods Enzymol* **225**, 900-18.

Wilkinson, D. G., Bailes, J. A. and McMahon, A. P. (1987). Expression of the proto-oncogene int-1 is restricted to specific neural cells in the developing mouse embryo. *Cell* **50**, 79-88.

Willert, K., Shibamoto, S. and Nusse, R. (1999). Wnt-induced dephosphorylation of axin releases beta-catenin from the axin complex. *Genes Dev* **13**, 1768-73.

Willert, K., Brown, J. D., Danenberg, E., Duncan, A. W., Weissman, I. L., Reya, T., Yates, J. R., 3rd and Nusse, R. (2003). Wnt proteins are lipid-modified and can act as stem cell growth factors. *Nature* **423**, 448-52.

Wilson, P. A. and Hemmati-Brivanlou, A. (1995). Induction of epidermis and inhibition of neural fate by Bmp-4. *Nature* **376**, 331-3.

Wilson, S. I. and Edlund, T. (2001). Neural induction: toward a unifying mechanism. *Nat Neurosci* **4 Suppl**, 1161-8.

Wilson, S. W. and Houart, C. (2004). Early steps in the development of the forebrain. *Dev Cell* **6**, 167-81.

Wilson, S. I., Rydstrom, A., Trimborn, T., Willert, K., Nusse, R., Jessell, T. M. and Edlund, T. (2001). The status of Wnt signalling regulates neural and epidermal fates in the chick embryo. *Nature* **411**, 325-30.

Winston, J. T., Strack, P., Beer-Romero, P., Chu, C. Y., Elledge, S. J. and Harper, J. W. (1999). The SCFbeta-TRCP-ubiquitin ligase complex associates specifically with phosphorylated destruction motifs in IkappaBalpha and beta-catenin and stimulates IkappaBalpha ubiquitination in vitro. *Genes Dev* **13**, 270-83.

Wobus, A. M. (2001). Potential of embryonic stem cells. *Mol Aspects Med* **22**, 149-64.

Wobus, A. M., Guan, K. and Pich, U. (2001). In vitro differentiation of embryonic stem cells and analysis of cellular phenotypes. *Methods Mol Biol* **158**, 263-86.

Wobus, A. M., Holzhausen, H., Jakel, P. and Schoneich, J. (1984). Characterization of a pluripotent stem cell line derived from a mouse embryo. *Exp Cell Res* **152**, 212-9.

Wobus, A. M., Wallukat, G. and Hescheler, J. (1991). Pluripotent mouse embryonic stem cells are able to differentiate into cardiomyocytes expressing chronotropic responses to adrenergic and cholinergic agents and Ca2+ channel blockers. *Differentiation* **48**, 173-82.

Wobus, A. M., Kaomei, G., Shan, J., Wellner, M. C., Rohwedel, J., Ji, G., Fleischmann, B., Katus, H. A., Hescheler, J. and Franz, W. M. (1997). Retinoic acid accelerates

embryonic stem cell-derived cardiac differentiation and enhances development of ventricular cardiomyocytes. *J Mol Cell Cardiol* **29**, 1525-39.

Wodarz, A. and Nusse, R. (1998). Mechanisms of Wnt signaling in development. *Annu Rev Cell Dev Biol* **14**, 59-88.

Wong, G. T., Gavin, B. J. and McMahon, A. P. (1994). Differential transformation of mammary epithelial cells by Wnt genes. *Mol Cell Biol* **14**, 6278-86.

Wood, H. B. and Episkopou, V. (1999). Comparative expression of the mouse Sox1, Sox2 and Sox3 genes from pre-gastrulation to early somite stages. *Mech Dev* **86**, 197-201.

Yamaguchi, T. P., Takada, S., Yoshikawa, Y., Wu, N. and McMahon, A. P. (1999). T (Brachyury) is a direct target of Wnt3a during paraxial mesoderm specification. *Genes Dev* **13**, 3185-90.

Yamaguchi, T. P. (2001). Heads or tails: Wnts and anterior-posterior patterning. *Curr Biol* **11**, R713-24.

Yamashita, J., Itoh, H., Hirashima, M., Ogawa, M., Nishikawa, S., Yurugi, T., Naito, M., Nakao, K. and Nishikawa, S. (2000). Flk1-positive cells derived from embryonic stem cells serve as vascular progenitors. *Nature* **408**, 92-6.

Yarbrough, D., Wachter, R. M., Kallio, K., Matz, M. V. and Remington, S. J. (2001). Refined crystal structure of DsRed, a red fluorescent protein from coral, at 2.0-A resolution. *Proc Natl Acad Sci U S A* **98**, 462-7.

Yin, Y., Lim, Y. K., Salto-Tellez, M., Ng, S. C., Lin, C. S. and Lim, S. K. (2002). AFP(+), ESC-derived cells engraft and differentiate into hepatocytes in vivo. *Stem Cells* **20**, 338-46.

Ying, Q. L., Nichols, J., Chambers, I. and Smith, A. (2003a). BMP induction of Id proteins suppresses differentiation and sustains embryonic stem cell self-renewal in collaboration with STAT3. *Cell* **115**, 281-92.

Ying, Q. L., Stavridis, M., Griffiths, D., Li, M. and Smith, A. (2003b). Conversion of embryonic stem cells into neuroectodermal precursors in adherent monoculture. *Nat Biotechnol* **21**, 183-6.

Yoshida, K., Chambers, I., Nichols, J., Smith, A., Saito, M., Yasukawa, K., Shoyab, M., Taga, T. and Kishimoto, T. (1994a). Maintenance of the pluripotential phenotype of embryonic stem cells through direct activation of gp130 signalling pathways. *Mech Dev* **45**, 163-71.

Yoshida, T., Toyama-Sorimachi, N., Miyasaka, M. and Lee, Y. C. (1994b). A crucial effect of ligand clustering on the inhibition of binding by L-selectin in intercellular adhesion. *Biochem Biophys Res Commun* **204**, 969-74.

Yoshikawa, S., McKinnon, R. D., Kokel, M. and Thomas, J. B. (2003). Wnt-mediated axon guidance via the Drosophila Derailed receptor. *Nature* **422**, 583-8.

Yost, C., Torres, M., Miller, J. R., Huang, E., Kimelman, D. and Moon, R. T. (1996). The axis-inducing activity, stability, and subcellular distribution of beta-catenin is regulated in Xenopus embryos by glycogen synthase kinase 3. *Genes Dev* **10**, 1443-54.

Zakin, L. D., Mazan, S., Maury, M., Martin, N., Guenet, J. L. and Brulet, P. (1998). Structure and expression of Wnt13, a novel mouse Wnt2 related gene. *Mech Dev* **73**, 107-16.

Zakin, L., Reversade, B., Virlon, B., Rusniok, C., Glaser, P., Elalouf, J. M. and Brulet, P. (2000). Gene expression profiles in normal and Otx2-/- early gastrulating mouse embryos. *Proc Natl Acad Sci U S A* **97**, 14388-93.

Zechner, D., Fujita, Y., Hulsken, J., Muller, T., Walther, I., Taketo, M. M., Crenshaw, E. B., 3rd, Birchmeier, W. and Birchmeier, C. (2003). beta-Catenin signals regulate cell growth and the balance between progenitor cell expansion and differentiation in the nervous system. *Dev Biol* **258**, 406-18.

Zhang, Y., Riesterer, C., Ayrall, A. M., Sablitzky, F., Littlewood, T. D. and Reth, M. (1996). Inducible site-directed recombination in mouse embryonic stem cells. *Nucleic Acids Res* **24**, 543-8.

Zhu, A. J. and Watt, F. M. (1999). beta-catenin signalling modulates proliferative potential of human epidermal keratinocytes independently of intercellular adhesion. *Development* **126**, 2285-98.

Appendix A: List of Antibodies used for Immunoblotting and Immunocytochemistry

*may use different Alexa conjugate from described above, ab = antibody

DSHB = Developmental Studies Hybridoma Bank

Antibody (Company:Catalogue number)	Subtype	Western		Immunocytochemistry (ICC)	
		Primary ab	2° ab	Primary ab	*2° ab
HA-Peroxidase (3F10) (Roche:2013819)	Rat IgG1	1:1000	-	-	-
Mouse Dkk1 (R&D System: AF 1765)	Goat IgG	1:1000	Donkey anti-goat IgG-HRP (1:20,000) (Jackson ImmunoResearch: 705035003)	-	-
Mouse Wnt3a (R&D System: MAB 1324)	Rat IgG2A	1:500	Rabbit anti-rat IgG-HRP (1:750) (DakoCytomation:P0 450)	-	-
Mouse Wnt5a (R&D System: AF 645)	Goat IgG	1:500	Donkey anti-goat IgG-HRP (1:20,000)	1:20	Donkey anti-goat IgG-488 (1:1000)
Mouse Wnt7a (K15) (Santa Cruz Biotechnology:	Goat IgG	1:200	Donkey anti-goat IgG-HRP (1:20,000)	1:50	Donkey anti-goat IgG-488 (1:1000)
HA high afinity (Roche:1867423)	Rat IgG1	1:1000	Rabbit anti-rat IgG-HRP (1:750) (DakoCytomation:P0 450)	1:150	Goat anti-rat IgG-488 (1:1000) (Molecular Probes:A11006)
Class III ß-Tubulin (Sigma:T8660)	Mouse IgG2B	-	-	1:100	Goat anti-mouse IgG2b-488 (1:1000) (Molecular Probes:A21141)
FoxG1	Mouse IgG	1:200			
GFAP (Dakocytomation:	Rabbit IgG	-	-	1:200	Goat anti-rabbit IgG-488 (1:1000) (Molecular Probes:A11008)
Islet (DSHB:)	Mouse IgG1	-	-	1:200	Goat anti-mouse IgG1-488 (1:1000)
Nestin (DSHB:)	Mouse IgG1	-	-	1:50	Goat anti-mouse IgG1-488 (1:1000)
NeuN (4G2) (Abcam:ab13938)	Mouse IgG1	-	-	1:100	Goat anti-mouse IgG1-488 (1:1000)
Pax6 (DSHB:)	Mouse IgG1	-	-	1:75	Goat anti-mouse IgG1-488 (1:1000)
RC2 (DSHB:)	Mouse IgM	-	-	1:100	Goat anti-mouse IgM-546 (1:1000)

Appendix B: Cloning and Subcloning strategies

A) Construction of *Wnt1*-HA/pCAG-floxed-neopA

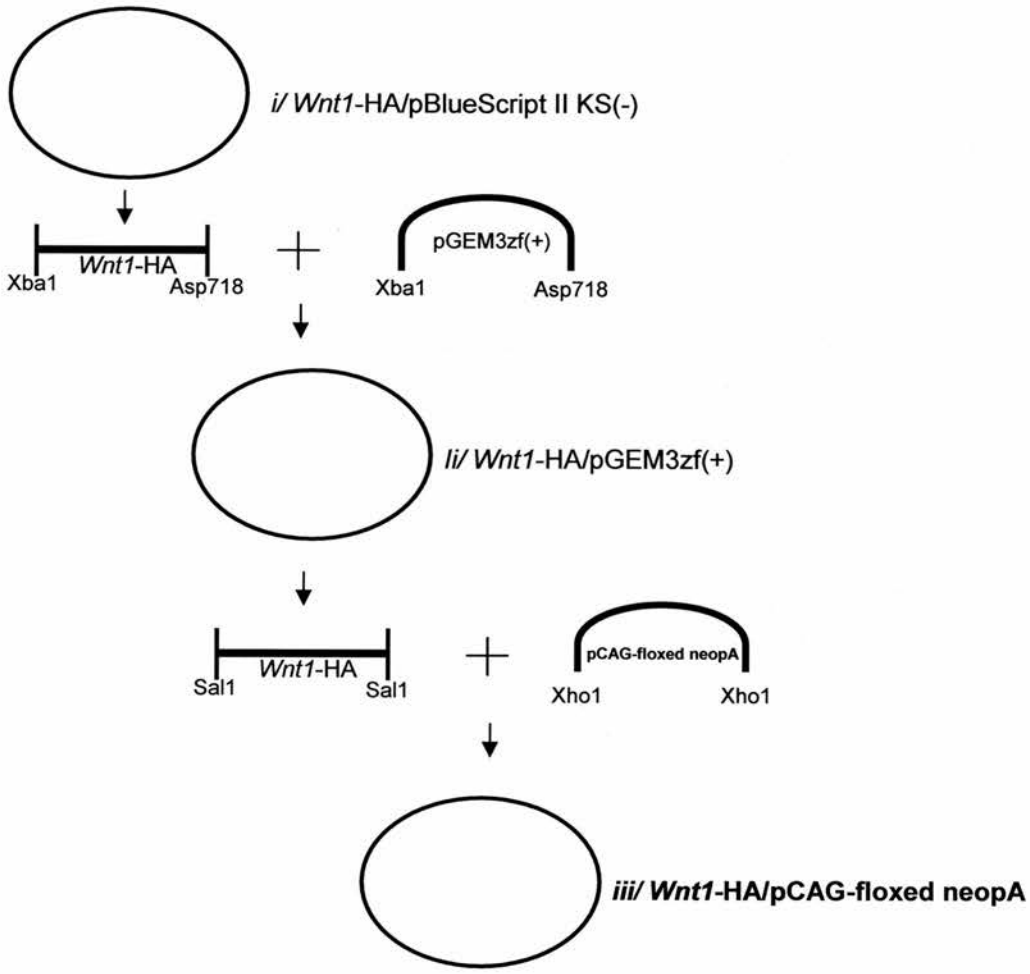

Confirmed by restriction enzyme digestion with:
Cla1, BamH1, Acc1, Xho1, EcoR1, EcoRV, Sal1, Nae1

A-i) Wnt1-HA/pBSII KS$^-$

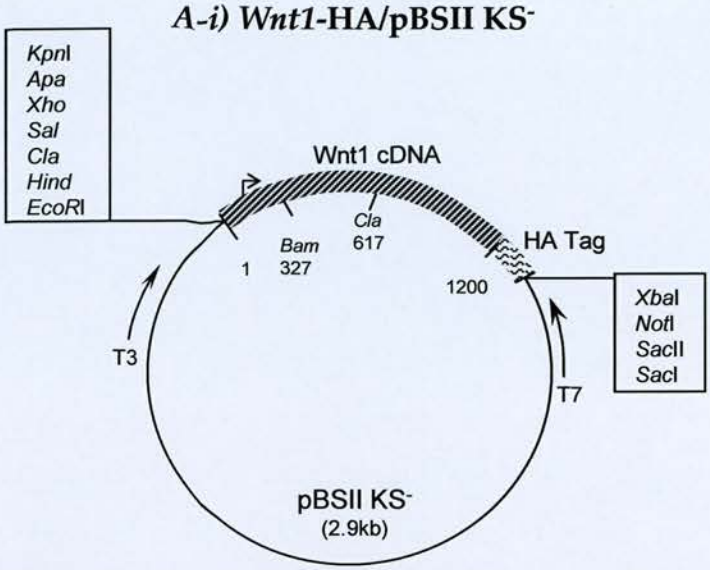

Ref: **Shimizu H**, Julius MA, Giarre M, Zheng Z, Brown AM, Kitajewski J. Transformation by Wnt family proteins correlates with regulation of beta-catenin. Cell Growth Differ. **1997** Dec; 8(12): 1349-58.

A-iii/ pCAG-floxed neopA-*Wnt1*-HA

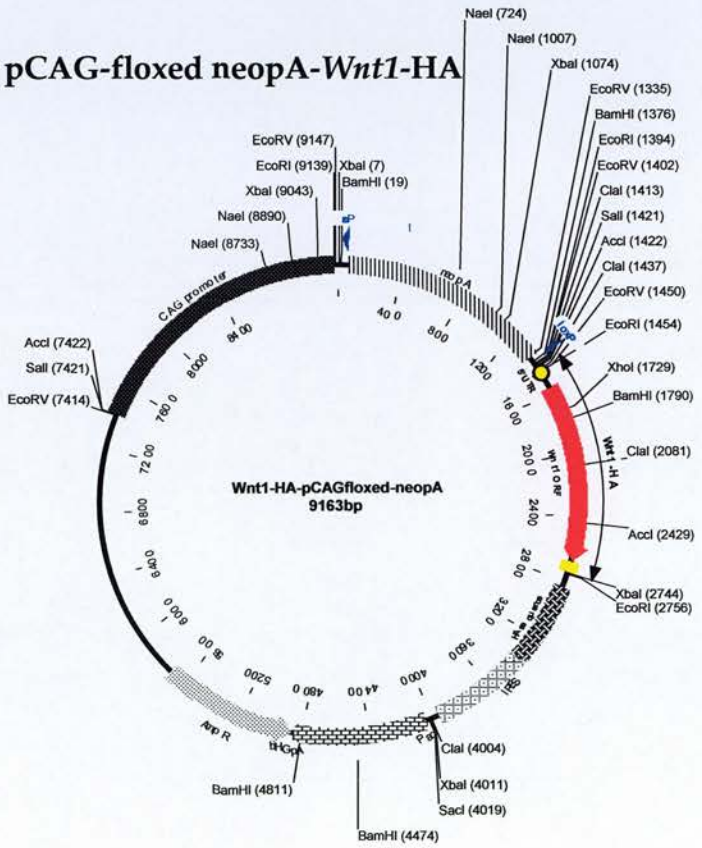

B) Construction of *Dkk1*/pCAG-floxed-neopA

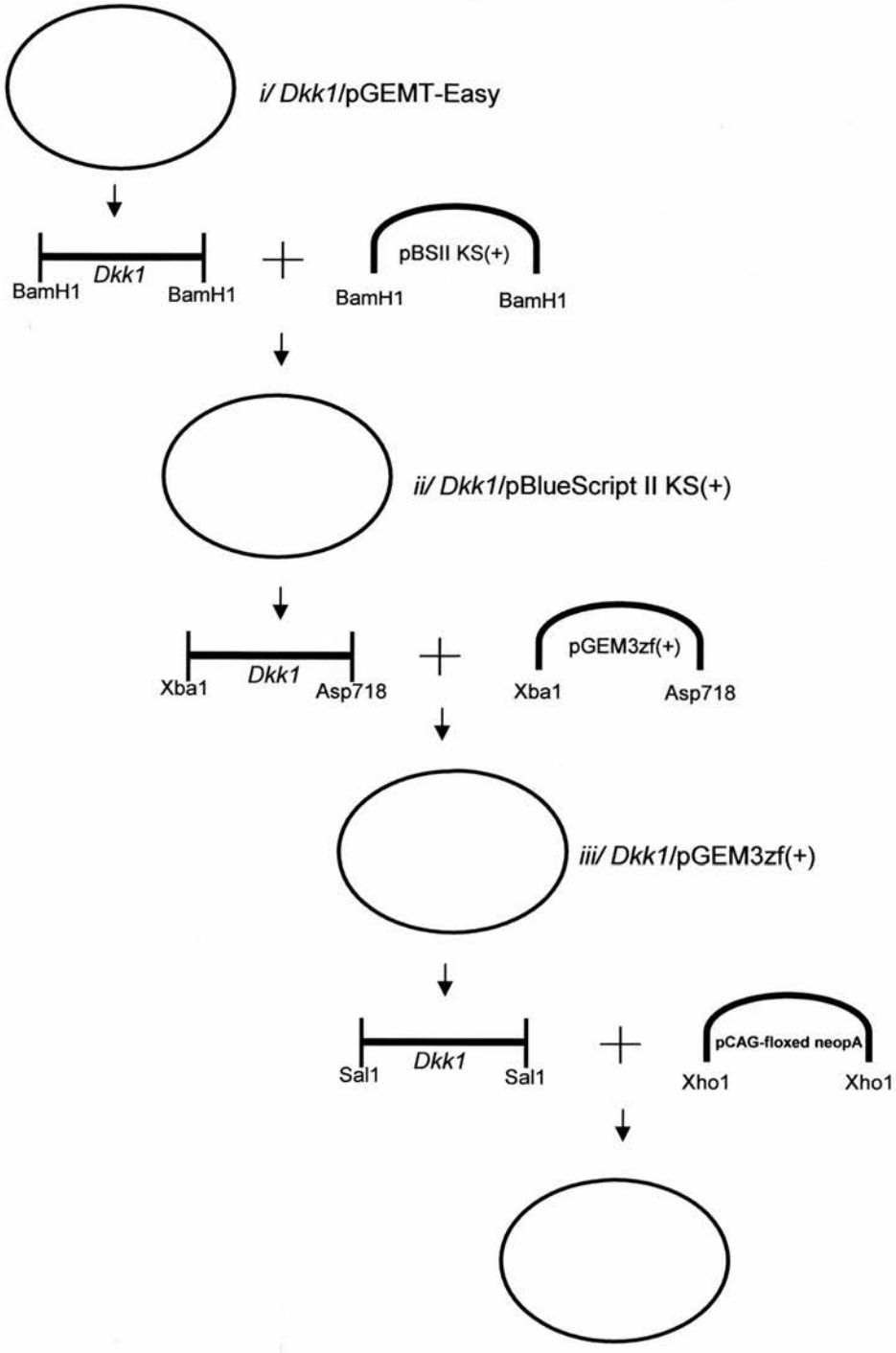

***Iv/ Dkk1*/pCAG-floxed neopA**

Confirmed by restriction enzyme digestion with:
Cla1, BamH1, Acc1, Xho1, EcoR1, Sal1, Asp718

B-i) pGEM-T Easy + *BamH* I-*Dkk 1*-*BamH* I

mouse Dkk 1 (accession # AF 030433; nuc 24-869=846 bp)

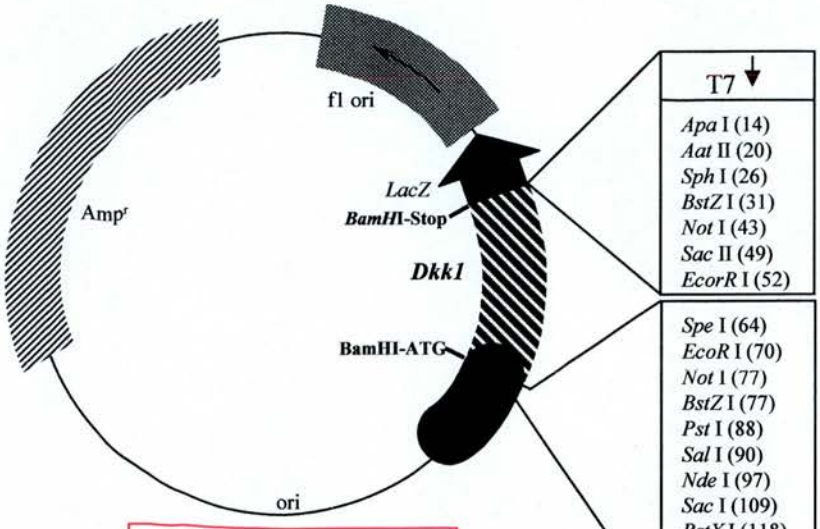

pGEM-T Easy Vector (3015 bp) + ***Dkk 1*** (860 bp)

A gift from Sarah Miller, University of Pennsylvania

B-ii) Dkk1 in pBlueScript II KS$^+$

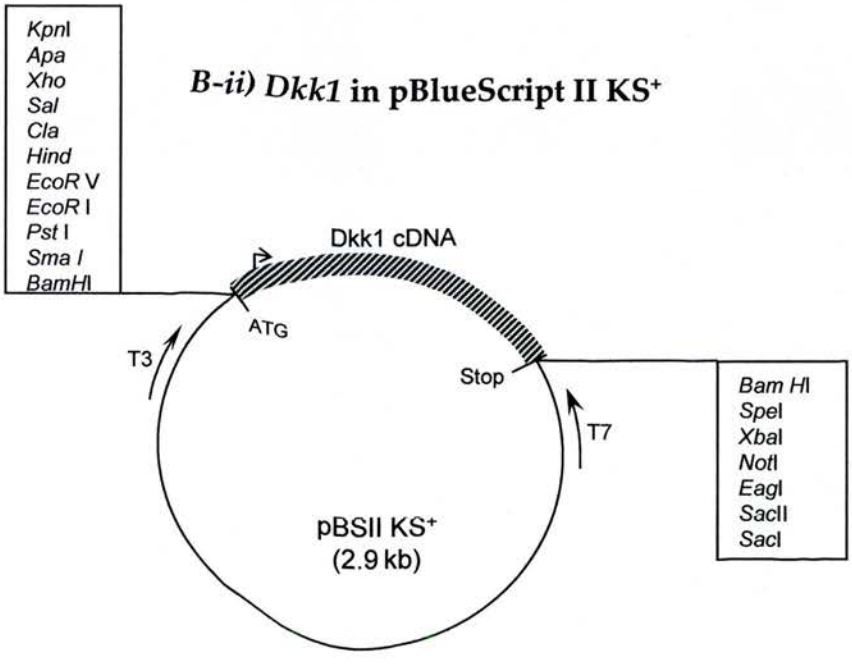

B-iv/ pCAG-floxed neopA-*Dkk1*

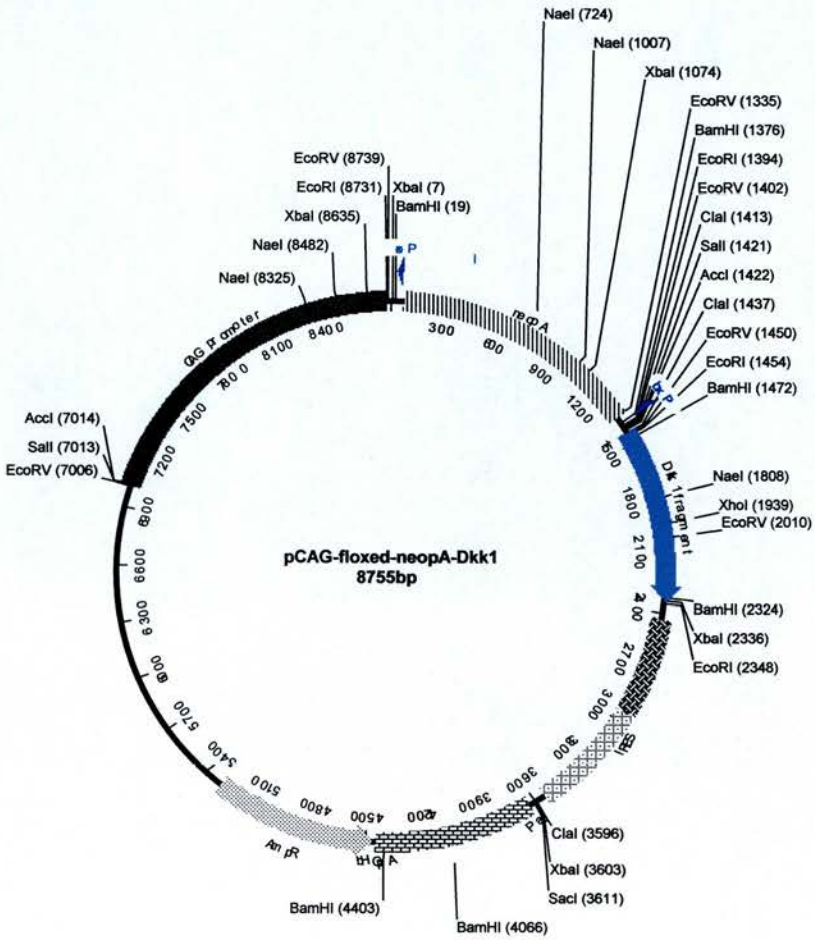

C) Construction of pCAG-floxed-*neo*pA-*Wnt3a*

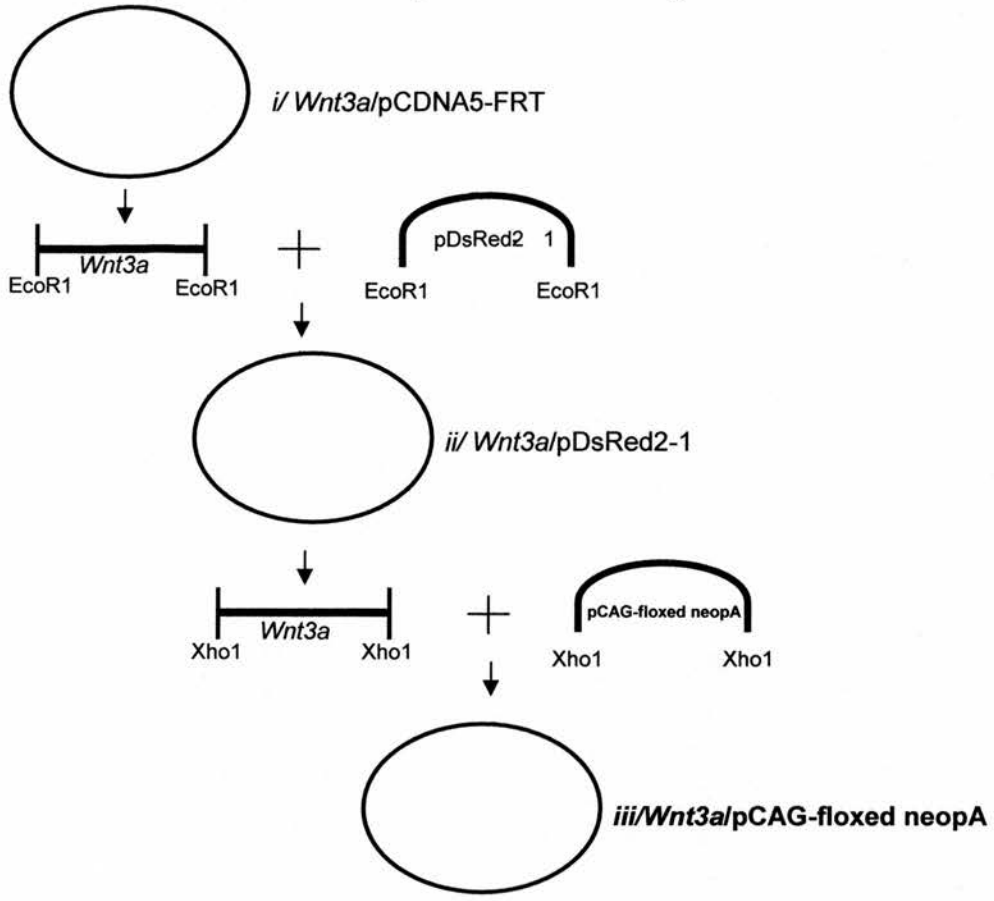

Confirmed by restriction enzyme digestion with:
Xho1, Sal1, Sac1, Not1, HindIII

D) Construction of pCAG-floxed-*neo*pA-*Wnt5a*

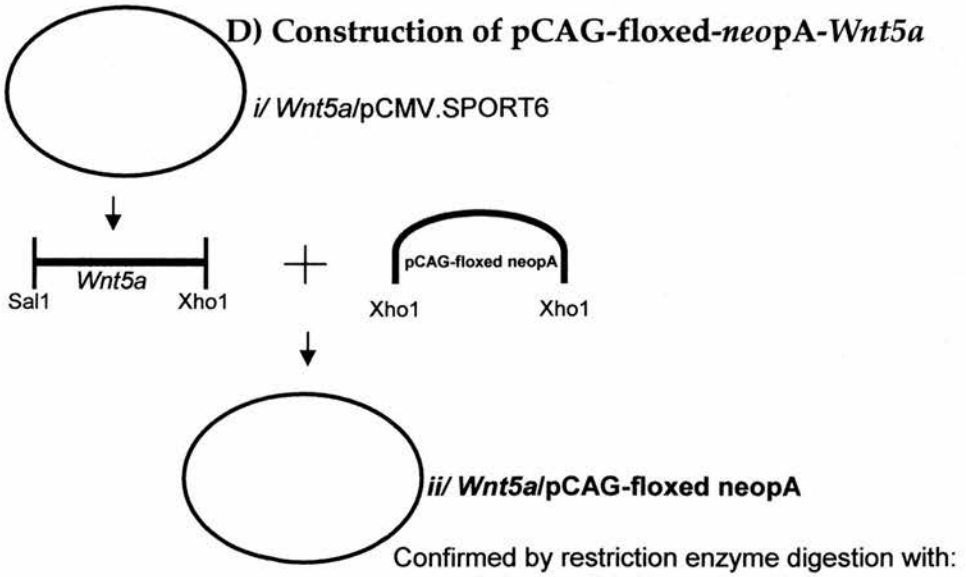

Confirmed by restriction enzyme digestion with:
Xho1, Sal1, EcoR1, Not1, Xho1/Sal1

C-i) pCDNA5-FRT-*Wnt3a*

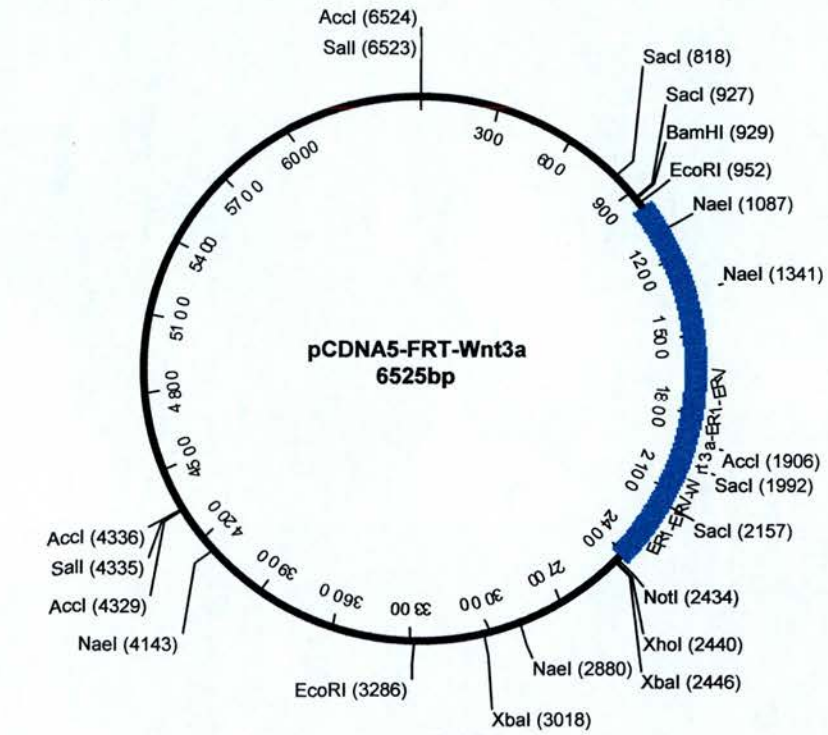

C-ii/ pDsRed2-1-*Wnt3a*

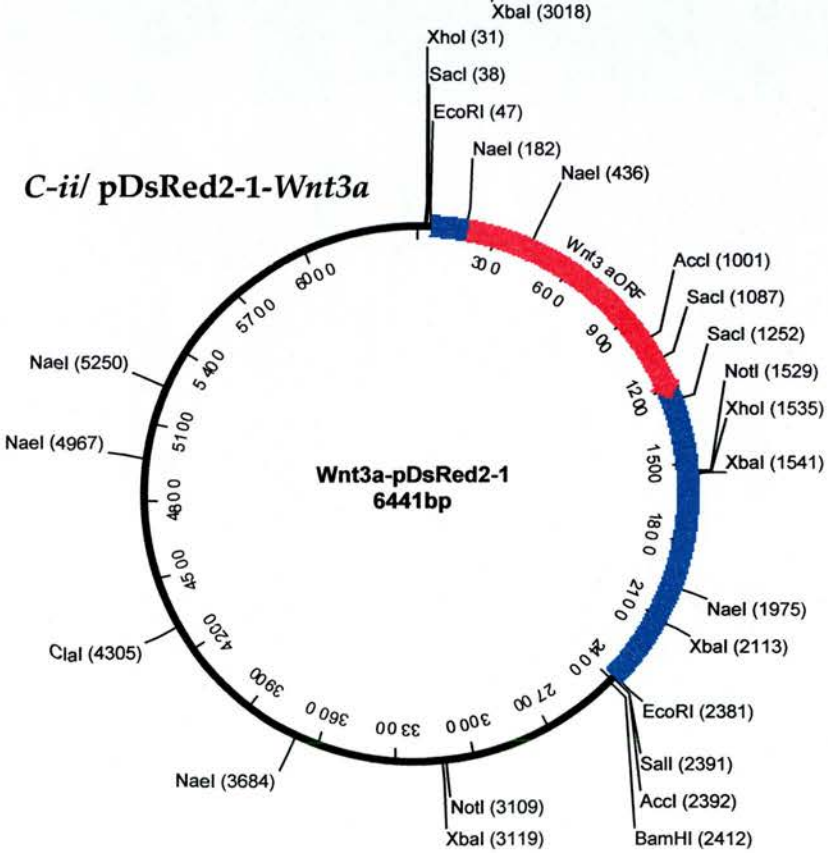

C-iii) pCAG-floxed-neopA-*Wnt3a*

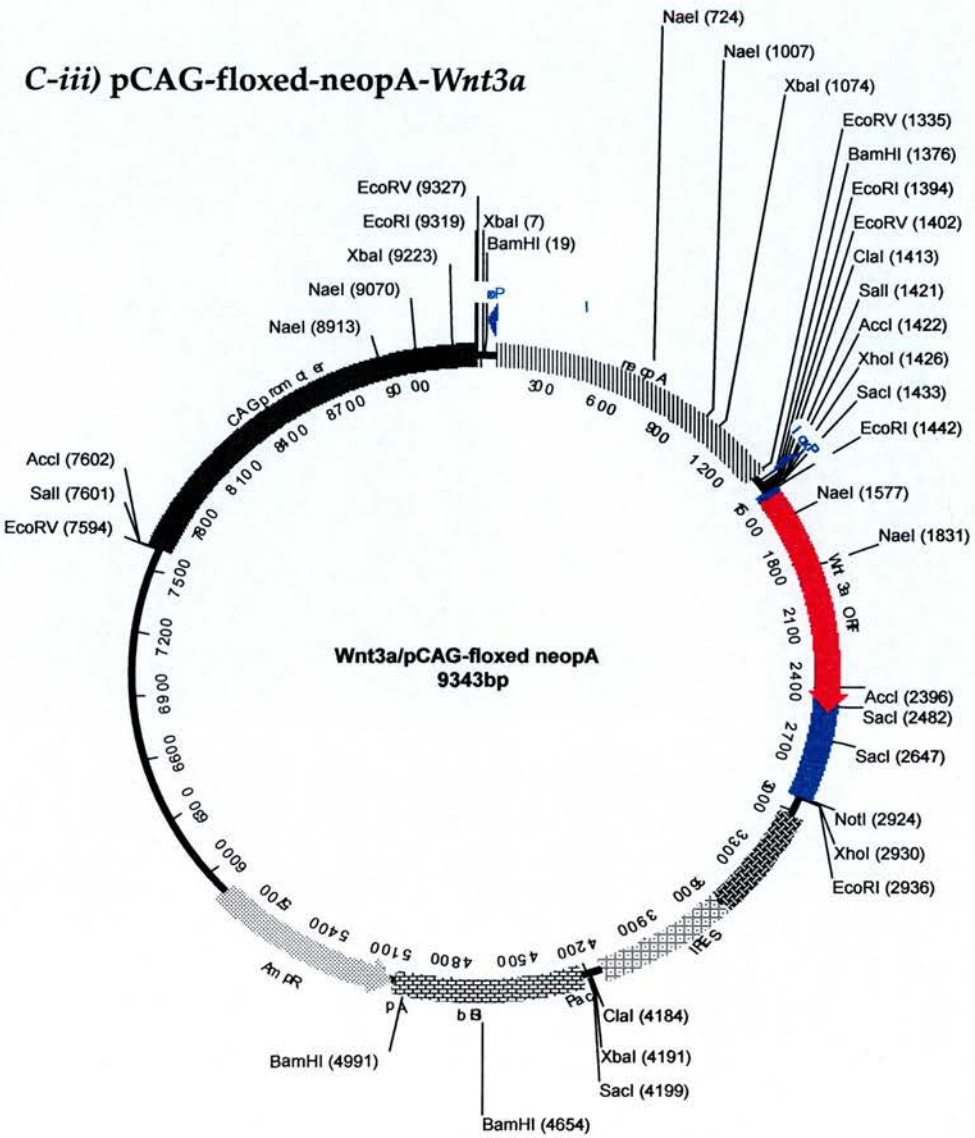

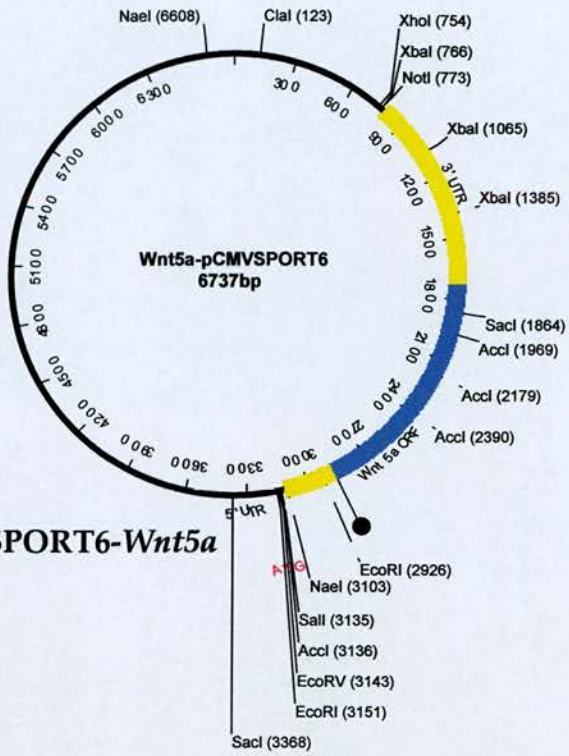

D-i)* pCMV.SPORT6-*Wnt5a

D-ii)* pCAG-floxed *neo*pA-*Wnt5a

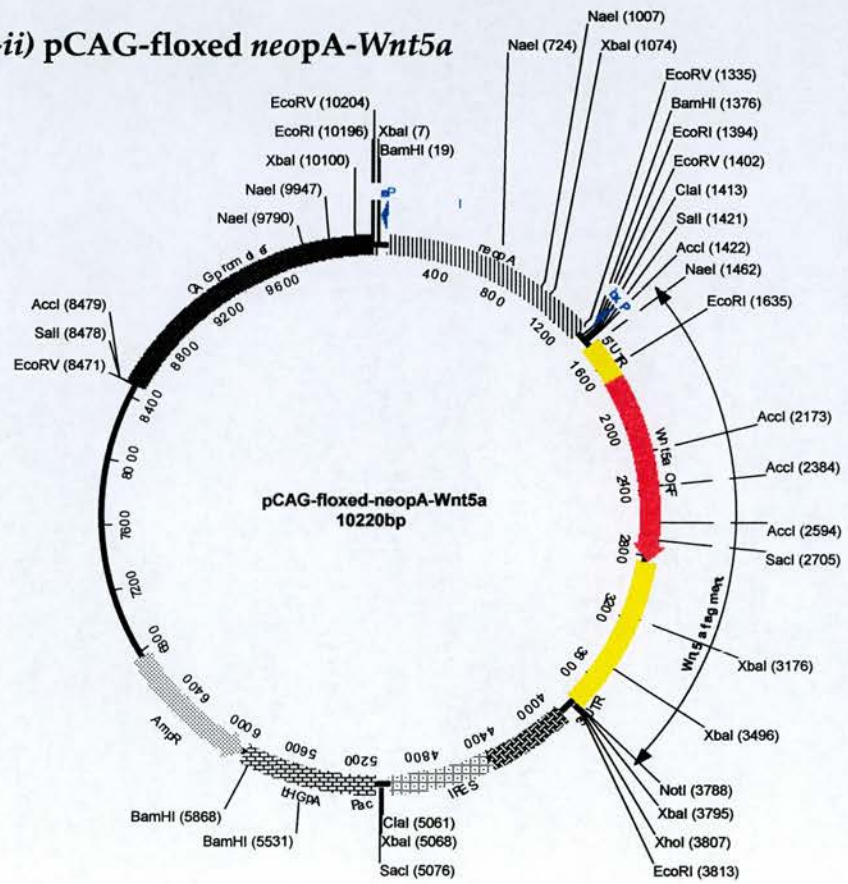

E) Construction of pCAG-floxed-*neo*pA-*Wnt7a* vector

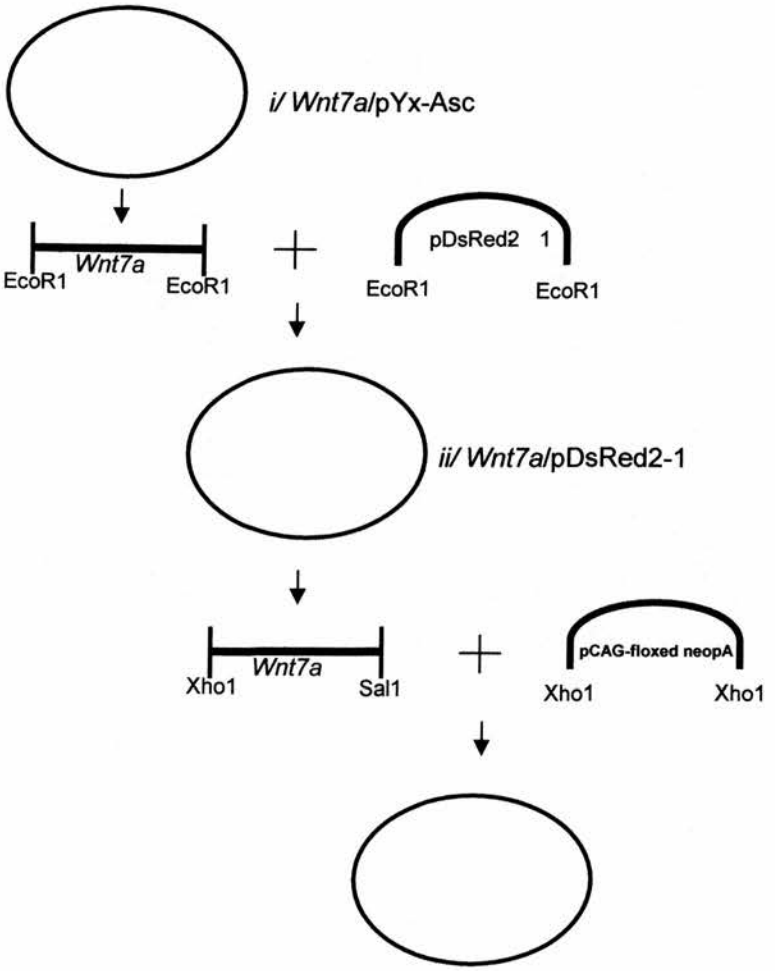

***iii/ Wnt7a*/pCAG-floxed neopA**

Confirmed by restriction enzyme digestion with:
Sac1, Xho1, EcoR1, Xho1/Sal1

E-i) **pYx-Asc-*Wnt7a***

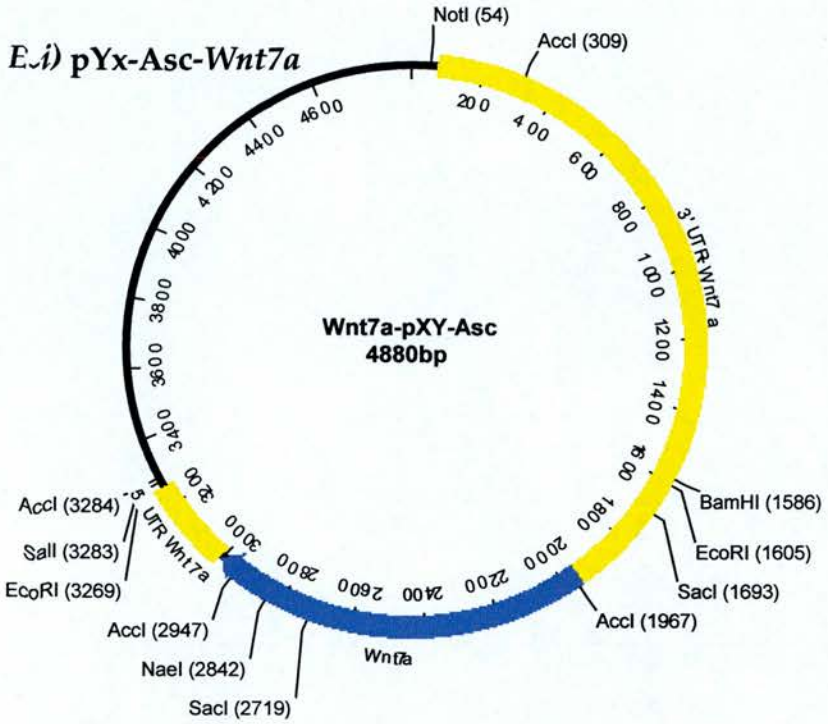

E-ii/ **pDsRed2-1-*Wnt7a***

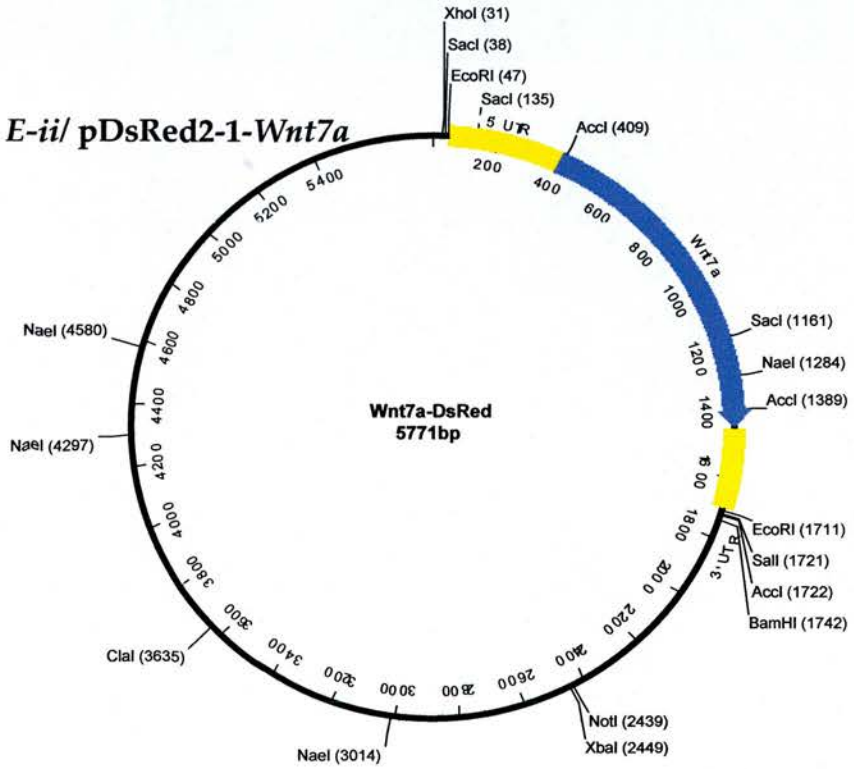

E-iii/ pCAG-floxed *neo*pA-*Wnt7a*

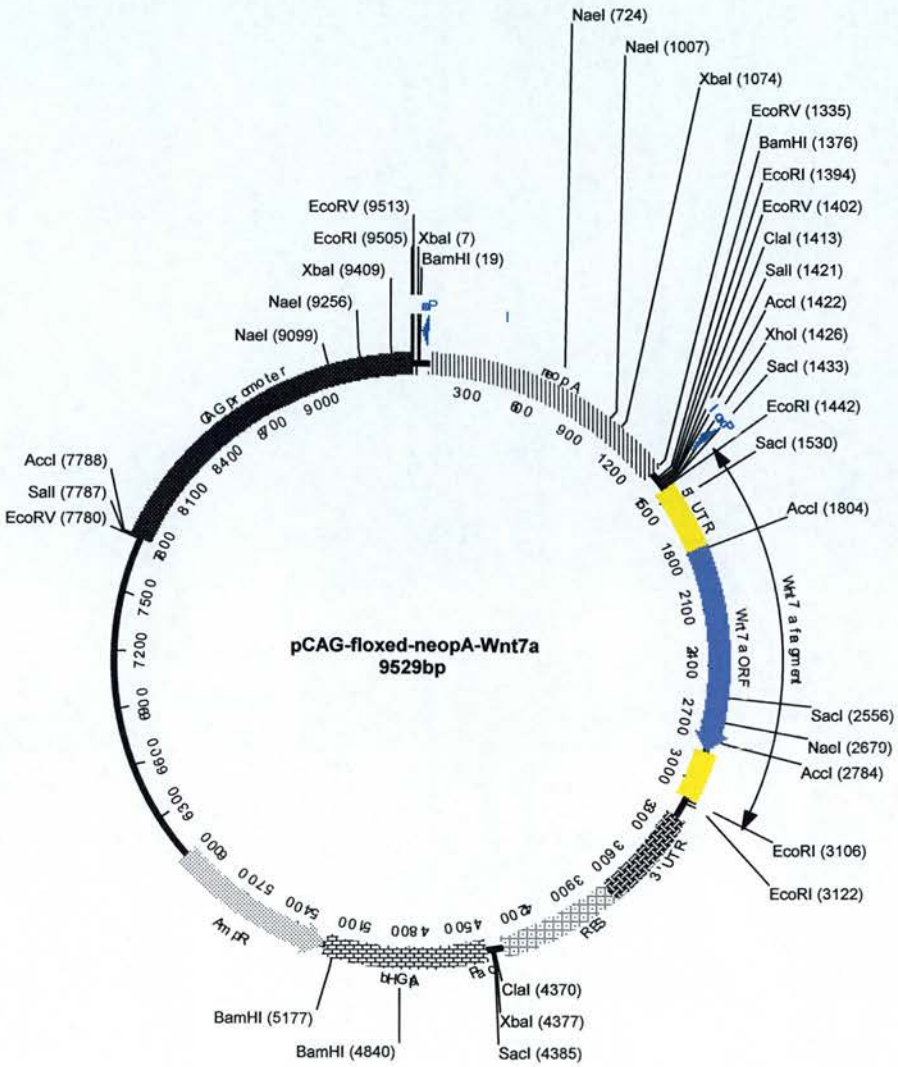

F) Construction of *pTOP-Red2 plasmid*

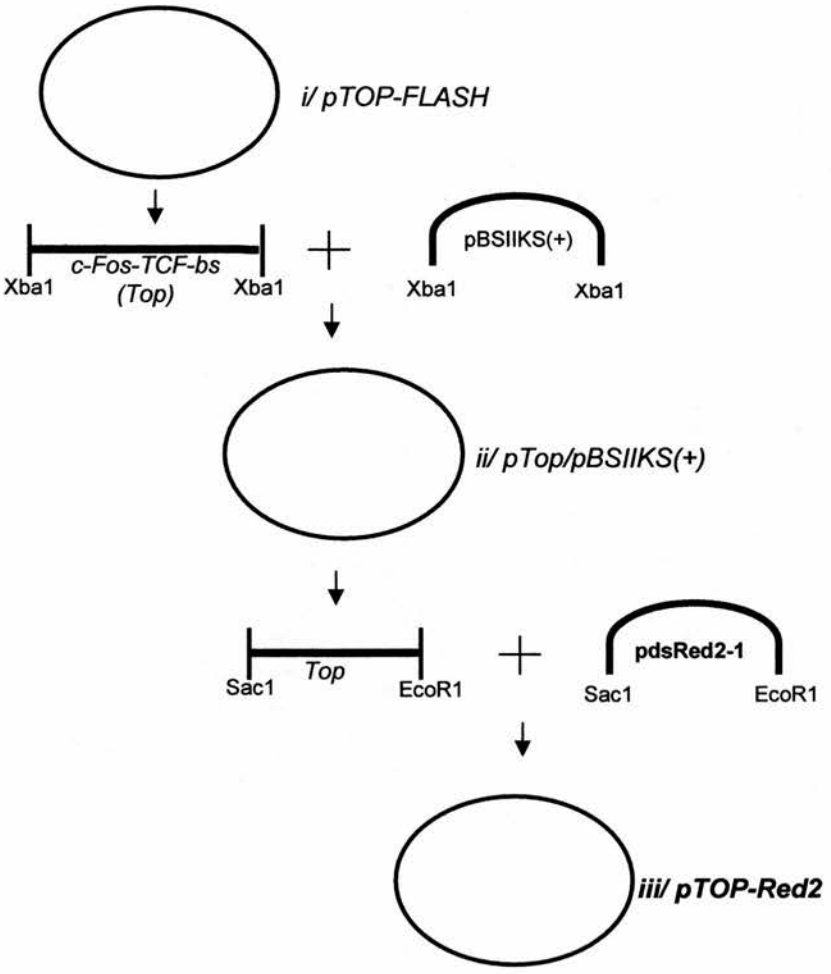

Confirmed by sequencing and restriction enzyme digestion with:
EcoR1/Sac1, Sal1

F-i) pTOP-FLASH (TCF-optimal-promoter)

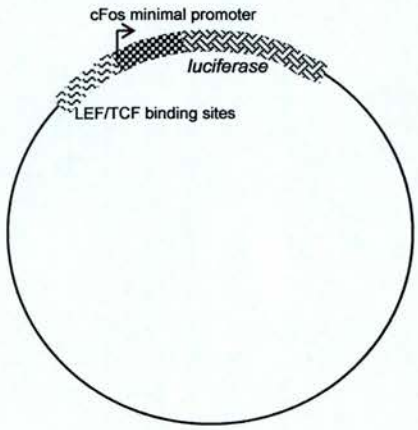

F-ii)*pTOP/pBSIIKS(+)*

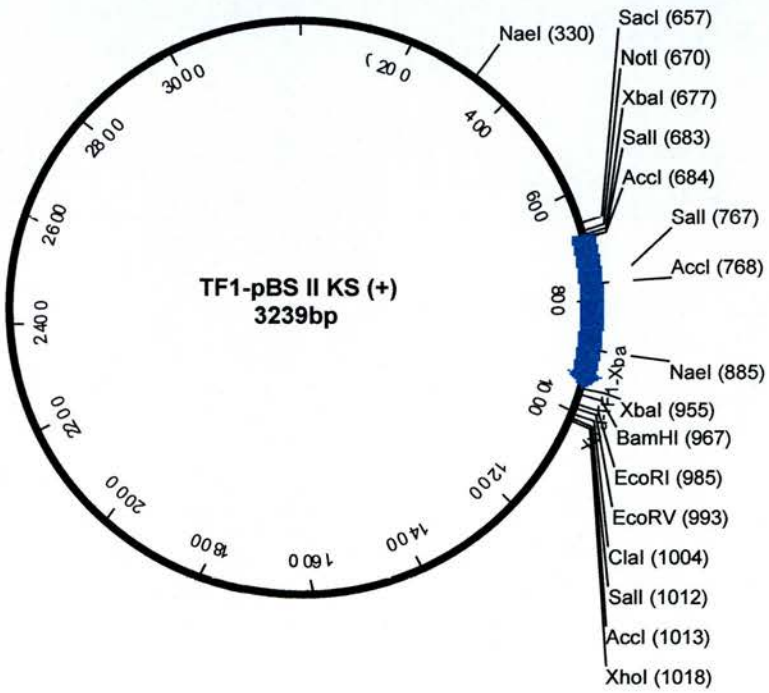

F-iii) pTOP-Red2

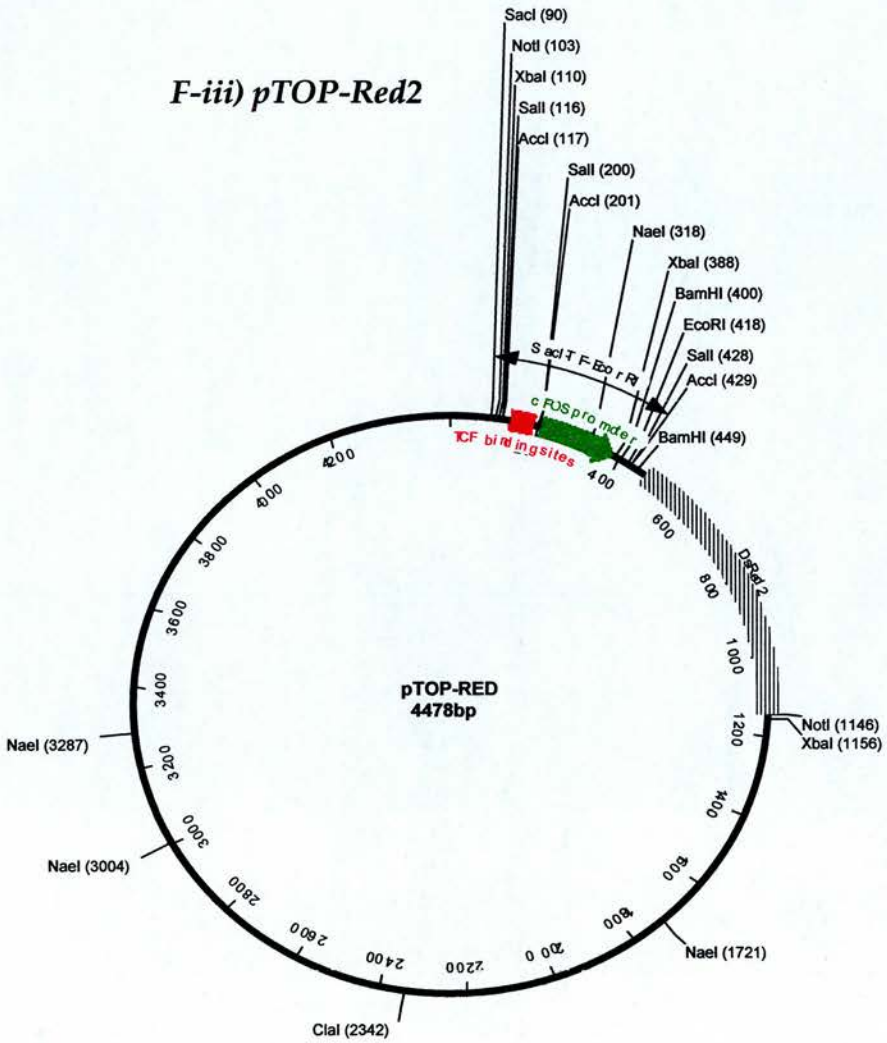

Appendix C: List of primers

i/ Primers for Reverse Transcription -Polymerase Chain Reaction (RT-PCR)

Name	Sequence	Size (bp)	Parameters
ß-Actin	ß-Actin-A1-forward: 5'GGCCCAGAGCAAGAGAGGTATCC3' ß-Actin-A2-reverse: 5'ACGCACGATTTCCCTCTCAGC3'	492	95°C – 3 minutes 95°C – 30 seconds 62°C – 30 seconds 72°C – 50 seconds } 35 cycles 72°C – 5 minutes
Dkk1	Dkk1-F-forward: 5' GCGTCCTTCGGAGATGATGG 3' Dkk1-R-reverse: 5'TTTAGACTGTCGGTTTAGTGTCTC 3'	846	95°C – 3 minutes 95°C – 30 seconds 58°C – 30 seconds 72°C – 50 seconds } 30 cycles 72°C – 5 minutes
Oct4	Oct4-forward: 5'GGCGTTCTCTTTGGAAAGGTGTTC3' Oct4-reverse: 5'CTCGAACCACATCCTTCTCT 3'	312	95°C – 3 minutes 95°C – 30 seconds 62°C – 30 seconds 72°C – 40 seconds } 30 cycles 72°C – 5 minutes
SFRP2	SFRP2-forward: 5'ATGCCGCGGGGCCCTGCCTCGCTG 3' SFRP2-reverse: 5'CTAGCATTGCAGCTTGCGGATGCT 3'		95°C – 3 minutes 95°C – 30 seconds 62°C – 30 seconds 72°C – 50 seconds } 30 cycles 72°C – 5 minutes
Sox1	Sox1-F-forward: 5'CCTCGGATCTCTGGTCAAGT 3' Sox1-R-reverse: 5'TACAGAGCCGGCAGTCATAC3'	593	95°C – 3 minutes 95°C – 30 seconds 62°C – 30 seconds 72°C – 50 seconds } 30 cycles 72°C – 5 minutes
Wnt1	Wnt1-F-forward: 5' TGCACCTGCGACTACCGGCG 3' Wnt1–R-reverse: 5' GTGCGCGGGGTGTTCGGGCT 3'	392	95°C – 3 minutes 95°C – 30 seconds 62°C – 30 seconds 72°C – 40 seconds } 35 cycles 72°C – 5 minutes
Wnt2	Wnt2-F-forward 5' CGGCCTTGTTTACGCCATC 3' Wnt2-R-reverse 5'TGAATACAGTAGTCTGGAGAA3'	496	95°C – 3 minutes 95°C – 30 seconds 55°C – 30 seconds 72°C – 45 seconds } 30 cycles 72°C – 5 minutes
Wnt2b	Wnt2b-F-forward 5' GCCAAAGAGAAGAGGCTTAA 3' Wnt2b-R-reverse 5' TCAGTCCGGGTGGCGTGGCG 3'	290	95°C – 3 minutes 95°C – 30 seconds 54°C – 30 seconds 72°C – 45 seconds } 35 cycles 72°C – 5 minutes
Wnt3	Wnt3- F-forward 5' GCCGACTTCGGGGTGCTGGT 3' Wnt3-R-reverse 5' CTTGAAGAGCGCGTACTTAG 3'	320	95°C – 3 minutes 95°C – 30 seconds 62°C – 30 seconds 72°C – 45 seconds } 30cycles 72°C – 5 minutes

Wnt3a	Wnt3a-F-forward 5′ ATTGAATTTGGAGGAATGGT 3′ Wnt3a-R-reverse 5′ CTTGAAGTACGTGTAACGTG 5′	320	95°C – 3 minutes 95°C – 30 seconds 55°C – 30 seconds 72°C – 45 seconds } 35 cycles 72°C – 5 minutes
Wnt4	Wnt4-F-forward 5′ GGCGTAGCCTTCTCACAGTC 3′ Wnt4-R-reverse 5′ TGCATTCCGAGGCACCAGCG 3′	300	95°C – 3 minutes 95°C – 30 seconds 62°C – 30 seconds 72°C – 45 seconds } 35 cycles 72°C – 5 minutes
Wnt5a	Wnt5aF1-forward 5′ TCCTATGAGAGCGCACGCAT 3′ Wnt5aR1-reverse 5′ CAGCTTGCCCCGGCTGTTGA 3′	230	95°C – 3 minutes 95°C – 30 seconds 59°C – 30 seconds 72°C – 45 seconds } 35 cycles 72°C – 5 minutes
Wnt5b	Wnt5bF1-forward 5′ CAGCTTGCCCTGGCGGGTGA 3″ Wnt5bR1-reverse 5′ TCGGAGGAGCAGGGCCGAGC3′	230	95°C – 3 minutes 95°C – 30 seconds 59°C – 30 seconds 72°C – 45 seconds } 30 cycles 72°C – 5 minutes
Wnt6	Wnt6- F-forward 5′ ATGGATGCGCAGCACAAGCG 3′ Wnt6-R-reverse 5′ TTTGCCGTCGTTGGTGCCCA 3′	310	95°C – 3 minutes 95°C – 30 seconds 62°C – 30 seconds 72°C – 40 seconds } 35 cycles 72°C – 5 minutes
Wnt7a	Wnt7a-F-forward 5′ CAAGGCCAGTACCACTGGGA 3′ Wnt7a-R-reverse 5′ GGCTCCACGTGGACGGCCTC 3′	310	95°C – 3 minutes 95°C – 30 seconds 55°C – 30 seconds 72°C – 45 seconds } 35 cycles 72°C – 5 minutes
Wnt7b	Wnt7b-F-forward 5′ CAAGGCTACTACAACCAGGC 3′ Wnt7b-R-reverse 5′ CACCTCCACCTGCACCGCTG 3′	310	95°C – 3 minutes 95°C – 30 seconds 62°C – 30 seconds 72°C – 40 seconds } 35 cycles 72°C – 5 minutes
Wnt8a	Wnt8aF1-forward 5′ GCAGCGACAACGTGGAGTTC 3′ Wnt8aR1-reverse 5′ GCTTCCTGAGATGCCATGAC 3′	170	95°C – 3 minutes 95°C – 30 seconds 62°C – 30 seconds 72°C – 40 seconds } 35 cycles 72°C – 5 minutes
Wnt8b	Wnt8b-F-forward 5′ AACGTGGGCTTCGGAGAGGC 3′ Wnt8b-R-reverse 5′ GCCCGCGCCCTGCAGCAGGT 3′	270	95°C – 3 minutes 95°C – 30 seconds 62°C – 30 seconds 72°C – 40 seconds } 30 cycles 72°C – 5 minutes
Wnt9a (14)	Wnt14-F2-forward 5′ CAGCACTACCAATGAAGCCA 3′ Wnt14-R2-reverse 5′CCTCGGCCACAACAAATACT 3′	220	95°C – 3 minutes 95°C – 30 seconds 58°C – 30 seconds 72°C – 45 seconds } 35 cycles 72°C – 5 minutes
Wnt9b (15)	Wnt15-F1-forward 5′ CTACGCTATGACACGGCTGT 3′ Wnt15-R1-reverse 5′ GTACTTGCTGGGCCGGCAGA 3′	171	95°C – 3 minutes 95°C – 30 seconds 62°C – 30 seconds 72°C – 40 seconds } 30 cycles

			72°C – 5 minutes
Wnt10a	Wnt10aF1-5′ AAAGTCCCCTACGAGAGCCC 3′ Wnt10aR1-5′ CAGCTTCCGACGGAAAGCTT 3′	180	95°C – 3 minutes 95°C – 30 seconds 55°C – 30 seconds 72°C – 40seconds } 30 cycles 72°C – 5 minutes
Wnt10b	Wnt10b-F1-forward 5′ CGGCTGCCGCACCACAGCGC 3′ Wnt10b-R1-reverse 5′ CAGCTTGGCTCTAAGCCGGT 3′	180	95°C – 3 minutes 95°C – 30 seconds 62°C – 30 seconds 72°C – 40 seconds } 35 cycles 72°C – 5 minutes
Wnt11	Wnt11-F1-forward 5′ GCCATGAAGGCCTGCCGTAG 3′ Wnt11-R1-reverse 5′ GATGGTGTGACTGATGGTGG 3′	160	95°C – 3 minutes 95°C – 30 seconds 62°C – 30 seconds 72°C – 40 seconds } 35 cycles 72°C – 5 minutes
Wnt16	Wnt16-F1-forward 5′ CCCTCTTTGGCTATGAGCTG 3′ Wnt16-R1-reverse 5′ CATGCCGTACTGGACATCAT 3′	209	95°C – 3 minutes 95°C – 30 seconds 62°C – 30 seconds 72°C – 45 seconds } 30 cycles 72°C – 5 minutes

ii/ qRT-PCR primers

Gene	Primer name-Sequence	Size (bp) /annealing Temperature
ß-Actin	ß-ActinF2-forward: 5′ CCTGTCAGCAATGCCTGGGT 3′ ß-Actinr2-reverse: 5′ CCAGCCTTCCTTCTTGGGTA 3′	150/ 58°C
Dkk1	Dkk1-LCF-forward: 5′ AGTGCGGCTCTGACGAGTAC 3′ Dkk1-LCR-reverse: 5′ GGTCAGAGGGCATGCATATTC 3′	165/58°C
GAPDH	GAPDH-1F-forward: 5′ TGGTGAAGCAGGCATCTGAG 3′ GAPDH-1R-reverse: 5′ TAGGCCATGAGGTCCACCAC 3′	121/58°C
Neomycin resistant (neo^r)	NeoF-forward: 5′ ATCAGGATGATCTGGACGAA 3′ NeoR-reverse: 5′ CAATATCACGGGTAGCCAAC 3′	225/56°C
SFRP2	sFRP2-F-forward: 5′AAGTTCCTGTGCTCGCTCTT 3′ sFRP2-R-reverse: 5′TGTCGTTGTCGTCCTCATTC 3′	309/58°C
Wnt1	MHWnt1LCfor-forward: 5′ATACGACCCCGTTTCTGCTG3′ MHWnt1LCrev-reverse:5′TTCCACTCCCTCACCTCAAAGC3′	138/58°C
Wnt1	Wnt1LC-F-forward: 5′CAAATGGCAATTCCGAAAC 3′ Wnt1LC-R-reverse: 5′AAGATGAACGCTGTTTCTCG 3′	105/54°C
Wnt2b	Wnt2b-F-forward:5′ GCCAAAGAGAAGAGGCTTAA 3′ Wnt2b-R-reverse:5′ TCAGTCCGGGTGGCGTGGCG 3′	290/54°C
Wnt3a	Wnt3aLC-F-forward: 5′ TGAACCGTCACAACAATGAG 3′ Wnt3aLC-R-reverse: 5′ CCAGCAGGTCTTCACTTCC 3′	107/55°C
Wnt4	Wnt4-F-forward: 5′ GGCGTAGCCTTCTCACAGTC 3′ Wnt4-R-reverse: 5′ TGCATTCCGAGGCACCAGCG 3′	300/58°C
Wnt5a	Wnt5aF1-forward: 5′ TCCTATGAGAGCGCACGCAT 3′ Wnt5aR1-reverse: 5′ CAGCTTGCCCCGGCTGTTGA 3′	230/58°C
Wnt5b	Wnt5bF1-forward: 5′ CAGCTTGCCCTGGCGGGTGA 3″ Wnt5bR1-reverse: 5′ TCGGAGGAGCAGGGCCGAGC3′	230/58°C
Wnt6	Wnt6- F-forward: 5′ ATGGATGCGCAGCACAAGCG 3′ Wnt6-R-reverse: 5′ TTTGCCGTCGTTGGTGCCCA 3′	310/58°C
Wnt7a	Wnt7a-F-forward: 5′ CAAGGCCAGTACCACTGGGA 3′ Wnt7a-R-reverse: 5′ GGCTCCACGTGGACGGCCTC 3′	310/55°C
Wnt7b	Wnt7b-F-forward: 5′ CAAGGCTACTACAACCAGGC 3′ Wnt7b-R-reverse: 5′ CACCTCCACCTGCACCGCTG 3′	310/58°C
Wnt8a	Wnt8aF1-forward: 5′ GCAGCGACAACGTGGAGTTC 3′ Wnt8aR1-reverse: 5′ GCTTCCTGAGATGCCATGAC 3′	170/58°C
Wnt9a (14)	Wnt14-F2-forward: 5′ CAGCACTACCAATGAAGCCA 3′ Wnt14-R2-reverse: 5′CCTCGGCCACAACAAATACT 3′	220/58°C
Wnt10b	Wnt10b-F1-forward: 5′ CGGCTGCCGCACCACAGCGC 3′ Wnt10b-R1-reverse: 5′ CAGCTTGGCTCTAAGCCGGT 3′	180/58°C
Wnt11	Wnt11-F1-forward: 5′ GCCATGAAGGCCTGCCGTAG 3′ Wnt11-R1-reverse: 5′ GATGGTGTGACTGATGGTGG 3′	160/58°C

iii/ Sequencing primers

Name of Plasmid	Sequence
TopFLASH	TF1-SF-forward: 5′ TTCAGTCGACCCCAGTGA 3′ LuciTF-SS-reverse: 5′ CTGACGCAGGCAGTTCTA 3′
Ds-Red2-1	Ds-Red2-1F-forward: 5′ AGCTGGACATCACCTCCCACAACG 3′ Ds-Red2-1R-reverse: 5′ GTACTGGAACTGGGGGGACAG 3′
pCAG-floxed	pCAGF-F1-forward: 5′ TCATGTCTGGATCTCCCG 3′ pCAGF-R1-reverse: 5′ AAGACGGCAATATGGTGG 3′

Appendix D: Consistency of ß-actin expression during neural differentiation of ES cells by qRT-PCR

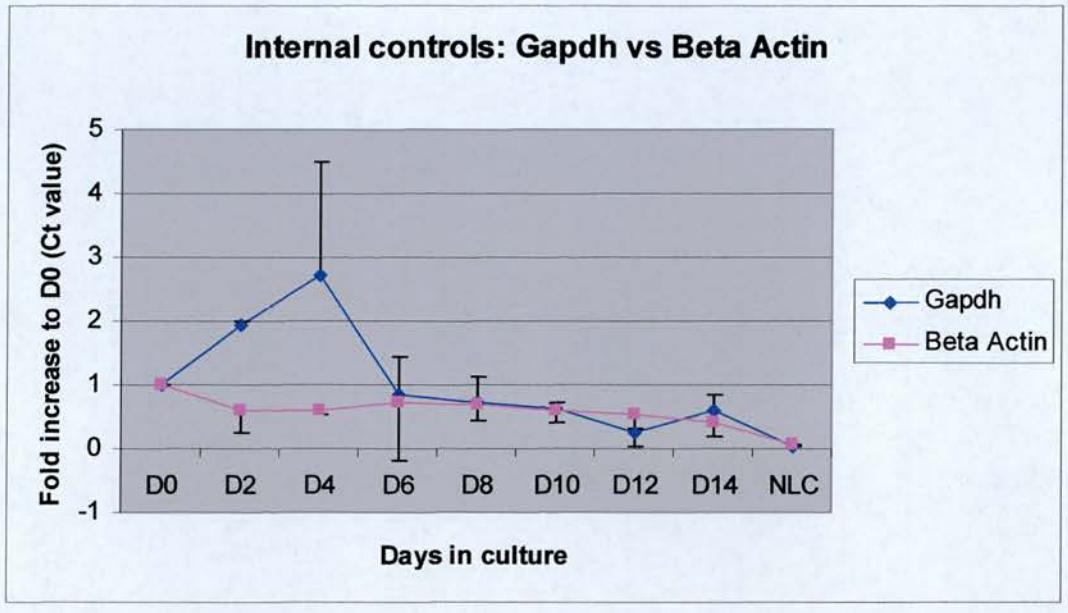

Comparison between expression of ß-Actin and Gapdh during neural differentiation of ES cells was carried out in order to examine the consistency of their expression during the process. It was discovered than expression of ß-Actin was more consistent than Gapdh, hence was used as an internal control for quantitative analysis of RT-PCR (qRT-PCR, Chapter 3). Results were from two independent experiments. Error bars are mean ± range between the two values.

Appendix E: Inducible expression system-pBigT/Pac-Asc

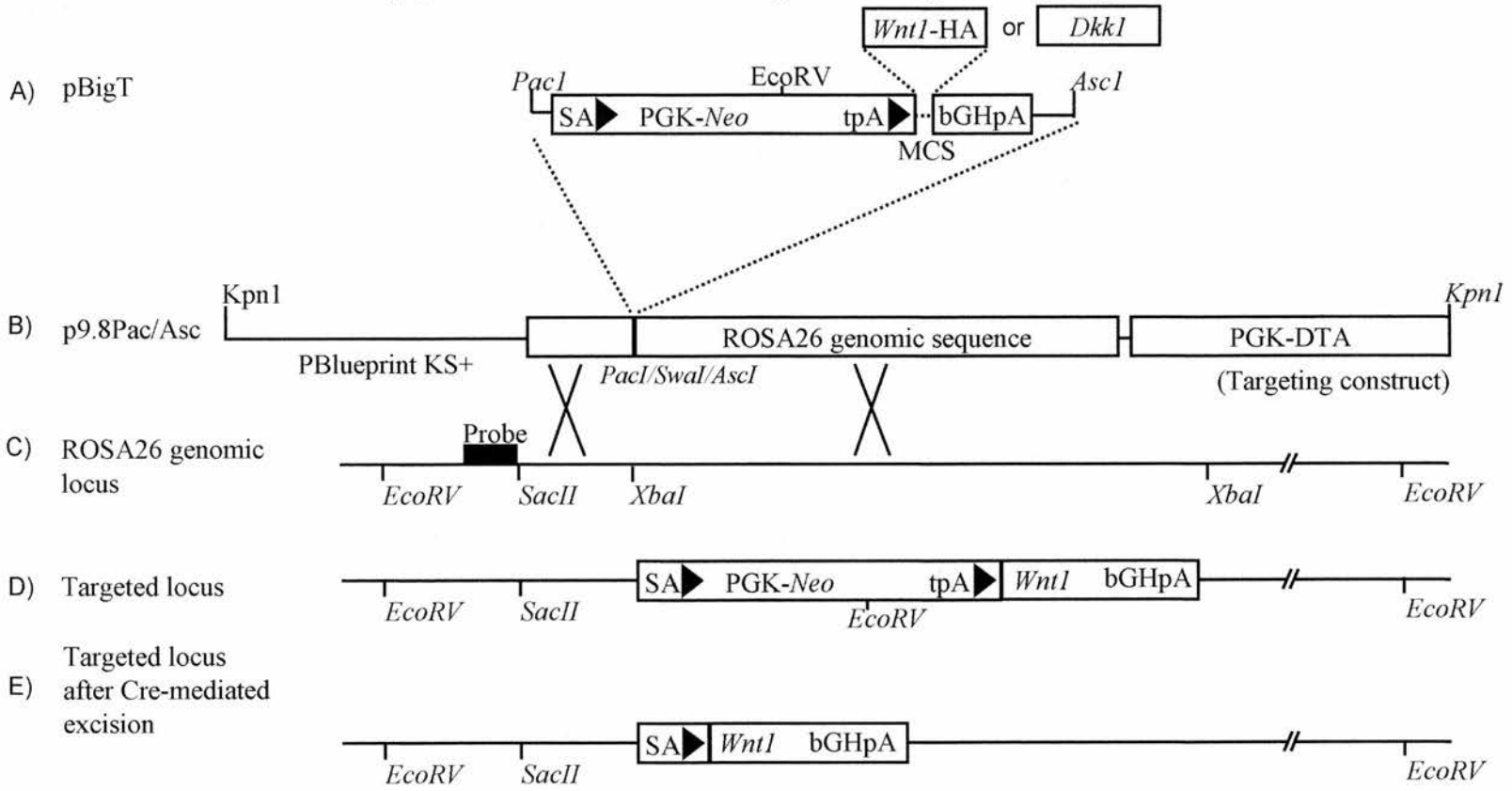

Gene Targeting strategy for ROSA26-Wnt1-HA and ROSA26-Dkk1. To generate a targeting construct, *Wnt1*-HA or *Dkk1* was cloned into pBigT (A), which was then ligated into ROSA26 vector, p9.8PAc/Asc vector (B). The generated construct will be then targeted into the ROSA26 locus (C) of R26CT2S ES cells to establish ROSA26-*Wnt1*-HA and ROSA26-*Dkk1* ES cells (D). The expression of the transgene will be induced upon excision of the floxed cassette by treatment with tamoxifen/4'-OHT. Diagram was adapted from Srinivas *et al.*, 2001). Generation of these targeting constructs were hampered due to technical problems.

Appendix F: Manual Cell Counting

A) pCAG-floxed-*neo*pA : Nestin

Manual Counting	- 4'-OHT				with 4'-OHT			
	ToPRO-3	Nestin +	Nestin -	% +ve cells	ToPRO-3	Nestin +	Nestin -	% +ve cells
f1	121	48	73	39.66942	98	61	37	62.2449
f2	90	53	37	58.88889	73	28	45	38.35616
f3	90	45	45	50	98	41	57	41.83673
f4	81	29	52	35.80247	108	64	44	59.25926
f5	152	96	56	63.15789	60	12	48	20
f6	66	30	36	45.45455	169	87	82	51.47929
Total	**600**	**301**	**299**		**606**	**293**	**313**	
Flowcytometry								
Gated				43.07				42.83

	- 4'-OHT	with 4'-OHT
Average % Nestin +ve	48.82887	45.529391
std dev	10.70388	15.6215201
SEM	4.36984	6.37745887
Flocytometry	43.07	42.83
T-test		
% no 4'-OHT to + 4'-OHT on D2		**0.67857566**

	- 4'-OHT	with 4'-OHT
Nestin Positive	50.16667	48.833333
Nestin negative	49.83333	52.166667
Std dev +	24.4738	27.154496
Std dev -	13.84798	15.992707
SEM +	9.991385	11.085777
SEM -	5.653416	6.5289952

B) pCAG-floxed-*neo*pA : ß-tubulin

	No 4'-OHT				4'-OHT on D2				4'-OHT on D7			
	ToPRO-3	ß-Tubulin +	ß-Tubulin -	% +ve cells	ToPRO-3	ß-Tubulin +	ß-Tubulin -	% +ve cells	ToPRO-3	ß-Tubulin +	ß-Tubulin -	% +ve cells
f1	183	67	116	36.61202	165	43	122	26.0606	129	47	82	36.43411
f2	151	51	100	33.77483	112	39	73	34.8214	130	46	84	35.38462
f3	46	16	30	34.78261	161	66	95	40.9938	150	54	96	36
f4	173	60	113	34.68208	141	46	95	32.6241	141	52	89	36.87943
f5	115	38	77	33.04348	156	60	96	38.4615	141	62	79	43.97163
f6	107	32	75	29.90654	165	59	106	35.7576	131	45	86	34.35115
f7	118	55	63	46.61017	123	54	69	43.9024	157	53	104	33.75796
f8	168	62	106	36.90476	117	46	71	39.3162	144	51	93	35.41667
Total	**1061**	**381**	**680**		**1140**	**413**	**727**		**1123**	**410**	**713**	

	No 4'-OHT	4'-OHT on D2	4'-OHT on D7
Average % B-tubulin +ve	35.7896	36.49222	36.52445
std dev	4.89104	5.530963	3.179687
SEM	1.72925	1.955491	1.124189
T-test			
% untreated to 4'-OHT D2	0.7917		
% untreated to 4'-OHT D7	0.7269		

	No 4'-OHT	4'-OHT on D2	4'-OHT on D7
Average ß-Tubulin +	47.625	51.625	51.25
Average ß-Tubulin -	85	90.875	89.125
Std dev +ve	17.476	9.516	5.496752
SEM +ve	6.1787	3.3644	1.943395
Std dev -ve	29.4812	18.712	8.219098
SEM -ve	10.4232	6.6156	2.90589

C) CAG-floxed-*neo*pA-*Wnt1*-HA: NPC 1-2 hours after plating

	- 4'-OHT				+ 4'-OHT on D2				Tp			
W1-8	ToPro3	Nestin +	Nestin -	% +ve	ToPro3	Nestin +	Nestin -	% +ve	ToPro3	Nestin +	Nestin -	% +ve
f1	277	231	46	83.3935	243	123	120	50.617	171	99	72	57.8947
f2	247	194	53	78.54251	272	174	98	63.971	111	49	62	44.1441
f3	307	258	49	84.03909	270	156	114	57.778	170	96	74	56.4706
f4	245	217	28	88.57143	356	208	148	58.427	108	47	61	43.5185
f5	311	269	42	86.49518	339	171	168	50.442	161	86	75	53.4161
f6	302	231	71	76.49007	284	103	181	36.268	107	50	57	46.729
f7	323	241	82	74.613	295	179	116	60.678				
f8	233	180	53	77.25322	259	151	108	58.301				
Total	**2245**	**1821**	**424**		**2318**	**1265**	**1053**		**828**	**427**	**1255**	

	- 4'-OHT				+ 4'-OHT on D2				Tp	
W1-3	ToPro3	Nestin +	Nestin -	% +ve	ToPro3	Nestin +	Nestin -	% +ve	Total cell score	
f1	252	185	67	73.4127	125	96	29	76.8	- 4'-OHT	3915
f2	184	141	43	76.63043	282	173	109	61.348	+ 4'-OHT on D2	3892
f3	207	173	34	83.57488	170	109	61	64.118	Tp	828
f4	183	143	40	78.14208	181	115	66	63.536		
f5	217	174	43	80.18433	172	94	78	54.651		
f6	162	121	41	74.69136	211	136	75	64.455		
f7	249	219	30	87.95181	189	100	89	52.91		
f8	216	183	33	84.72222	244	122	122	50		
Total	**1670**	**1339**	**331**		**1574**	**945**	**629**			

	- 4'-OHT	+ 4'-OHT on D2	Tp		- 4'-OHT	+ 4'-OHT on D2	Tp
Average	80.54	59.222	50.362	pos	197.5	138.125	71.1667
std dev	4.997	8.9506	6.3573	std dev	31.02	26.292	25.0393
SEM	1.249	2.2377	2.5954	SEM	7.7551	6.57299	10.2223

	- 4'-OHT	+ 4'-OHT on D2	Tp
FACS	61.73	54.59	40.09

T-test manual counting	
%Non-induced to Induced on D2	6.6E-10
%Non-induced to Tp	2E-10
T-test manual counting	
# pos.cells Non-induced to Induced on D2	0.00018
# pos cells Non-induced to Tp	1.5E-06

D) CAG-floxed-*neo*pA-*Wnt1*-HA: Nestin after 24 hrs plating

No 4'-OHT				4'-OHT on D2			
ToPro3	Nestin +	Nestin -	% +ve	ToPro3	Nestin +	Nestin -	% +ve
229	67	162	29.25764	117	25	92	21.36752
264	78	186	29.54545	185	29	156	15.67568
261	81	180	31.03448	194	32	162	16.49485
206	45	161	21.84466	226	42	184	18.58407
303	112	191	36.9637	252	35	217	13.88889
226	46	180	20.35398	298	31	267	10.40268
261	49	212	18.77395	291	24	267	8.247423
229	42	187	18.34061	277	27	250	9.747292
214	35	179	16.35514	265	20	245	7.54717
190	26	164	13.68421	219	13	206	5.936073
169	30	139	17.75148	179	20	159	11.17318
210	22	188	10.47619	229	20	209	8.733624
317	128	189	40.37855	221	41	180	18.55204
321	127	194	39.56386	187	32	155	17.1123
274	88	186	32.11679	219	31	188	14.15525
243	72	171	29.62963	218	49	169	22.47706
293	86	207	29.35154	295	41	254	13.89831
269	96	173	35.68773	287	32	255	11.14983
440	130	310	29.54545	305	42	263	13.77049
377	117	260	31.03448	276	29	247	10.50725
215	55	160	25.5814	164	16	148	9.756098
199	49	150	24.62312	160	9	151	5.625
138	33	105	23.91304	187	13	174	6.951872
171	45	126	26.31579	216	25	191	11.57407

Constitutive expression (Tp)							
ToPro3	Nestin +	Nestin -	% +ve		No 4'-OHT	4'-OHT D2	Tp
150	94	56	62.66667	Nestin positive	69.125	28.25	86.45833
180	81	99	45	Nestin negative	181.6667	199.5417	76.41667
135	70	65	51.85185		No 4'-OHT	4'-OHT D2	Tp
196	78	118	39.79592	std dev	34.74918	10.35983	18.40127
192	68	124	35.41667	SEM +ve	7.093146	2.114692	3.756144
162	83	79	51.23457	std dev	40.7342	47.72929	23.22277
167	82	85	49.1018	SEM -ve	8.314835	9.742701	4.740328
162	84	78	51.85185				
178	113	65	63.48315		No 4'-OHT	4'-OHT D2	Tp
199	108	91	54.27136	% Nestin	26.33845	12.63867	53.56444
166	84	82	50.60241	std dev	7.827768	4.622236	10.54133
138	78	60	56.52174	SEM	1.597836	0.94351	2.15174
158	28	130	17.72152				
146	78	68	53.42466	T-Test			
149	87	62	58.38926	% Non-induced to induced on D2			0.0000000042
162	94	68	58.02469	% Non-induced to Tp			4.8555E-13
154	94	60	61.03896	T-test non-induced +ve cells to D2's			1.49541E-06
201	123	78	61.19403	T-test non-induced +ve cells to Tp's			0.03605404
174	101	73	58.04598				
197	107	90	54.31472				
111	75	36	67.56757				
140	87	53	62.14286				
148	92	56	62.16216				
144	86	58	59.72222				

E) pCAG-floxed-neopA-Wnt1-HA: ß-Tubulin

	- 4-OHT				+4'-OHT on D2			
Clone1	ToPRO-3	ß-Tubulin +	ß-Tubulin -	% +ve cells	ToPRO-3	ß-Tubulin +	ß-Tubulin -	% +ve cells
f1a	417	195	222	46.7626	152	126	26	82.89474
f1b	452	172	280	38.0531	216	163	53	75.46296
f1c	241	138	103	57.2614	118	109	9	92.37288
f2a	255	118	137	46.2745	230	126	104	54.78261
f2b	334	168	166	50.2994	278	161	117	57.91367
f2c	295	154	141	52.2034	232	195	37	84.05172
Total	**1994**	**945**	**1049**		**1226**	**880**	**346**	
Clone1								
f1a	435	211	224	48.5057	345	264	81	76.52174
f1b	636	407	229	63.9937	376	295	81	78.45745
f1c	648	242	406	37.3457	277	268	9	96.7509
f2a	367	204	163	55.5858	388	307	81	79.12371
f2b	419	159	260	37.9475	364	266	98	73.07692
f2c	613	199	414	32.4633	377	320	57	84.88064
Total	**3118**	**1422**	**1696**		**2127**	**1720**	**407**	
Clone2								
f1a	181	102	79	56.3536	175	154	21	88
f1b	353	118	235	33.4278	225	195	30	86.66667
f1c	274	107	167	39.0511	304	254	50	83.55263
f1d	373	143	230	38.3378	193	158	35	81.86528
f2a	382	224	158	58.6387	370	304	66	82.16216
f2b	362	213	149	58.8398	228	207	21	90.78947
f2c	413	244	169	59.0799	251	195	56	77.68924
f2d	342	217	125	63.4503				
Total	**2680**	**1368**	**1312**		**1746**	**1467**	**279**	
Total	**7792**				**5099**			

Clone1	+ 4'-OHT on D7				Constitutive expression (Tp)			
f1a	ToPRO-3	ß-Tubulin +	ß-Tubulin -	% +ve cells	ToPRO-3	ß-Tubulin +	ß-Tubulin -	% +ve cells
f1b	252	110	142	43.6508	203	54	149	26.60099
f1c	113	56	57	49.5575	214	19	195	8.878505
f2a	132	72	60	54.5455	221	11	210	4.977376
f2b	330	212	118	64.2424	139	17	122	12.23022
f2c	202	141	61	69.802	171	29	142	16.95906
Total	274	163	111	59.4891	191	6	185	3.141361
Clone1	**1303**	**754**	**549**		**1139**	**136**	**1003**	
f1a								
f1b	420	301	119	71.6667	121	27	94	22.31405
f1c	304	166	138	54.6053	181	34	147	18.78453
f2a	376	190	186	50.5319	147	40	107	27.21088
f2b	319	229	90	71.7868	214	19	195	8.878505
f2c	430	334	96	77.6744	236	23	213	9.745763
Total					141	18	123	12.76596
Clone2	**1849**	**1220**	**629**		**1040**	**161**	**879**	
f1a								
f1b	270	171	99	63.3333				
f1c	297	187	110	62.963				
f1d	564	331	233	58.6879				
f2a	322	223	99	69.2547				
f2b	293	190	103	64.8464				
f2c	281	158	123	56.2278				
f2d	278	140	138	50.3597				
Total	352	235	117	66.7614				
	2657	**1635**	**1022**					
	5809				**2179**			

	No 4'-OHT	on D2	on D7	Tp
Ave	48.6938	80.36923	61.05192	14.3739
std dev	10.3106	10.37669	9.095819	8.01667
SME	2.30551	2.380575	2.086724	2.31421

	No 4'-OHT	on D2	on D7	Tp
pos	186.75	214.0526	189.95	24.75
neg	202.85	54.31579	115.79	156.8333
std dev	68.30032	68.33616	75.989	13.18487
SEM	15.27242	15.67739	17.433	3.806145

	No 4'-OHT	on D2	on D7	Tp
neg	202.85	54.31579	115.78947	156.8333
std dev	88.30585	32.49111	42.045714	41.40231
SEM	19.74579	7.453973	9.6459484	11.95182

T-test	
% untreated to 4'-OHT D2	1.54E-11
% Untreated to 4'-OHT D7	0.000327
% Untreated to Tp	6.37E-11

T-test	
#pos untreated to 4'-OHT D2	0.220063
#pos untreated to 4'-OHT D7	0.890719
# pos Untreated to Tp	5.15E-09

F) CAG-floxed-*neo*pA-*Wnt3a*: Nestin

	No 4'-OHT				4'-OHT on D2				Constitutive expresion (Tp)			
	B-tubulin +	B-tubulin -	total cells	%	B-tubulin	B-tubulin -	total cells	%	B-tubulin	B-tubulin -	total cells	%
f1	864	63	927	93.2	895	229	1124	79.63	687	113	800	85.88
f2	735	76	811	90.63	956	152	1108	86.28	784	121	905	86.63
f3	952	61	1013	93.98	864	323	1187	72.79	920	155	1075	85.58
f4	993	111	1104	89.95	686	360	1046	65.58	724	183	907	79.82
f5	834	88	922	90.46	334	242	576	57.99	989	149	1138	86.91
f6	895	79	974	91.89	441	204	645	68.37	753	124	877	85.86
f7	1181	80	1261	93.66	564	220	784	71.94	870	123	993	87.61
Total	**6454**		**7012**	92.04	**4740**		**6470**	73.26	913	113	1026	88.99
									635	106	741	85.7
	No 4'-OHT	4'-OHT on D2	Constitutive expresion (Tp)		No 4'-OHT	4'-OHT on D2	Constitutive expresion (Tp)		**7275**		**7662**	94.95
Average	91.965	71.7967	85.886	pos	922	677.143	808.333		No 4'-OHT	4'-OHT on D2	Tp	
std dev	1.663	9.24831	2.5267	neg	79.7143	247.143	131.889	std pos	141.32	240.3223	120.104	
SEM	0.6286	3.49553	0.8422					SEM pos	53.4139	90.83329	40.0347	
T-test % control to untreated on D2			1E-04					std neg	16.79	71.29383	25.2064	
T-test % control to Tp			1E-04					SEM neg	6.34603	26.94653	8.40212	
	No 4'-OHT	4'-OHT on D2	Tp		T-test #pos untrested to D2			0.039				
Flowcytometry	88.62	79.22	72.07		T-test #pos untrested to Tp			0.104				

G) CAG-floxed-*neo*pA-*Wnt3a*: ß-tubulin

	No 4'-OHT				4'-OHT on D2			
	positive cells	total cells	negative cells	% +ve cells	positive cells	total cells	negative cells	% +ve cells
f1a	141	188	47	75	53	53	0	100
f2a	133	184	51	72.2826	24	24	0	100
f3a	190	289	99	65.7439	33	45	12	73.3333
Total A	464	661	197	70.1967	110	122	12	90.1639
f4b	156	228	72	68.4211	16	36	20	44.4444
f5b	92	114	22	80.7018	21	23	2	91.3043
f6b	131	168	37	77.9762	25	26	1	96.1538
Total B	379	510	131	74.3137	62	85	23	72.9412

	4'-OHT on D7				Constitutive expresion (Tp)			
f1a	positive cells	total cells	negative cells	% +ve cells	positive cells	total cells	negative cells	% +ve cells
f2a	340	477	137	71.2788	112	141	29	79.4326
f3a	187	218	31	85.7798	93	133	40	69.9248
Total A	261	359	98	72.7019	95	149	54	63.7584
f4b	788	1054	266	74.7628	300	423	123	70.922
f5b	363	481	118	75.4678	54	85	31	63.5294
f6b	200	246	46	81.3008	95	133	38	71.4286
Total B	311	421	110	73.8717	62	116	54	53.4483
	874	1148	274	76.1324	211	334	123	63.1737

	No 4'-OHT	4'-OHT on D2	4'-OHT on D7	Tp
Average	73.3543	0	76.73349	
std dev	5.68257	0	5.630183	
SEM	2.3199	0	2.298513	0

	No 4'-OHT	4'-OHT on D2	4'-OHT on D7	Tp
positive cells	140.5	28.667	277	85.1667
negative cella	54.6667	5.8333	90	41
std	32.2165	13.155	73.22022	22.2838
SEM +	13.1523	5.3707	29.89203	9.09731
std	27.2666	8.3046	42.12838	10.8812
SEM -	11.1315	3.3903	17.19884	4.44222

T-test			
T-test % pos untreated to D2	0.26667	# pos untreated to D2	1.4E-05
T-test % pos untreated to D7	0.32516	# pos untreated to D7	0.00189
T-test % pos untreated to Tp	0.16396	# pos untreated to Tp	0.00612

H) CAG-floxed-*neo*pA-*Dkk1*: Nestin

	No 4'-OHT				4'-OHT on D2			
	Nestin +	Total	Nestin -	%+ve	Nestin +	Total	Nestin -	%+ve
f1	143	158	15	90.506329	159	207	48	76.811594
f2	167	229	62	72.925764	219	275	56	79.636364
f3	174	220	46	79.090909	270	318	48	84.90566
f4	307	432	125	71.064815	280	330	50	84.848485
f5	96	140	44	68.571429	257	312	55	82.371795
f6	127	185	58	68.648649	219	258	39	84.883721
f7	144	169	25	85.207101	165	201	36	82.089552
f8	139	161	22	86.335404	202	240	38	84.166667
Total	1297	**1694**	397		1771	**2141**	370	

	Constitutive expresion (Tp)			
	Nestin +	Total	Nestin -	%+ve
f1	70	133	63	52.631579
f2	87	136	49	63.970588
f3	100	177	77	56.497175
f4	68	102	34	66.666667
f5	93	124	31	75
f6	97	157	60	61.783439
f7	85	104	19	81.730769
f8	118	160	42	73.75
Total	718	**1093**	375	

	No 4'-OHT	4'-OHT on D2	Tp		No 4'-OHT	4'-OHT on D2	Tp
% Nestin +ve	77.7938	82.46423	66.503777	pos	162.125	221.375	89.75
sd dev	8.6921134	2.939765	9.8405137	neg	49.625	46.25	46.875
SEM	3.0731262	1.0393639	3.479147	std dev pos	63.232988	45.55354	16.298554
T-test				SEM pos	22.356237	16.105608	5.762409
% Non-induced to D2		0.1719495		std dev neg	34.883224	7.7228788	19.134393
% Non-induced to Tp		0.0290243		SEM neg	12.333082	2.73045	6.7650296
				T-Test			
				# pos Non-treated to D2			0.0494832
				# pos Non-treated to Tp			0.0073078

I) CAG-floxed-*neo*pA-*Dkk1*:Foxg1

	No 4'-OHT			4'-OHT on D2			Constitutive expression (Tp)		
	Foxg1 +	Total	%+ve	Foxg1 +	Total	%+ve	Foxg1 +	Total	%+ve
f1	26	72	36.111111	76	189	40.21164	31	70	44.285714
f2	13	97	13.402062	61	173	35.260116	39	77	50.649351
f3	3	264	1.1363636	1	152	0.6578947	41	60	68.333333
f4	1	236	0.4237288	50	136	36.764706	47	78	60.25641
Total	43	669	6.4275037	188	650	28.923077	158	285	55.438596

	Non-induced	Induced on D2 EBs	PuromycinR
Average	12.768316	28.223589	55.881202
Std dev	16.663122	18.493641	10.583409
SEM	8.3315608	9.2468204	5.2917044

T-test	
% untreated to D2	0.2606755
% untreated to Tp	0.0047289

J) CAG-floxed-*neo*pA-*Dkk1*: ß-tubulin

	No 4'-OHT				4'-OHT on D2			
	B-tub +ve	Total cells	Btub -ve	% +ve	B-tub +ve	Total cells	Btub -ve	% +ve
f1	291	548	257	53.102	178	265	87	67.17
f2	175	329	154	53.191	237	306	69	77.451
f3	149	269	120	55.39	223	300	77	74.333
f4	265	532	267	49.812	336	487	151	68.994
f5	134	285	151	47.018	327	448	121	72.991
f6	255	625	370	40.8	170	226	56	75.221
f7	211	462	251	45.671	156	201	45	77.612
f8	192	395	203	48.608	172	220	48	78.182
f9	236	548	312	43.066	438	637	199	68.76
f10	227	411	184	55.231	215	291	76	73.883
Total	2135	**4404**	2269	48.479	2452	**3381**	929	72.523

	4'-OHT on D7				Constitutive expresion (Tp)			
	B-tub +ve	Total cells	Btub -ve	% +ve	B-tub +ve	Total cells	Btub -ve	% +ve
f1	56	109	53	51.38	64	97	33	65.97938
f2	93	144	51	64.58	58	94	36	61.70213
f3	63	80	17	78.75	44	71	27	61.97183
f4	148	175	27	84.57	86	113	27	76.10619
f5	57	86	29	66.28	89	132	43	67.42424
f6	79	104	25	75.96	59	80	21	73.75
f7	35	60	25	58.33	44	60	16	73.33333
f8	74	89	15	83.15	77	117	40	65.81197
f9	121	148	27	81.76	47	58	11	81.03448
f10	99	118	19	83.9	58	83	25	69.87952
Total	825	**1113**	288	74.12	626	**905**	279	69.17127

	- 4'-OHT	D2	D7	Tp	T-test	
Average	49.189	73.46	72.8656	69.699	Non-induced to induced on D2 (+ve cells)	0.356
std dev	5.077	3.9628	11.8915	6.2979	Non-induced to induced on D7 (+ve cells)	2E-06
SEM	1.6055	1.2531	3.76041	1.9916	Non-induced to Tp (+ve cells)	5E-08

T-test% non-induced to induced D2	5.6E-10
T-test % non-induced to induced D7	1.7E-05
T-test % non-induced to Tp	2.4E-07

	Non-induced	Induced on D2	Induced on D7	Tp
Average +	213.5	245.2	82.5	62.6
Average -	226.9	92.9	28.8	27.9
std +	51.1	92.536	33.712	16.48
SEM +	16.159	29.262	10.6607	5.2115
std -ve	78.69	49.709	13.0792	10.279
SEM -ve	24.884	15.719	4.13602	3.2505

Appendix G: FACS analysis

CAG-floxed-*neo*pA: Nestin

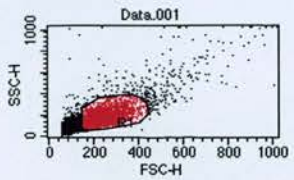

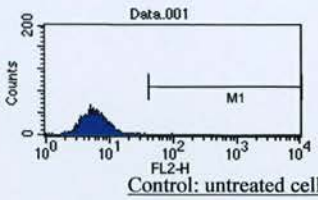

File: Data.001 Acquisition Date: 20-Dec-05
Gate: G1 Gated Events: 3828
Total Events: 12030 X Parameter: FL2-H (Log)

Marker	Events	% Gated	% Total	Mean	Geo Mean	Median
All	3828	100.00	31.82	6.32	5.79	5.62
M1	1	0.03	0.01	94.75	94.75	94.75

Control: untreated cell-fixed only

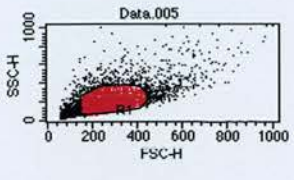

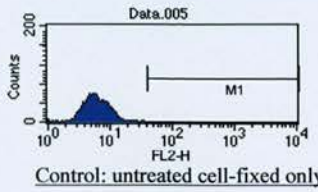

File: Data.005 Acquisition Date: 20-Dec-05
Gate: G1 Gated Events: 5416
Total Events: 7110 X Parameter: FL2-H (Log)

Marker	Events	% Gated	% Total	Mean	Geo Mean	Median
All	5416	100.00	76.17	6.39	5.89	5.78
M1	0	0.00	0.00	***	***	***

Control: untreated cell-fixed only with primary antibody only

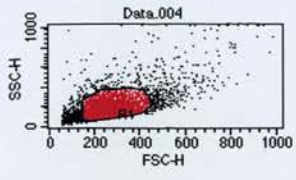

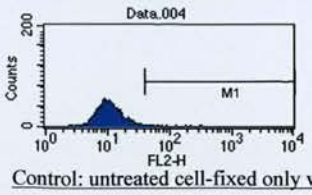

File: Data.004 Acquisition Date: 20-Dec-05
Gate: G1 Gated Events: 4566
Total Events: 5895 X Parameter: FL2-H (Log)

Marker	Events	% Gated	% Total	Mean	Geo Mean	Median
All	4566	100.00	77.46	11.89	10.65	10.32
M1	23	0.50	0.39	90.85	72.03	59.35

Control: untreated cell-fixed only with secondary antibody only

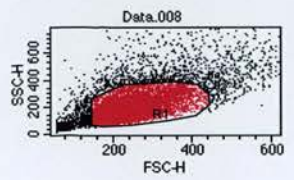

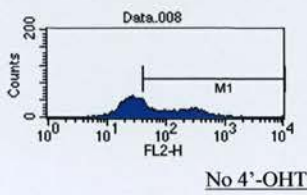

File: Data.008 Acquisition Date: 20-Dec-05
Gate: G1 Gated Events: 6847
Total Events: 8989 X Parameter: FL2-H (Log)

Marker	Events	% Gated	% Total	Mean	Geo Mean	Median
All	6847	100.00	76.17	99.84	51.70	35.55
M1	2949	43.07	32.81	198.70	144.98	156.79

No 4'-OHT-Nestin/PE

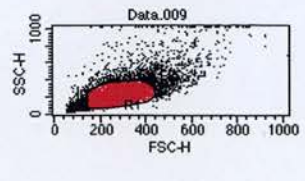

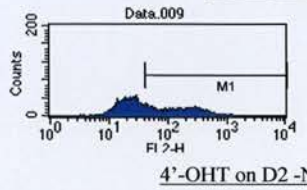

File: Data.009 Acquisition Date: 20-Dec-05
Gate: G1 Gated Events: 6496
Total Events: 8691 X Parameter: FL2-H (Log)

Marker	Events	% Gated	% Total	Mean	Geo Mean	Median
All	6496	100.00	74.74	97.43	48.24	32.49
M1	2782	42.83	32.01	197.65	147.67	156.08

4'-OHT on D2 -Nestin/PE

FACS analysis on nestin expression in stably-transfected R26CT2S cells with pCAG-floxed-*neo*pA empty vector was carried out using controls as described above (for setting up the R1 and M1 gate). The same procedure was used for all antibodies staining analysed by FACS.